Superleder tapes karakteriseret fra nanometer pinning til meter store spoler

Abrahamsen, Asger Bech

Publication date:
2013

Document Version
Også kaldet Forlagets PDF

Karakterisering
på alle længdeskalaer

DMS

DANSK METALLURGISK SELSKAB
Vintermødet
2013
Koldingfjord

Foredrag
præsenteret ved
Vintermødet 16. til 18. januar 2013
Hotel Koldingfjord
Kolding

Redaktion:
Trine Nybo Lomholt

FORORD

Dansk industri skal bl.a. overleve på kvalitet, og det er vigtigt, at virksomhederne kan dokumentere denne kvalitet overfor deres kunder. Vintermødet 2013 har derfor fokus på karakterisering af materialer, processer og komponenter, som spænder fra nanometer til meterskala og fra forskning & udvikling til monitorering af komponenter i drift.
Vintermødet sigter mod en bred dækning af emnet med foredrag, der bl.a. dækker mikroskopi, kemisk analyse, mekanisk prøvning, skadesanalyse, kvalitetskontrol mm.

Dette års virksomhedsbesøg foregik på Alfa Laval i Kolding. Alfa Laval Kolding er specialist i løsninger til håndtering af væsker af enhver viskositet, hurtig rengøring af lukket procesudstyr og intelligent, automatiseret kontrol. På fabrikken i Kolding produceres pumper og ventiler til fødevareindustrien, bryggerier, mejerier, farmaceutiske- og kosmetiske industrier. Alfa Laval Kolding beskæftiger i dag ca. 550 medarbejdere.

Trine Nybo Lomholt

INDHOLDSFORTEGNELSE

Fracture mechanics - Some basic concepts and recent trends

Erling Østby, SINTEF

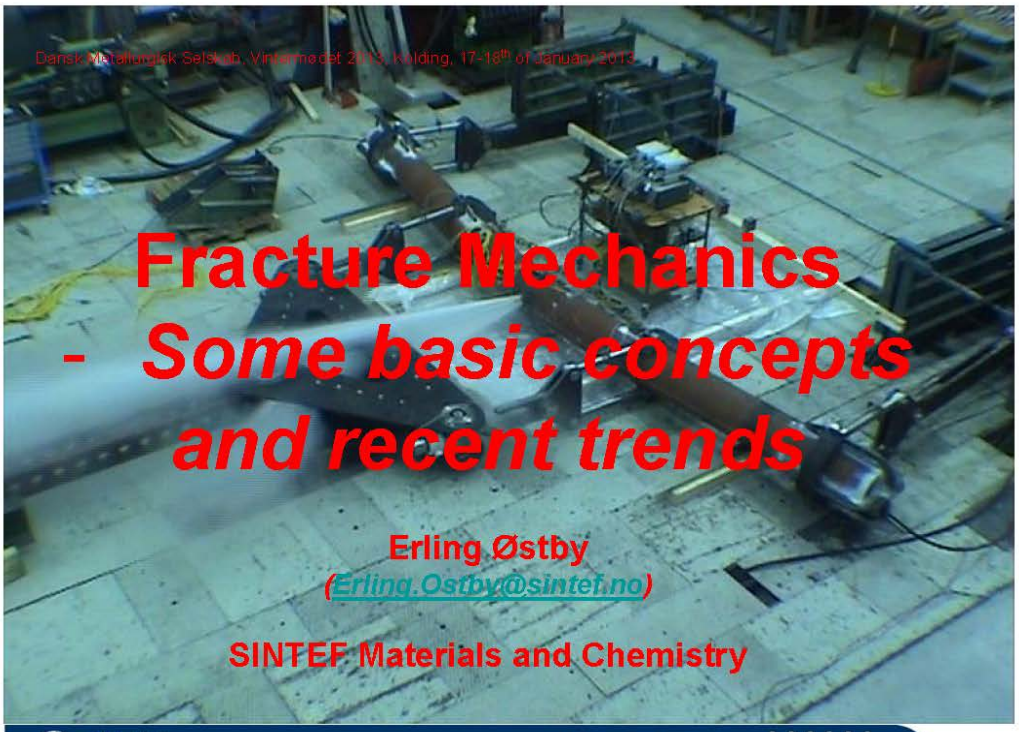

SINTEF Materials and Chemistry

- SINTEF Materials and Chemistry is a contract research division offering high competence within
  - materials technology,
  - applied chemistry,
  - and applied biology
- 400 employees
  - 100 Oslo, 300 Trondheim, approx. 25% non-Norwegian from 44 countries
- 8 departments + staff
- Core areas of R&D
  - Oil & Gas industry, approx. 150 man-years
    - along the whole value chain from increased oil production, drilling, flow assurance, pipelines, to refineries and petrochemical
    - the largest independent research institution in the world on oil spill
  - Land-based industries, approx. 120 man-years
    - aluminum, ferro alloys, mineral industry, manufacturing industry, pharmaceutical industry (biotech), and food industry.
  - Environmentally friendly energy, approx. 120 man-years
    - Silicon-based solar, CCS, bio-refinery, offshore wind, hydrogen technology.

Executive Vice President Torstein Haarberg together with former and present employees at SINTEF Materials and Chemistry

Outline

- Some basic fracture mechanics concepts
- Examples of emerging/new topics
  - Constraint effect – *"new knowledge"*
  - Fracture under large global deformations - *"application under harsher conditions"*
  - Use of numerical simulation tools – *"taking the analysis further"*
  - Testing techniques – *"new information"*
  - Probabilistic fracture assessments – *"quantified safety level"*
  - .. and a few words on multi-scale approaches – *"tomorrow"*
- Wrap-up

Some basic fracture mechanics

Basic fracture mechanics

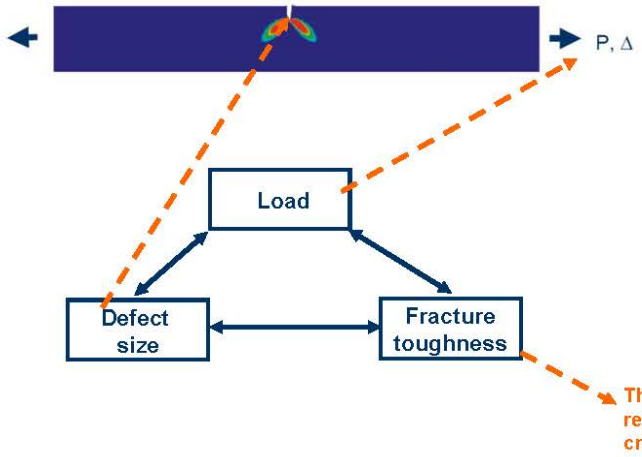

Types of fracture – global perspective

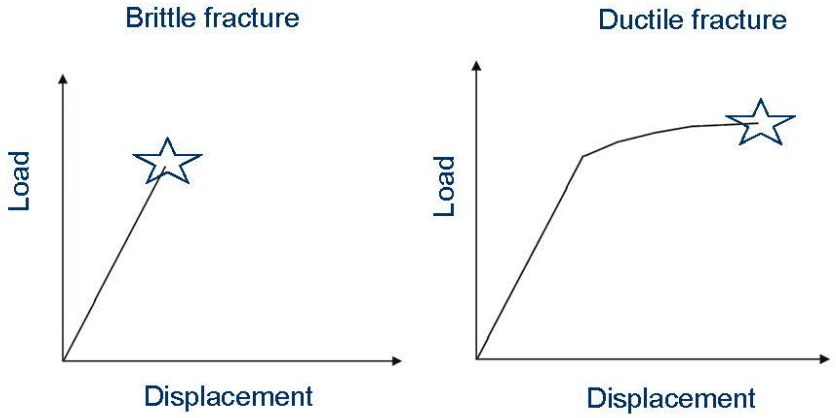

Types of fracture – materials perspective

Brittle fracture (cleavage fracture)

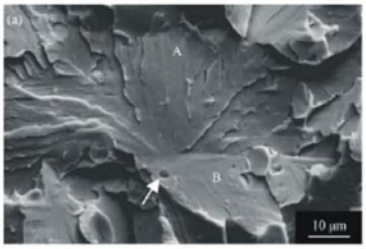

-Fracture propagates along given planes in the crystal
-Requires little energy for crack propagation

Ductile fracture

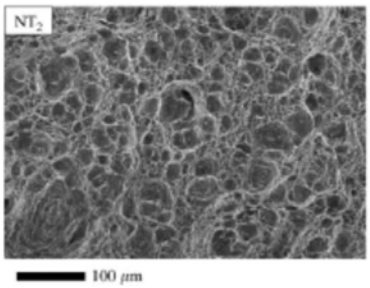

- Fracture propagates through formation and coalescence of voids in the material
- Requires more energy (and local deformation)

How to qunantify the loading of the crack

- Elastic conditions – Stress intensity factor, K

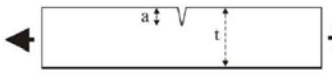

$$K = \sigma\sqrt{\pi a}\, f(a/t) \quad [\mathrm{MPam}^{1/2}]$$

- With significant plasticity – J-integral or CTOD (δ)

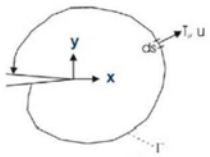

$$J = \int_{\Gamma} \left(w\,dy - T_i \frac{\partial u_i}{\partial x}\, ds\right)$$

$$J = m\sigma_y\delta$$

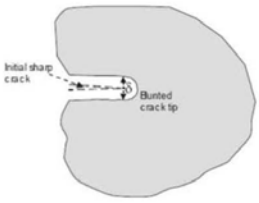

When will the material fracture?

- Brittle fracture:
  - Fracture occurs when a critical K, J or CTOD value is reached

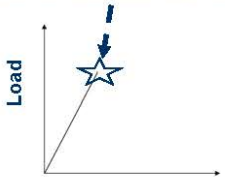

- Ductile fracture:
  - The fracture resistance is not represented with a single value, but with a curve (either using J or CTOD)

A transition in fracture mechanism may sometimes occur

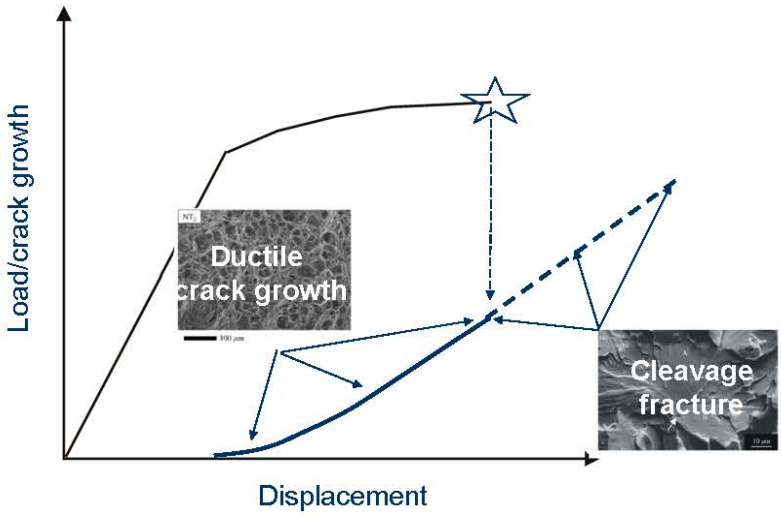

Crack arrest – *when cracks stop growing*

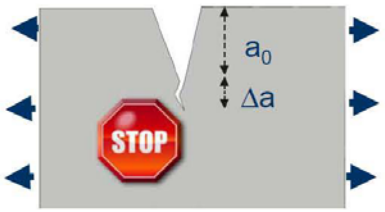

Materials barriers

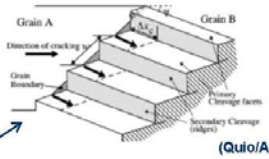

(Quio/Argon 2003)

Reduced loading with crack growth

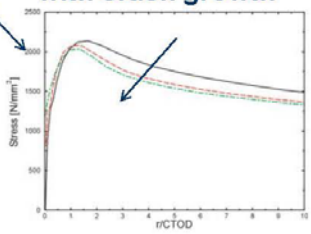

Emerging/new topics

Constraint effects in fracture

- Key points:
  - *Fracture toughness no longer a material parameter!!!*
  - There is an influence from the geometry and mode of loading applied

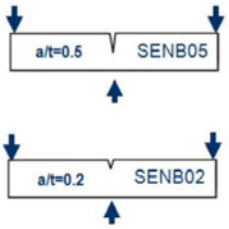

- Case:
  - The effect of specimen geometry in brittle fracture toughness of a HAZ microstructure

Classical fracture mechanics parameters – *Believed to fully describe the crack tip conditions….*

- Elastic conditions – Stress intensity factor, K

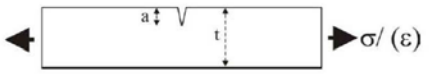

$$K = \sigma\sqrt{\pi a}\, f(a/t) \quad [\mathrm{MPam}^{1/2}]$$

- With significant plasticity – J-integral or CTOD (δ)

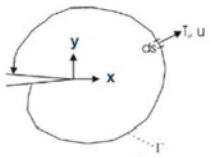

$$J = \int_{\Gamma} (w\,dy - T_i \frac{\partial u_i}{\partial x} ds)$$

$$J = m\sigma_y\delta$$

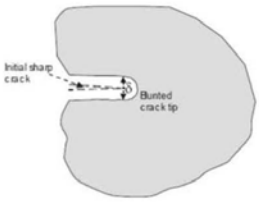

"… but there was more"

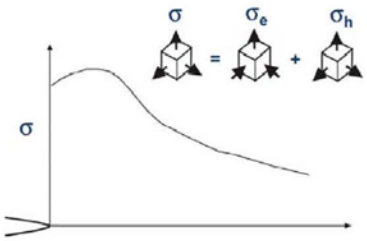

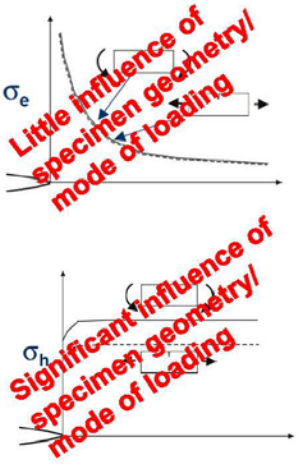

..and the so-called constraint effect was "born"

Example – effect of constraint on local crack-tip stress field/fracture toughness

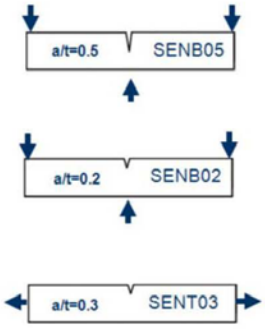

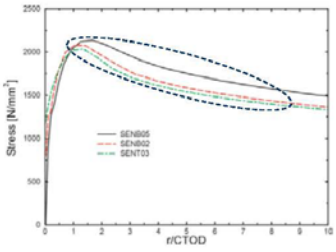

Specimen geometry affects the local stress level in front of the crack, i.e. the constraint level...

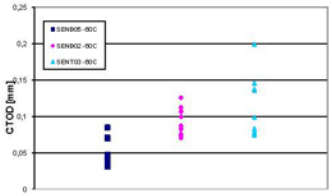

..which in turns affects the fracture toughness

Fracture under large imposed deformations

- Key points:
  - Most fracture mechanics approaches developed for situations with macroscopic elastic behaviour
  - Technological pull to allow for larger utilization of materials
  - Need fracture assessment schemes that applies under large global deformations
- Case:
  - Fracture under large deformations in pipelines/strain-based design

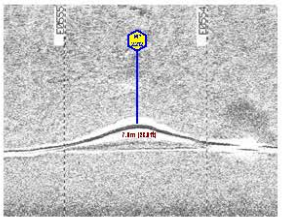

Large deformation scenarios for pipelines

Pipeline installation

Ice loading

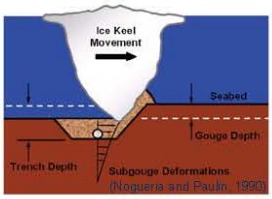

On-bottom snaking

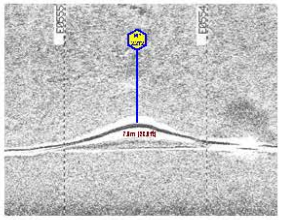

Earthquakes

Pipelines must in many cases be designed to withstand a given deformation or strain level – i.e. strain-based design principles should be used

Some effects to consider

Misalignment

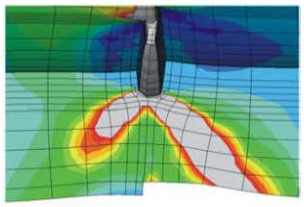

Mismatch

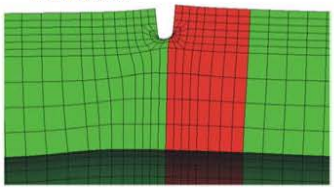

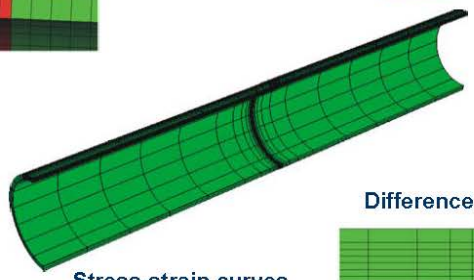

Defect size

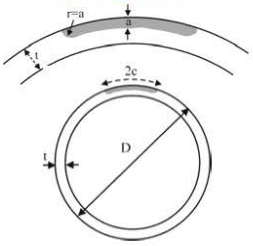

Difference in wall thickness

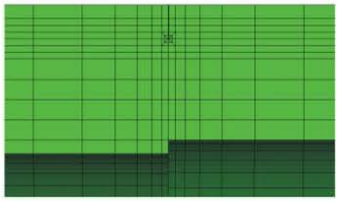

Stress-strain curves

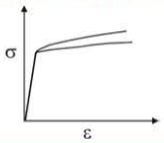

The effect of biaxial loading

Initial FE studies

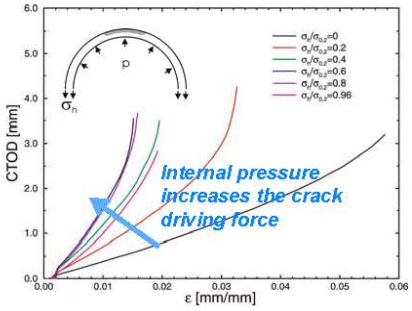

(Jayadevan et al. 2004, Østby et al. 2005)

Large-scale experimental validation

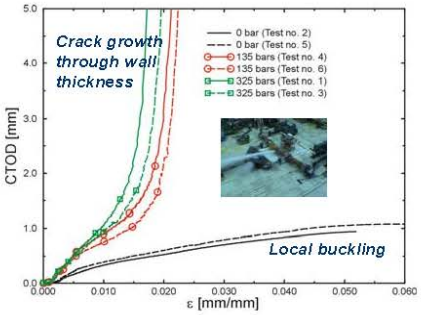

(Østby and Hellesvik 2007,2008)

Simplified strain-based fracture assessment model

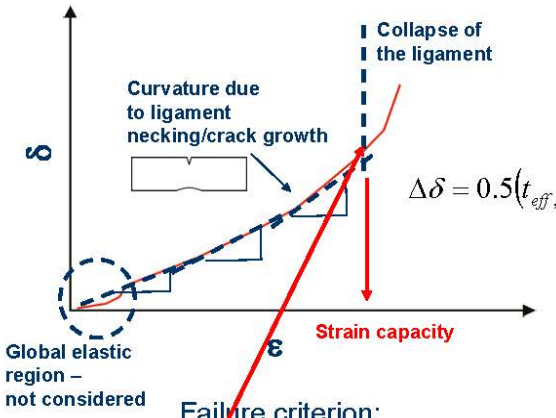

Calibrated by use of FE

$$\Delta\delta = 0.5\left(t_{eff,1} f_1 g_1 cor_1 + t_{eff,2} f_2 g_2 cor_2\right)\Delta\varepsilon$$

Crack depth, crack length, Y/T, biaxial loading, mismatch, misalignment

Failure criterion:

$$\delta_{\max,x} = 0.5(0.03L_{0,eff,x} + \delta_{\Delta a=1mm} - 0.61)\left(-12.1\left(\frac{\sigma_{02,BM}}{\sigma_{TS,BM}}\right)^2 + 18.9\left(\frac{\sigma_{0.2,BM}}{\sigma_{TS,BM}}\right) - 6.28\right)$$

Fracture toughness

(Østby 2007)

Numerical simulations

- Key points:
  - Analytical solutions often not accurate enough
  - Numerical (FE) fracture mechanics simulations becoming more usual *also in the industry*
  - Quicker implementation of new knowledge
  - Coupling with more advanced material models and micromehanical-based fracture criteria becomes easier
- Cases:
  - Small and large-scale modelling of ductile fracture in pipelines
  - The effect of local materials properties in ductile fracture
  - Geometry and materials constraint effects in brittle fracture
  - Including "microstructure"

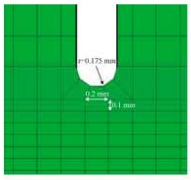

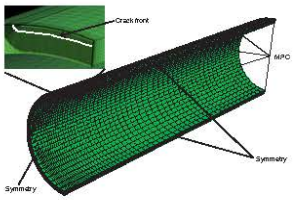

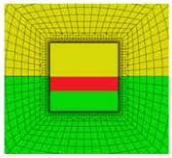

The Gurson-Tvergaard-Needleman model and criterion for void coalescence

Yield function:

$$\Phi(q,\bar{\sigma},f,\sigma_m)=\frac{q^2}{\bar{\sigma}^2}+2q_1 f\cosh\left(\frac{3q_2\sigma_m}{2\bar{\sigma}}\right)-1-(q_1 f)^2=0$$

Thomason's limit load criterion

$$\frac{\sigma_1}{\bar{\sigma}}<\left(\alpha\left(\frac{1}{r}-1\right)^2+\frac{\beta}{\sqrt{r}}\right)(1-\pi r^2)$$

Void growth

$$\mathrm{d}f_{growth}=(1-f)\mathrm{d}\varepsilon^{\mathrm{p}}:\mathbf{I}$$

$$r=\sqrt[3]{(3f/4\pi)e^{\varepsilon_1+\varepsilon_2+\varepsilon_3}}\Big/\sqrt{e^{\varepsilon_1+\varepsilon_3}/2}$$

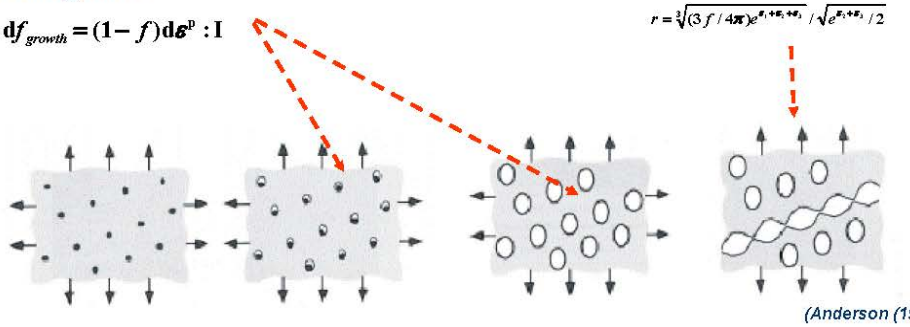

(Anderson (1995))

- An interesting approach for modelling of ductile crack growth

Crack growth modelling – SENT small-scale testing

Seamless X65 pipe

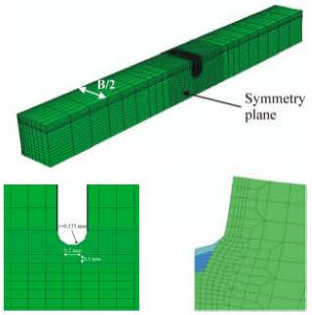

Comparisons between experiment and simulation

Load vs. CMOD

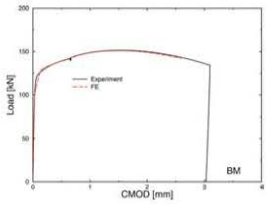

CTOD vs. Δa

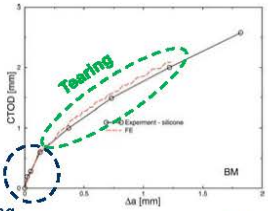

Blunting

(Østby et al. 2008)

Crack growth modelling - Large-scale testing

325 bar internal pressure

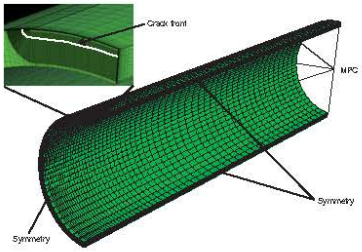

CTOD vs. global strain

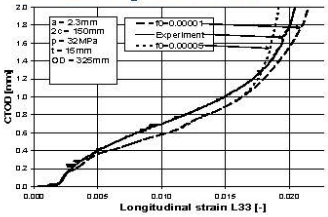

(Sandvik et al. 2008)

Ductile tearing resistance

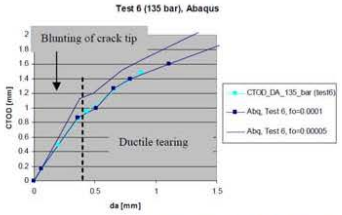

(Dybwad et al. 2009)

Invers modelling… to help understanding the influence of local features – Ex. HAZ X80 weld

FE configuration

Comparison with experiment

Defect at fusion line

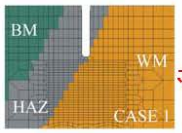

Defect shifted somewhat into HAZ
-The effect of defect position

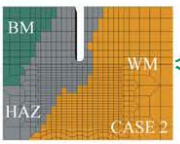

Defect shifted somewhat into HAZ with local increase in strength
-The effect of defect position
-The effect of crack-tip shielding

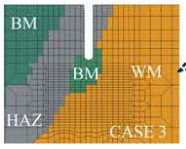

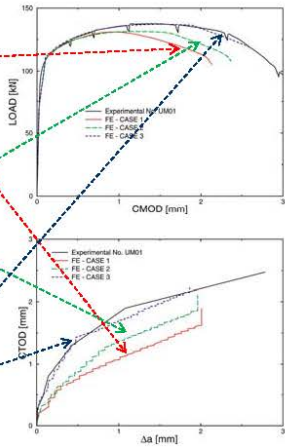

(Østby et al. 2009)

Micromechanical models for brittle fracture – The Weibull stress approach

Failure probability, P_f:

$$P_f = 1 - \exp\left(-\left(\frac{\sigma_w}{\sigma_u}\right)^m\right)$$

The Weibull stress:

$$\sigma_w = \sqrt[m]{\frac{1}{V_0}\int (\sigma_1)^m dV}$$

Scaling volume

Principal stress

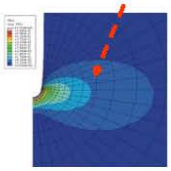

Toughness scaling principle

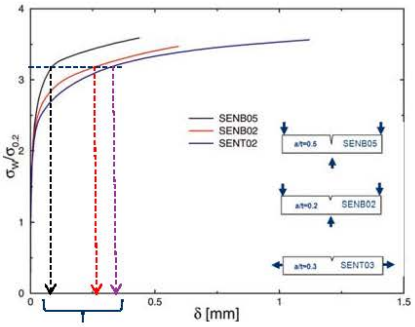

Equivalent CTOD values in different specimen geometries

Constraint effect – Ex. HAZ microstructure

ICCGHAZ 420 Mpa steel

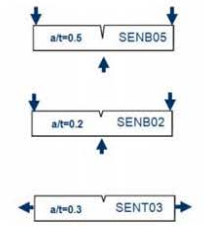

Experimental CTOD values

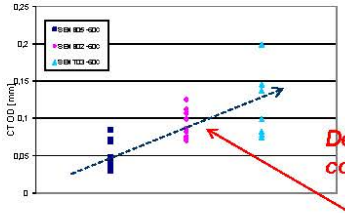

Description of constraint effect

FE modeling

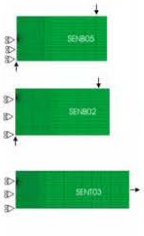

Local crack tip fields

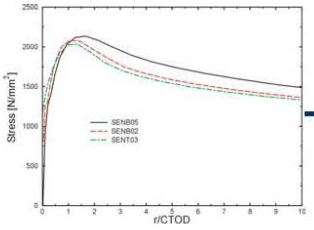

Calibration using Weibull stress

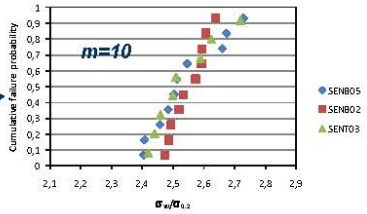

(Østby et al. 2011b)

FE modeling of inhomogeneous material systems - HAZ

Real HAZ

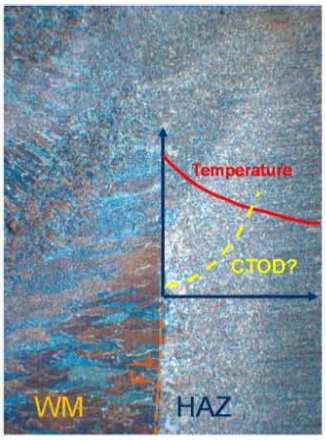

Idealized FE representation

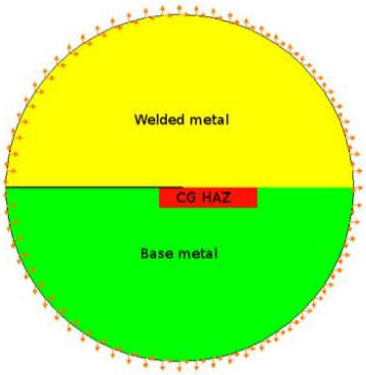

Transferability from weld thermal simulation to real HAZ toughness using the Weibull stress model

"Homogeneous" HAZ

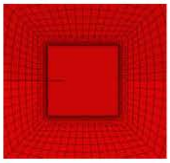

"HAZ" in weld

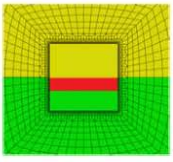

"How to get from to "

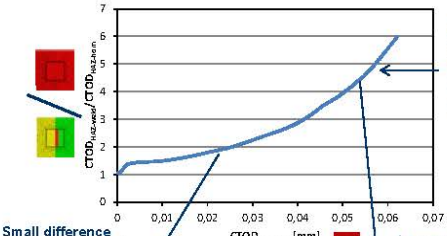

Derived from Weibull stress analysis/toughness scaling principle

Small difference between simulated and real HAZ

Larger difference between simulated and real HAZ

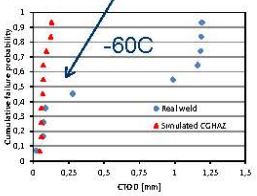

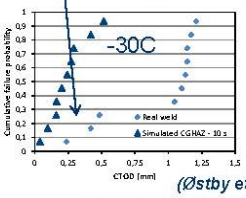

(Østby et al. 2012)

Including "microstructure"…

Grains

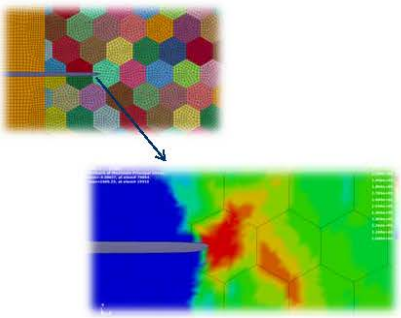

Crystal plasticity – accounting for grain orientation

(Kane et al. 2011)

Particles/inclusions

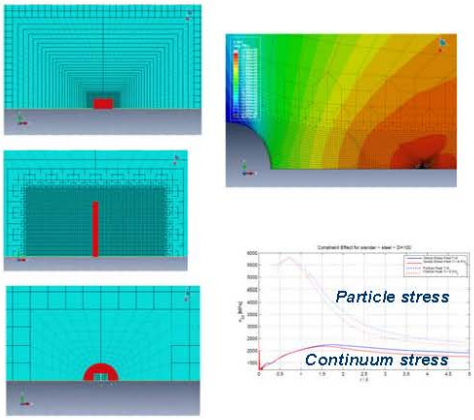

Testing techniques

- Key points:
  - More knowledge about properties at lower levels ("Karakterisering på alle længdeskalaer")
  - Helpful for improved understanding of fracture
  - Modelling requires more input regarding material properties

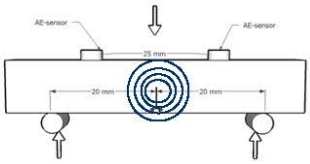

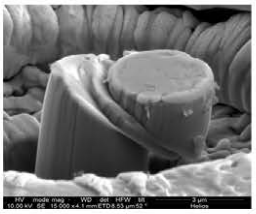

- Cases:
  - Acoustic emission and local crack arrest
  - FIB/Nano indentation
  - FIB/TEM

Interpretation of acoustic emission signals

- AE signal:

$$A = 20\log\left(\frac{V}{V_{ref}}\right) - A_{pre\_amp}\ [\mathrm{dB}]$$

  - A – amplitude in dB
  - V – voltage signal transducer
  - V_{ref} – reference voltage (1µV)
  - A_{pre_amp} – pre-amplification used (in this case -20dB)

101 dB signal

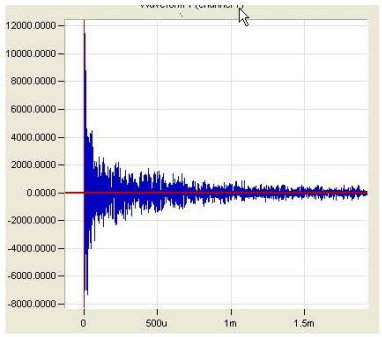

t

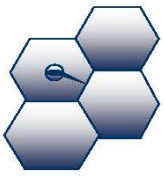

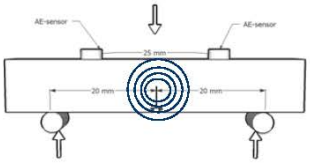

Correlation between AE signals and arrested microcracks

Experimentally observed microcrack

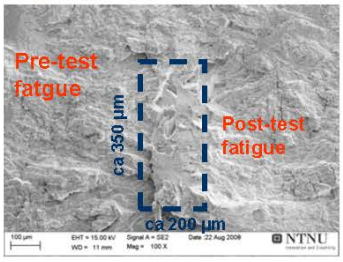

FE modelling of microcrack extension

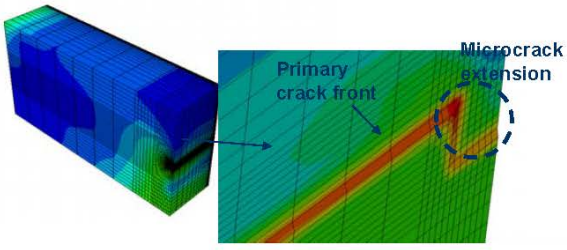

Load drop due to introduction of microcrack

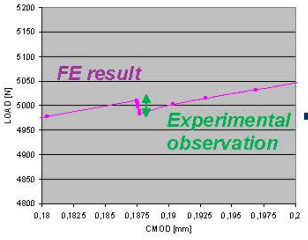

Assistance in validation of correlation between AE signal amplitude and microcrack size

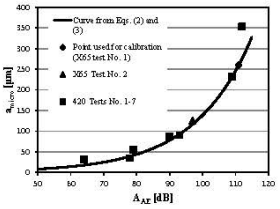

(Østby et al. 2012)

FIB/nano indentation/TEM

FIB/nanoindentation

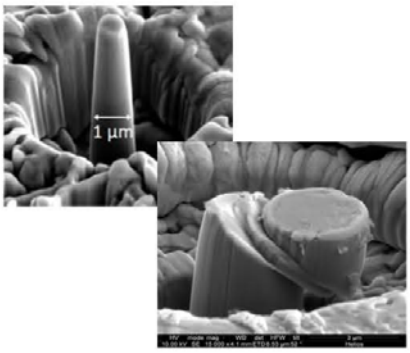

FIB/TEM

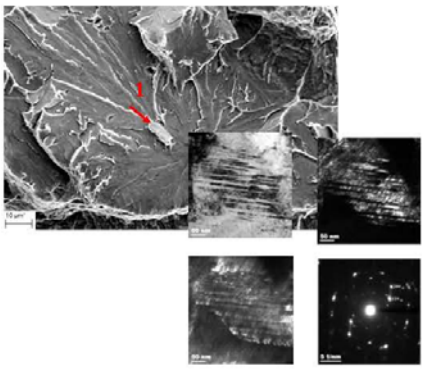

Plastic properties at small-scales

(Haugen et al. 2012)

Investigation of nature of fracture initiating particles

(Mohseni et al. 2012)

Probabilistic fracture mechanics

- Key points:
  - Natural scatter and variability in parameters entering the problem
  - Deterministic analysis in some cases of limited value
  - Uncertainty around accuracy of models
  - Probabilistic approaches open for linking to given failure probabilities/safety levels

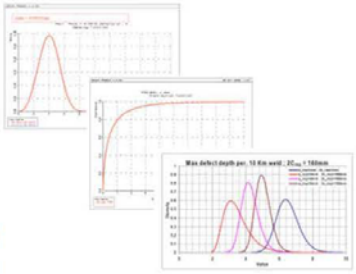

- Case:
  - Calibration of safety factors in fracture assessment of pipelines

Simplified fracture assessment model

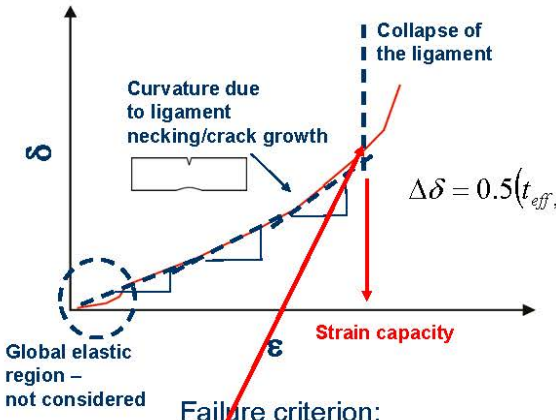

Calibrated by use of FE

$$\Delta\delta = 0.5\left(t_{eff,1} f_1 g_1 cor_1 + t_{eff,2} f_2 g_2 cor_2\right)\Delta\varepsilon$$

Crack depth, crack length, Y/T, biaxial loading, mismatch, misalignment

Failure criterion:

$$\delta_{\max,x} = 0.5(0.03L_{0,eff,x} + \delta_{\Delta a=1mm} - 0.61)(-12.1\left(\frac{\sigma_{02,BM}}{\sigma_{TS,BM}}\right)^2 + 18.9\left(\frac{\sigma_{0.2,BM}}{\sigma_{TS,BM}}\right) - 6.28)$$

Fracture toughness

(Østby 2007)

Calibration of partial safety factors

- Scatter in input parameters
- Model uncertainty
- Variability in applied strains (basis from Hotpipe project)
- Statistical distributions of defects (valuable input from Hydro)

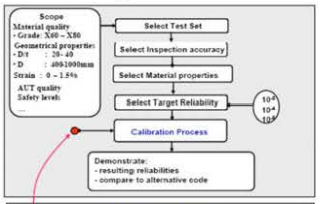

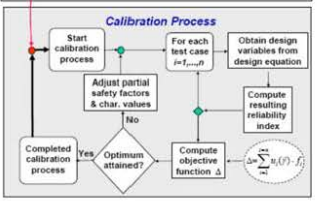

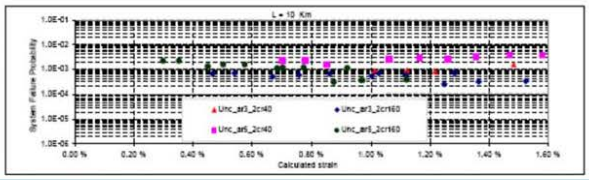

(G. Sigurdsson, DNV)

Proposed design format

$$\varepsilon_{max} \le \min\left\{ \frac{0.015}{\gamma_L}, \frac{\varepsilon^c_{cap}\left(t_c; \sigma_h; a_c \cdot \gamma_a; 2c_c; \alpha_c / \gamma_j; (a_{rep} \text{ or } Std(a_m))\right)}{\gamma_L} \right\}$$

- ε_{max} – best estimate applied strain
- ε_{cap} – deformation capacity (calculated based on simplified model)

- γ_L – safety factor applied strain
- γ_a – safety factor defect depth
- γ_j – safety factor fracture toughness

- Safety factors depend on the safety class
- Different safety factors for installation (system effect) and operation
- Safety factor for applied strain under operation depends upon "CoV" of best estimate

Tomorrow….?

Multiscale modelling – *The way of tomorrow?*

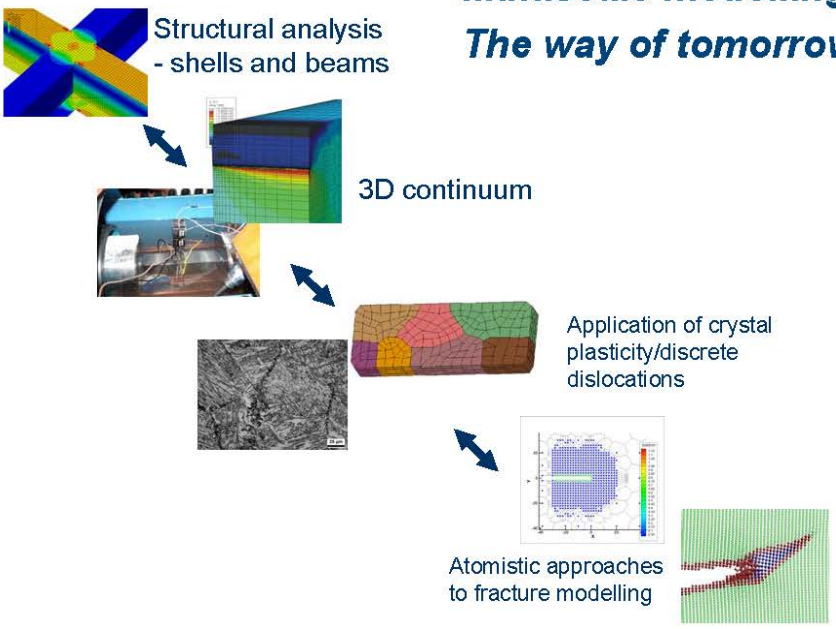

Wrap-up…

- Fracture mechanics has been developed into a useful tool:
  - Materials developments
  - Design/structural integrity assessments
- New issues are being introduced and new application areas emerge
- The use of numerical simulation tools is becoming increasingly more important
- Important future development trends:
  - Further development of link to materials science
  - Development of multiscale schemes
- ***Vision…***
  - ***…predictions rather than calibration/"description"***

Acknowledgments

- The financial support from the Norwegian Research Council and the industry to the Fracture Control Offshore Pipelines and Arctic Materials projects is greatly acknowledged
- The contributions from colleagues at SINTEF, NTNU, and DNV is also highly acknowledged

Off-line testing af friktion og smøring i pladeformgivning

Niels Bay, DTU Mekanik

Off-line testning af friktion og smøring i pladeformgivning

Niels Bay, Ermanno Ceron

DTU-Mekanik

Projektpartnere:

Grundfos, SSAB, Outokumpu Stainless, Uddeholm

Dansk Metallurgisk Selskabs Vintermøde

Kolding

Januar 2013

Indhold

- Introduktion
- Faldgruber ved off-line testning
- Off-line plade-tribo-testning
- Eksempel på analyse af konkret produktion
- Off-line test resultater
- Produktionstest resultater, sammenligning med off-line test
- Konklusion

Introduction

Legislation

Since 2000 legislation in Europe and Japan has been increasingly restrictive as regards industrial application of hazardous lubricants

2006-2007 EU introduced new legislations, REACH, aiming at high level of protection of human health and the environment from risk posed by chemicals.

REACH makes industry responsible for assessing and managing the risks and providing appropriate safety information to their users.

The new legislations have forced metal forming industry to look for new environmentally benign tribo-systems.

This causes however great challenges.

Lubrication in tribologically difficult sheet metal forming

Tribologically difficult materials:

High strength steel, stainless steel, aluminium, titanium

Tribologically difficult processes:

Deep drawing with low radius of curvature

Ironing

Fine blanking

Chlorinated additives

Chloroparaffins suspected to have harmful effects on human health

- Risk of dioxin formation
- High recycle costs

Tribological problems in sheet metal forming

- High normal pressures
- Elevated tool/work piece interface temperatures

i.e. severe stressing of the lubricant with possible breakdown as a consequence.

Breakdown may cause:
- Local pick-up on tool surface
- Scoring of subsequently formed work piece surface

The sequence of events normally referred to as galling

Challenges

- Introduction of new lubricants in manufacturing production is costly (production breaks, cleaning of tools)
- Industry is reluctant to carry out production tests due to bad experience (premature galling leading to unexpected production stops)
- Off-line testing of new tribo-systems
- It is vital to ensure testing conditions emulate production conditions
- Otherwise a tribo-system, which is approved in the simulative test, may turn out to be malfunctioning in the production tool, thus leading to the problems described above.

Environmentally friendly sheet forming lubricants (except dry film)

Only a few lubricant manufacturers have focused on development of new, environmentally friendly lubricants

- **Masa Oil, Finland:** Biodegradable oils derived from tall oil extracted from fir tree. Fatty acid ester based.
- **Rhenus Lub, Germany:** Refined mineral oils with special additives of natural fatty components, synthetic esters, sulphur additives.
- **IRMCO Fluids, USA:** Oil free, low viscosity, water soluble lubricants made from vegetables and fruit.

Simulative sheet tribo-tests

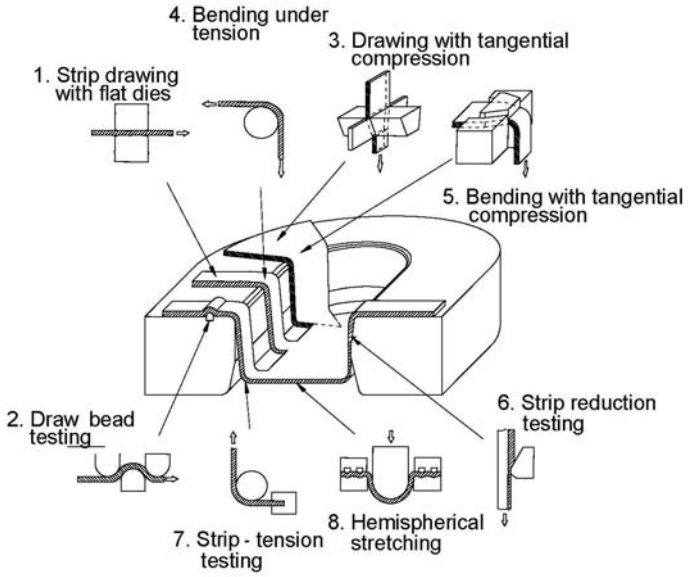

Indhold

- Introduktion
- **Faldgruber ved off-line testning**
- Off-line plade-tribo-testning
- Eksempel på analyse af konkret produktion
- Off-line test resultater
- Produktionstest resultater, sammenligning med off-line test
- Konklusion

Selected off-line tests
Sheet forming tribology

Bending-Under-Tension

Draw Bead Test

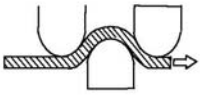

Strip Reduction Test

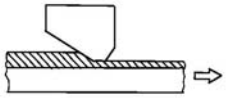

PUnching Test

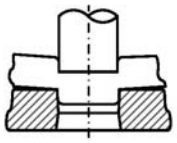

Test	Normal pressure	Surface expans.	Temp.	Tribological severety
BUT	low	0	low	low
DBT	medium	0	medium	medium
SRT	high	medium	high	high
PUT	medium-high	infinite	very high	very high

Bending under tension - BUT

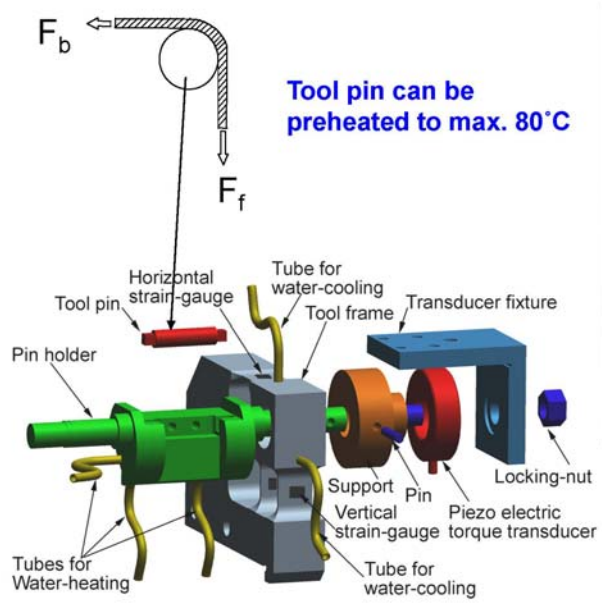

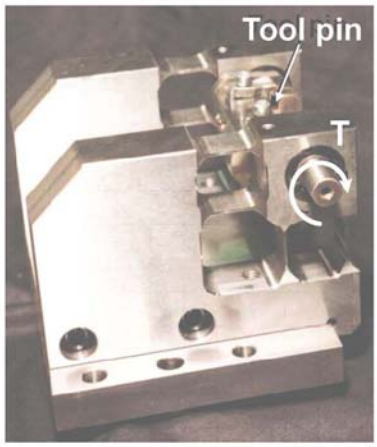

D.D. Olsson, K. Chodnikiewicz, J.L. Andreasen, N. Bay

Bending Under Tension - BUT

Stainless steel Wn.1.4401, Plain mineral oil without additives, v=80mm/s

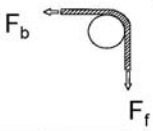

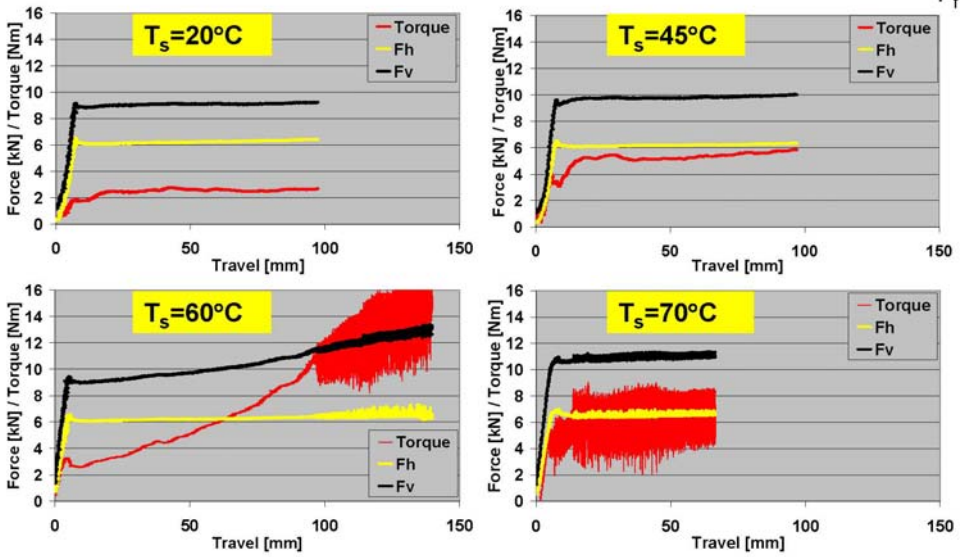

J.L. Andreasen, D.D. Olsson, K. Chodnikiewicz, N. Bay

Faldgruber ved off-line testning -1

- For lav værktøjstemperatur
- For lav emnetemperatur (flertrinsoperationer)
- Ændrede procesparametre
  - Normaltryk
  - Glidelængde
  - Glidehastighed
  - Overfladeekspansion
  - Tid mellem tests
  - Kontakt/ikke kontakt mellem slag
- Ændrede smørebetingelser
  - Påføringsteknik
  - Emne- og værktøjsgeometri
- For få gentagelser

Faldgruber ved off-line testning - 2

- Ændrede egenskaber af emnemateriale
  - Flertrins operationer, f.eks. dybtrækning + krængetrækning/re-trækning
  - Dybtrækning + strækningsreduktion
- Ændret overfladetopografi
  - Emne (f.eks. ved flertrinsoperationer)
  - Værktøj (retning af hypper ved drejning, slibning, polering)

Production tool

Simulative tool (BUT)

Indhold

- Introduktion
- Faldgruber ved off-line testning
- **Off-line plade-tribo-testning**
- Eksempel på analyse af konkret produktion
- Off-line test resultater
- Produktionstest resultater, sammenligning med off-line test
- Konklusion

New, universal sheet tribotester

BUT

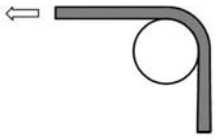

DBT

SRT

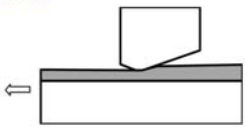

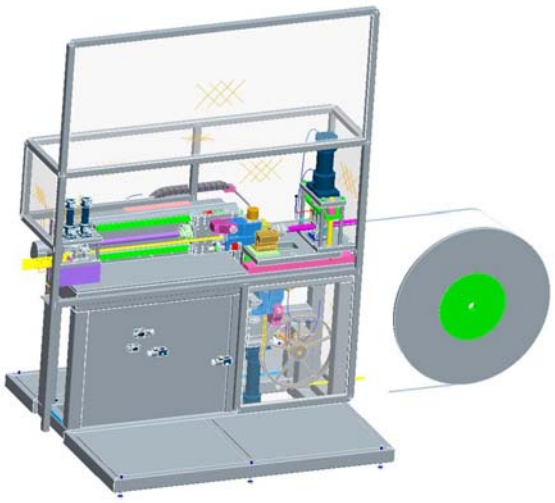

Universal sheet tribo-tester

- Automatic PLC controlled running of repeated tests
- Material feed from coil of more than 1000m
- Adjustable sliding lengths, speed, cycle time and total number of strokes
- Ensuring appropriate emulation of production conditions with heating and cooling cycle
- Easy programming by Labview

BUT_test_running_detail.avi

BUT_test_running.avi

E. Ceron, N. Paldan,
J. Gregersen, N. Bay

17

Methodology for predicting lubrication performance in production

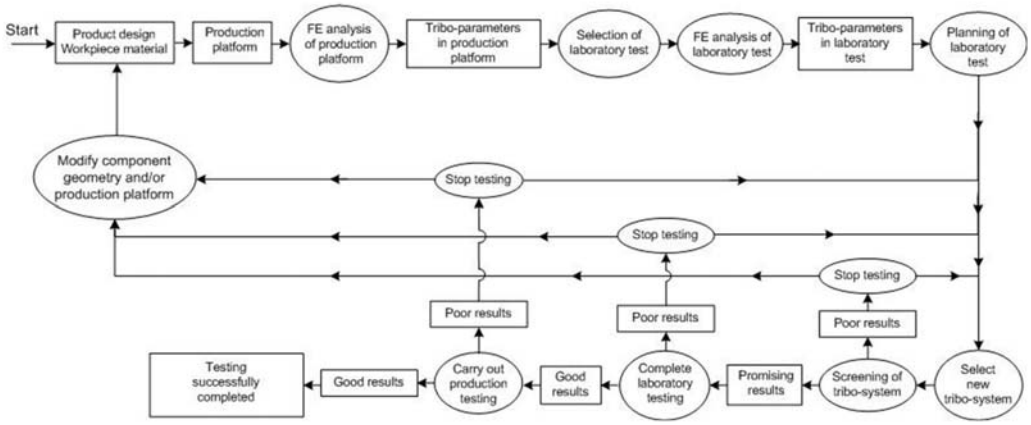

E. Ceron, N. Bay

18

Indhold

- Introduktion
- Faldgruber ved off-line testning
- Off-line plade-tribo-tester
- **Eksempel på analyse af konkret produktion**
- Off-line test resultater
- Produktionstest resultater, sammenligning med off-line test
- Konklusion

Production test example

Deep drawing in progressive tool - Grundfos

a. Deep drawing
b. 1st redrawing
c. 2nd redrawing Tribologically the most severe operation
d. Sharp pressing of flange

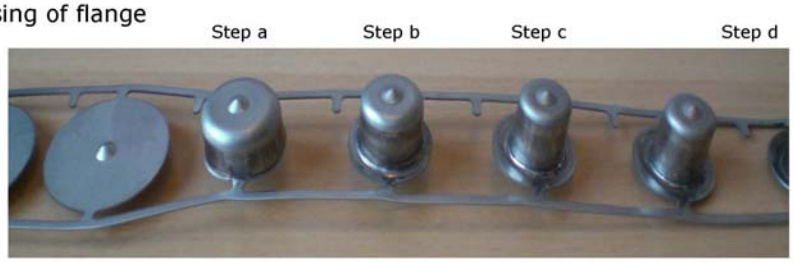

Workpiece material: EN 1.4301

Production rate: 40 spm

Step c

Deep drawing in progressive tool Grundfos

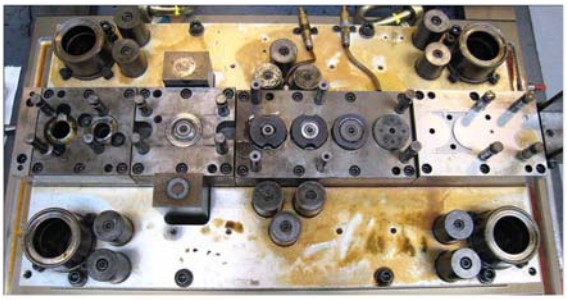

E. Ceron, E. Madsen, N. Bay

Simulation of deep drawing and 2 redrawings

- LS-DYNA 2D implicit model
- The blank is transferred from one process to the following updating flow stress and equivalent strain

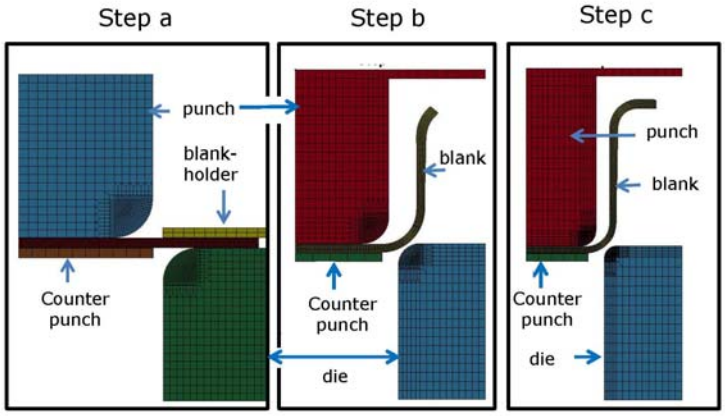

22

E. Ceron, N. Bay

Distribution of radial stress in step c

Maximum contact pressure p_{max} = 900 MPa

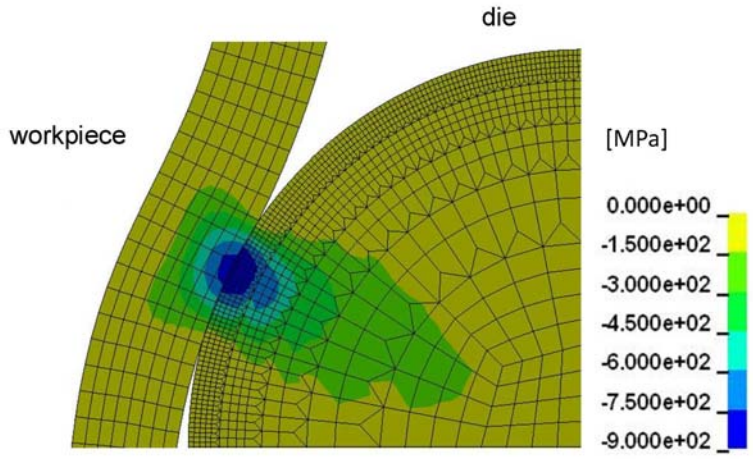

Simulation of BUT test

Round pin with radius R = 3,5

Maximum contact pressure 360 Mpa
with maximum back tension 300 MPa

(i.e. only 40% of maximum pressure in production tool)

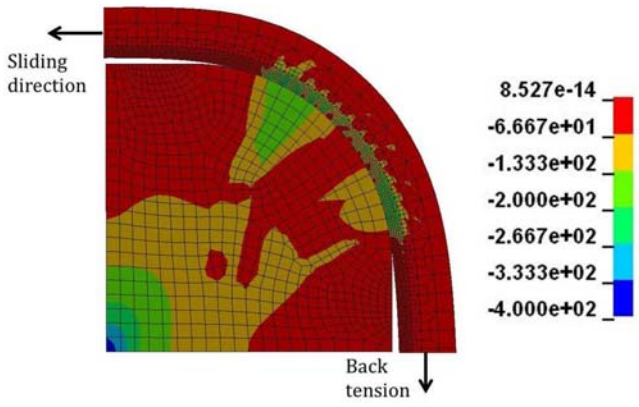

Distribution of radial stresses in BUT test

By modifying the BUT test tool to a 45° contact instead, sufficient contact pressure can be reached

Maximum contact pressure p_{max} = 1000 MPa with back tension 300 MPa

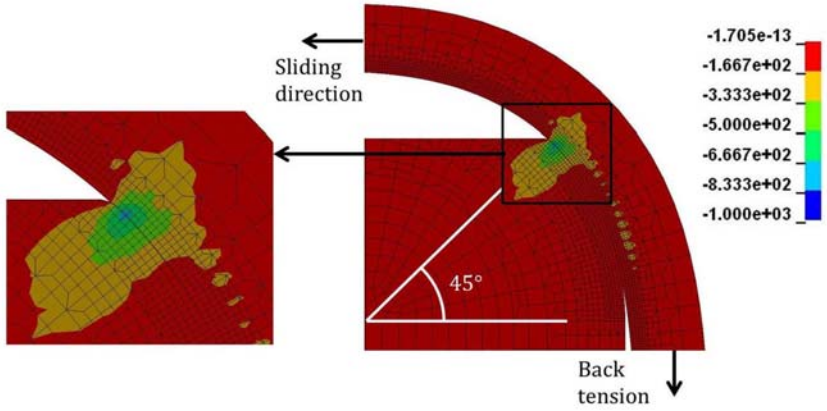

Lubricant film breakdown in BUT test

Severe pick and galling

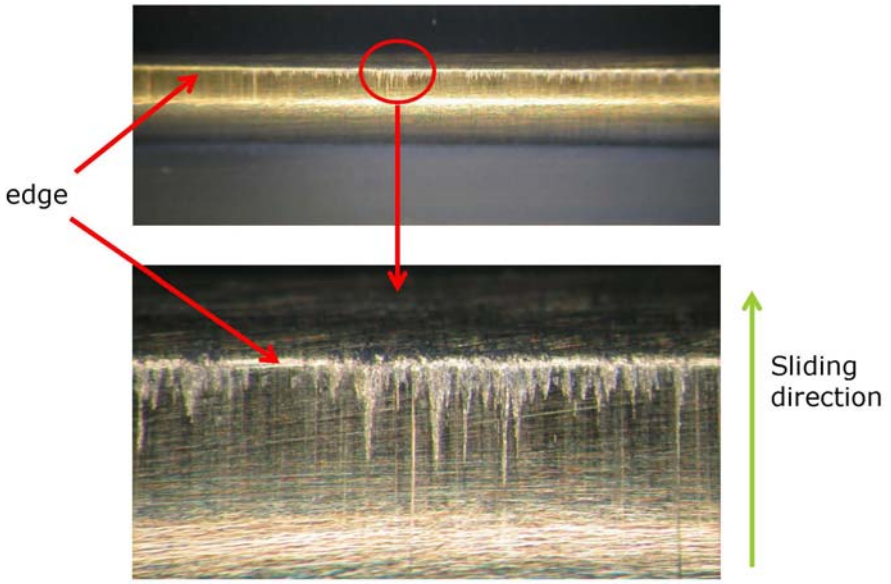

Tribo-systems investigated

Tribo-system	Workpiece material	Tool material	Lubricant
1	EN 1.4301	Vancron 40	rhenus SU 166 A
2	DP 800	Vancron 40	ANTICORIT PLS 100T
3	EN 1.4162 LDX 2101®	Vancron 40	rhenus SU 166 A

rhenus SU 166 A: mineral oil with EP additives, 160 mm^2/s at 40°C

ANTICORIT PLKS 100T: mineral oil, 100 mm^2/s at 40°C

Indhold

- Introduktion
- Faldgruber ved off-line testning
- Off-line plade-tribo-tester
- Eksempel på analyse af konkret produktion
- **Off-line test resultater**
- Produktionstest resultater, sammenligning med off-line test
- Konklusion

BUT test

Tribo-system 1:

Material: EN 1.4301

Lubricant: rhenus SU 166 A

Test rate: 40 and 95 spm

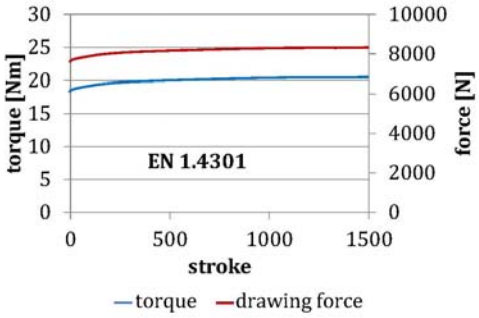

Tool after 1500 tests

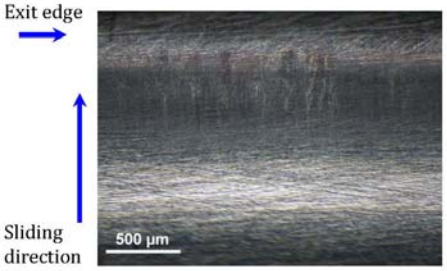

BUT test

Tribo-system 2:

Material: DP 800

Lubricant: ANTICORIT PLS 100T

Test rate: 40 and 95 spm

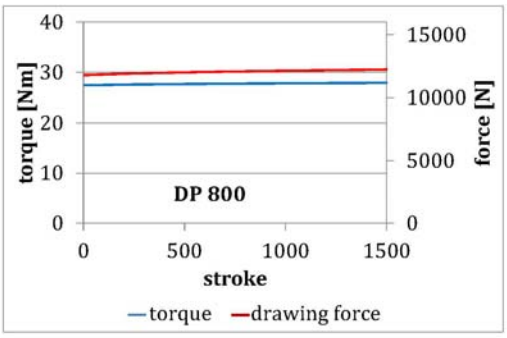

Tool after 1500 tests

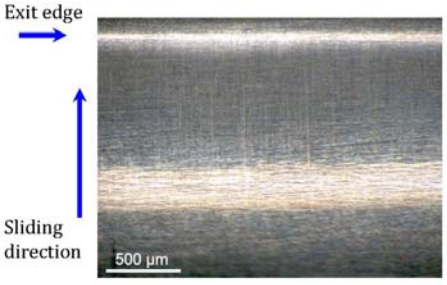

BUT test

Tribo-system 3

Material: EN 1.4162, LDX 2101®

Lubricant: rhenus SU 166 A

Test rate: 40 spm

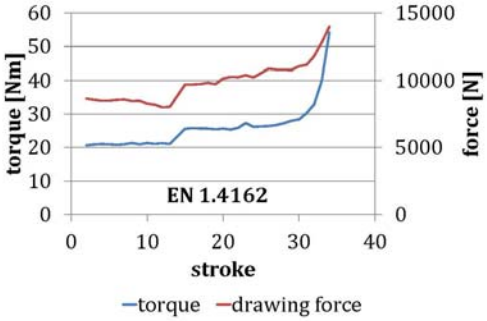

Tool after 32 tests

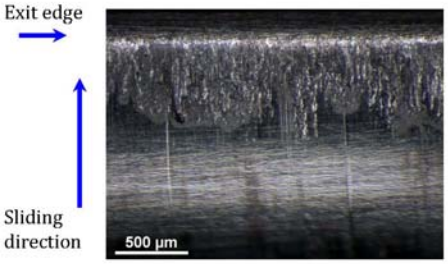

Indhold

- Introduktion
- Faldgruber ved off-line testning
- Off-line plade-tribo-tester
- Eksempel på analyse af konkret produktion
- Off-line test resultater
- **Produktionstest resultater, sammenligning med off-line test**
- Konklusion

Production tests

Tribo-system 1

Cup No. 1500

Tribo-system 2

Cup No. 1500

Tribo-system 3

Cup No. 40

Tribo system 1 and 2: no galling even at 95 spm

Tribo system 3: heavy galling after drawing 10 cups

SEM pictures of tools - EN 1.4301

- Few scratches on the surface
- Slight amount of pick up can be seen like on BUT tool
- (part in EL RØR has less chromium oxide due to previous redrawing, may cause fewer scratches on tool surface?)

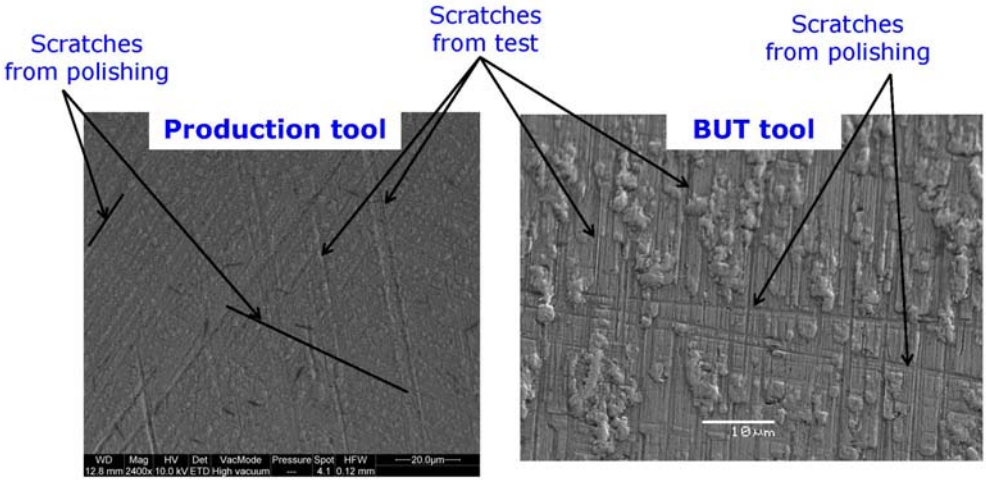

Tool temperature development – EN 1.4301

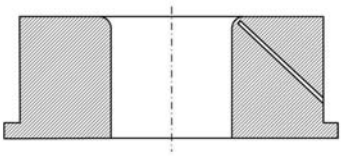

Temperature increases fast
in the first 50 strokes

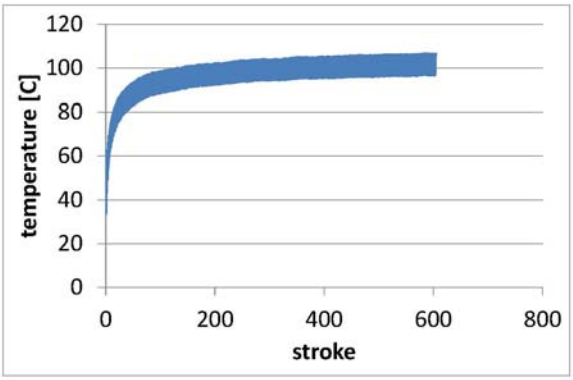

SEM pictures of tools – DP 800

- SEM picture of the tool surface
- Similar micro pick-up in production tool as in the BUT tool

Production tool

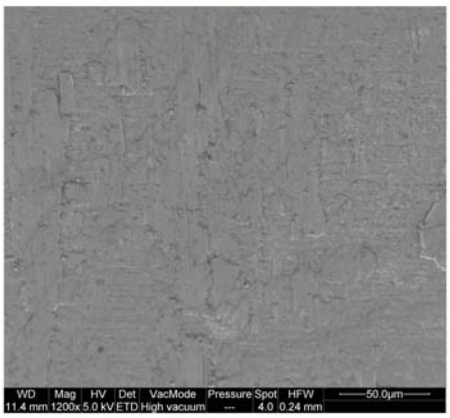

BUT tool

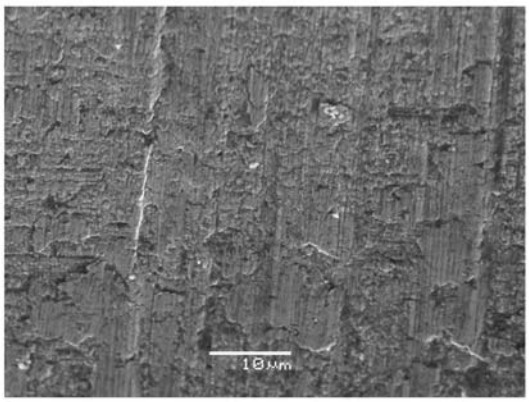

Production tool 2 – LDX 2101

- Parts are not acceptable. Severe galling along rolling direction
- Pick-up occurs already in operation 2.

Production tool 3 – LDX 2101

- Pick-up occurs also in operation 3

Tool temperature development

Comparison between LDX and EN 1.4301

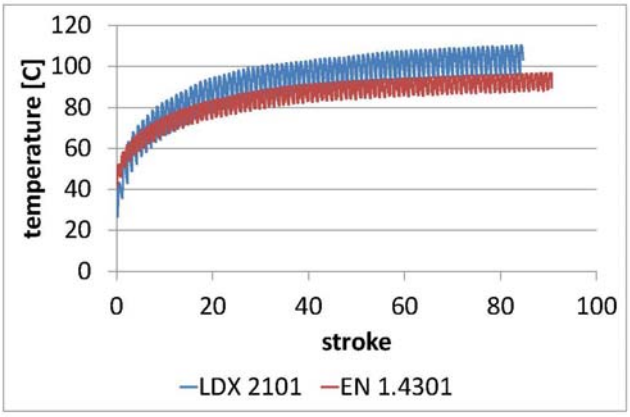

Evaluation of a tribo-system for deep drawing production

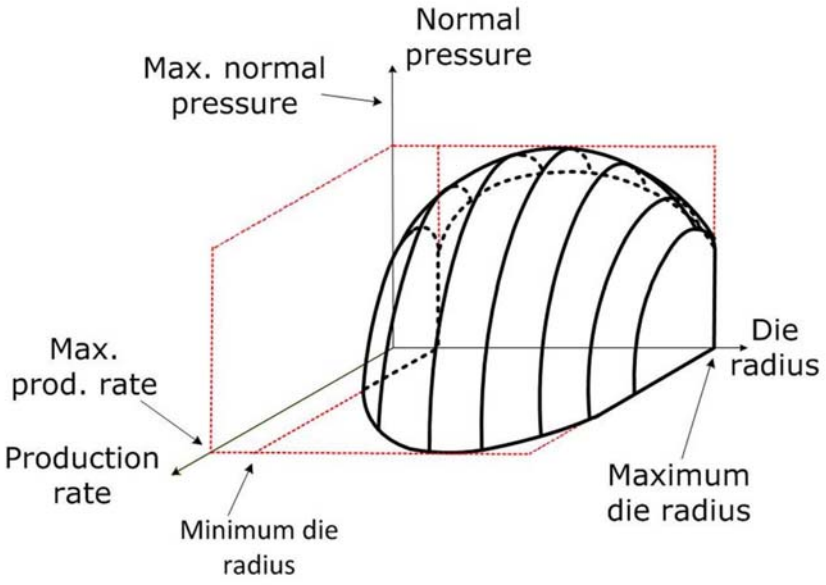

Evaluation of a tribo-system for deep drawing production

Poor tribo-system
production point above threshold surface

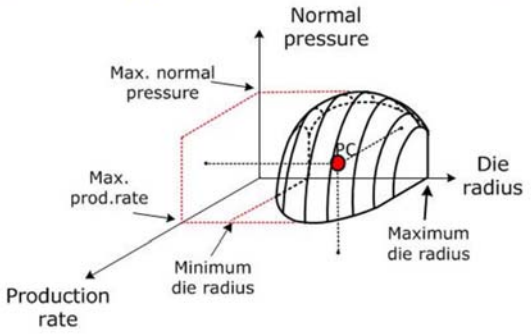

Promising tribo-system
Production point below threshold surface

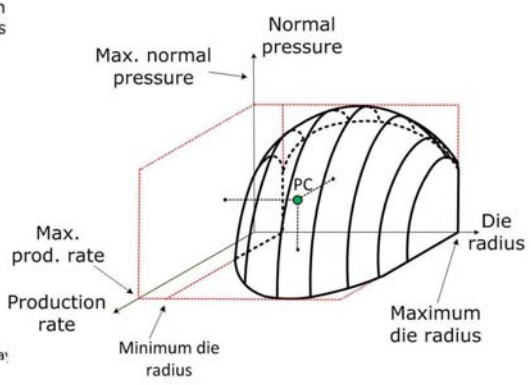

41 E. Ceron, N. Bay Niels Bay

Conclusion – differences between production and laboratory

	Production	Laboratory
Work hardening	High (max strain = 2)	Low (max strain = 0,2)
Surface topography	Completely different from original	Original
Normal pressure	≈1000 MPa	≈1000 MPa but smaller contact area
Initial specimen temperature	≈110C	25C
Temperature developed in the specimen	≈200C	≈90-100C
Temperature developed in the tool	≈110C (EN1.4301)	≈45C (EN1.4301)
Sliding speed	100-150mm/s	50mm/s
Thermal exchange	No workpiece/tool contact during idle time	workpiece/tool contact during idle time

42 E. Ceron, N. Bay

Indhold

- Introduktion
- Faldgruber ved off-line testning
- Off-line plade-tribo-tester
- Eksempel på analyse af konkret produktion
- Off-line test resultater
- Produktionstest resultater, sammenligning med off-line test
- **Konklusion**

Konklusion

Metodik til forudsigelse af smøremiddel performance i produktion

- Numerisk modellering af produktionsbetingelser
- Valg af simulativ test
- Numerisk modellering af simulativ test
- Off-line testning
- Produktions testning

Miljøvenlige alternativer til kloreret paraffinolie

- rhenus SU 166 A

END

Industriens udnyttelse af de store internationale røntgen neutronfaciliteter

Henning Friis Poulsen, DTU Fysik

Industriens udnyttelse af de store internationale Røntgen og neutron faciliteter

Hening Friis Poulsen, DTU Fysik
hfpo@fysik.dtu.dk

ESS & MAX-IV

- ESS og MAX IV i Lund
  - ESS (2019), verdens bedste neutronkilde, finansieret af 17 europæiske lande (ca. 1,5 mia. euro)
  - MAX IV (2015), synkrotron, svensk finansieret (500 mio. euro)
- Det danske bidrag
  - ESS: 1.4 Mia kroner + 12.5% drift
  - Data Management Center i Kbh (62 ansatte)
  - MAX-IV: Dansk beamlinie (74 Mkr) ?
- Science parks omkring Lund og Københavnsområdet

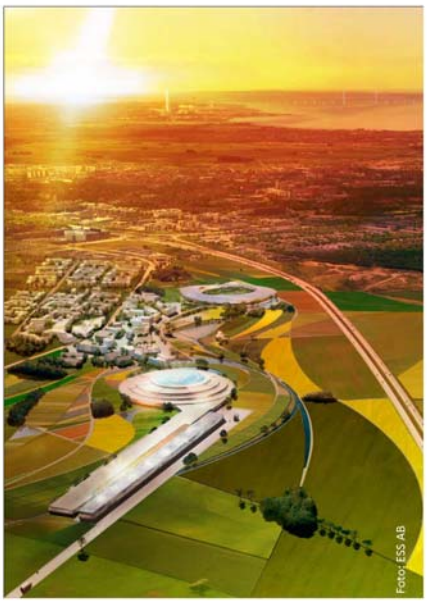

Verdens største mikroskop

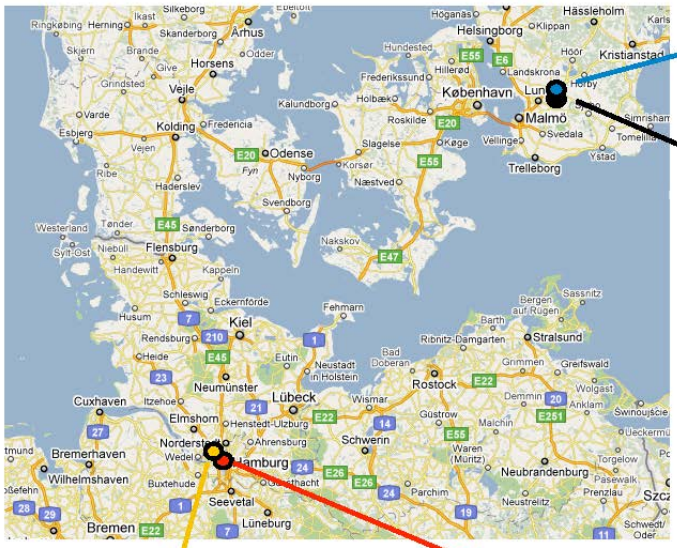

ESS, 2019
Neutroner
Dk medværk: 1.4 Gkr

Max-IV 2016
Medium energi Røntgen
Dk beamlinie: 74 Mkr ?

E-XFEL, 2016
Kohærent Røntgen
DK medlemskab: 11 Mkr/år

PETRA-III, 2011
Høj energi Røntgen
Dk bruger

Hvad er en synktroton?

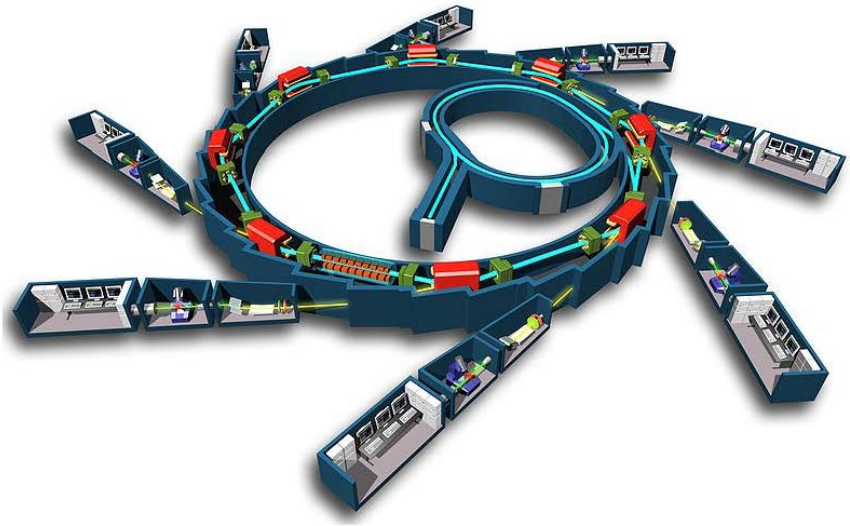

Hvorfor bruge en synktroton?

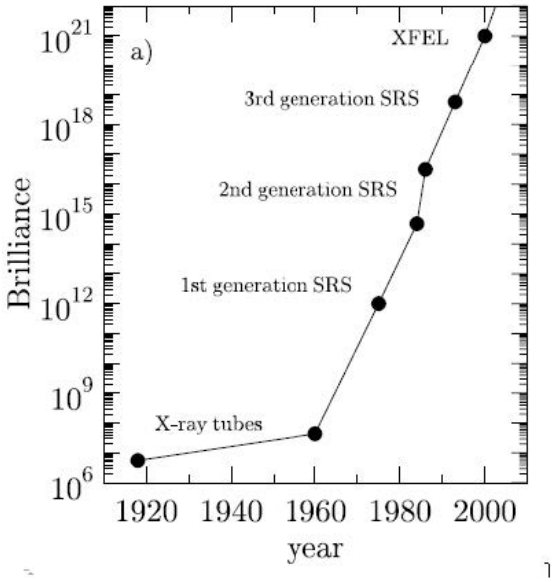

Forskel i tværsnit

Neutroner

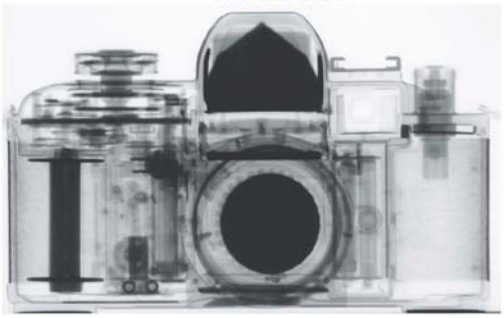

Ser: H, C, O, ….

Røntgen

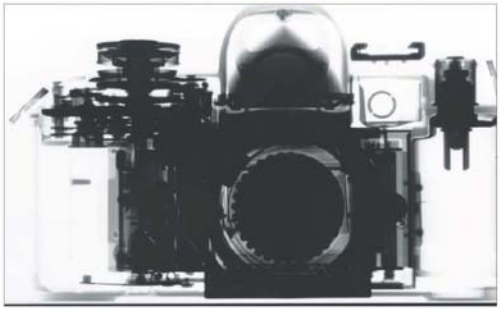

Ser: høje Z-numre

Virksomheder som brugere af store faciliteter

Udfordringer:

- Manglende kendskab og ekspertise
- Ventetid og usikkerhed omkring måletid
- "Data analysen koster en halv PhD"

Haldor Topsøe, Astra Zeneca, Novo Nordisk, Carlsberg .. er stærkt involveret

Mulige danske løsninger:

- Strategiske partnerskaber
- Portaler/science hubs

Individuelle løsninger:

- Opsøg akademiske partnere
- Ansæt erhvervs-PhD studerende
- Science Link

SCIENCE LINK

Part-financed by the European Union (European Regional Development Fund)

SCIENCE LINK opens up research facilities for commercial R&D purposes

Partners:

MAX-lab, Lund
Desy, Hamburg
HZG & HZB, Berlin

DTU is Danish representative

Offers:

- Access to beamtime for industry
- Consultant for preparing, and executing beamtime
- Help with analyzing data

Contact: Martin Meedom Nielsen
DTU Physics
Phone: 51801561
mmee@fysik.dtu.dk

SCIENCE LINK

Forslag fra MAX IV:

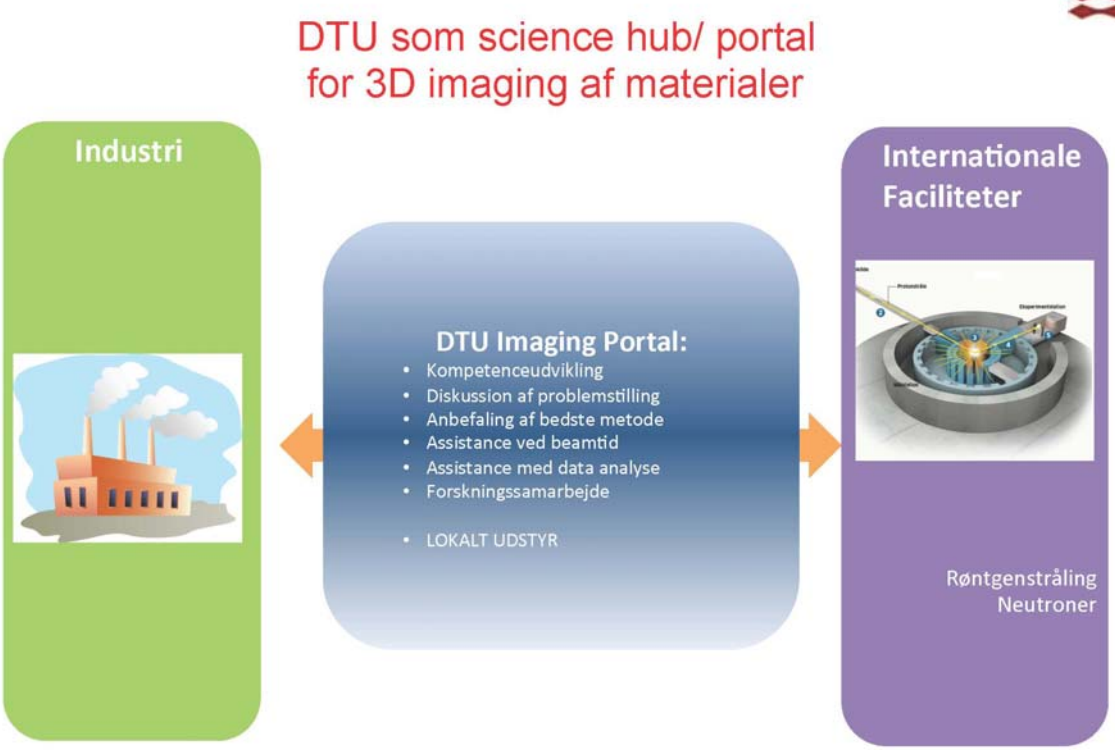

Best practice: University of Manchester
Strukturfondsprojekt (2013-2014): ESS og MAX-IV som vækstmotorer i regionen

Neutron Imaging

Courtesy: PSI, HMI/HZB, FRM2

Residual Spændinger

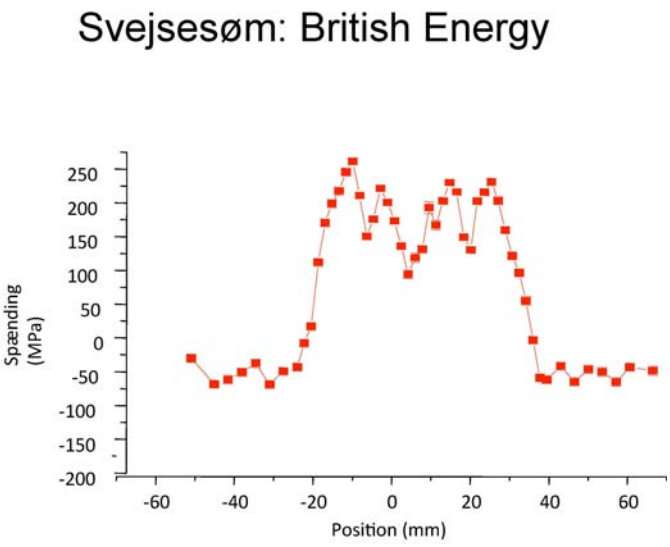

Courtesy: Open University, UK

3D strain map of friction stir weld

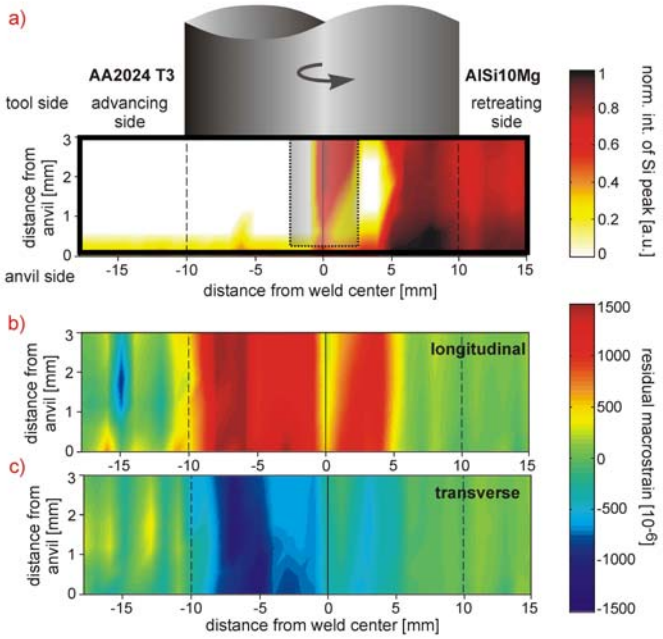

3D imaging af energimaterialer

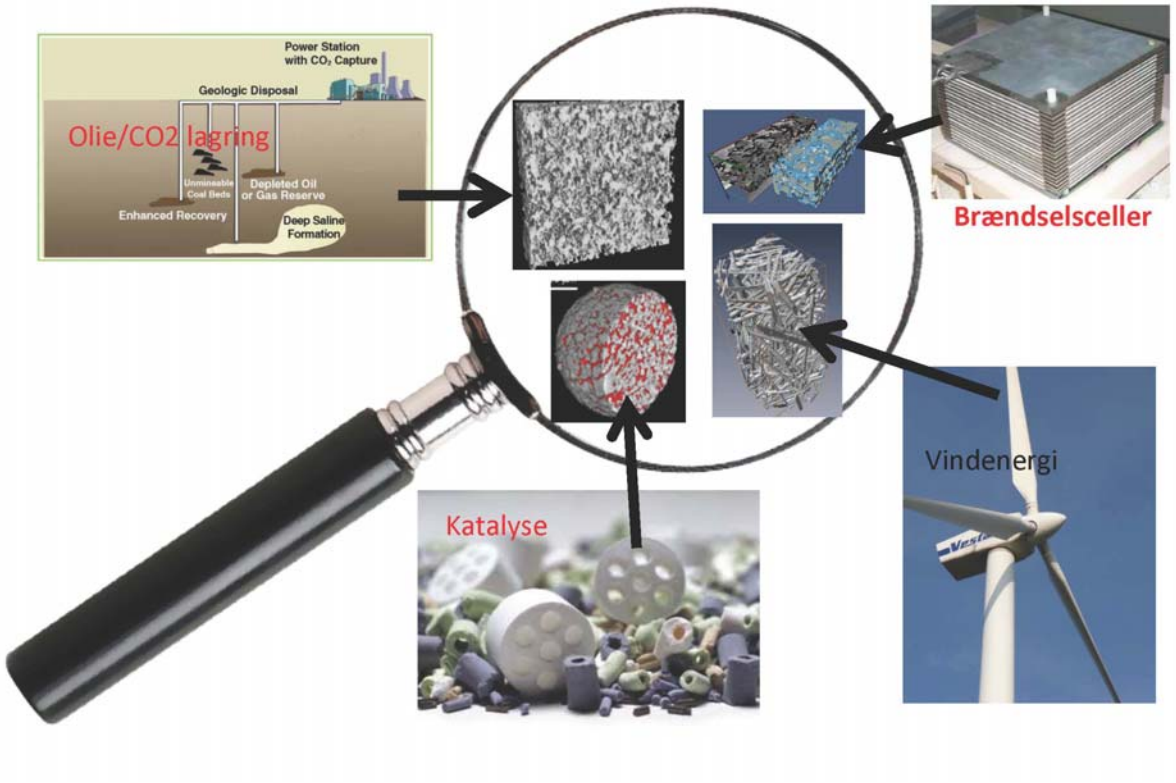

Fase kontrast tomografi af Al folie

Materiale: Alcan Al folie
Type:Al8079
Energi: 17.5 keV
Volumen:
$90x90x48\mu m^3$
Voxel størrelse: $60nm^3$

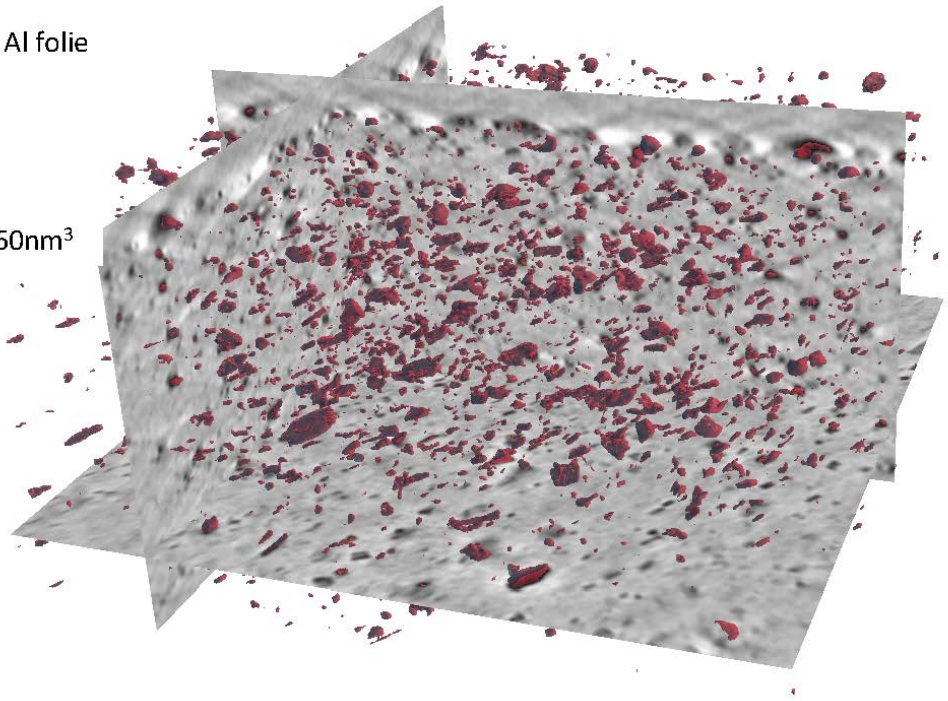

Slide fra P. Cloetens, ESRF

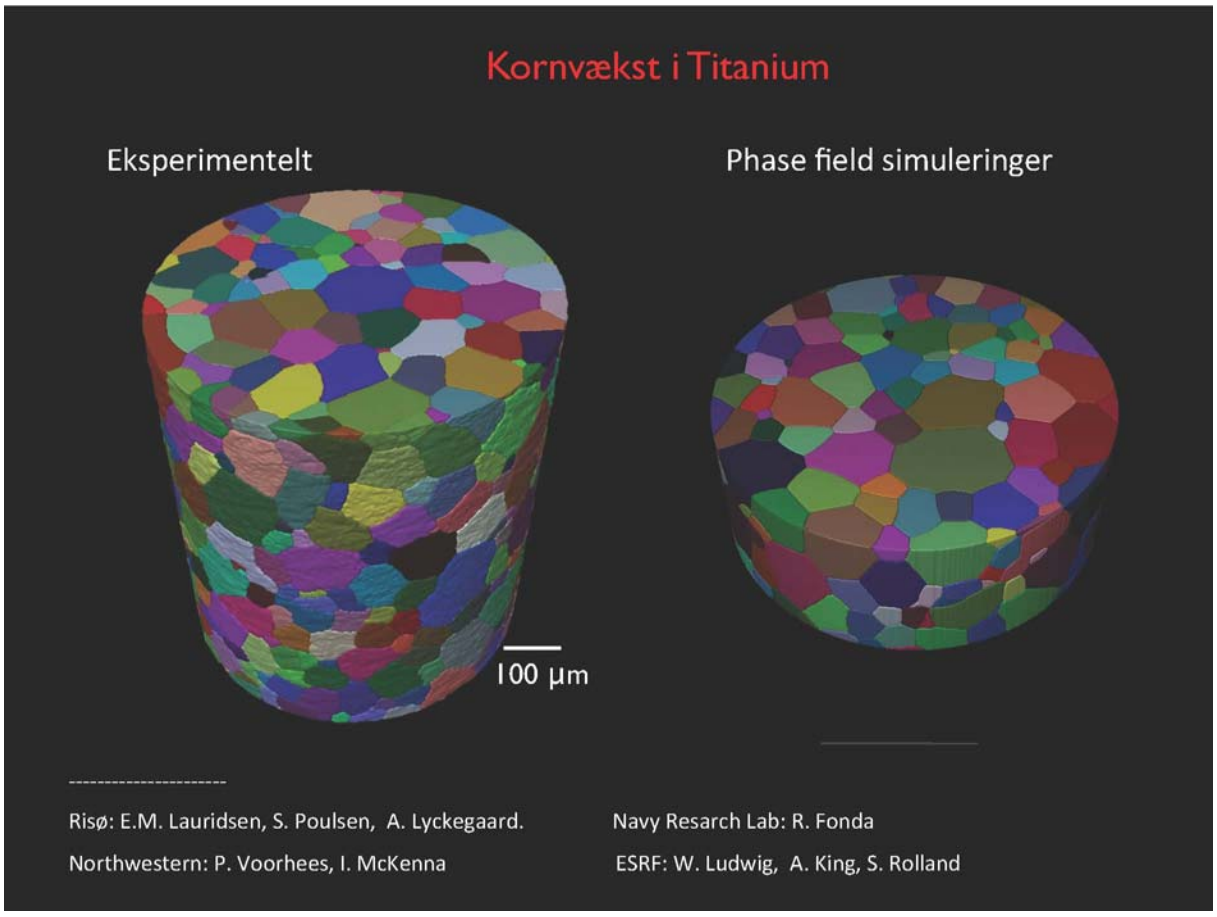

Stress corrosion revnedannelse i stål

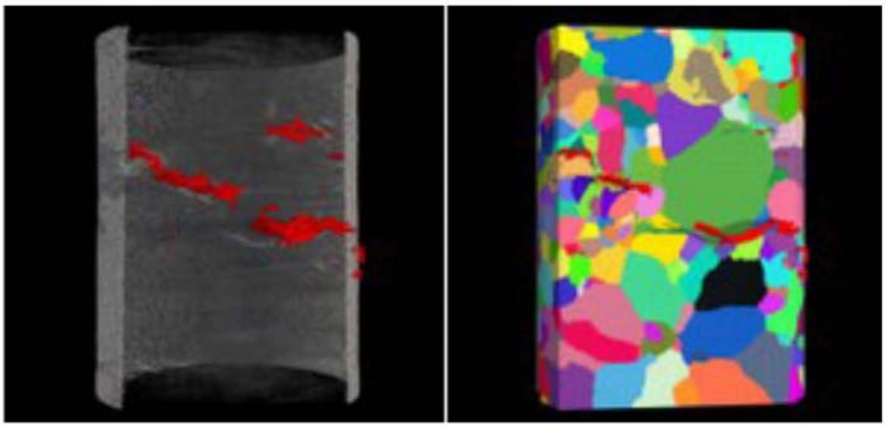

A. King, G. Johnson, D. Engelberg, W. Ludwig, and J. Marrow, *Science* (2008) **321**, 382 - 385

Spændinger omkring revnespids i Mg

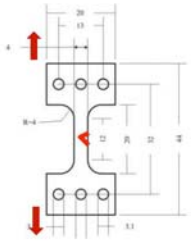

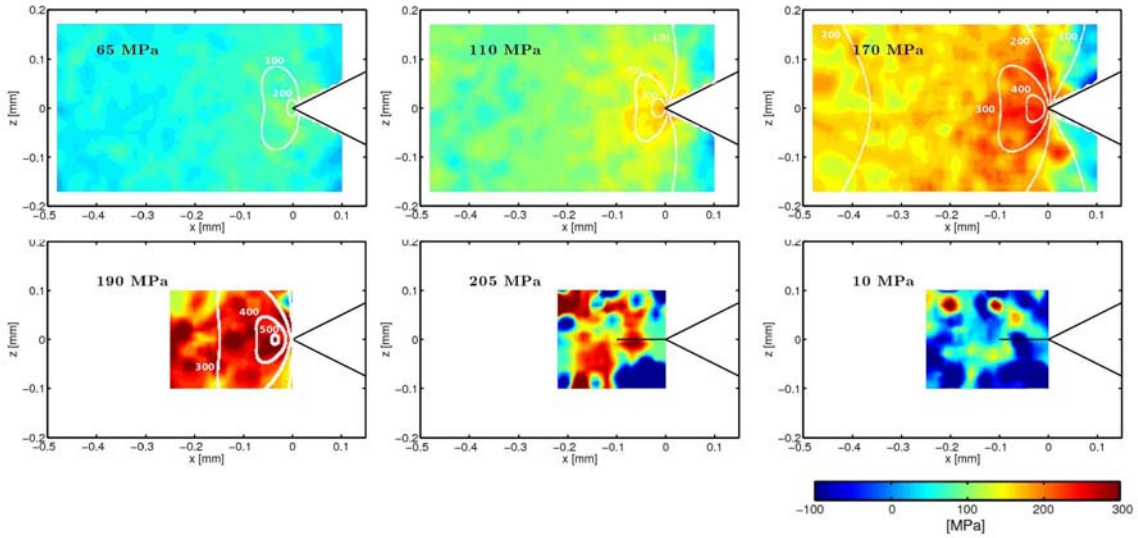

J. Oddershede, B. Camin, S. Schmidt, L.P. Mikkelsen, H.O. Sørensen, U. Lienert, H.F. Poulsen, W. Reimers.
Acta Mater. **60,** 3570-3580 (2012).

diffraktions baseret

TEM TXM

Opløsning:	1 Å	20-30 nm
Tykkelse:	1 korn in 2D	1000 korn in 4D
Orienteringer:	0.01-0.1 grad	0.001 – 0.1 grad
Spændinger:	(indirekte)	direkte

Diffraktions baseret Transmission Røntgen Mikroskopi

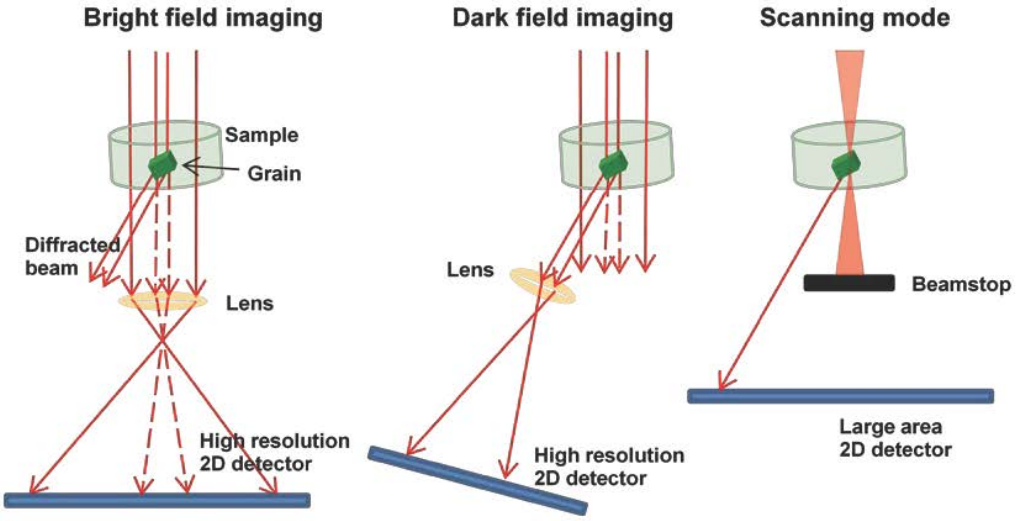

Arbejdsgruppe:

DTU: H.F. Poulsen, E.M. Lauridsen, S. Schmidt, W. Pantleon, J. Oddershede, Y. Zhang, H. Simons, J. Hübner, F. Jense

ESRF: A. Snigirev, I. Snigireva, W. Ludwig, A. King, C. Detlefs.

Mikroskopi

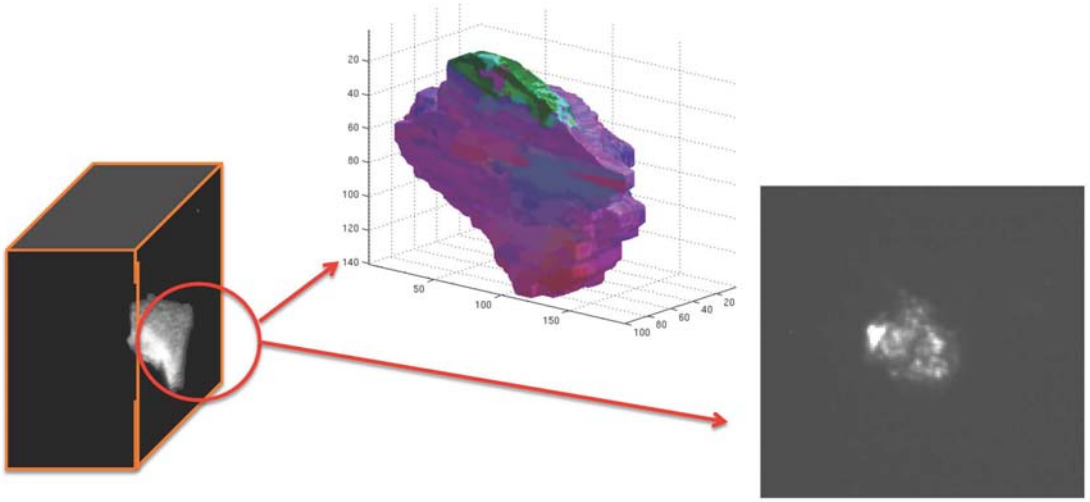

2 µm
0.5 deg

200 nm
0.15 deg

200 nm
0.01 deg

Arbejdsgruppe:

DTU: H.F. Poulsen, E.M. Lauridsen, S. Schmidt, W. Pantleon, J. Oddershede, Y. Zhang, H. Simons, J. Hübner, F. Jense

ESRF: A. Snigirev, I. Snigireva, W. Ludwig, A. King, C. Detlefs.

Studier af rekrystallisation med 3DXRD

Dorte Juul Jensen

Studier af rekrystallization med 3DXRD

D. Juul Jensen

Risø campus

DTU Wind Energy
Department of Wind Energy

Staff	MAC	KOM
Senior scientists (incl emerit.)	7	8
Scientists	3	0
Engineers	0	6
Postdocs	3	3
PhD students	3	5
Technicians	3	7
Secretary	1	1
Guest scientists	3	1

Aim for Materials Science and Advanced Characterization (MAC) section

To perform materials science and development on a high international level with focus in particular on materials and components for wind energy applications

To advance existing techniques and to implement new characterization techniques and data analysis tools to match the needs of the scientific and engineering projects

Covering the whole range from basic science to applications

Work on length scales from nanometer to meter

DTU Wind Energy

Sections

Composites and Materials Mechanics

Materials Science and Advanced Characterization

Fluid Mechanics

Test and Measurement

Wind Turbines

Aeroelastic Design

Meteorologic Section

Wind Energy Systems

DTU Wind Energy

WIND ENERGY SYSTEMS
Wind resources and siting
Wind power integration and control
Offshore wind energy
Wind energy and society

WIND TURBINE TECHNOLOGY
Aeroelastic design
Structural design and safety
Mechanical components
Electro-technical components

BASICS FOR WIND ENERGY
Aero and hydrodynamics
Boundary-layer meteorology and turbulence
Light, strong materials
Remote sensing and measurement technology

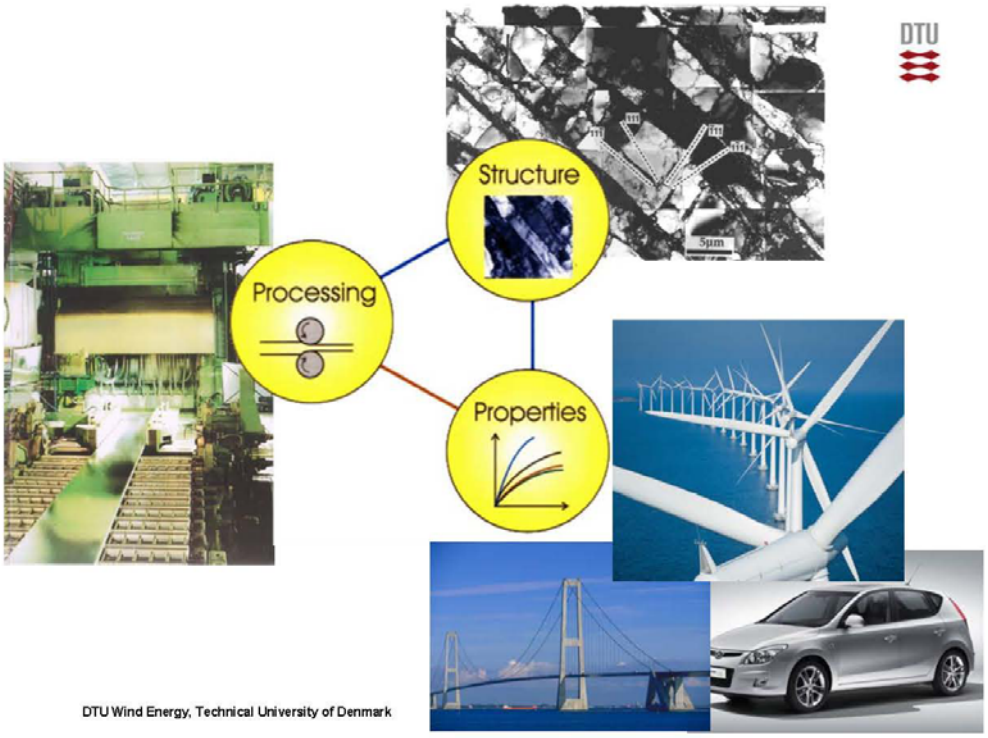

Materials:
Light and strong metals and alloys
Steels
Nanostructured materials

- Processing
  Rolling, extrusion, etc.
  Very high strain: ARB, DPD HPT
  Annealing
- Structure
  Advanced electron microscopy
  Advanced x-ray characterization
  Serial sectioning
- Properties
  Mechanical testing (KOM)
  Calometry
  Hardness
  Physical proporties

DTU Wind Energy, Technical University of Denmark

Electron microscopes @ DTU Wind Energy

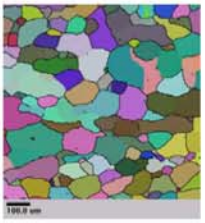

3 SEM & 3 TEM

ZEISS SUPRA 35

JEOL JMS-840

ZEISS EVO 60

JEOL JEM-3000F

JEOL JEM-2000FX

Funding achieved
Microscope
installed

200 kV

DTU Wind Energy, Technical University of Denmark

3D X-ray microscopes at ESRF in France, APS in USA and Hasylab in Germany

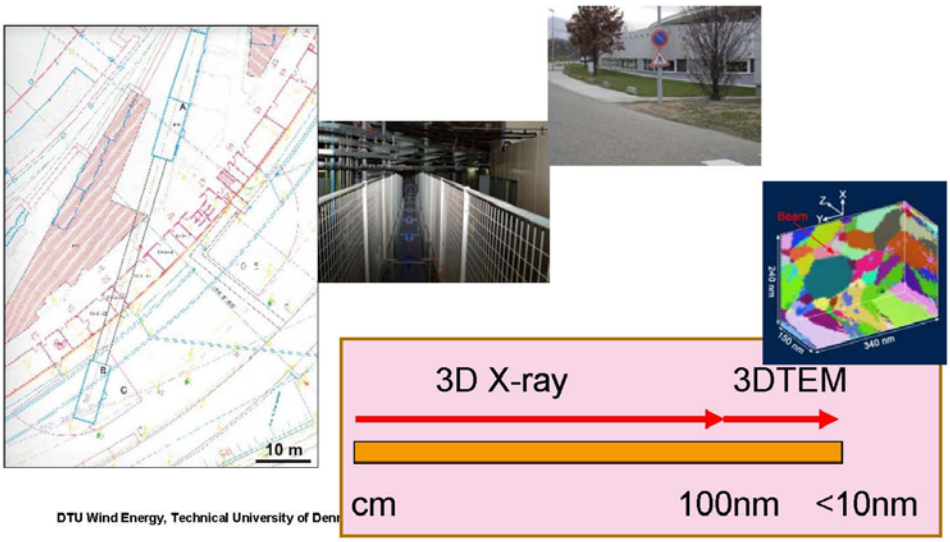

Hard and wear resistant steel components

- Characterize structure to determine stress and strain gradients as input for numerical modelling of e.g. friction and wear
- Develop reliable testing techniques (e.g. microsamples) to analyse structure and properties of components damaged by impact, wear or fatigue

Light and strong metals and alloys

- Optimize strength and formability by thermomechanical processing – bulk samples and multilayers
- Advance analytical and numerical modelling of receovery and recrystallization through 2D and 3D characterization

Technique development

- Implement and develop techniques for characterization of damaged samples (incl lab residual stress measurements)
- Develop techniques for optimizing metals including surface hardening
- Superusers of all relevant 3D/4D techniques with focus on research results

Recrystallization Kinetics

DTU Wind Energy, Technical University of Denmark

Recrystallization kinetics - standard measurements

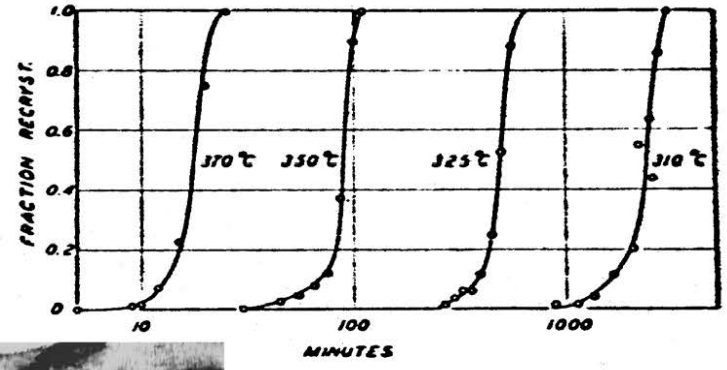

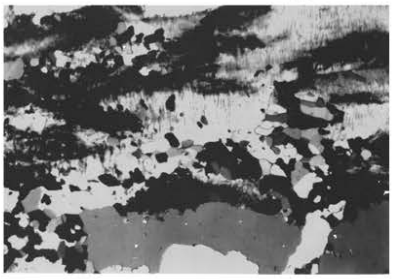

W.A. Anderson and R.F. Mehl: Trans. AIME, 1945, **161**, 140-172.

Recrystallization Kinetics – Standard model

Assuming:

- Random distribution of nucleation sites
- All grains grow with the same time-independent growth rate
- All nuclei develop at t = o or as a linear function of t

$V_v = 1 - \exp(-Bt^k)$

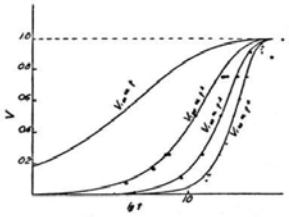

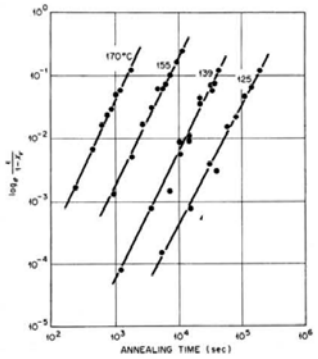

t Time
B, k Constants related to nucleation rate, growth rate and dimensionality of growth

Experimental results - examples

Problems

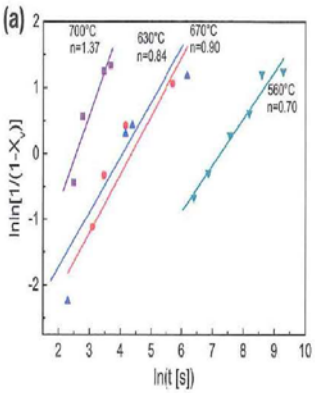

Yaping Lü, Dmitri A. Molodov, Günter Gottstein, Acta Mat. 59 (2011) 3229-3243

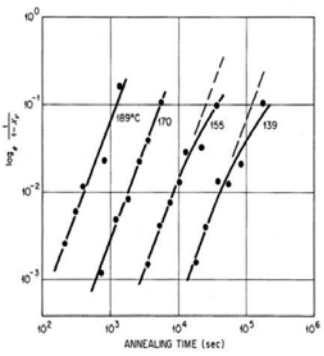

R.A. Vandermeer and P. Gorden: in ´Recovery and recrystallization of metals`, (ed. L. Himmel), Interscience New York, 1963, 211-240

Clustered nucleation

Optical microscopy combined with serial sectioning

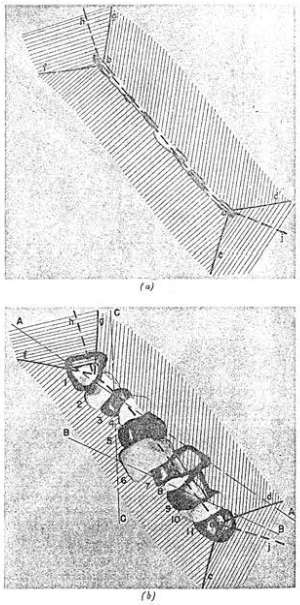

R.A. Vandermeer and P. Gorden: Trans. TMS-AIME, 1959, **215**, 577-588.

JMAK model

Assuming:

- ~~Random distribution of nucleation sites~~
- All grains grow with the same time-independent growth rate
- All nuclei develop at t = o or as a linear function of t

Experimental methods and results

Average growth rates – time and orientation dependencies

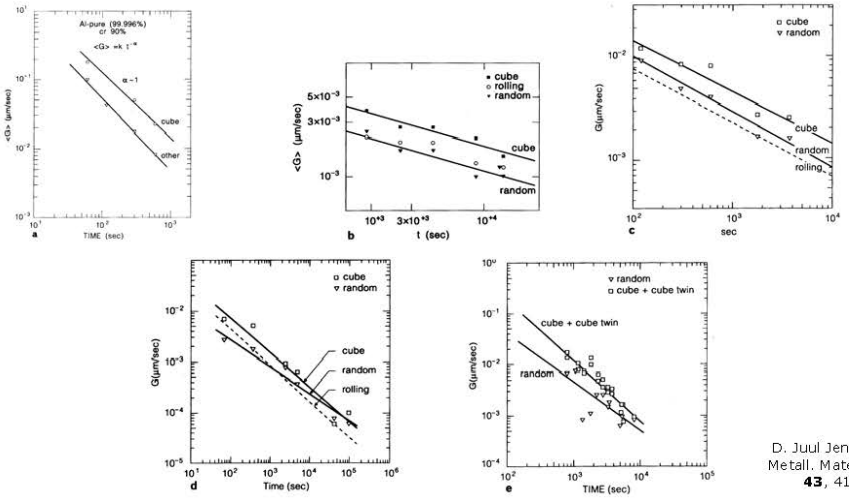

D. Juul Jensen: Acta Metall. Mater., 1995, **43**, 4117-4129.

Growth rates

- ~~All grains grow with the same time-independent growth rate~~

- On avarage grains grow as $\langle G \rangle = k \cdot t^{-\alpha}$ or they have a fast decreasing growth rate followed by a period of constant growth and on average, cube grains often grow faster than other grains

- **What do individual grains do?**

3D X-ray Diffraction (3DXRD)
3D Microscope for in-situ characterization of recrystallization kinetics

- Sub-μm spatial resolution
- Bulk penetration (0.1 mm – 1 cm)
- Non-destructive
- Fast measurements (seconds – minutes)

Recystallization kinetic measurements

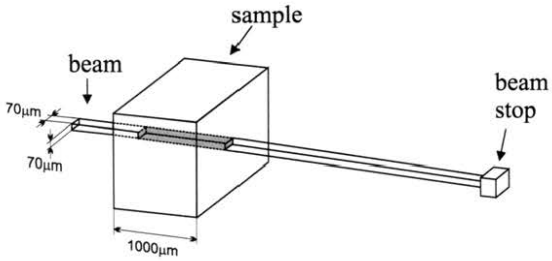

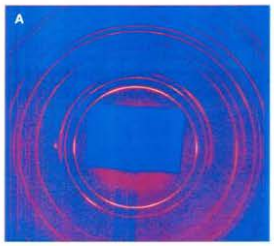

T = 0 min

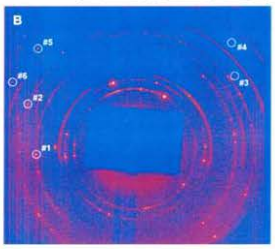

T = 162 min

Al (AA 1050) cr 90%

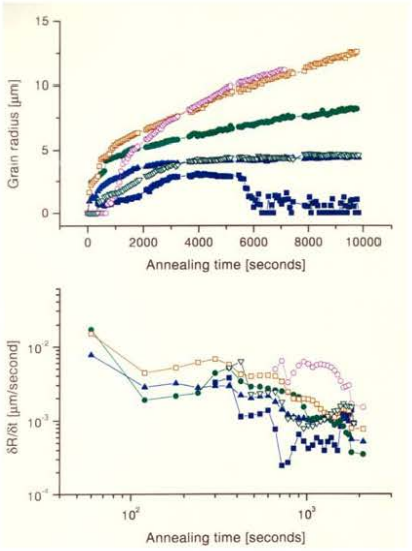

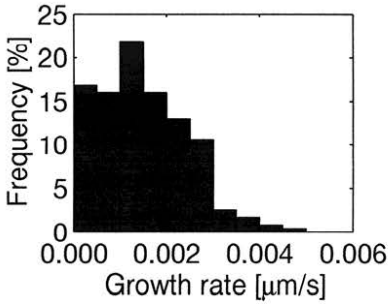

E.M. Lauridsen, H.F. Poulsen, S.F. Nielsen and D. Juul Jensen: Acta Mater., 2003, **51**, 4423-4435
E.M. Lauridsen, D. Juul Jensen, H.F. Poulsen and U. Lienert: Scripta Mater., 2000, **43**, 561-566

Al (AA 1050) cr 50%

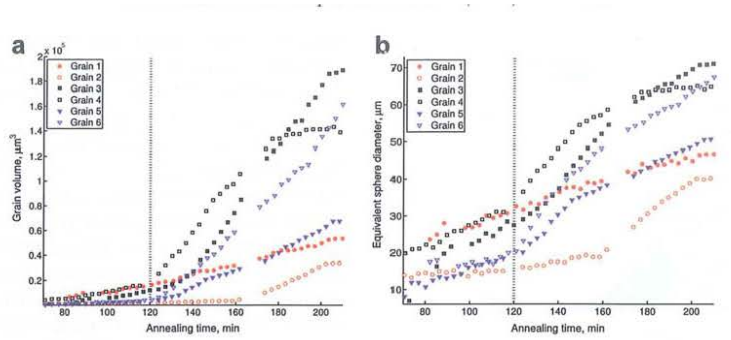

S.O. Poulsen et al. (2011)
Scripta Mater. **64**, 1003-1006.

Grain averaged activation energy for individual grains determined by 3DXRD

$$v = M \bullet F$$

$$v = Mo \exp\left(\div \frac{Q}{RT}\right) F$$

$$Q = R\left(\frac{1}{T_1} \div \frac{1}{T_2}\right) \ln \frac{v_2}{v_1}$$

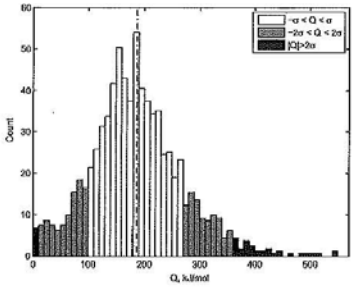

Figure 2. Distribution of grain-averaged activation energies. The mean of the distribution, $\langle Q \rangle = 187\ \mathrm{kJ\ mol^{-1}}$, is indicated by the vertical line. The standard deviation is $\sigma = 82.9\ \mathrm{kJ\ mol^{-1}}$, and the 1σ and 2σ confidence intervals are indicated by the colour of the bars.

v	Growth rate
M	Mobility
F	Driving force
R	Gas constant
T	Absolute temperature
Q	Activation energy

S.O. Poulsen et al. (2011) Scripta Mater. **64**, 1003-1006

Grain growth during recrystallization in weakly rolled aluminum single crystal

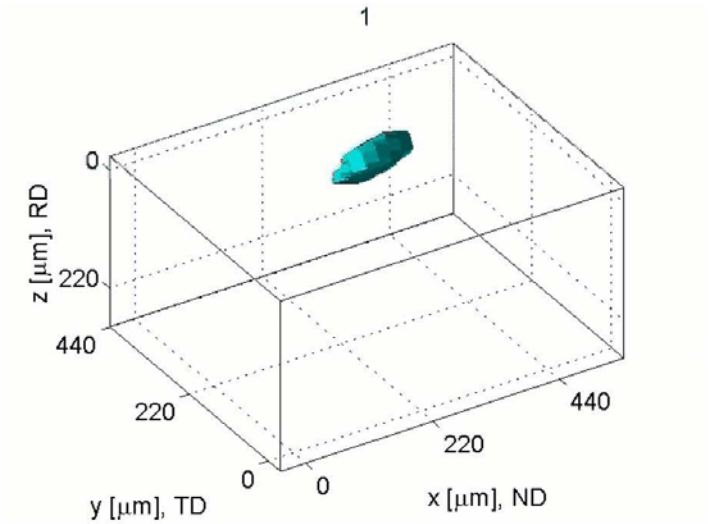

Schmidt, S., Nielsen, S.F., Gundlach, G., Margulies, L., Huang, X., Juul Jensen, D., Science, 2004, 229-232.

Simulations of effects of distribution of growth rates

$$r = A \cdot t^{1-\alpha}$$

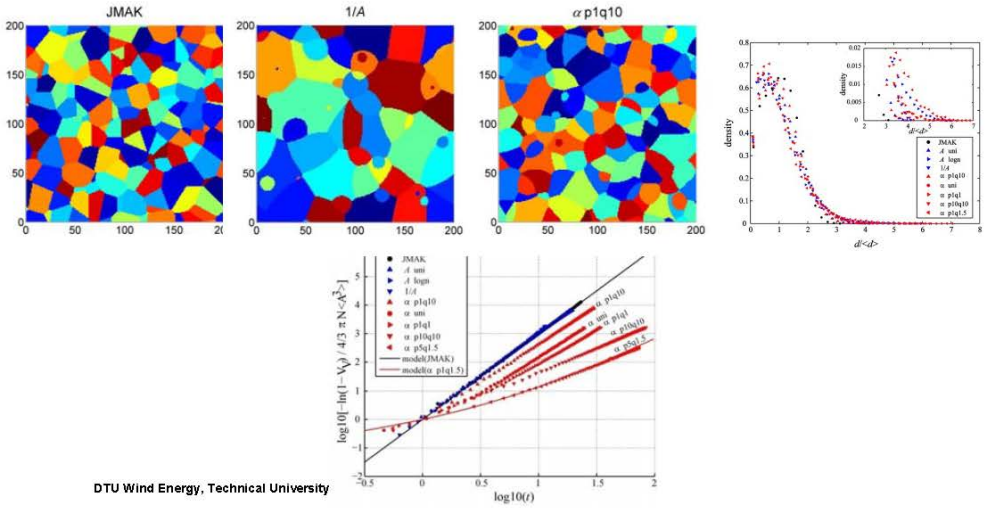

Nanometals

Kinetics in nanostructured copper

Copper DPD to ε = 2.0

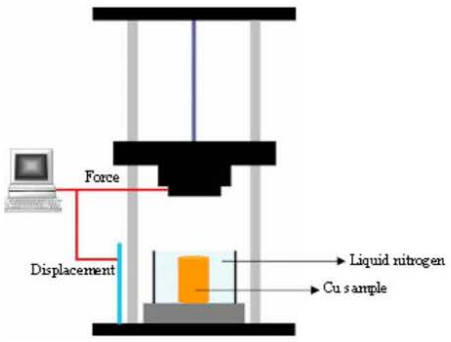

Lin et al., Risø 2012

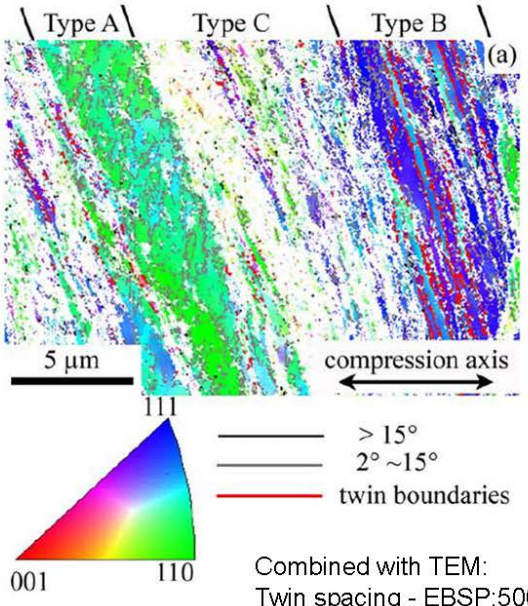

Combined with TEM:
Twin spacing - EBSP:500nm, TEM:44nm
Type C – TEM: <100nm

DTU Wind Energy, Technical University of Denmark

3DXRD measurements anneal at 120C

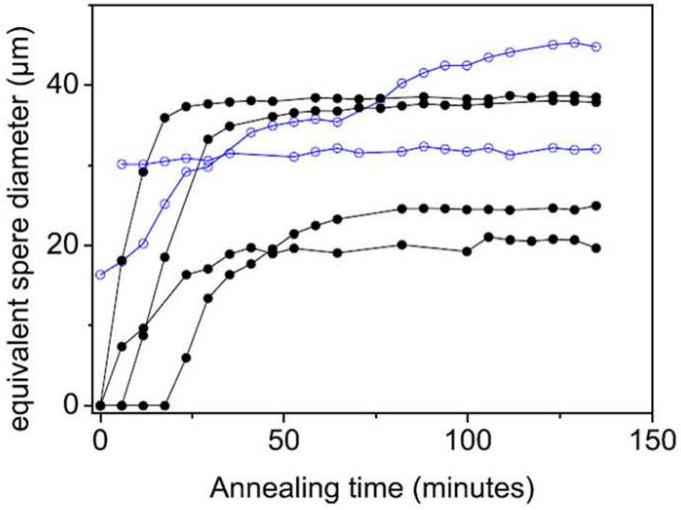

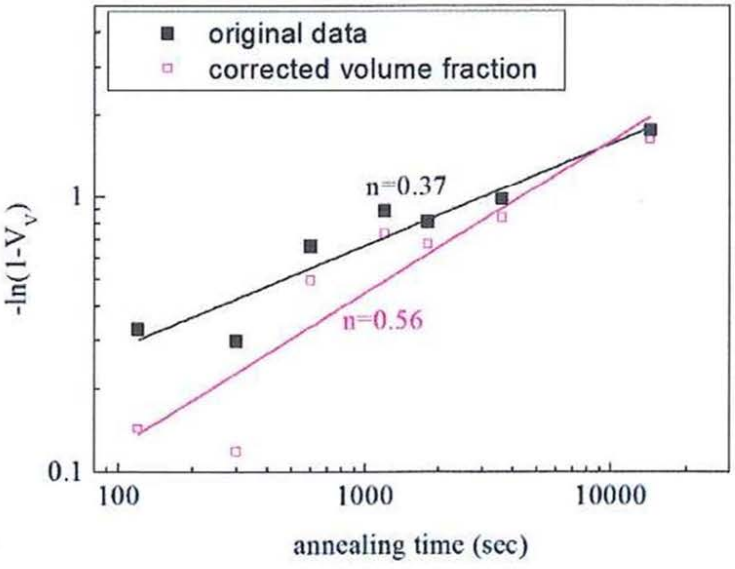

Kinetics in inhomogeneous deformed microstructures

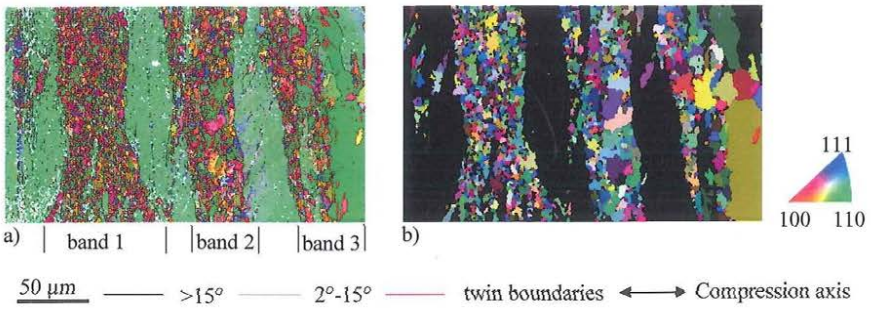

Lin et al., Risø 2012

Kinetics in inhomogeneous deformed microstructures

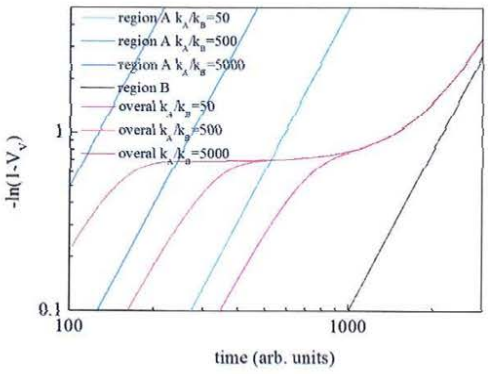

Lin et al., Risø 2012

See also Doherty et al., Risø 1986

Conclusions

Recrystallization kinetics is strongly affected by:

- Spatial distribution of nucleation sites
- Time dependent and texture dependent growth rates
- Each recrystallizing grain has its own kinetics
- Wide distribution of activation energies
- Inhomogeneous deformation microstructures

3DXRD combined with electron microscopy are efficient tools to study recrystallization kinetics

Den nyeste generation af røntgen diffraktometre med tilhørende temperaturcelle

Flemming Grumsen, DTU Mekanik

DTU

DTU Mekanik
Institut for Mekanisk Teknologi

Den nyeste generation af XRD med tilhørende temperatur celle

Flemming Bjerg Grumsen

Outline

- Hvad er XRD?
- Hvad er nyt?
- Strip detektoren. Hvad kan den?
- Mikrodiffraktion med et eksempel
- Temperatur cellen
- Expanderet austenit
- Varmebehandling af expanderet austenit

Hvad er XRD?

- Braggs lov: $n\lambda = 2d\sin\theta$

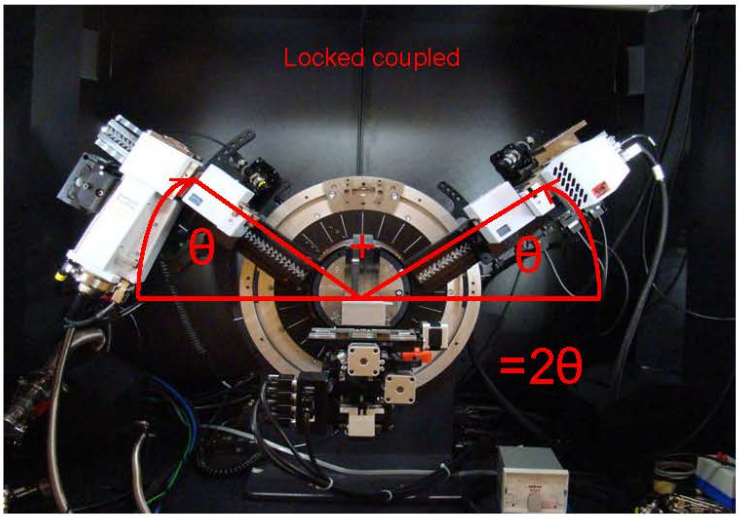

Hvad er XRD?

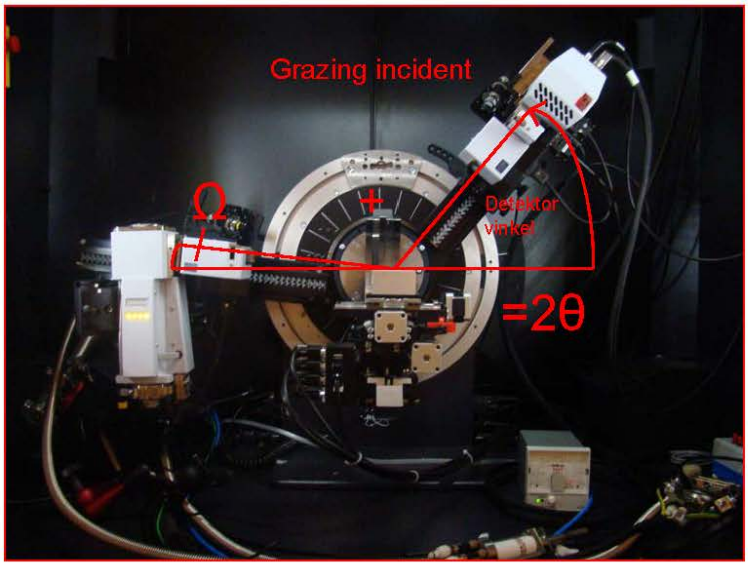

Hvad er nyt?

- Twist tube: linie- og punktfocus

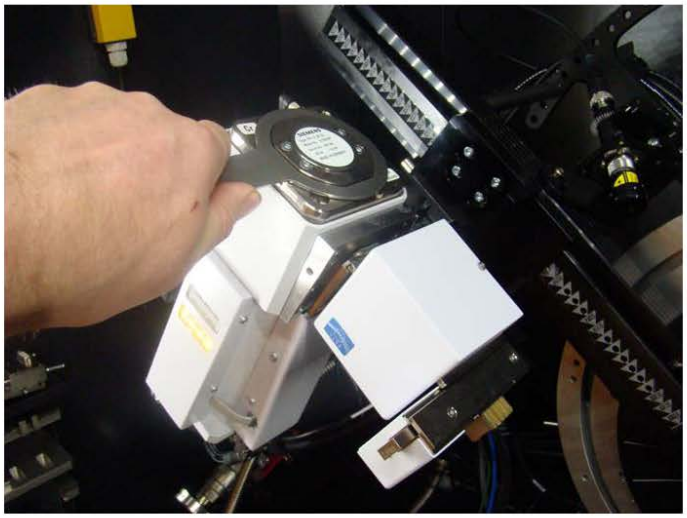

Hvad er nyt?

- Snap lock til skift mellem polycap, göbelspejl og divergence assembly

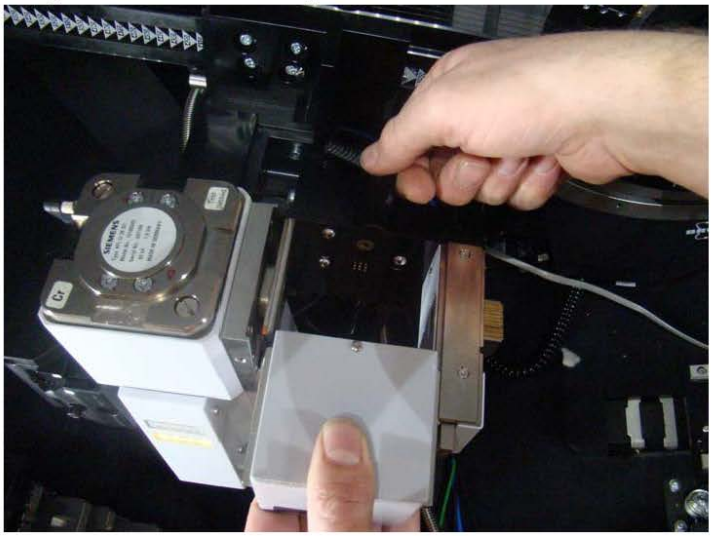

Hvad er nyt?

- Polycap til punkt fokus

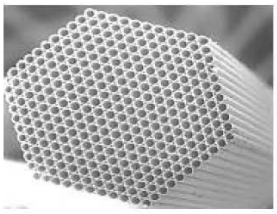

Mikrofibre til guided Røntgen beam

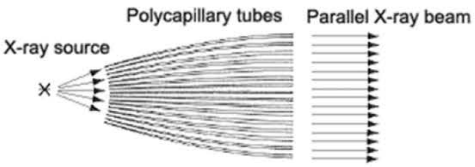

Fra kilde til næsten parralel beam

Hvad er nyt?

- Automatisk registrering at optik (Da Vinci)

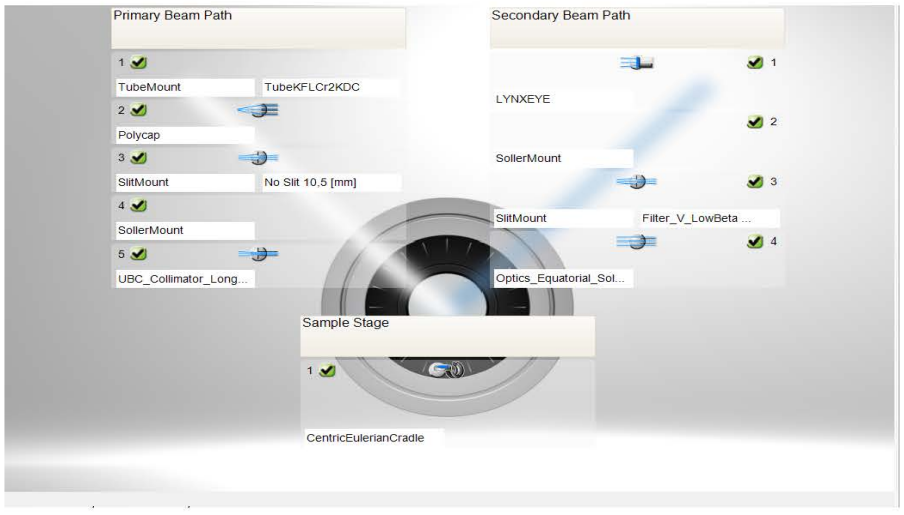

Hvad er nyt?

- Silicon strip 1d detektor (lynxeye)

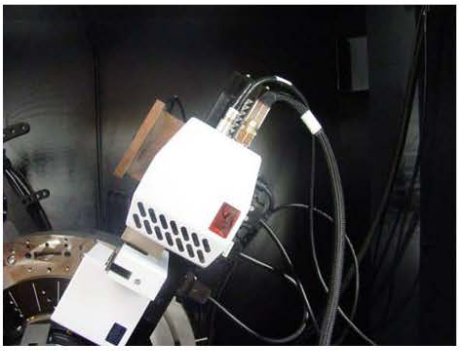

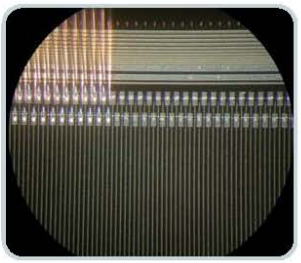

192 strips af 75 µm tykkelse
og 16 mm lange

Billede venligst udlånt af Bruker AXS

Stripdetektoren

- 0D: sammenlægger alle strips til en detektor
- 1D: hver strip fungerer separat og kompenserer for positionen

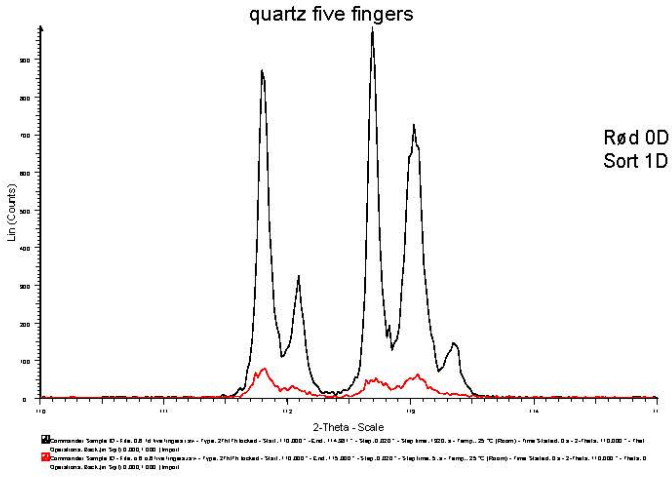

Rød 0D 0.6 mm detektor slit
Sort 1D detektor fuldt åben

Mikrodiffraktion på Friction stir welding

Polycap med 0.3 mm collimator

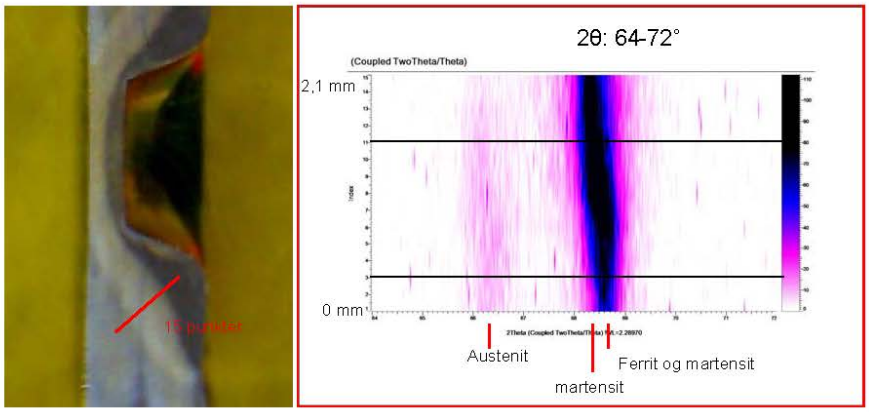

Temperatur cellen

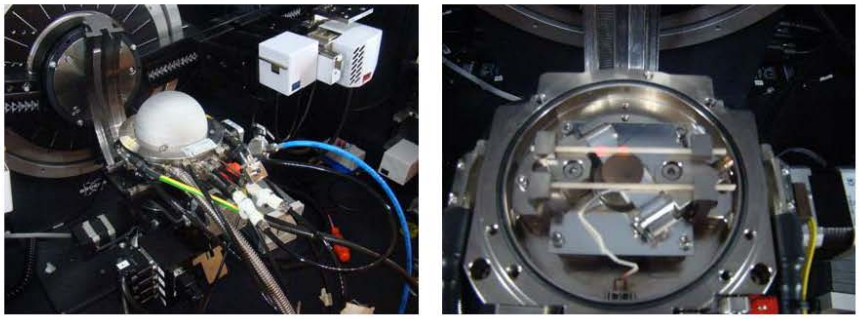

Temperatur spænd: 25-1100 ˚C eller -180 til 450 ˚C
Vacuum eller gas flow
Ramping 0,1 – 1 grad pr. sekund

nedbrydning og (Oxidation☹) af ekspanderet austenit

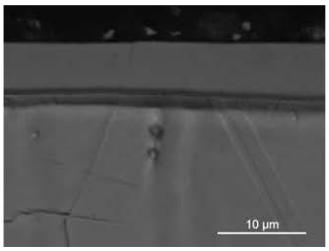

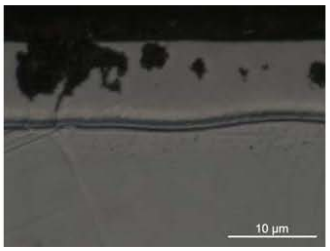

- Expanded austenit is metastabilt
- Ved temperaturer over 450 ˚C ned brydes den til
  - CrN
  - Ferrit

Forsøgsparametre

- Grazing incident 2, 5 og 15 grader, 2θ: 53˚ til 87˚ 30 min for hvert scan
- 30˚C, 100 - 400 ˚C med 50 ˚C interval. Ramping: 1 ˚C pr s.
- 400 ˚C til 560 ˚C med 5 ˚C interval. Ramping: 0,1 ˚C pr s.
- Afkøling til 30 ˚C. ramping: 1 ˚C pr s.

Resultater

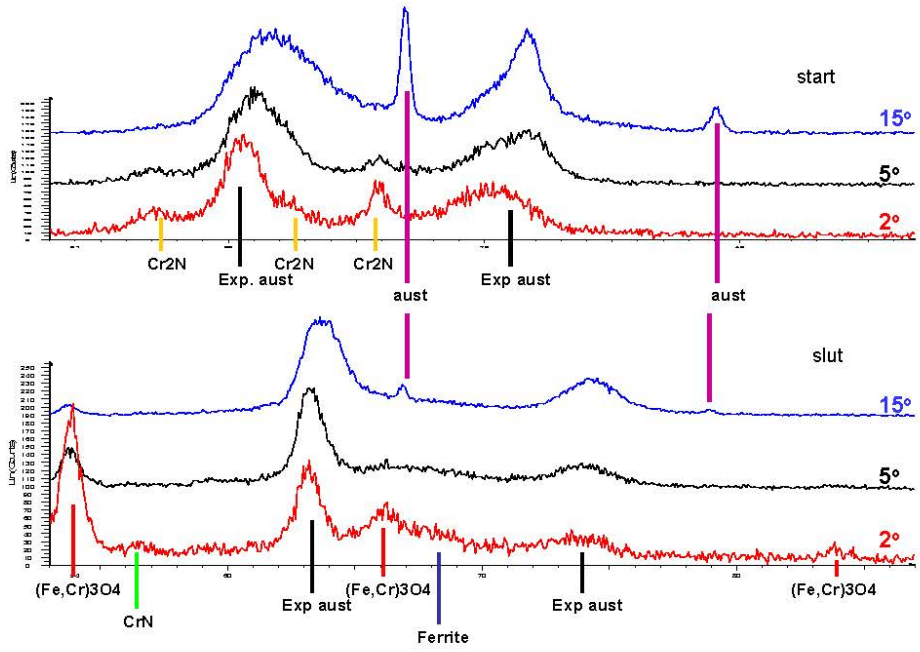

Resultater

2 ° grazing incident

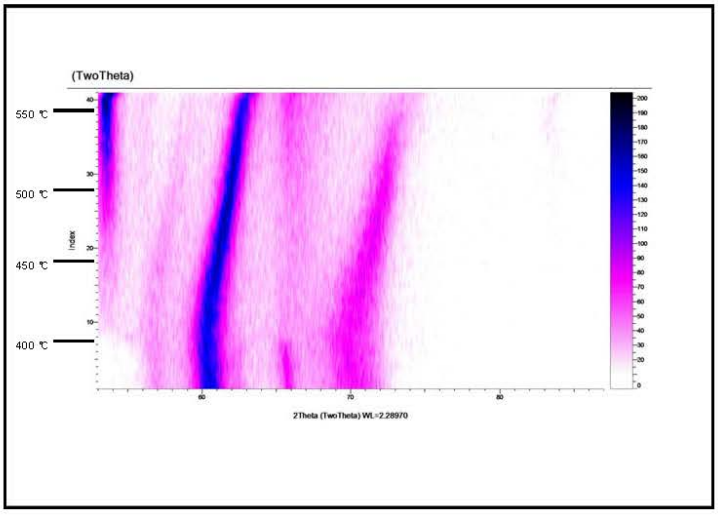

resultater

5 ° grazing incident

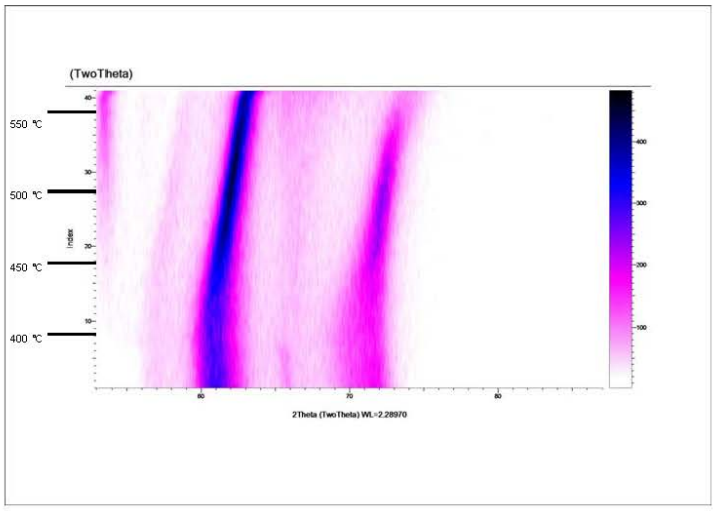

Resultater

15 ° grazing incident

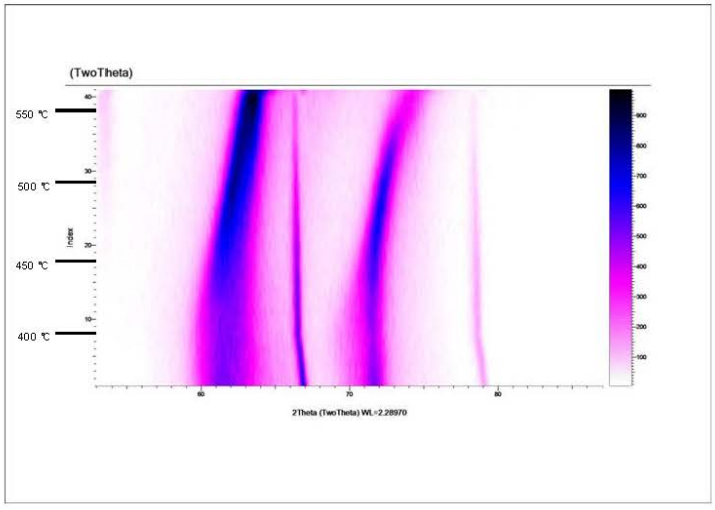

Hvad kan man gøre for at undgå oxidation?

- Au eller Pt coating?
- Ar/H2 gas?
- Metal med større affinitet til O2 end prøven i kammeret?

- Og til sidst tak til Christian Hansson fra Bruker for support og til Trine Nybo Lomholt for nye ideer, når problemerne syntes uoverskuelige

NDT – relevant teknikkers muligheder og begrænsninger

Peter Willumsen, Force

NDT af svejsninger




Af Peter Villumsen
DS/EN 473 niveau 3

NDT af svejsninger

Metoder:

- Røntgen
- Ultralyd
- Magnetpulverprøvning
- Penetrantprøvning
- Tæthedsprøvning
- Hvirvelstrømsprøvning

NDT af svejsninger

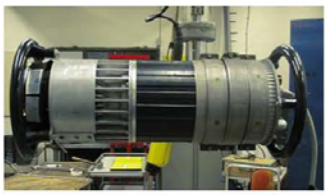

Radiografi

Røntgen op til 300 kv.

Isotop (Gamma)

- Selen 75
- Ir 192
- Cobolt 60

NDT af svejsninger

Radiografi

Følsomhed 1-2% af godstykkelse

Radiografi bruges på alle emner/svejsninger i alle former for industri både i forbindelse med ny produktion og vedligehold.

NDT af svejsninger

Radiografi bruges til af finde fejl i volumen
Radiografi er 2 dimensional.

Fordele:
God til runde fejl eks. Pore
God til tynde godstykkelser

Ulemper:
Stråling
Begrænset godstykkelser

NDT af svejsninger

Ultralyd

Manuel eller automatisk

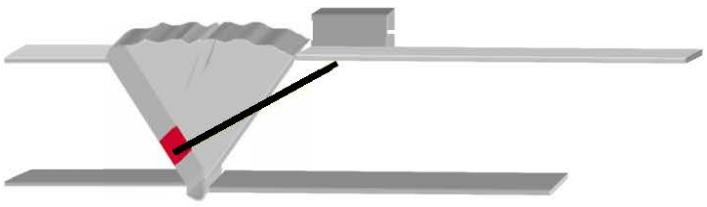

NDT af svejsninger

Manuel ultralyd bruges til:

- Tykkelse måling
- Lagdelings kontrol
- Materialefejl
- Svejsekontrol

0.37 mm i mindst 2 retninger

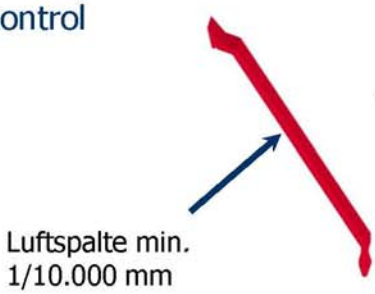

Luftspalte min.
1/10.000 mm

NDT af svejsninger

Manuel Ultralyd

Fordele:
God til plane fejl
God til tykke godstykkelser

Ulemper:
Kræver plads
Ingen dokumentation

NDT af svejsninger

Højt ydende automatiseret ultralyd inspektion

- Hurtig automatiseret inspektion
- Optimeret inspektion
- Dokumenteret
- Gentagen inspektion
- Stål, rustfrit stål, etc.

NDT af svejsninger

Magnetpulverprøvning

For indikationer åben til overfladen og kun på magnetiske materialer.

Følsomhed

Ca. 0,1 – 1mų

NDT af svejsninger

Magnetpulverprøvning

Kan udføres som prøvning med kontrast farve under alm. belysning.

Eller som fluorescerende prøvning i mørke med ultraviolet belysning

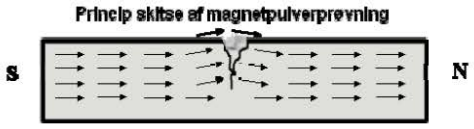

NDT af svejsninger

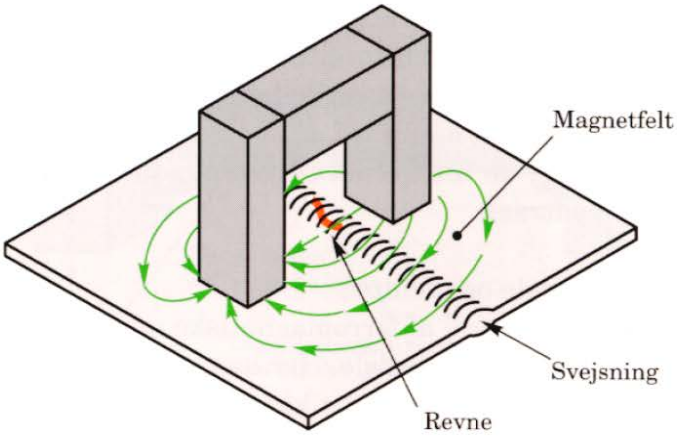

NDT af svejsninger

Fordele:
God til plane fejl åben til overfladen
Hurtig

Ulemper:
Kun overflade fejl
Ingen dokumentation

NDT af svejsninger

Penetrantprøvning
(Kapillarprøvning)

Kan udføres som prøvning med kontrast farve under alm. belysning.

Eller som fluorescerende prøvning i mørke med ultraviolet belysning
Den mest følsomme metode

NDT af svejsninger

Penetrant bruges på ikke porøse materialer

Primært på umagnetiske som eks, rustfrit stål, aluminium, magnesium osv.

For indikationer åben til overfladen

Følsomhed
Ca. 0,1 – 1mų

NDT af svejsninger

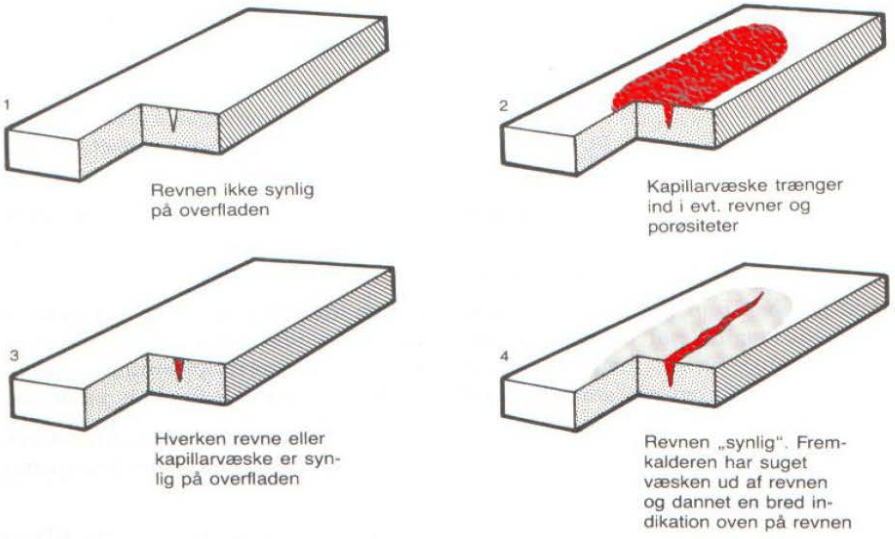

NDT af svejsninger

Fordele:
God til fejl åben til overfladen
Kan bruges som tætheds prøvning
Let at udføre

Ulemper:
Kun overflade fejl
Ingen dokumentation
Kræver meget rengøring

NDT af svejsninger

Tæthedsprøvning

(Lækageprøvning)

Lækageprøvning er ikke bare en, men mange metoder

De følgende er nogle af de mest anvendte

Visuelle - Akustiske – Trykforandring – Sporstoffer - Radioaktive sporstoffer - Termografi – Hvirvelstrøm - Farveforandring – Røggasser – Krydskorrelator – kabilarprøvning

NDT af svejsninger

Vakuum box

NDT af svejsninger

Hvirvelstrømsprøvning

Undersøgelse af elektrisk ledende materialer, primært metaller.

Metoden anvendes bl.a. til revne- og korrosionsdetektion samt tykkelsesmålinger, fx til undersøgelse af varmevekslerrør og i flyindustrien til kontrol af fx turbineblade og understel.

Slut...

Metrology and Quality Assurance

Maria Holmberg, Teknologisk Institut

THE DANISH TECHNOLOGICAL INSTITUTE

Founded 1906 by Gunnar Gregersen

"To support Danish industry, mainly small enterprises, by providing technical assistance in the form of teaching, advice, testing and technological research"

"Technological research - developed with the necessary scientific approach, but without the means of making science. The purpose is to develop new field for manufacturing "
Gunnar Gregersen

DTI - DIVISIONS AND CENTRES

DANISH TECHNOLOGICAL INSTITUTE

BUILDING TECHNOLOGY
Concrete
Building Processes
Indoor Climate and Humidity
Masonry and Building Components
New Industrialization
Swimming Pool Technology
Timber and Textiles

LIFE SCIENCE
Food Technology
IT Development
Chemistry and Water Technology

ENERGY AND CLIMATE
Energy Efficiency and Ventilation
FEM-Secretariat
Installation and Calibration
Refrigeration and Heat Pump Technology
Pipe Centre
Renewable Energy and Transport
Automobile Technology

MATERIALS
Materials Testing
Plastics Technology
Production Development
Tribology
Packaging and Transport

PRODUCTION
Micro technology and Surface Analysis
Metrology and Quality Assurance
Robot Technology

BUSINESS DEVELOPMENT
Policy and Business Development
Human Resources Development
Creativity and Growth
Technology Partnership

TRAINING
IT Training
Conferences
Leadership and Management Training

INTERNATIONAL CENTRE

METROLOGY & QUALITY ASSURANCE

DANISH TECHNOLOGICAL INSTITUTE

Geometrical measurements – shape and dimensions of physical objects

Commercial activities
- Pilot production
- Product development
- Subcontractors/customers
- Training and courses

R&D activities
- Trouble shooting
- Product development
- Metrology
- Production and productivity

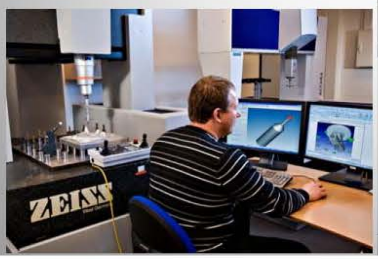

METROLOGY & QUALITY ASSURANCE

DANISH TECHNOLOGICAL INSTITUTE

Metrology – DPLL (Danish Primary Laboratory for Length)

Designated institute within length – mechanical calibration of gauge block

Accreditation within geometrical measurements

EURAMET, TC-L (Technical Committee for Length)

CMC (Calibration and Measurement Capabilities)

EMRP projects

Multi-sensor metrology for microparts in innovative industrial projects

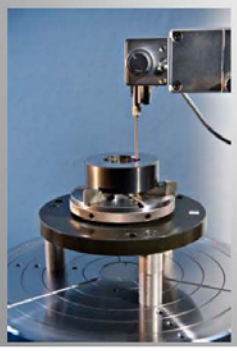

DANISH TECHNOLOGICAL INSTITUTE

Fra programmet:

Dansk industri skal bl.a. overleve på kvalitet, og det er vigtig, at virksomhederne kan **dokumentere denne kvalitet overfor deres kunder**. Vintermødet 2013 har derfor fokus på **karakterisering af materialer, processer og komponenter**, spændende fra nanometer til meterskala og fra **forskning & udvikling** til **monitorering af komponenter i drift**.

Dokumentere kvalitet overfor deres kunder

Geometrisk opmåling kan kvantificere dette – tolerancer, dimensioner, data
Reproducerbarhed

Karakterisering af materialer, processer og komponenter

Kombinere opmåling (dimension, form) med materiale karakterisering (densitet, homogenitet, struktur)
Hvilke parametre repræsenterer hvad?

Forskning & Udvikling

Trouble shooting – vi ved ikke helt hvad vi kigger efter…
Metrologi & måleteknik i fremtiden – inklusive CT Scanning

Monitorering af komponenter i drift

CT Scanning som ikke-destruktiv analyse med mulighed for 3D karakterisering

CT SCANNING

DANISH TECHNOLOGICAL INSTITUTE

CT – Computed Tomography – Scanning

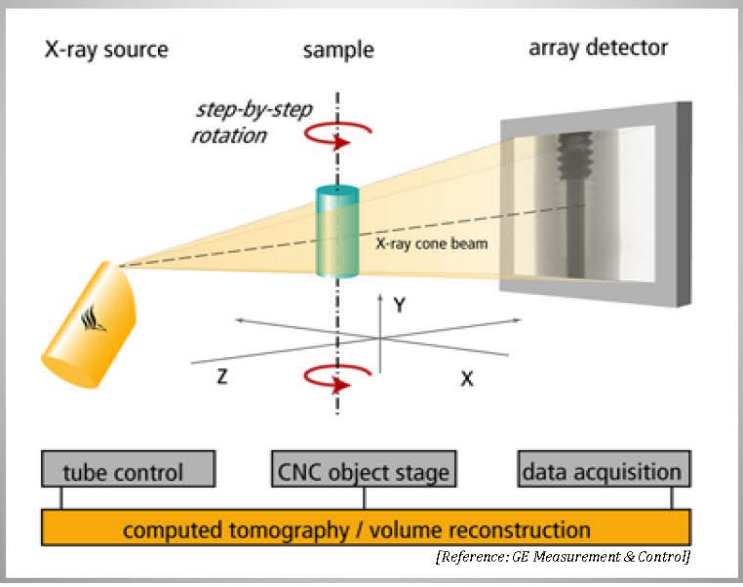

CT SCANNING

DANISH TECHNOLOGICAL INSTITUTE

- Measuring size, form and position of geometrical features
- Non-destructive analysis of inner structures

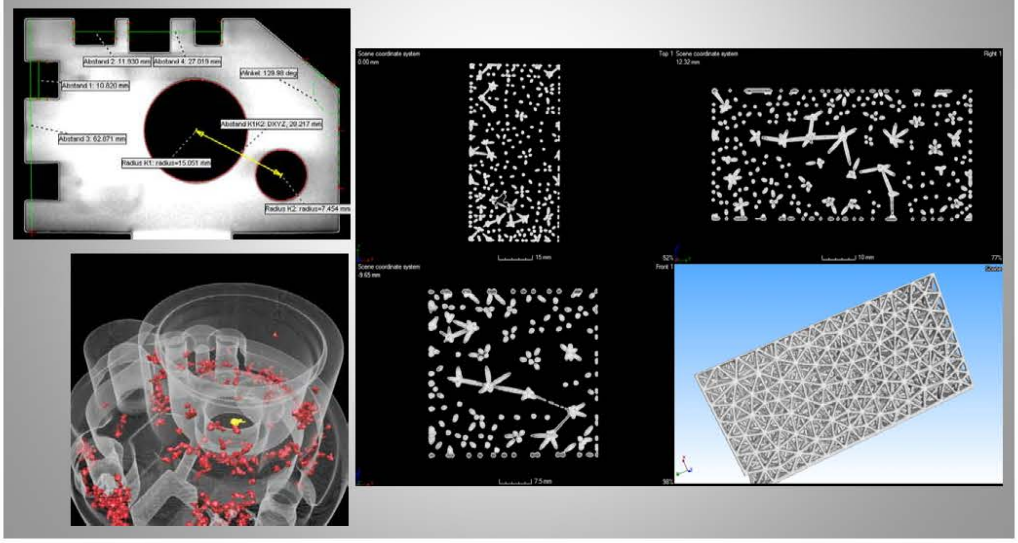

CT SCANNING

DANISH TECHNOLOGICAL INSTITUTE

Zeiss METROTOM 1500

X-Ray tube:	225 kV
Detector:	1024 x 1024 pixels
Sample size:	30 x 30 x 30 cm
'Detectability':	< 10 µm

Industrial CT Scanner
Manufacturing, Production,
In-line Scanning etc.

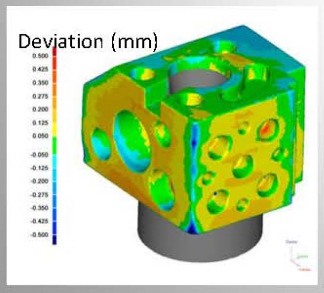

CT SCANNING

DANISH TECHNOLOGICAL INSTITUTE

Bruker microCT, Skyscan 1172

X-Ray tube:	100 kV
Detector:	4000 x 2300 pixels
Sample size:	2 x 2 cm (possibility to combine scans)
'Detectability':	< 1 µm

µCT Scanner
Material characterisation, R&D,
high resolution etc.

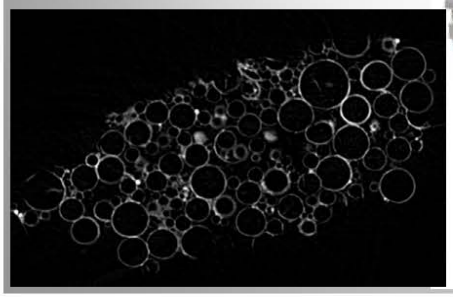

Document quality in regards to customers

DANISH TECHNOLOGICAL INSTITUTE

Documentation in regards to customers and subcontractors in a supply chain

Often a combination of different technologies, for example CMM and CT Scanning

Manufacturing

'Quantification of quality' using geometrical measurements

Example - release of moulds for injection moulding into production

Characterisation of materials, processes and components

DANISH TECHNOLOGICAL INSTITUTE

Combining geometrical measurements with material characterisation

How are used processes related to characteristics of resulting component?

Combining data on micro- and macro-scale

Material for use as a matrix aluminium syntactic metal foam

Hollow glass spheres (ø20-80 µm) that are bonded chemically to each other by water-based silane coating.

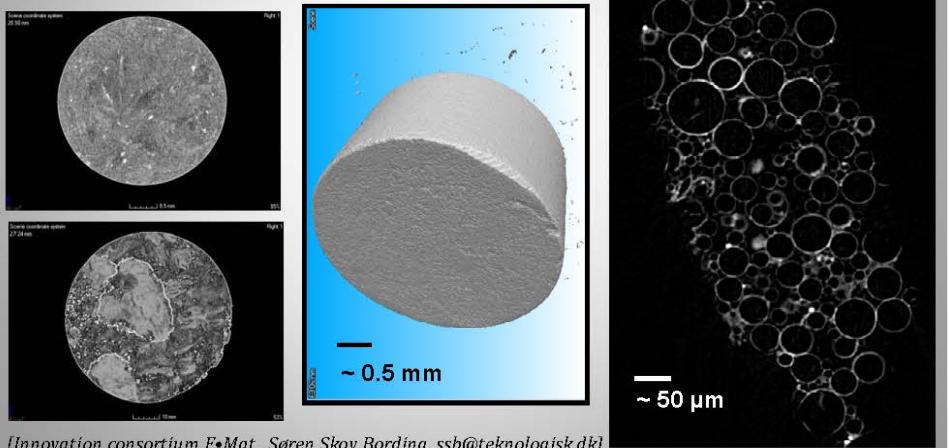

[Innovation consortium F•Mat., Søren Skov Bording, ssb@teknologisk.dk]

Research and Development

DANISH TECHNOLOGICAL INSTITUTE

Metrology and geometrical measurements

EMRP project: Multi-sensor metrology for microparts in innovative industrial projects
Transferring new methods, systems, protocols from laboratory to production facilities.

- Influence on uncertainty from parameter X
- Optimization of protocols (tolerances, time etc.)
- Data handling and data fusion

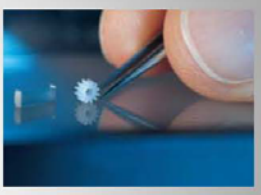

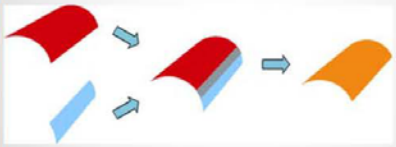

Development together with industry

Product development and trouble shooting
Designed/optimized solution for specific applications

- Automation and multiplying
- Sample holders for CT scan of several items simultaneously
- Software systems (macros) for automatic handling of data

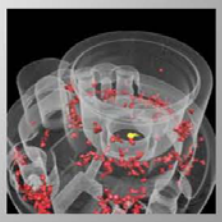

Monitoring components 'in-line'

DANISH TECHNOLOGICAL INSTITUTE

CT Scanning – Possibility to perform non-destructive testing in 3D

'In-line' CT Scanning system

Expensive and time consuming
Necessary to have 3D?
Need to be combined with software solutions

High-end products
Complex technology
Assembled items – components made of different materials etc.

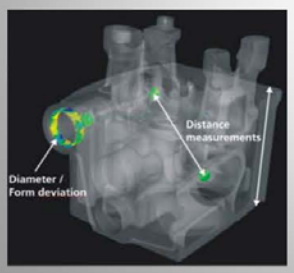

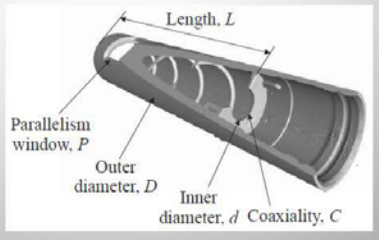

Characterization on all length scales - CT Scanning

DANISH TECHNOLOGICAL INSTITUTE

Industrial CT Scanning in combination with µCT

- From micro to cm range
- Low density material
- Complex geometry
- Non-destructive

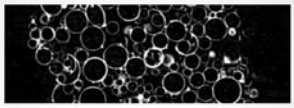

nano micro cm meter

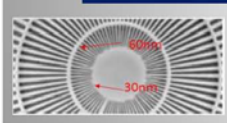

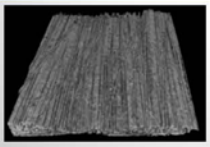

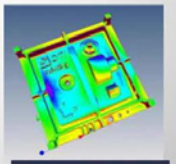

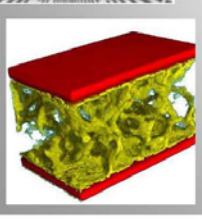

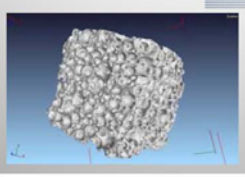

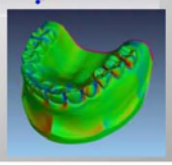

METROLOGY & QUALITY ASSURANCE

DANISH TECHNOLOGICAL INSTITUTE

Maria Holmberg

PhD, Senior Consultant

Metrology and Quality Assurance
Production
Danish Technological Institute
Gregersensvej 8B
DK-2630 Taastrup
Denmark

+45 72 20 30 06

mahg@teknologisk.dk
www.teknologisk.dk

CT SCANNING

DANISH TECHNOLOGICAL INSTITUTE

Image artifacts

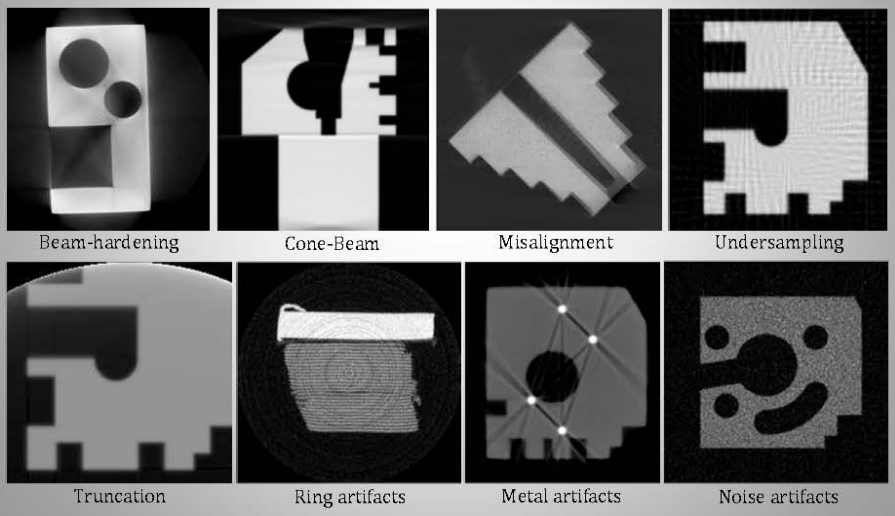

Determining geometrically necessary dislocation densities by EBSD

Philip Littlewood, DTU Mekanik

Determining geometrically necessary dislocation densities by EBSD

Philip Littlewood

DTU Mechanical Engineering
Department of Mechanical Engineering

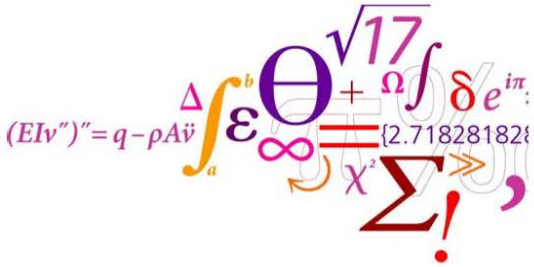

Overview

- Theoretical basis for determining dislocation density by EBSD
- Cross-correlation method for EBSD patterns
- Application to deformed Ti alloys

DETERMINING DISLOCATION DENSITIES BY EBSD

Dislocation and Curvature Tensors

- Dislocation Tensor [1]:

$$\alpha_{ij} = \sum nb_i r_j$$

- Relationship between Dislocation and Curvature Tensors (with/without elastic strain) [1,2]

$$\alpha_{ij} = \kappa_{ji} - \delta_{ij}\kappa_{kk}$$

$$\kappa_{pi} = -\alpha_{ip} + \frac{1}{2}\delta_{pi}\alpha_{kk} + e_{pjk}\epsilon^{el}_{ik,j}$$

[1] J. F. Nye. Acta Metallurgica, 1:153-162, 1953.

[2] E. Kröner. *Continuum Theory of Dislocations and Self Stresses*. Springer, Berlin, 1958.

Limitations on Determining Dislocation Densities with EBSD

- Only dislocations contributing to lattice curvature (GNDs) can be detected
  - Dipoles, other multipoles are "invisible" (SSD)
- Dislocation tensor gives only nine equations
  - Systems other than simple cubic have too many dislocation types – no unique solution
  - Linear programming can be used to generate lower-bound solutions [1]
- Surface nature of EBSD makes information unavailable
  - Z-components of curvature cannot be measured
  - 5 components of dislocation tensor & difference of two others can be derived [2]
  - Can be overcome by 3D FIB-EBSD [3]

[1] S. Sun, B.L. Adams, C. Shet, S. Saigal, W. King. Scripta Materialia, 39:501-508, 1998.
[2] W. Pantleon. Scripta Materialia 58:994-997, 2008.
[3] E. Demir, D. Raabe, N. Zaafarani, S. Zaefferer. Acta Materialia, 57:559-569, 2009.

Cross-Correlation-Based GND Measurement

- Standard EBSD error is ~1°
  - Magnified in calculations of misorientation
  - Cross-correlation method [1] was developed to improve resolution
- Distortion of crystal lattice causes shifts in EBSD patterns
  - Crystal distortion can be measured by measuring the shifts
  - Hydrostatic strains do not realign crystal planes and cannot be detected

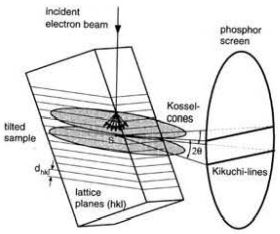

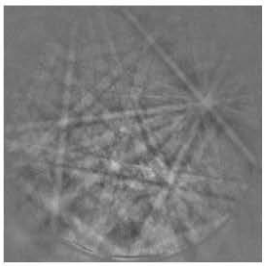

[1] A. J. Wilkinson, G. Meaden, D. Dingley. Ultramicroscopy 106:307-313, 2006.

Cross-Correlation-Based GND Measurement

- Standard EBSD error is ~1°
  - Magnified in calculations of misorientation
  - Cross-correlation method [1] was developed to improve resolution
- Distortion of crystal lattice causes shifts in EBSD patterns
  - Crystal distortion can be measured by measuring the shifts
  - Hydrostatic strains do not realign crystal planes and cannot be detected

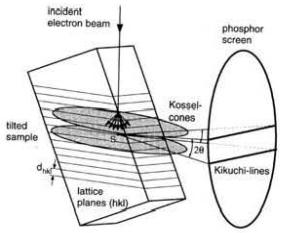

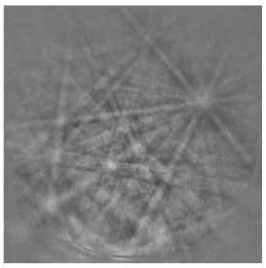

[1] A. J. Wilkinson, G. Meaden, D. Dingley. Ultramicroscopy 106:307-313, 2006.

Calculating GND densities from pattern shifts

- A reference pattern is divided into regions
- Shifts of each region are measured at each point
- One region gives two equations:

$$r_1 r_3 \left[\frac{\partial u_1}{\partial x_1} - \frac{\partial u_3}{\partial x_3}\right] + r_2 r_3 \frac{\partial u_1}{\partial x_2} + r_3^2 \frac{\partial u_1}{\partial x_3} - r_1^2 \frac{\partial u_3}{\partial x_1} - r_1 r_2 \frac{\partial u_3}{\partial x_2} = Q_1 r_3$$

$$r_2 r_3 \left[\frac{\partial u_2}{\partial x_2} - \frac{\partial u_3}{\partial x_3}\right] + r_1 r_3 \frac{\partial u_2}{\partial x_1} + r_3^2 \frac{\partial u_2}{\partial x_3} - r_2^2 \frac{\partial u_3}{\partial x_2} - r_1 r_2 \frac{\partial u_3}{\partial x_1} = Q_2 r_3$$

- Measuring 4 regions allows 8 elements of distortion tensor to be derived
  - 9th element must be derived from boundary conditions
  - More than 4 regions allows least-squares fitting to improve accuracy

APPLICATION: FATIGUE IN TITANIUM ALLOYS

Crystallography of Ti-6Al-4V

- Two phases: HCP α and BCC β
  - Ti-6Al-4V as received is mostly α
- Three main slip planes in α
  - Slip along **a** <11-20> and **c+a** <11-23> directions
  - **c+a** requires higher stress to activate (~3-4x)

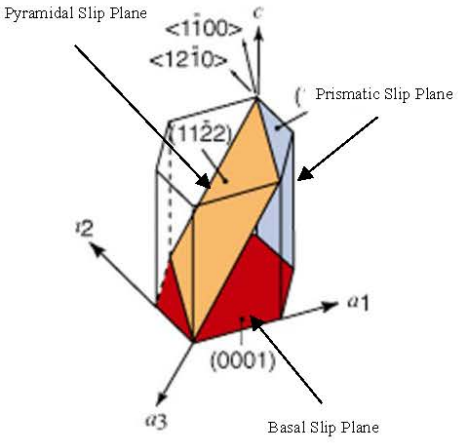

http://web.earthsci.unimelb.edu.au/wilson/icel/introduction.html

Crystal Anisotropy

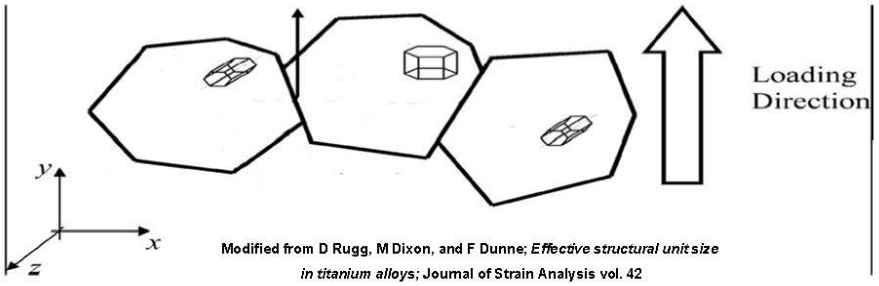

Modified from D Rugg, M Dixon, and F Dunne; *Effective structural unit size in titanium alloys*; Journal of Strain Analysis vol. 42

- No resolved shear stress on basal/prismatic planes in center grain
- Grain becomes resistant to plastic deformation relative to others

Fatigue Testing

- Material: Ti-6Al-4V rolled bar stock provided by Rolls-Royce
  - Globular primary α-phase grains, small amount of grain-boundary β phase
  - Average grain size ~12 μm
- Deformed in fatigue to failure
  - Peak stress 900 MPa, stress ratio 0.1
- Cross-correlation EBSD used to measure GND distributions

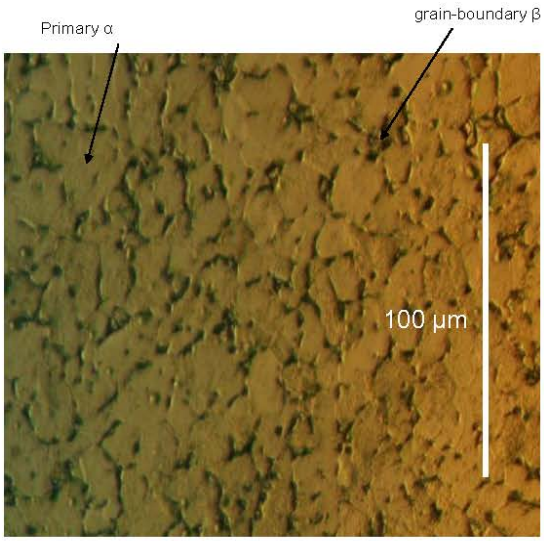

Relating GND Densities to Microstructure

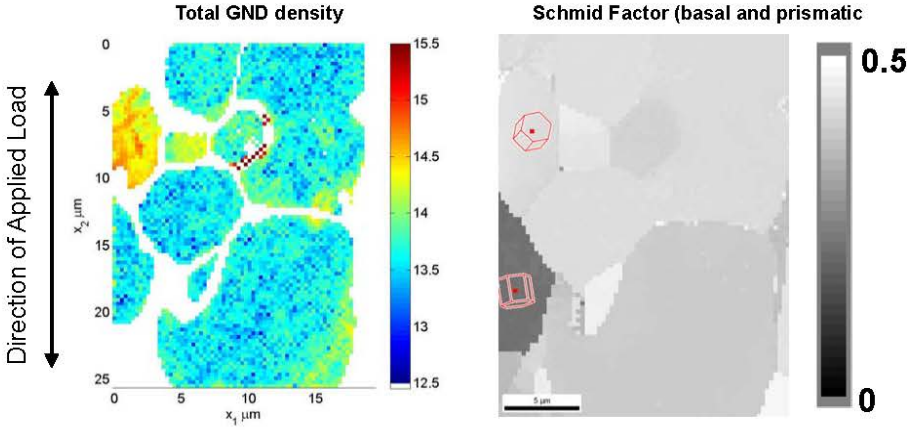

a vs c+a GND densities

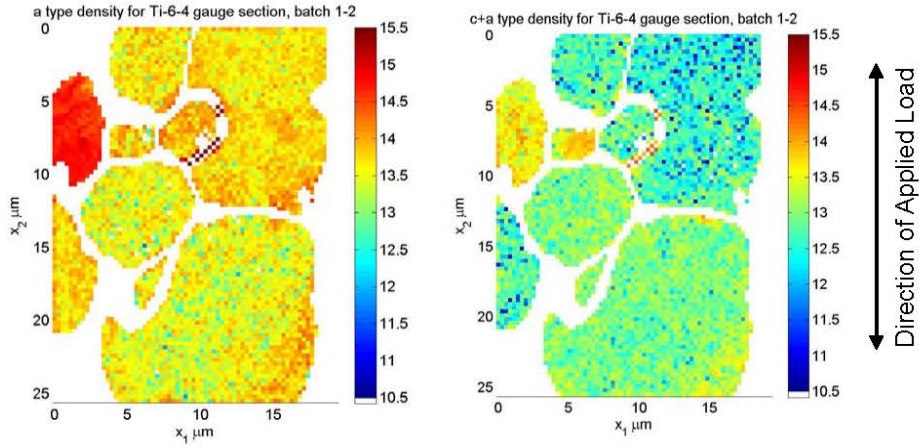

GND Pile-Up

- First proposed as a crack initiation method by Stroh [1]
- Suggested by Bache and Evans as a mechanism in cold-dwell sensitivity [2]

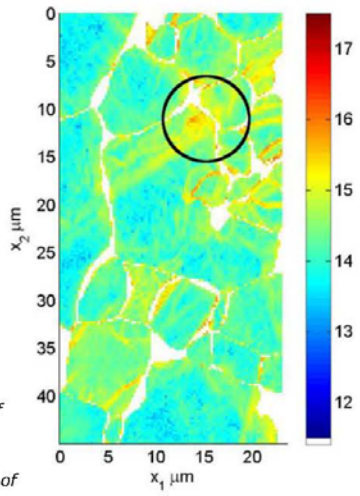

[1] A. N. Stroh. *Proceedings of the Royal Society of London. Series A, Mathematical and Physical Sciences*, 223:404-414, 1954.

[2] W. J. Evans, M. R. Bache. *International Journal of Fatigue*, 16:443-452, 1994.

GND Statistics

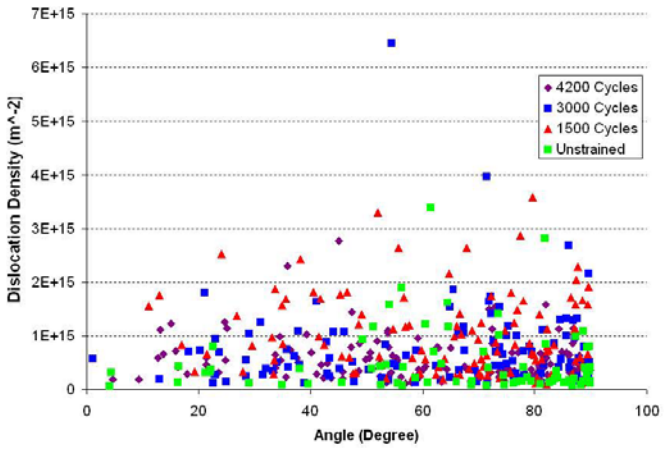

GND Statistics

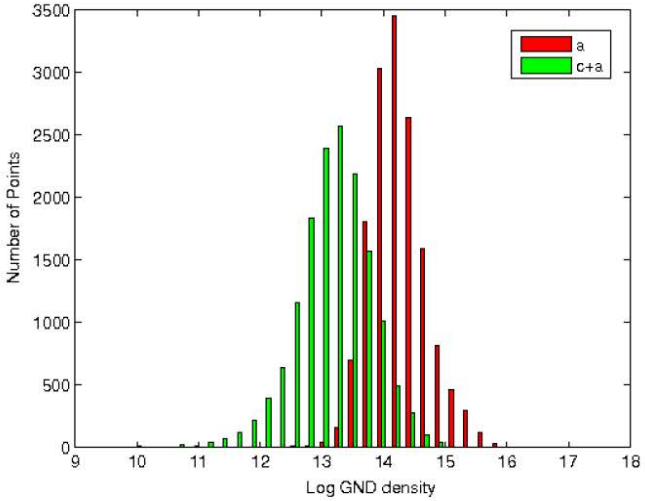

Conclusions

- Cross-correlation based EBSD can be used to study storage of geometrically necessary dislocations on a microstructural level
- Grain-grain interactions play a significant role in inhomogeneous deformation in Ti-6Al-4V
  - No direct link between crystal orientation and GND density
- Dislocation pile-up along a slip band, and slip penetration into a neighbouring grain, have been observed.

Transformation af udskillelser på atomar skala

Hilmar Danielsen, DTU Mekanik

Transformation af udskillelser på atomar skala

Hilmar K. Danielsen
DTU Mekanik

MN → CrMN

M = V, Nb or Ta

Two different 12%Cr martensitic steels investigated:

(V/Nb)N → Cr(V/Nb)N
TaN → CrTaN

Fremstilling af prøver til TEM (carbon extraction replica)

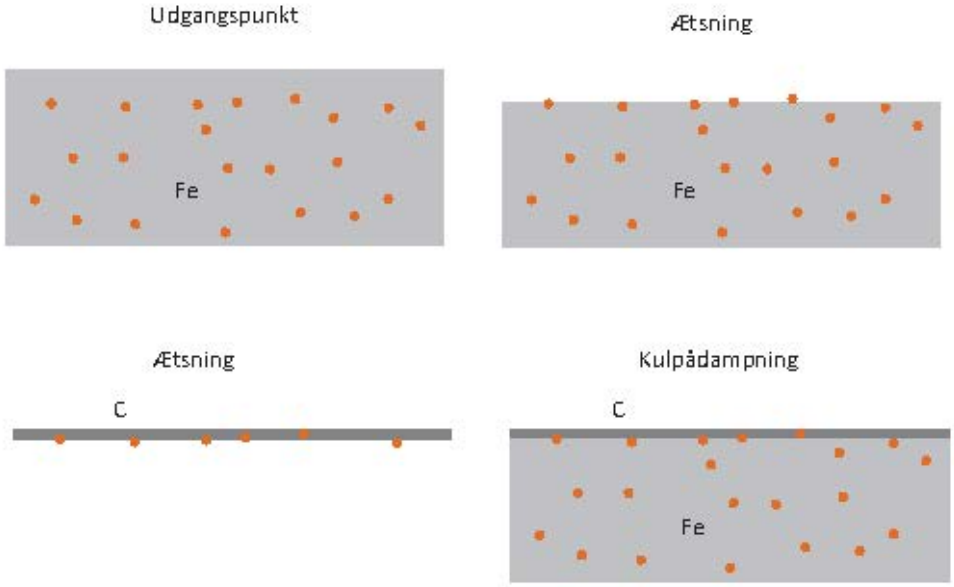

Investigations performed using FEI TITAN 300KV analytical TEM with High Angle Annular Dark Field (HAADF)

MN
(VN, NbN, TaN)

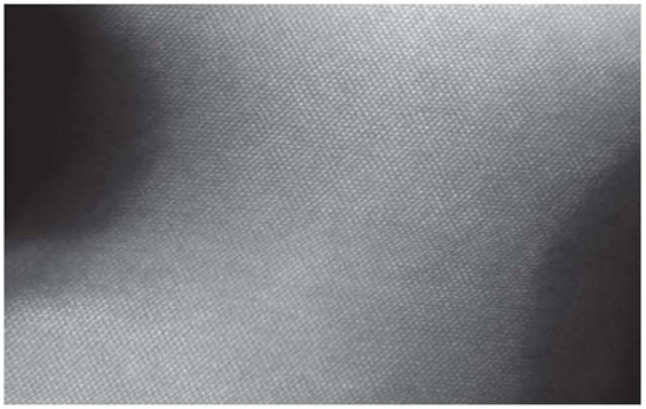

HAADF billede af (V,Nb)N

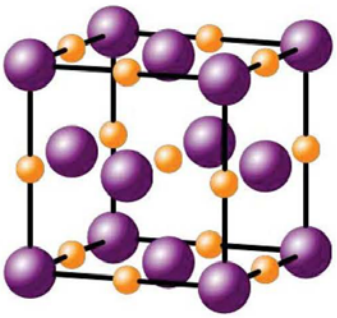

NaCl type enhedscelle

CrMN

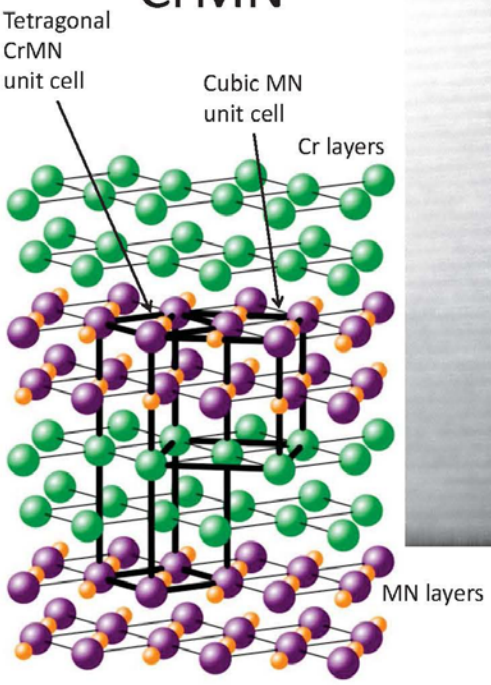

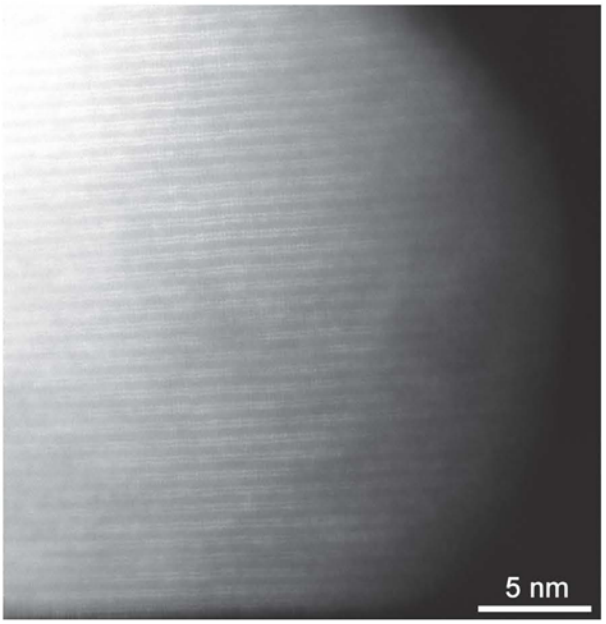

High resolution image of Cr(V,Nb)N showing double layered structure.

The cubic MN and tetragonal CrMN are bound together as one particle, it is possible to follow the atomic layers through the "interface".

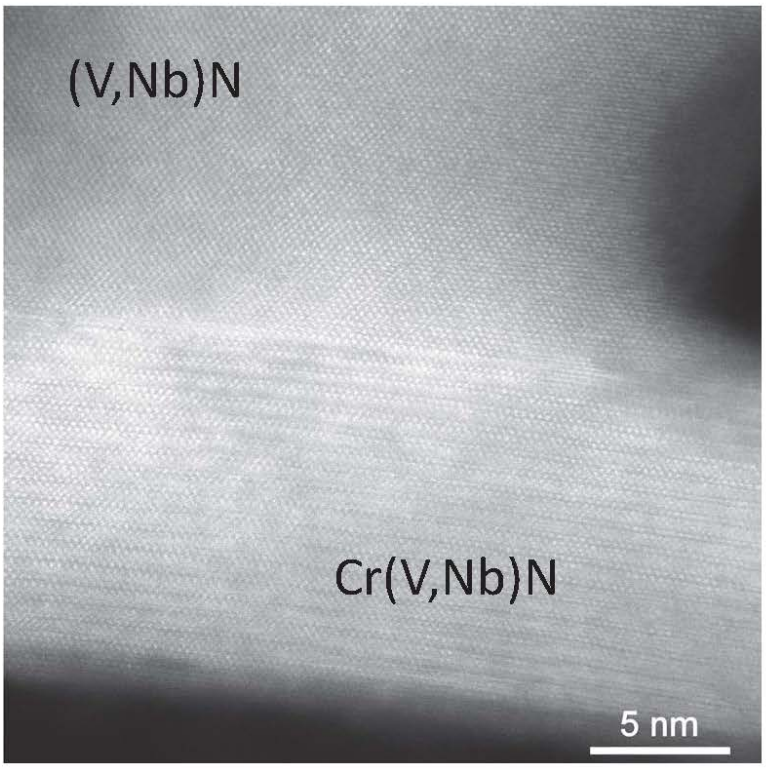

The Cr(V,Nb)N does not have a perfect lattice, there are triple layers, layers changing from Cr to (V,Nb)N etc.

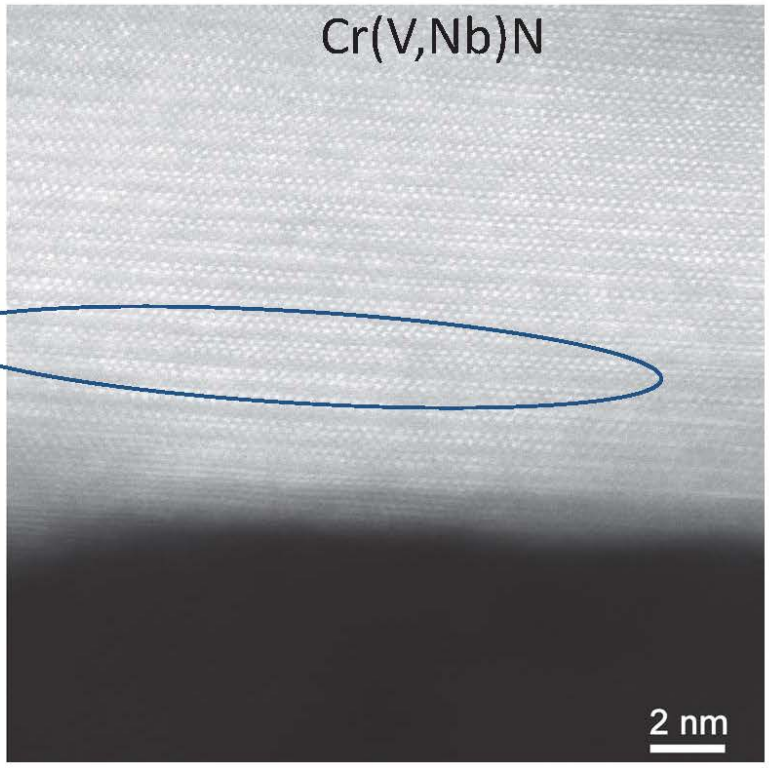

CrTaN has much clearer contrast as Ta atoms are very heavy compared to Cr atoms. Ta atoms are clearly visible while the Cr atoms are very dark.

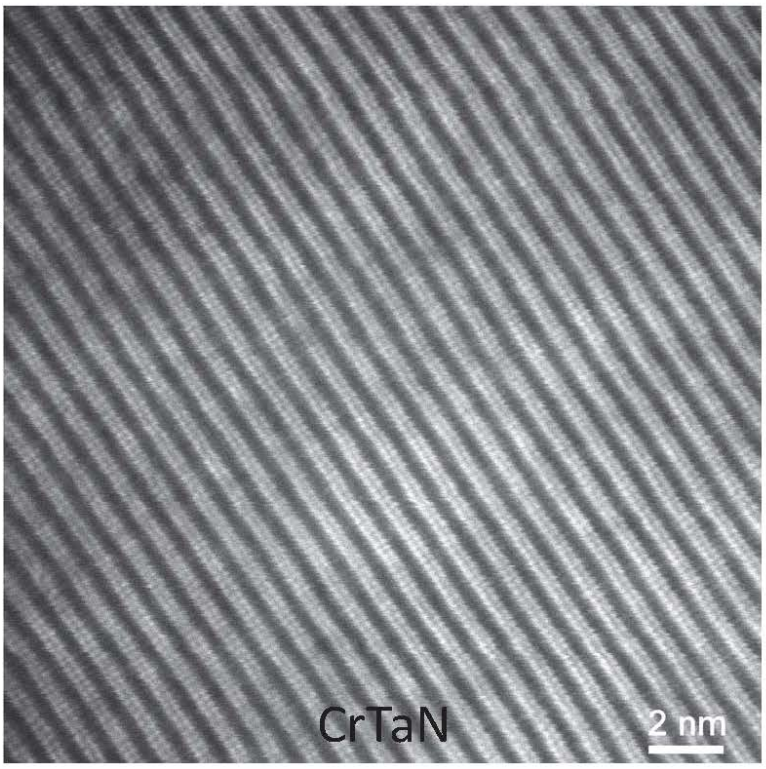

Cr atoms arrange themselves as double layers (dark lines)

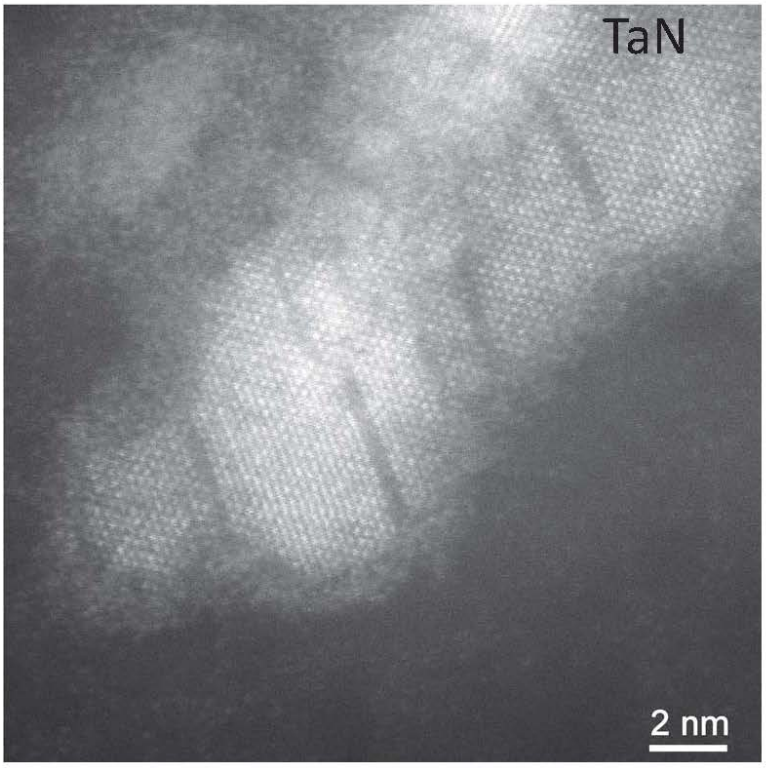

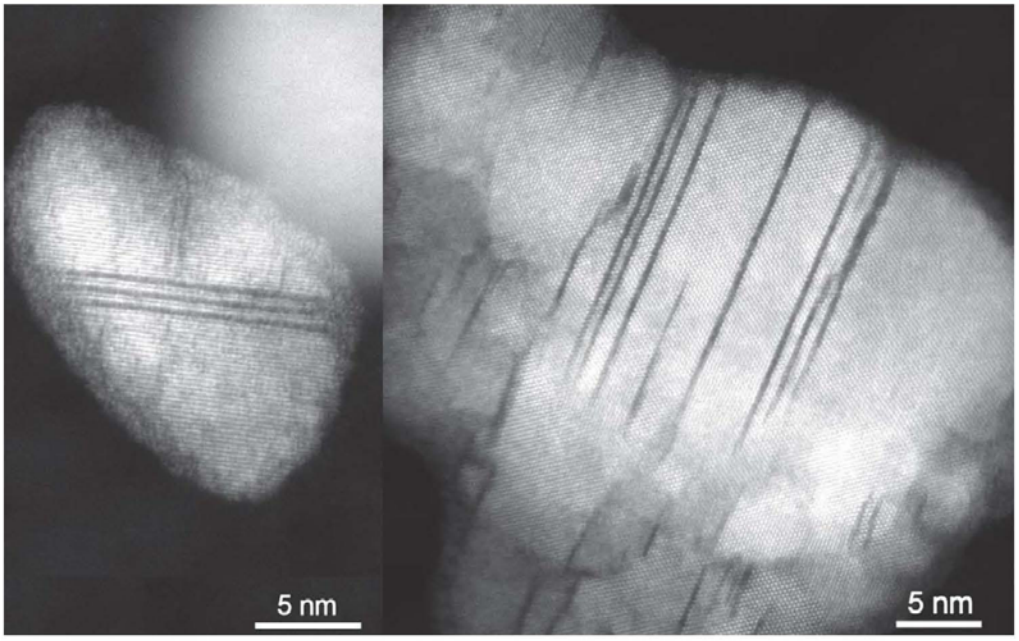

Transformation with a clear orientation relationship

Cr double layers appear as straight parallel lines through the TaN crystal structure

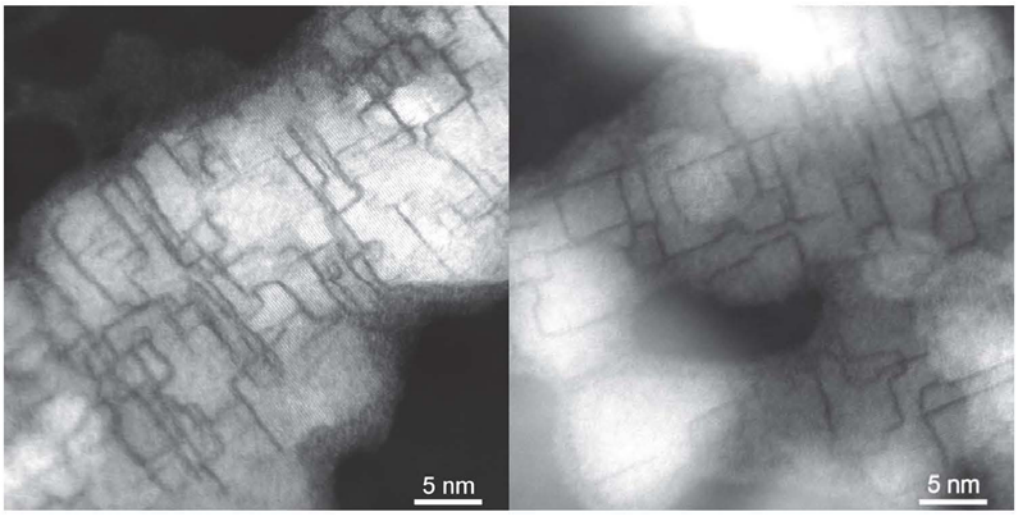

Transformation with a chaotic orientation relationship

Cr double layers have not decided upon the orientation of the future tetragonal crystal

Interface between CrMN and MN. The crystal structure can be followed from one region to the other.

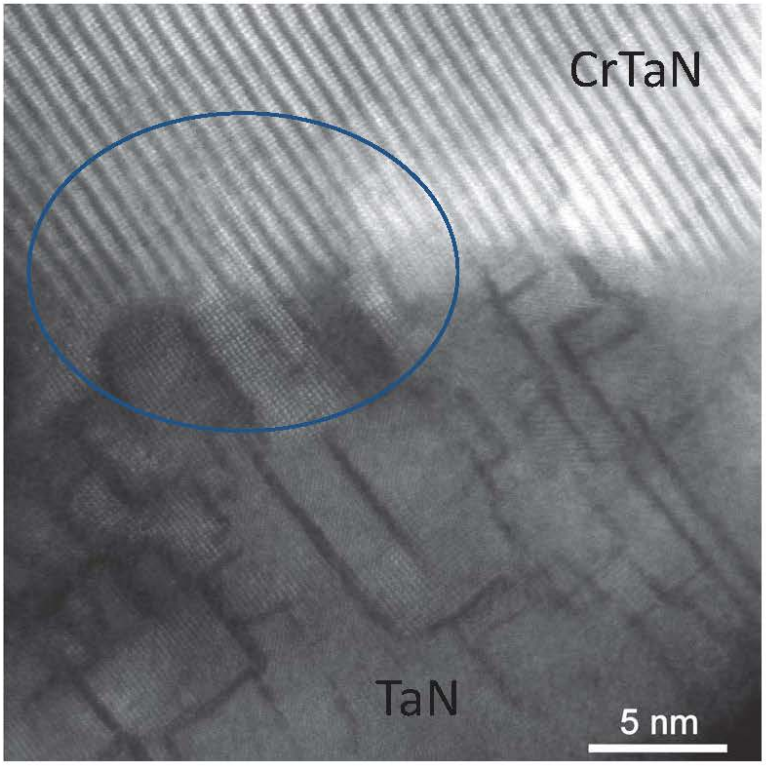

TaN particles with amorphous layer

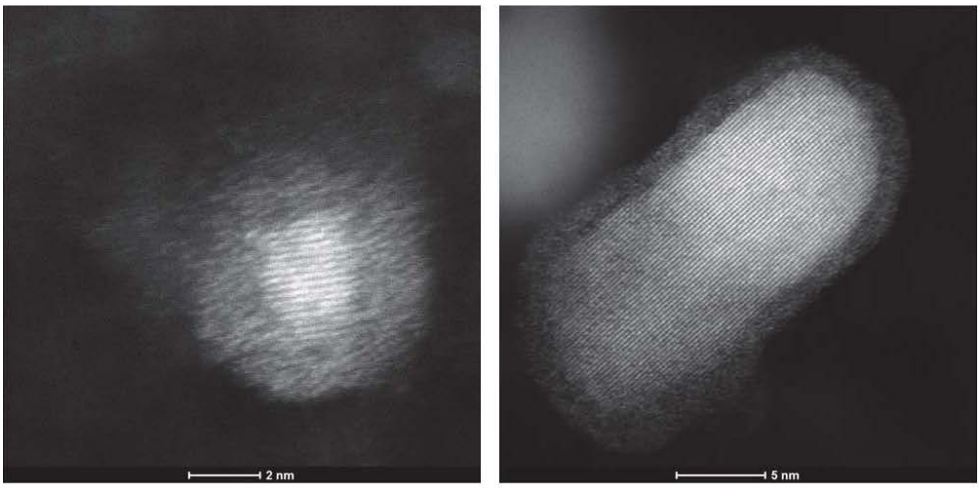

Areas where the electron beam has been concentrated crystallize

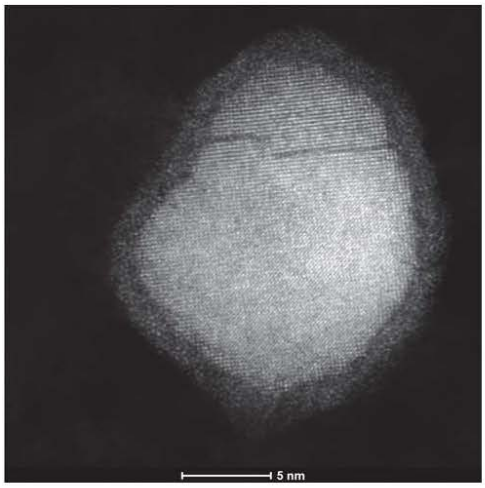

Before

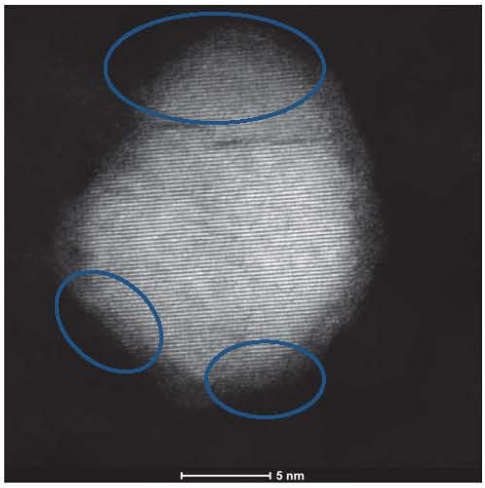

After

Entire interface crystallising after electron beam exposure

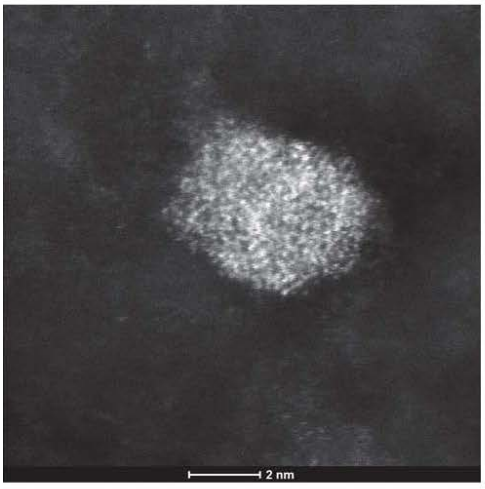

Before

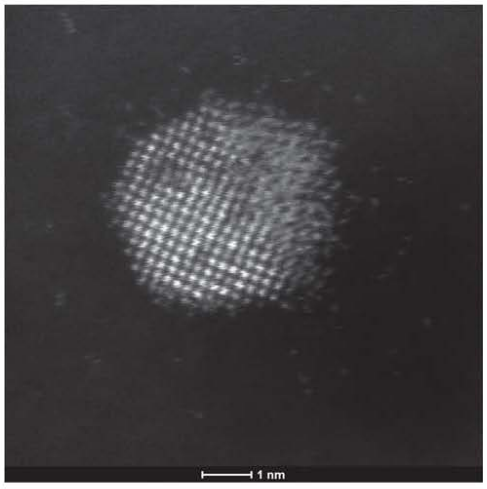

After

Precipitate interfaces

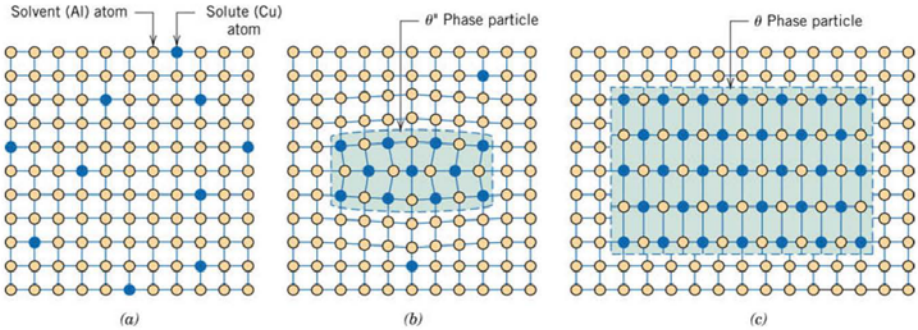

Solid solution | Semi-coherent precipitates | Incoherent precipitates

Semi and incoherent MN

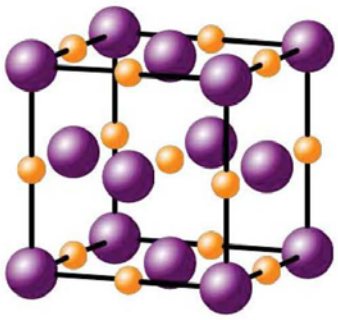

Lattice parameters

VN: 0.413 nm	misfit: 2%	no amorphous layer
NbN: 0.439nm	misfit: 9%	amorphous layer
TaN: 0.440nm	misfit: 9%	amorphous layer

Baker-nutting relationship

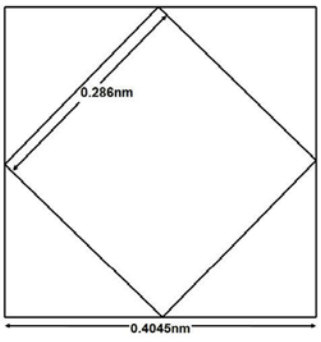

Edge of a large Fe_2W particle

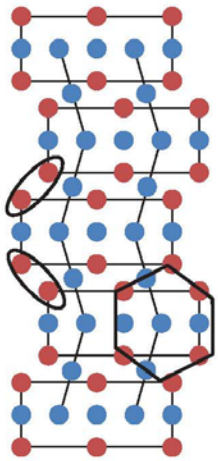

Small Fe_2W particle (thin)

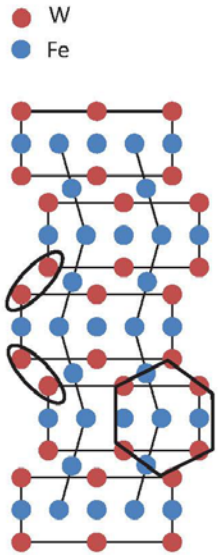

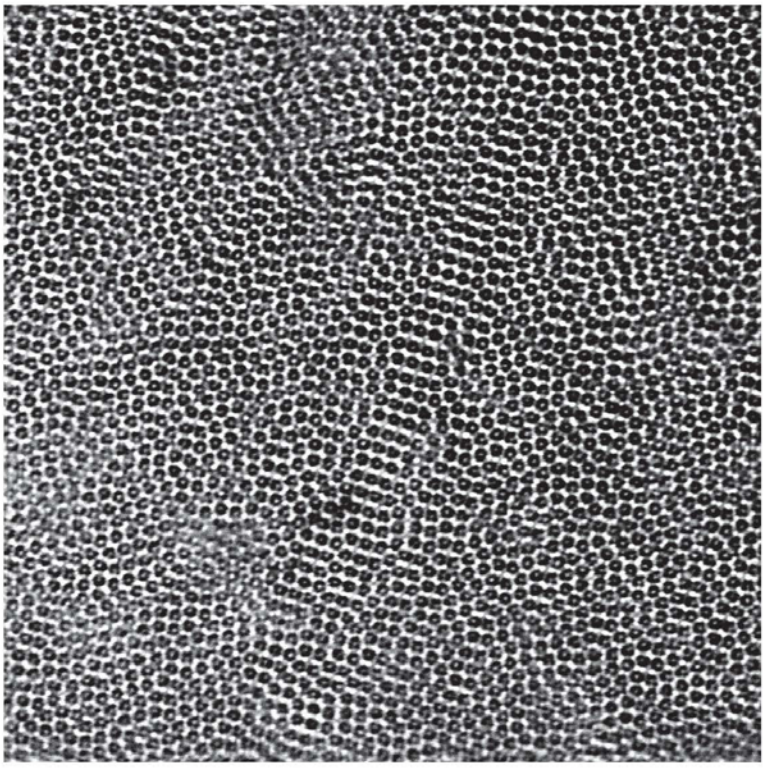

Konklusion

- TaN kan transformere deres sammensætning og krystalstruktur til en anden type partikler
- Partikler kan have en meget uordnet krystalstruktur
- På atomar skala er vores prøver lette at påvirke (elektron stråle, ætsning osv)

Structure and Chemical Characterization by Electron Microstrcopy – Spanning the micro and nano regime

Jakob Birkedal Wagner, DTU CEN

Structural and Chemical Characterization by Electron Microscopy – Spanning the micro and nano regime

Jakob B. Wagner

Acknowledgements:

DTU Cen, Technical University of Denmark:
Hossein Alimadadi, Christian D. Damsgaard, Thomas W. Hansen

EPFL:
Quentin Jeangros

FEI:
Jörg Jinschek

DTU Cen
Center for Electron Nanoscopy

DTU Center for Electron Nanoscopy

- Realized by a generous donation from the A.P. Møller og Hustru Chastine Mc-Kinney Møller's Fond til Almene Formaal
- DKK 100,000,000 ~ C14,000,000
- Grant announced in January 2006
- *"Establish a World Class Facility with a unique suite of advanced electron microscopes, in a purpose-built building"*
- Inaugurated in December 2007

- Hosting 7 electron microscopes
  - 2 high-end TEM (1 ETEM)
  - 1 work horse TEM
  - 2 dual beam SEM/FIB
  - 2 SEM

FEI Microscopes at DTU Cen

- SEMs
  - Inspect 'S'
    - Workhorse
    - EDX/WDS
  - Quanta 3D FIB/SEM
    - Sample prep
  - Quanta 200 FEG
    - High res
    - Cryo
    - EDX
  - Helios Nanolab FIB/SEM
    - EBSD
    - EDX
- TEMs
  - Tecnai T20 G2
    - Workhorse
    - EDX/GIF
  - Titan 80-300 probe corrected
    - Holography
    - EDX/GIF
  - Titan 80-300 image corrected
    - ETEM
    - EDX/GIF

More info on the web: www.cen.dtu.dk

Image Formation (at all scales)
-Beam-specimen interactions

- The fast electrons is focused and controlled easily by electro-magnetic lenses
- Interaction between fast electrons and matter creates a variety of signals

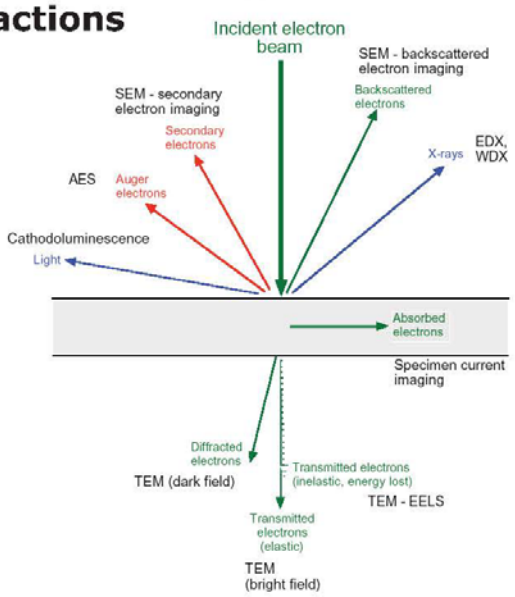

Dual Beam: EBSD, ion channeling imaging

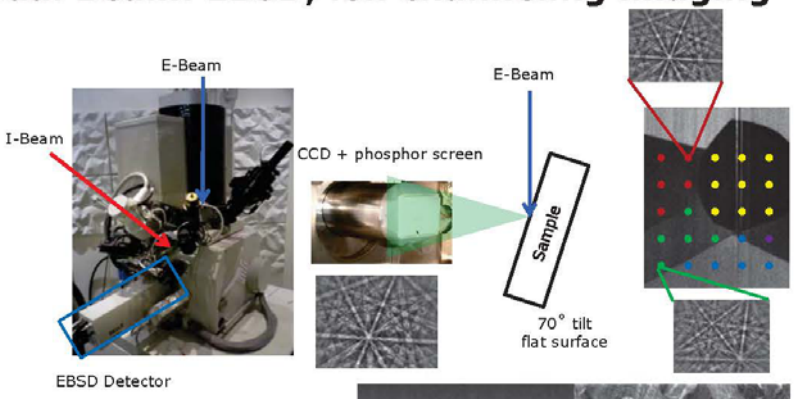

SE Contrasts:

Crystallographic orientation (channeling)
Chemistry
Topographic

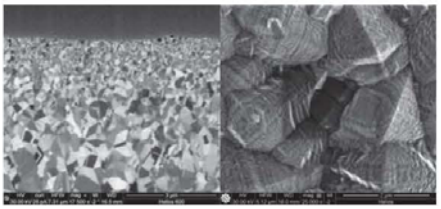

C.A. Volkert and A.M. Minor - MRS bulletin 32 -2007

Failure of Solid Oxide Fuel Cells

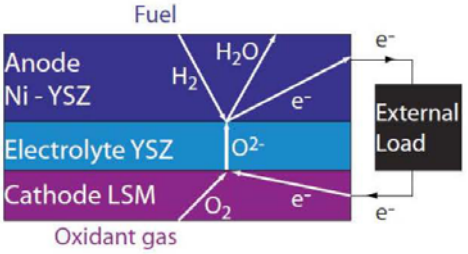

H_2O, excess fuel & oxidant gas to burner, gas turbine and heat exchanger

- Fuel Cell Anode Failure
  - Redox stability of NiO/YSZ based anode

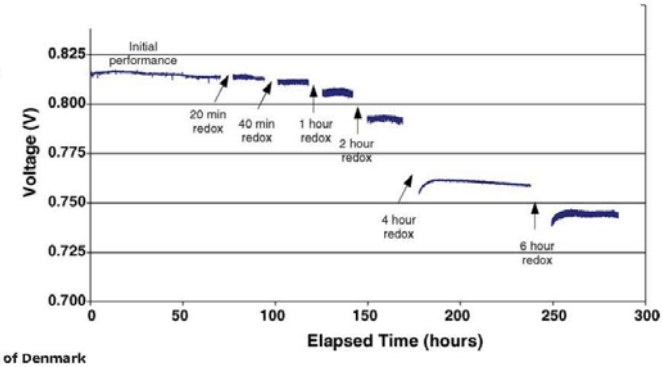

Environmental TEM

- C_S Image Corrector & Monochromator. E-cell
- Installed gas lines: N_2, He, Ar, O_2, H_2, CO, CO_2, CH_4 & H_2O
- Possible to attach other (premixed) gases
- Full control of composition using mass flow controllers
- Total pressure in E-Cell: up to 2000Pa
- Temperature depends on heating holder, gas pressure and gas composition (Example: approx. 700° C @ 100Pa H_2)
- Dynamic acquisition (at the moment 5 frames/s)
- EELS of gases possible

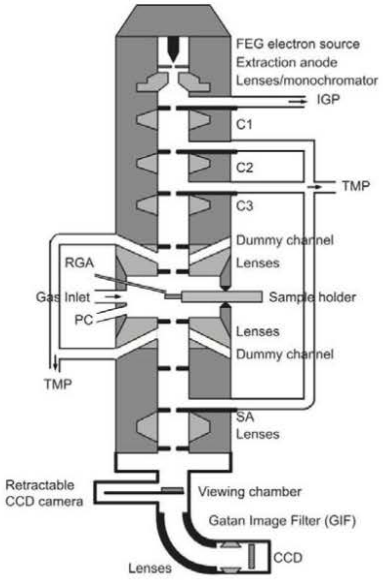

T. W. Hansen, J. B. Wagner and R. E. Dunin-Borkowski, *Mater. Sci. Tecnol.*, 26, 1338 (2010)

Imaging at Different Length Scales

-2D to 3D and irreversible changes

ETEM sample

FIB slice of NiOx/YSZ based SOFC

Complementary and dynamic information from multiple facilities on the same sample is needed

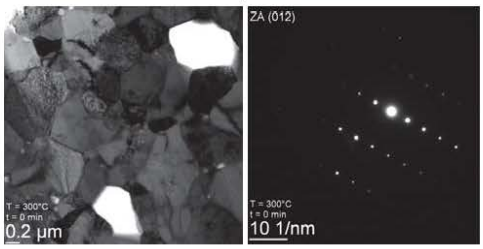

Reduction
150Pa H_2

SEM sample

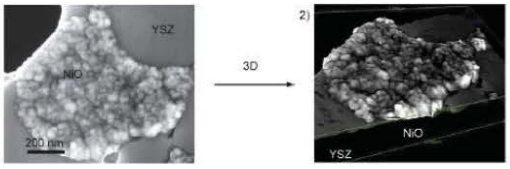

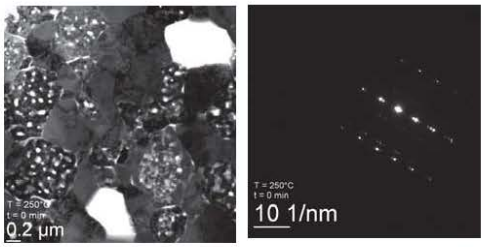

Oxidation
320Pa O_2

Q. Jeangros et al., Acta Materialia 58 (2010) 4578–4589

Elemental mapping (oxygen)

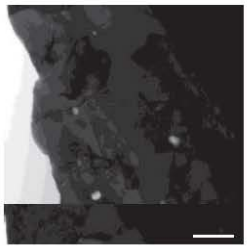

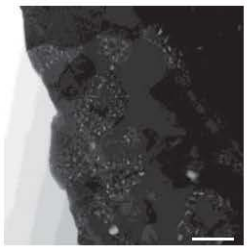

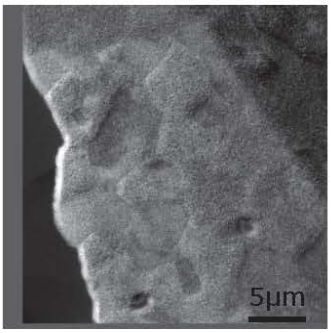

310°C → 430°C in 150Pa H_2

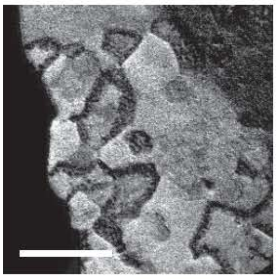

From Structure to Application

Q. Jeangros et al., Acta Materialia 58 (2010) 4578–4589

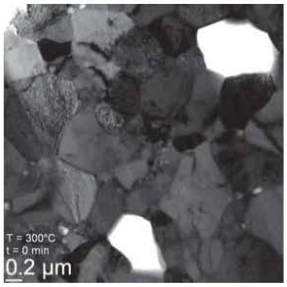

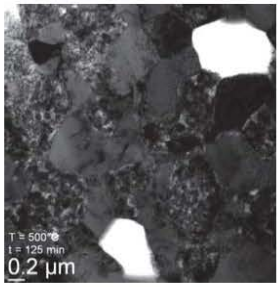

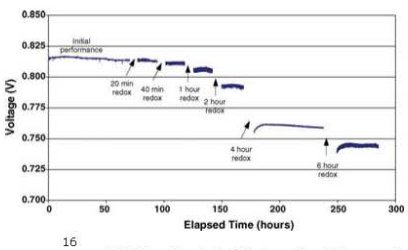

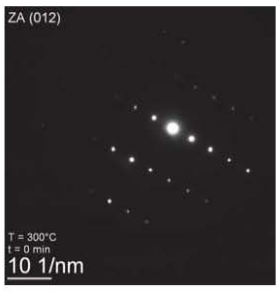

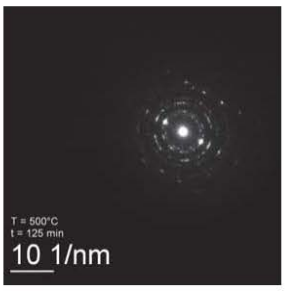

Deeper insight in Nickel reduction using model system

- NiO crystals
- 130Pa H_2

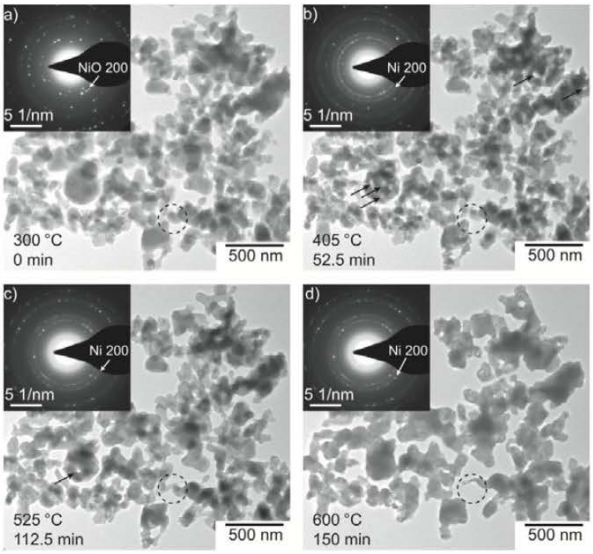

Evolution during reduction

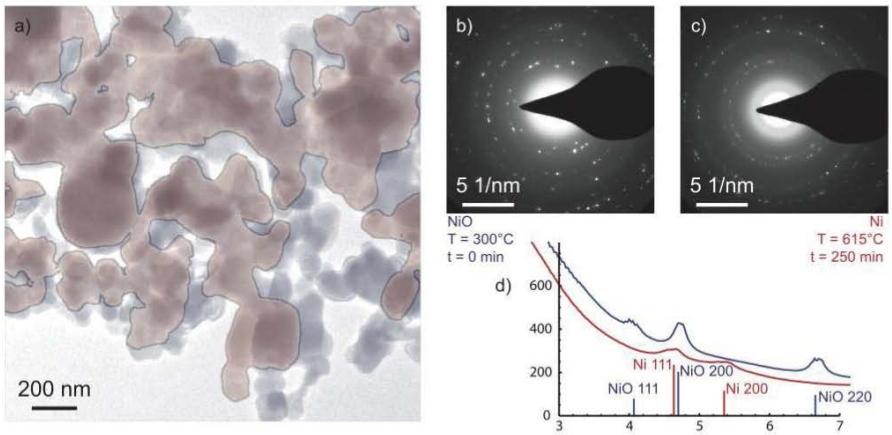

- In situ reduction in 130Pa H_2

Q. Jeangros et al., J. Mat. Sci. DOI 10.1007/s10853-012-7001-2

High Resolution ETEM

- Atomic arrangement visualized at 500°C in 130Pa H_2

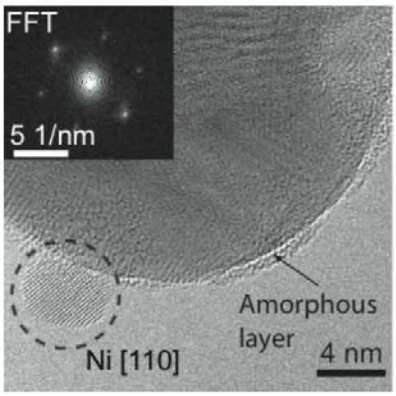

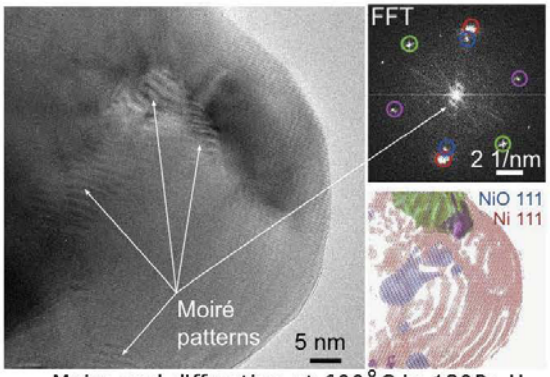

- Moire and diffraction at 600°C in 130Pa H_2

Q. Jeangros et al., J. Mat. Sci. DOI 10.1007/s10853-012-7001-2

Determination of Activation Energies - Spectroscopical Analysis

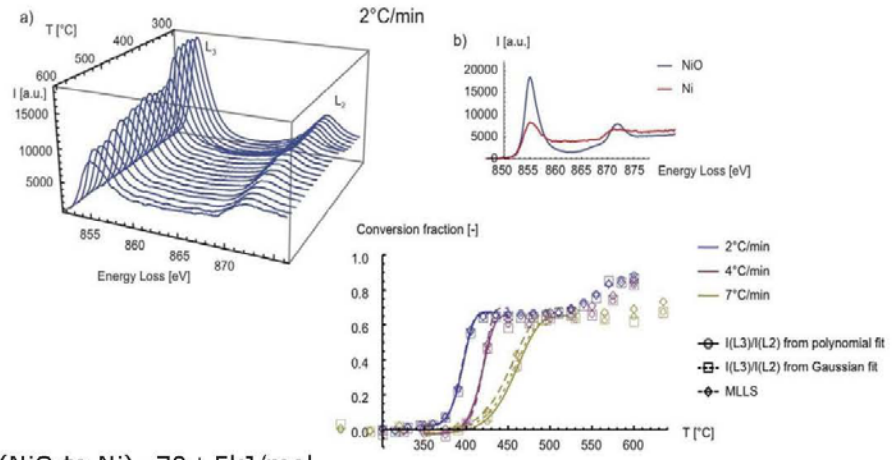

E_a (NiO to Ni) = 70 ± 5kJ/mol
Similar results obtained from diffraction analysis

Q. Jeangros et al., J. Mat. Sci. DOI 10.1007/s10853-012-7001-2

Methodology

- A complete dataset using different tools and techniques can be acquired
  - Different length scales
  - Different types of information (crystallographic, morphology, chemical, etc.)
- From analysis of such a dataset a coherent understanding of the process can be obtained

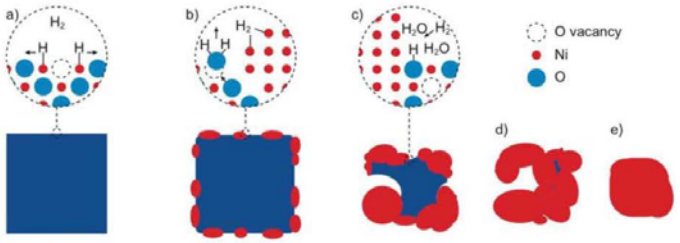

Q. Jeangros et al., J. Mat. Sci. DOI 10.1007/s10853-012-7001-2

Nanoparticle mobility

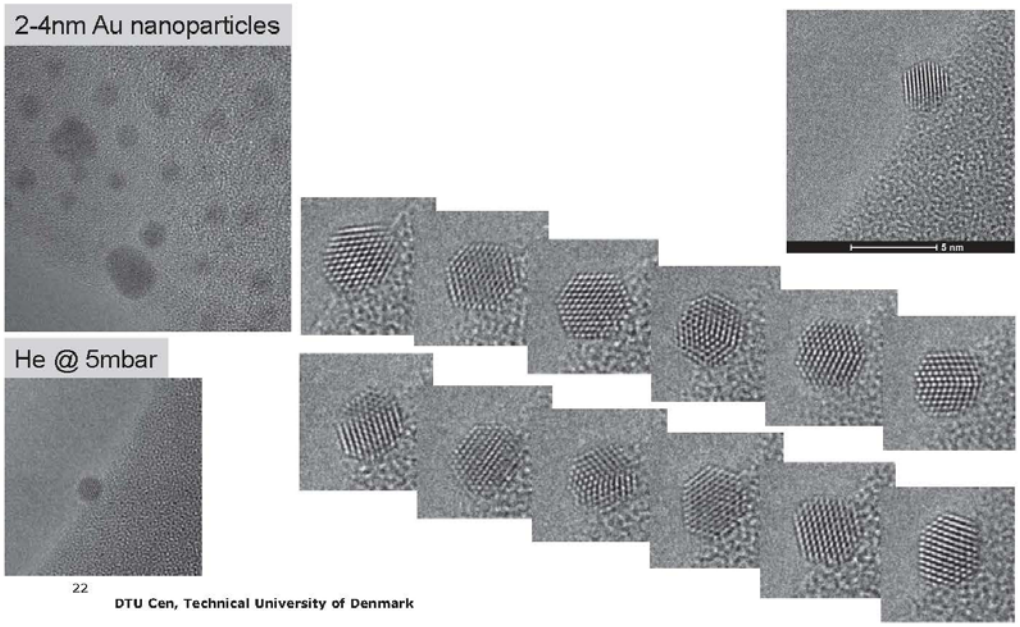

Au/Graphene

- Ca. 4x real time
- RT, Vacuum: Particles are mainly immobile
- Slight rotations are observed
- Coalescence events occur, but equilibrium shapes are only slowly obtained
- Surface reconstruction occurs
- All movies recorded at same beam current density (ca. 1A/cm^2)

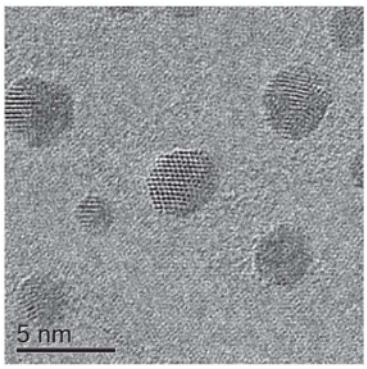

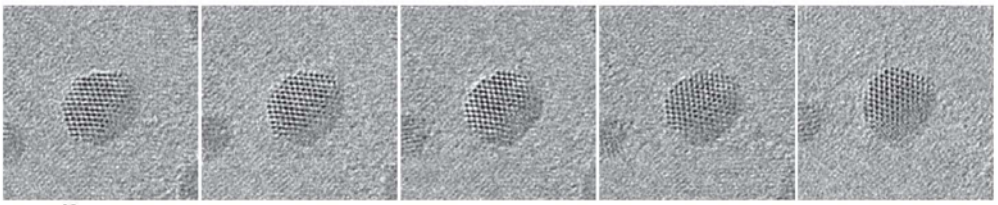

Au/Graphene

- Ca. 8x real time
- 104°C, 200Pa H_2
- Cross correlation used for image alignment
- At low temperatures, particles wobble around equilibrium positions, but do not tend to migrate long distances
- Particles in close proximity can coalesce into to single particles, but do not readily form single crystalline structures

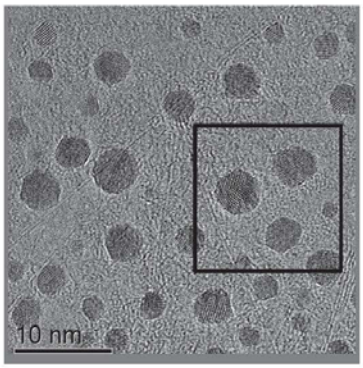

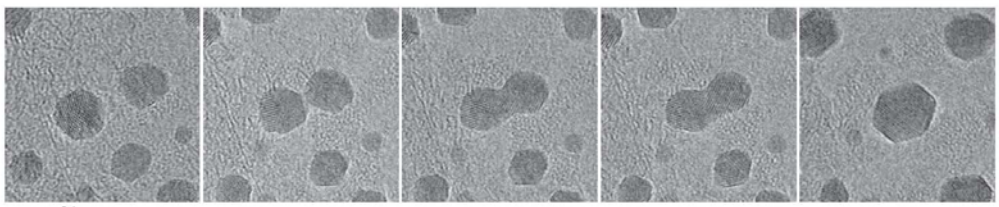

Outlook – longer term

Combining complimentary characterization and sample prep. techniques with TEM

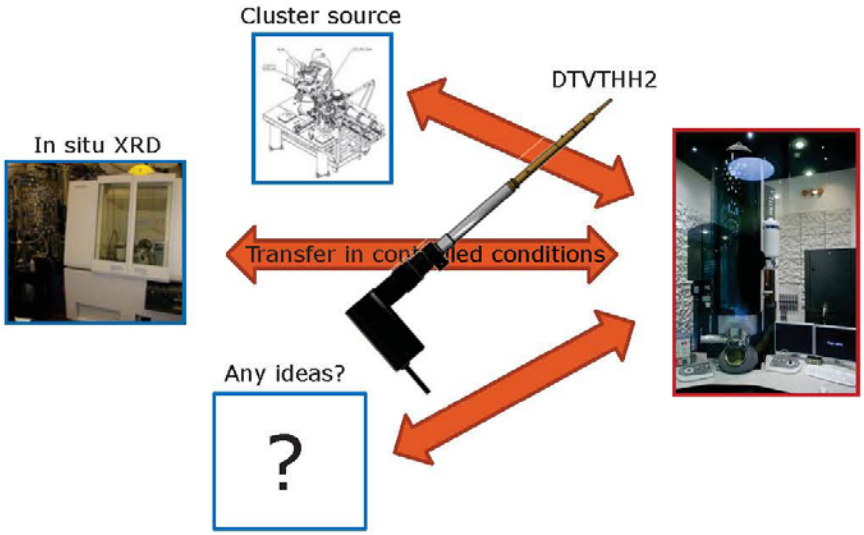

Interested in collaboration?

- Please contact us at cen.dtu.dk

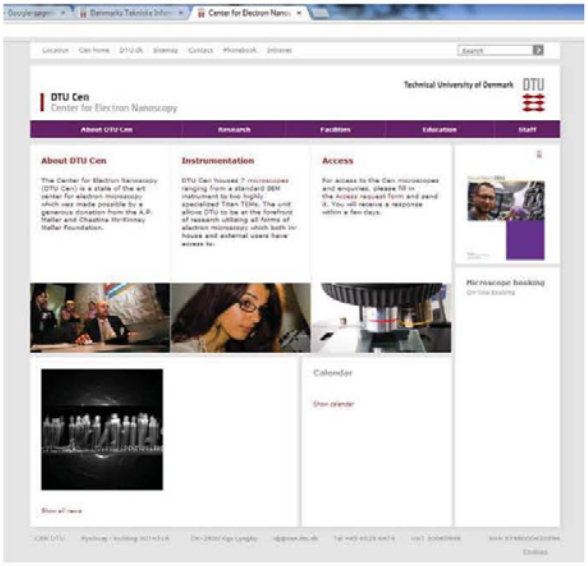

Nanostruktur og styrke af stål deformeret ved valsning og med shot peening

Niels Hansen, DTU Vindenergi

Dansk Metallurgisk Selskabs Vintermøde 2013

Nanostruktur og styrke af stål deformeret ved valsning og ved shot peening

N. Hansen[1], X.D. Zhang[1], Y. Gao[2], X. Huang[1]

[1]Danish-Chinese Center for Nanometals, Wind Energy Department, Technical University of Denmark, Campus Risø, DK-4000 Roskilde, Denmark

[2]Beijing Institute of Aeronautical Materials, AVIC, Beijing 100095, P.R. China

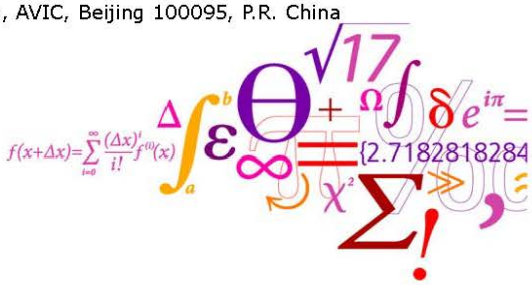

DTU Wind Energy
Department of Wind Energy

Plastisk deformation

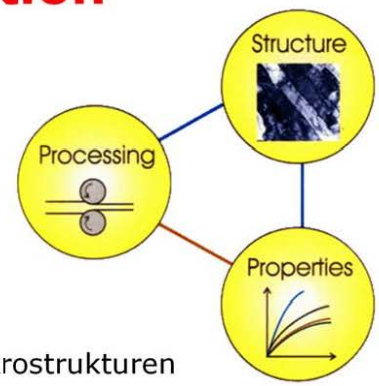

Generelle principper

- Plastisk deformation forfiner mikrostrukturen
- En finere mikrostruktur følges af højere styrke
- Høj styrke kan opnås gennem kraftig plastisk deformation

Evolution of deformation microstructures

Subdivision of grains/crystals by dislocation boundaries in characteristic 2D and 3D configurations.

Carpet structure in Cu

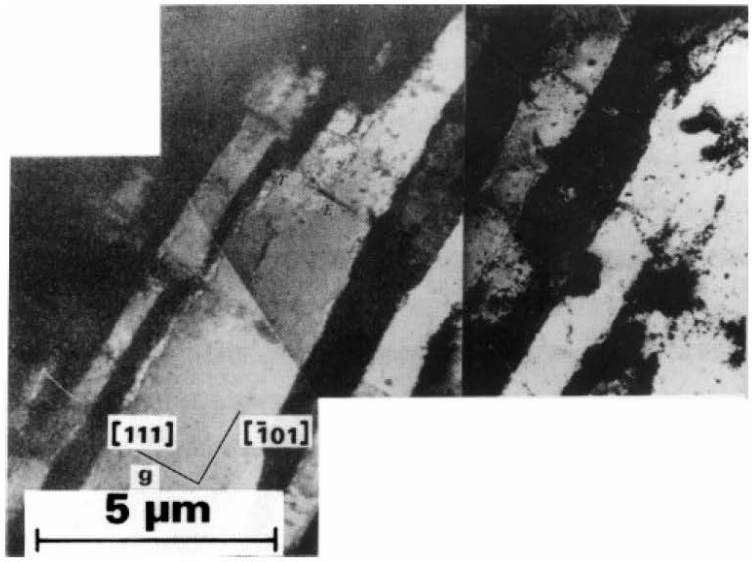

Cell structure in Fe

Cold deformed structures subdivided by extended almost planar boundaries (carpets) and short cell boundaries forming cell blocks

99.96% Al $\varepsilon_{vM} = 0.12$ 99.99% Ni $\varepsilon_{vM} = 0.26$

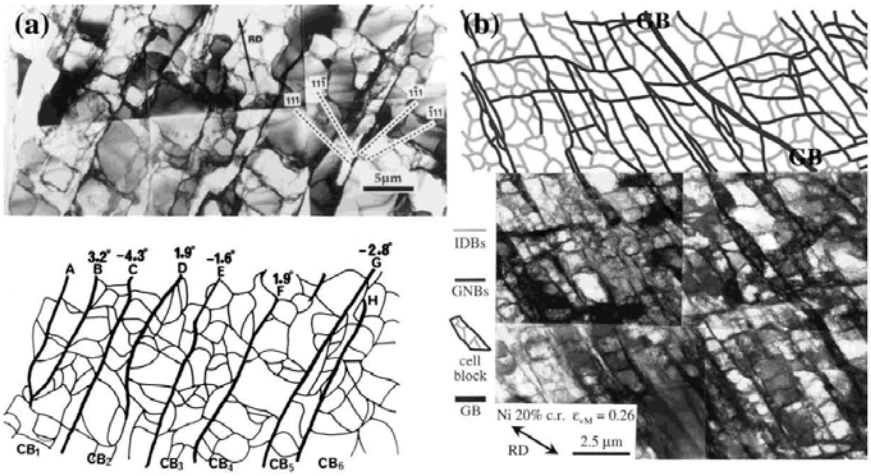

Structural evolution during plastic deformation

Grains/crystals subdivide by formation of dislocation and high angle boundaries, creating hierarchical structures in a finer and finer scale down to the nanometer dimension as the strain and stress increased to a high level.

Large strain deformation

Structural length scale > 100 – 300 nm

Process examples are:
Rolling
Torsion
Drawing
Accumulative roll bonding
Equal channel angular extrusion
Multidirectional deformation

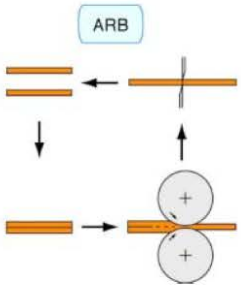

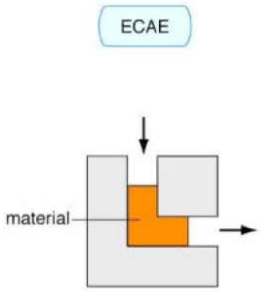

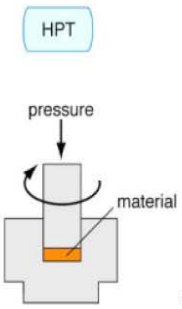

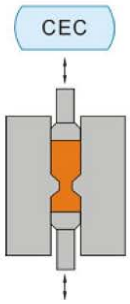

Al and Ni cold rolled to large strain

Al, ε_{vM}=6

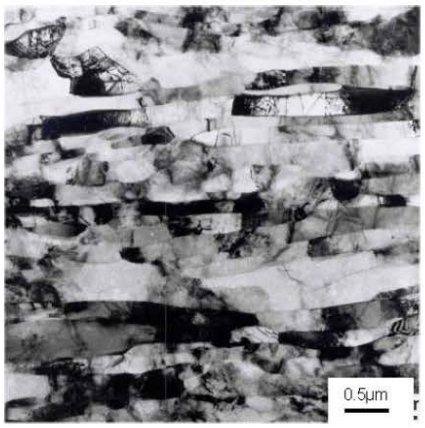

Ni, ε_{vM}=3.5

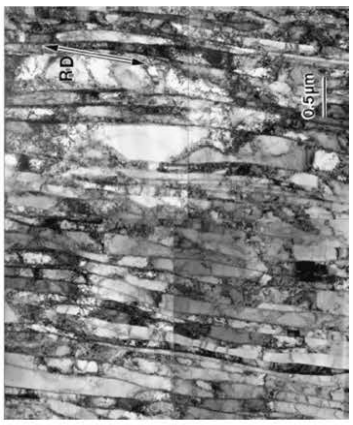

Large strain deformation

Structural length scale
> 50 nm

Process examples are:
High pressure torsion
Dynamic plastic deformation

Structural length scale
> 5 nm

Process examples are:
Ball milling
Surface mechanical attrition
Friction

TEM of 99.99% Ni cold-deformed by high pressure torsion to ε_{VM} 12. The shear direction is marked.

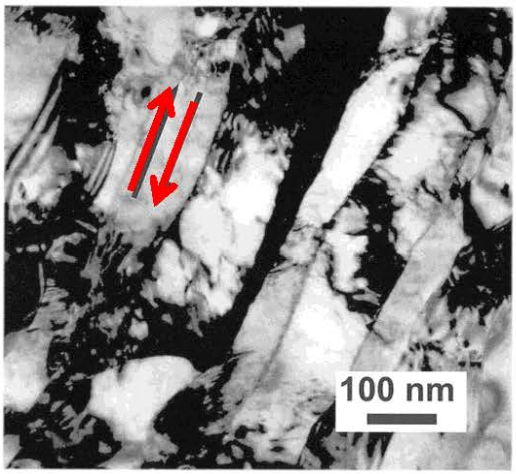

Surface mechanical attrition treatment (SMAT) of iron

- The surface layer is nanostructured with a boundary spacing about 10 nm.
- The subsurface layer is graded and extend to about 50 μm below the surface.

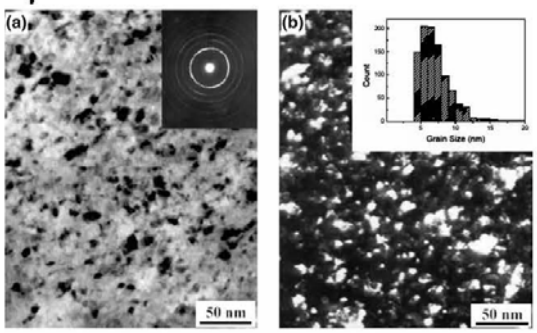

Bright field image (a) and dark field image (b) of 99.95% pure iron – surface layer

Analysis of structure and strength of low carbon steel deformed by shot peening and by cold rolling

Applications

Particle Impact

Shot-peening

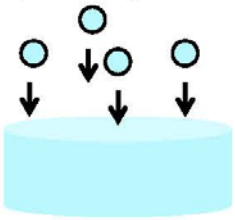

SMAT (surface mechanical attrition treatment)

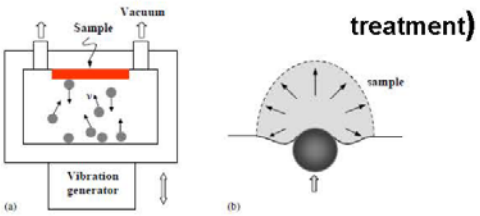

	Shot-peening	SMAT
Shot size	0.05 ~ 1 mm	1 ~ 10 mm
Shot velocity	~ 100 m/s	1 ~20 m/s
Shot direction	Single direction (~ 90°)	Multi-direction (vibration frequency: 20 ~ 50 HZ)
Temperature increase	50-100 °C	50-100 °C
Thickness of graded nanostructures	~ 20 μm	~ 40 μm

Shot Peening (1)

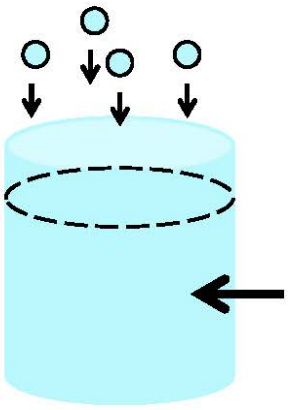

0.8 mm high-carbon steel balls
High shot velocity: 260-300 m/s

Cold rolling: low to high strain
Strain rate: about 0.3 s^{-1}

Material
Pure industrial iron: Fe-0.004C-0.44Al-0.017Ni-0.13Mn-0.0066P

Shot-peening (2)

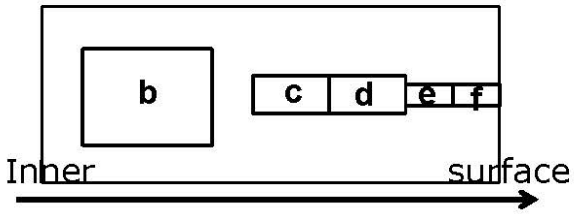

b) 1200 - 600 μm from surface
c) 460 - 260 μm from surface
d) 260 - 60 μm from surface
e) 60 - 30 μm from surface
f) 30 - 0 μm from surface

b: 1200 - 600 μm from surface

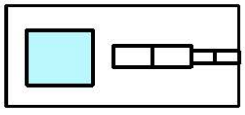

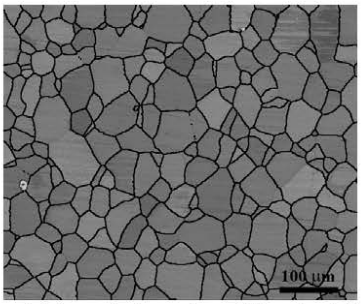

Inner surface

Black line: high angle boundary (Misorientation angle > 15°)

Shot-peening (3)

c: 460 - 260 μm from surface

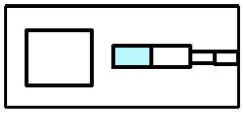

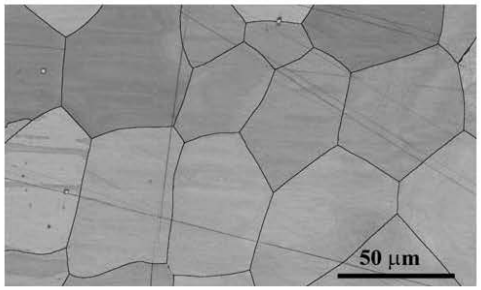

d: 260 - 60 μm from surface

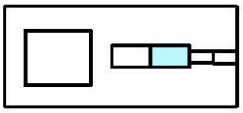

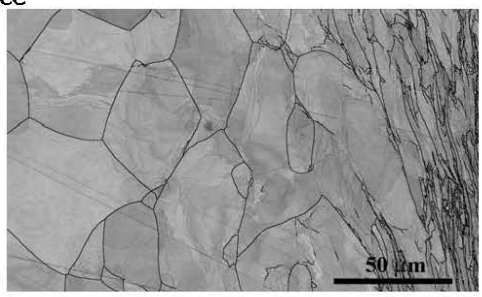

Inner surface

Black line: high angle boundary (Misorientation angle > 15°)

Shot-peening (4)

e: 60 - 30 μm from surface

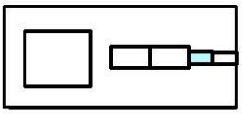

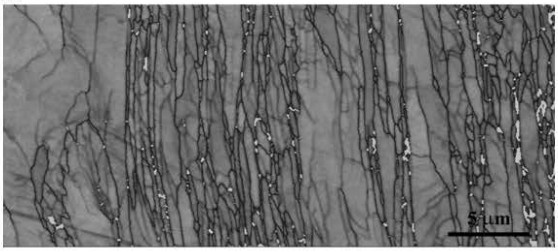

f: 30 - 0 μm from surface

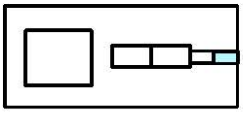

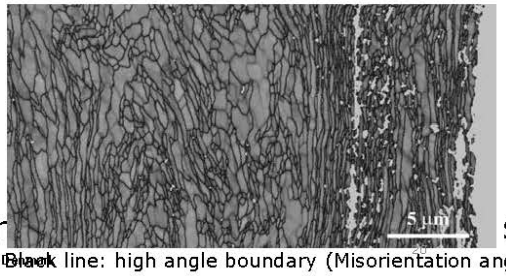

Inner surface

Black line: high angle boundary (Misorientation angle > 15°)

Shot-peening (5)

Lamellar boundary misorientation angle (EBSD)

1200 - 600 μm from surface

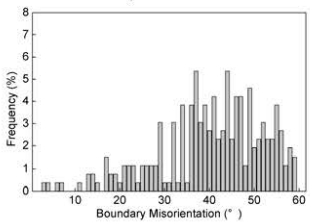

60 - 40 μm from surface

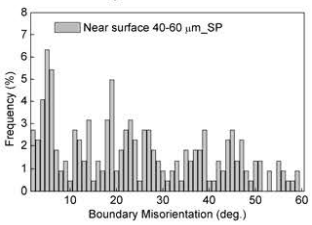

40 - 20 μm from surface

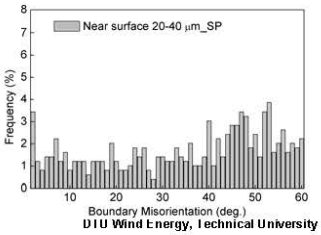

20 - 10 μm from surface

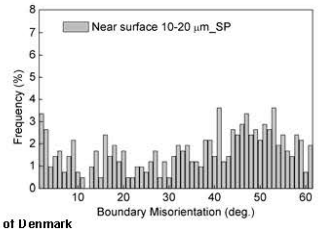

10 - 0 μm from surface

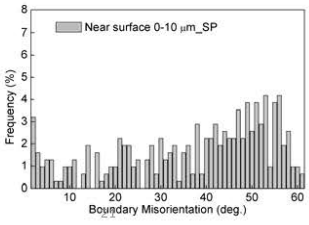

DTU Wind Energy, Technical University of Denmark

Shot-peening (6)

Structural parameters in a lamellar surface

	θ_{LB}(deg.)	D_{LB}(nm)	Fraction of HABs (%), F_{HAB}
Near surface 0-20μm_SP	35.4	223	80.6
Near surface 20-40μm_SP	34.9	301	80.7
Near surface 40-60μm_SP	24.6	515	65.2

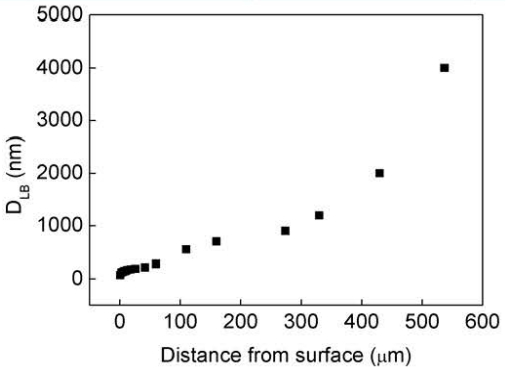

22 DTU Wind Energy, Te

Shot-peening (7)

Hardness vs distance from surface

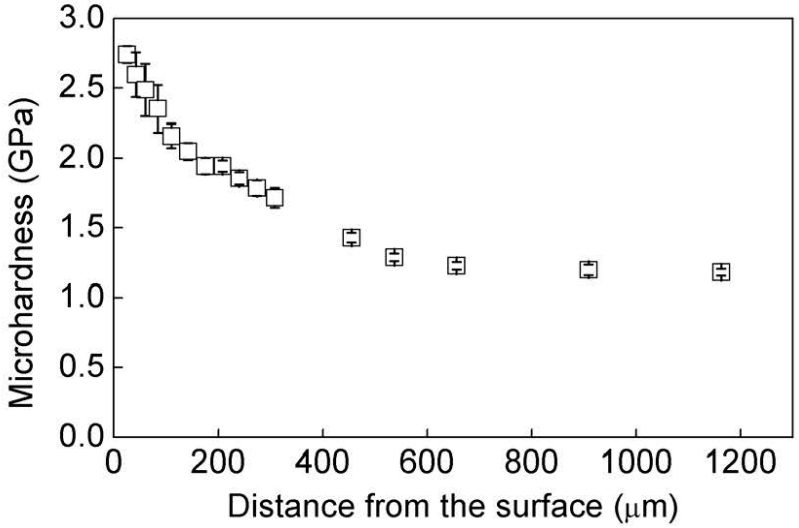

The microstructure in a shot-peened surface and subsurface is a graded lamellar structure, also observed in a friction and wear sample. The lamellar morphology also characterizes samples cold rolled to high strain.

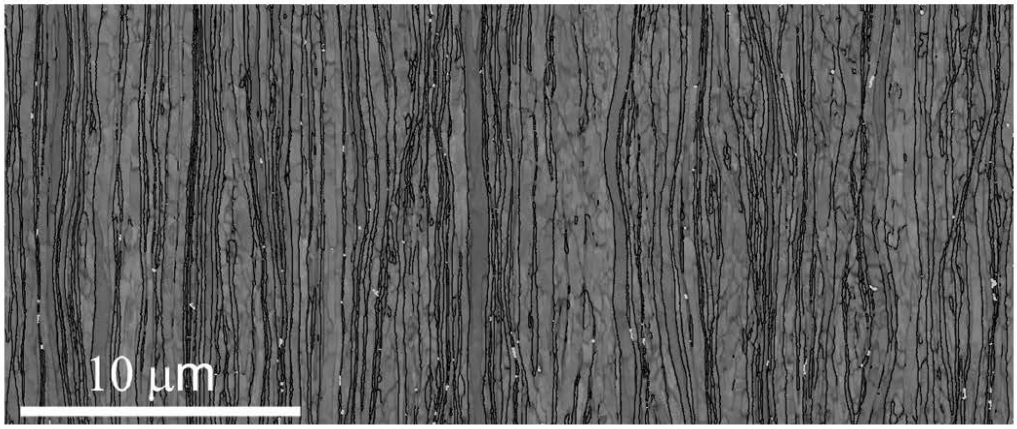

Microstructure of cold-rolled pure iron_Strain 4.26

Scaling of D^{GNB}

In samples deformed by shot peening (SP), cold rolling (CR), surface mechanical attrition (SMAT) and friction

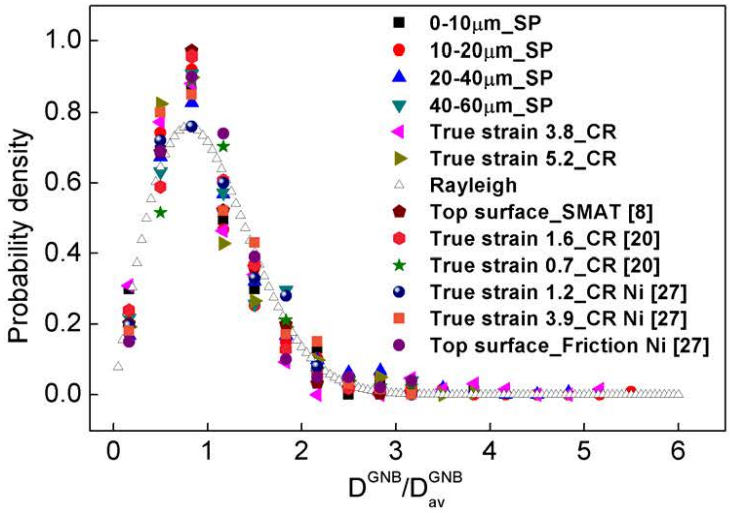

Relationships between microstructureal parameters and the stress and strain state in a graded surface layer as a basis for constitutive equations

- **Stress estimate: microhardness, nanoindentation, miniature test samples.**
- **Strain estimate: displacement of structural markers as grain boundaries, twin boundaries and embedded pins.**

Structure property relationships are difficult to obtain as surface layers are thin (< 50 ~ 100 μm) and the microstructure is graded at a nanostructural scale.

Indirect estimate of structure-property relationships in a graded structure

The deformed structures in shot-peened, friction and cold-rolled samples have similar characteristics, and is suggested to use the structure-property relationships for rolled (bulk) samples as a baseline for the analysis of graded surface structures.

Structure property relationships for cold-rolled samples

Establish master curves for the relationships:

- **Stress (σ) and strain (ε)**
- **Stress (σ) and boundary spacing (D_{av})**
- **Strain (ε) and boundary spacing (D_{av})**

Flow stress (σ) as a function of the rolling strain (ε)

Parabolic hardening (Stage Ⅲ)
Linear hardening (Stage Ⅳ)

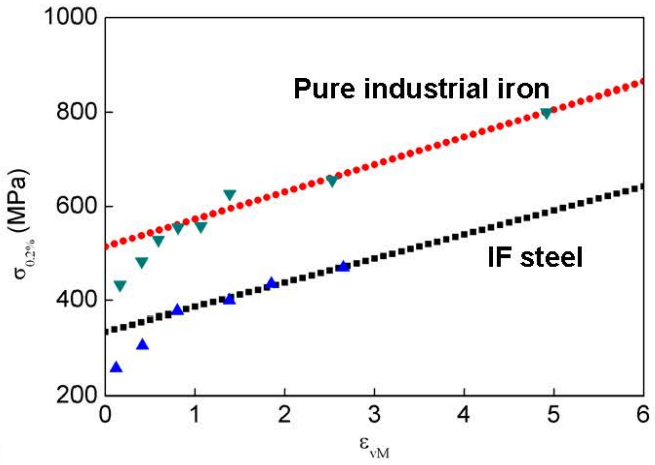

Flow stress (σ) as a function of boundary spacing (D_{av})

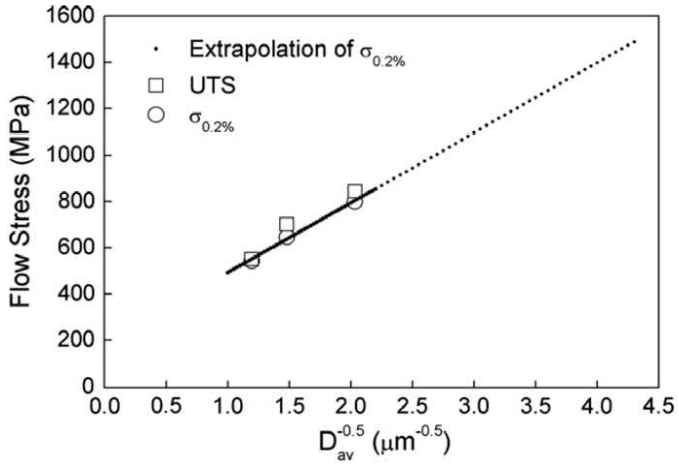

$$\sigma = 190.74 + 301.36 \times D_{av}^{-0.5}$$

Relationship between boundary spacing D_{av} (=2/S_v) and strain (ε)

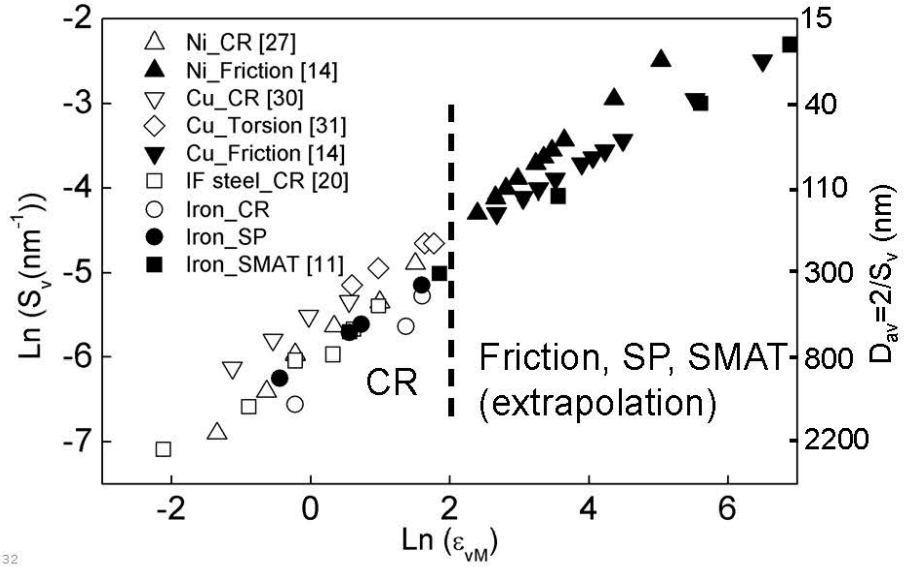

Stress and strain state in graded structures

Based on master curves for rolled samples the local stress and strain state in a graded surface strcture can be estimated by a measurement of D_{av} as a function of the distance from the surface.

Strain (ε) as a function of boundary spacing (D_{av})

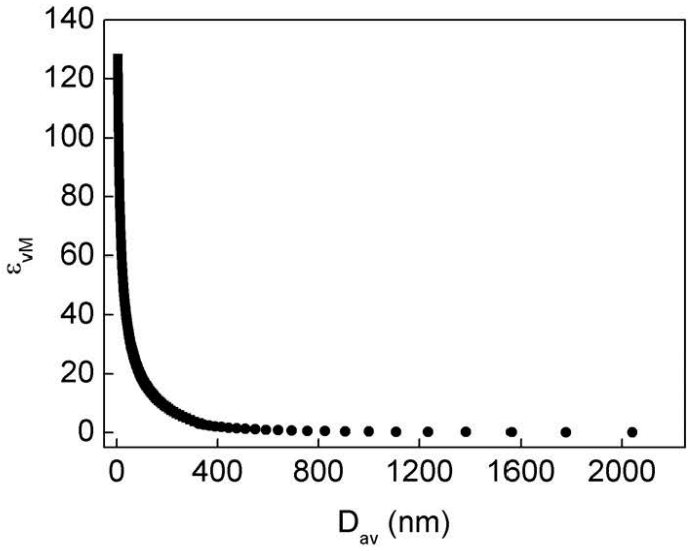

Stress distribution in a graded surface / subsurface layer

- Determined by microhardness, approx. 1/3 the flow stress
  - Determined inderectly based on a master curve for the relationship between σ and D_{av}

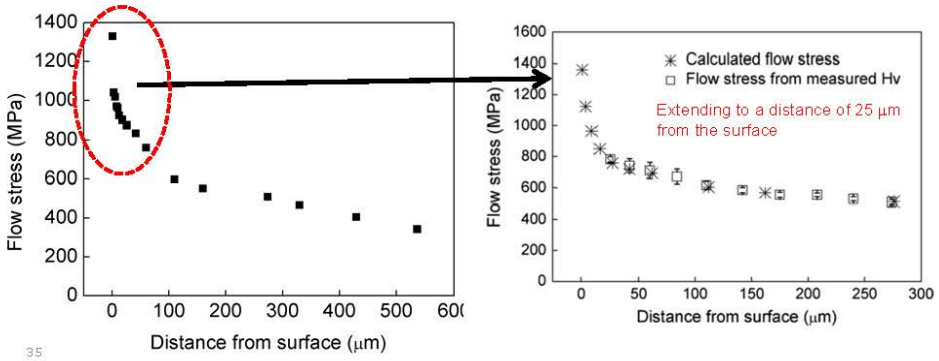

Stress distribution in the top surface layer (0-25 μm) of a SP sample

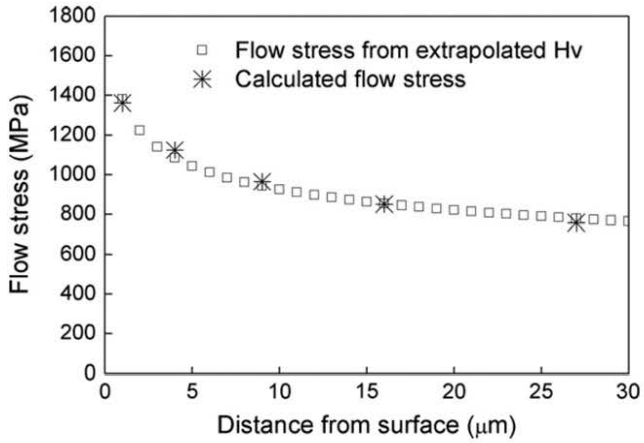

Konklusion

- Et hårdt overfladelag dannet ved plastisk deformation som f.eks. shot peening har en gradueret nanostruktur, der strækker sig 50-100 μm ind i materialet.
- Spændings- og tøjningstilstanden i overfladelaget kan analyseres ved lokalt at bestemme afstanden mellem dislokationsgrænser og korngrænser, D_{av}, der relaterer til styrken, σ, gennem ligningen

$$\sigma = K \bullet D_{av}^{-0.5}$$

K er en konstant for hårdt deformeret materiale, der kan bestemmes ved at måle sammenhørende værdier for D_{av} og σ for grundmaterialet deformeret f.eks. ved valsning til en høj deformationsgrad.

- Den foreslåede mikroskopiske metode til analyse af en lokal spændings- og tøjningstilstand i et deformeret materiale kan anvendes generelt ved analyse af deformationszoner, f.eks. nær revner, partikler og korngrænser.

Homogen og lokaliseret tøjningsudvikling af nanostruktureret aluminium

Jacob Kidmose, DTU Vindenergi

Homogen og lokaliseret tøjningsudvikling af nanostruktureret aluminium

Fordele ved brugen af ARAMIS

Jacob Kidmose

vejledere:
N. Hansen, G. Winther and X. Huang

DTU Wind Energy
Department of Wind Energy

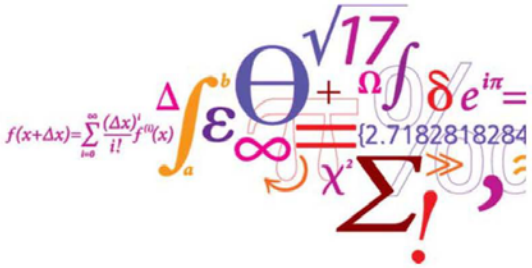

Start materiale

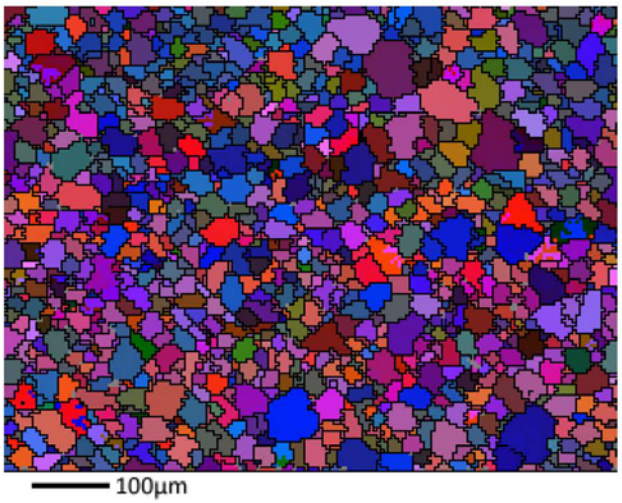

- Al1050 –99.5%
- Kornstørrelse 30 µm.

Accumulative Roll Bonding

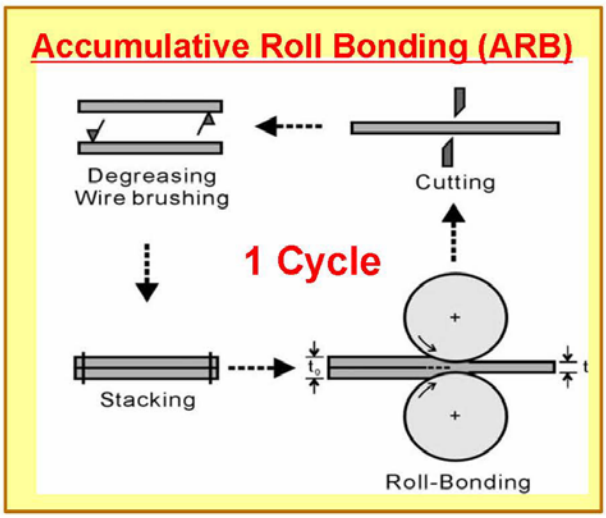

6C-ARB Microstruktur

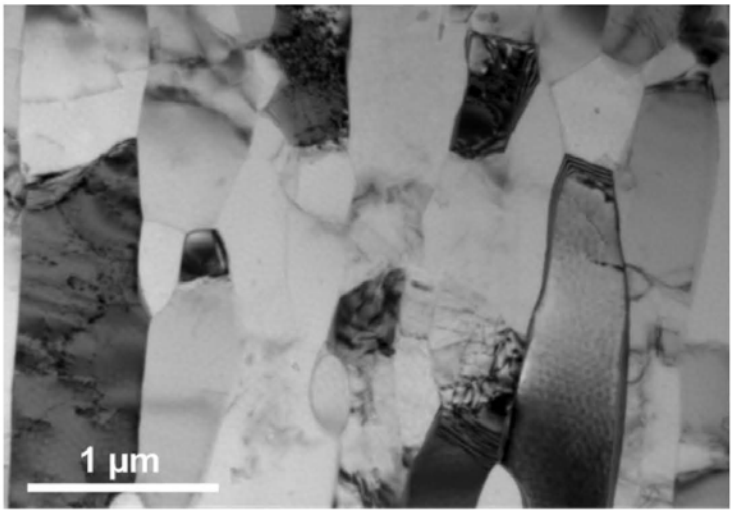

6C-ARB1050Al plade

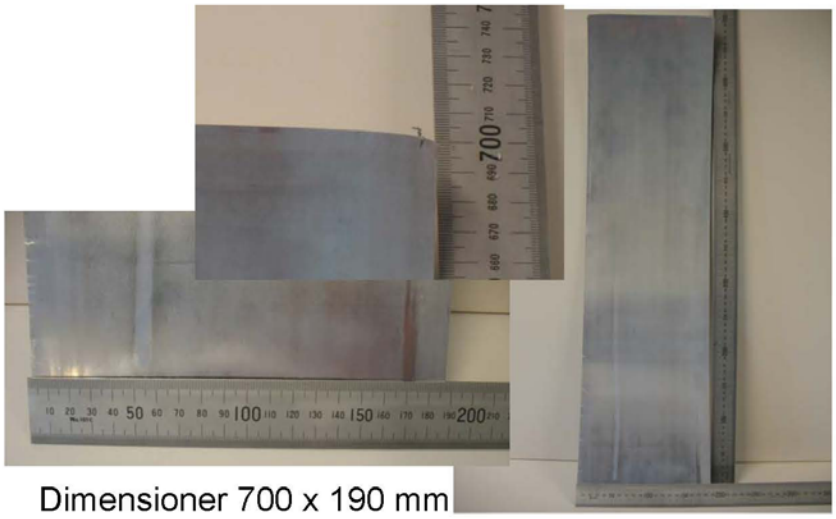

ARAMIS

- Dot pattern
- Facet size 0,75 mm

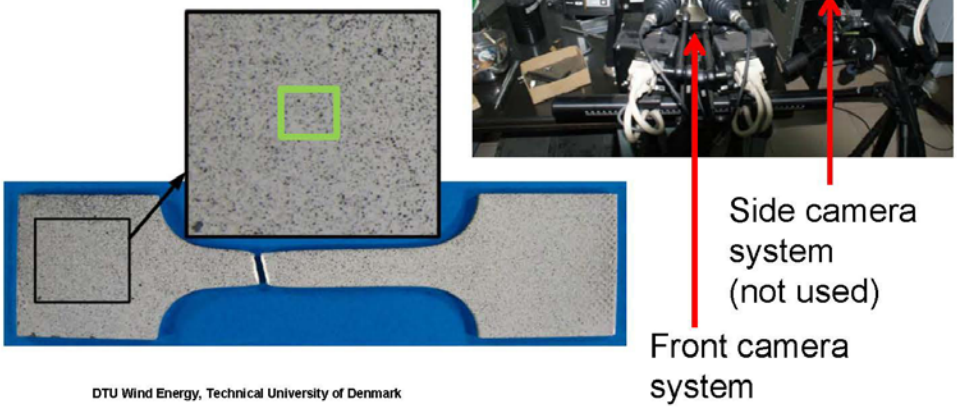

Mechanical properties

- AA1050
  - 6C-ARB
    - Varmbehandling
      - 6C-ARB-225
    - Valsning
      - 6C-ARB-CR50

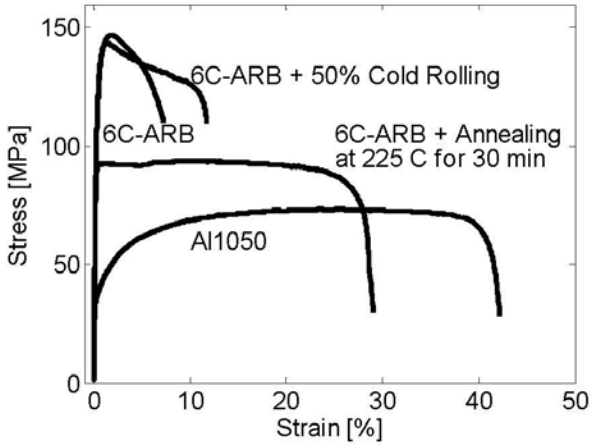

Homogen deformation

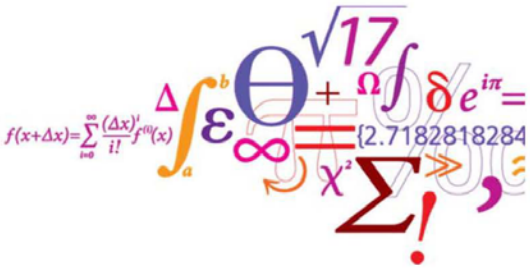

DTU Wind Energy
Department of Wind Energy

6C-ARB

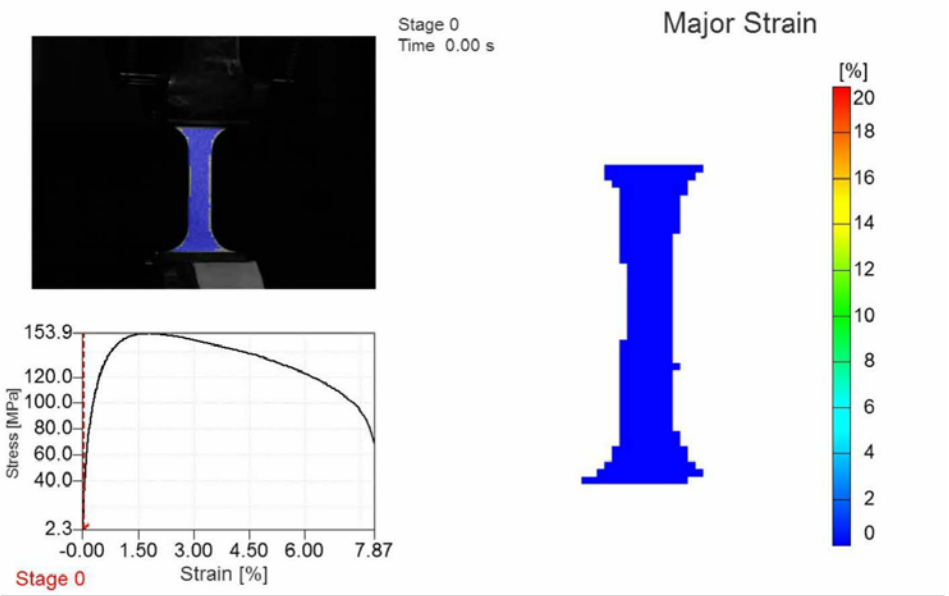

6C-ARB-CR50

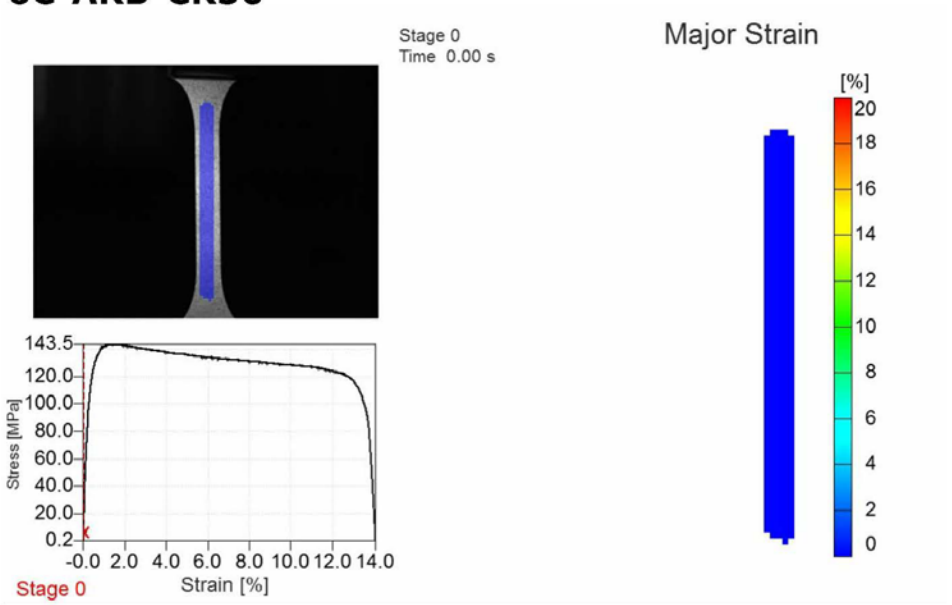

Results

- 6C-ARB udvikler shear band lige efter brud styrken
- 6C-ARB-CR50 har homogene deformation flere procent efter brud styrke

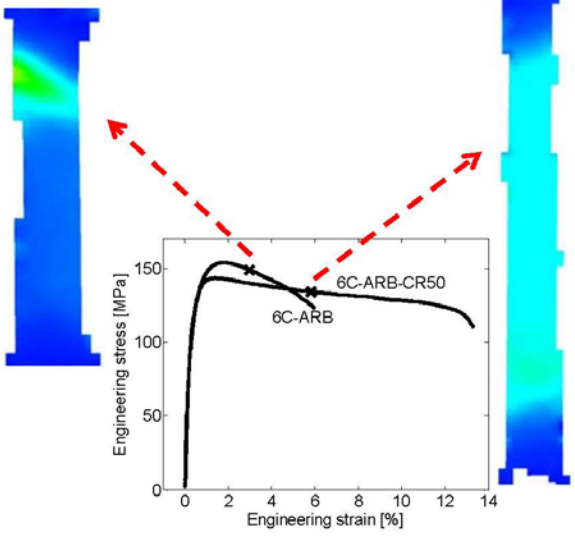

Varmbehandling

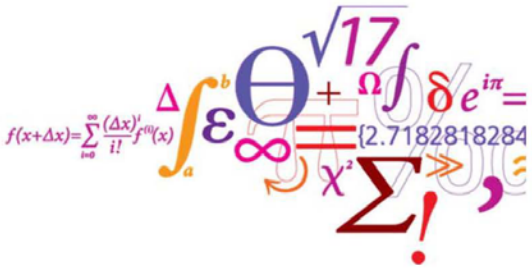

DTU Wind Energy
Department of Wind Energy

6C-ARB-225

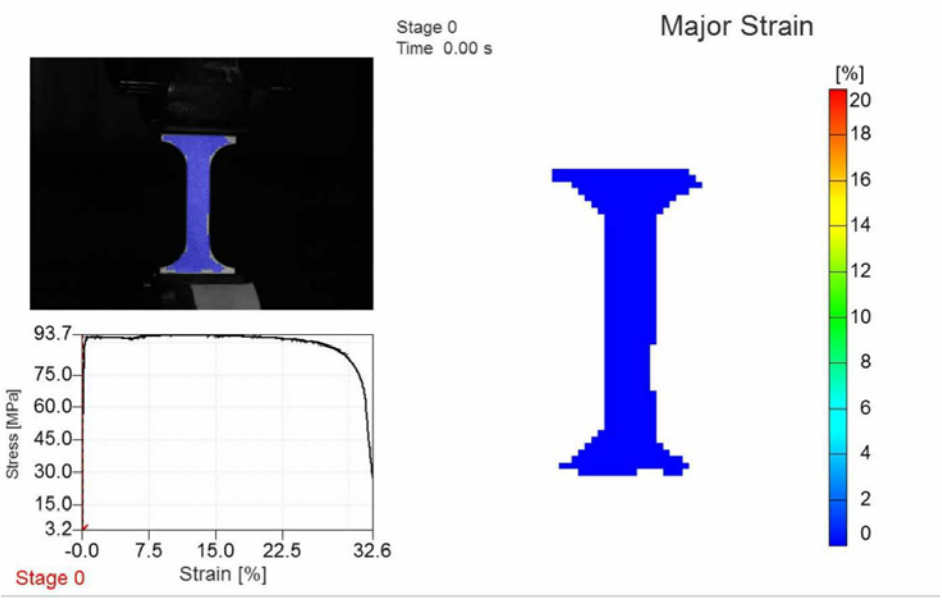

ARAMIS

- En-akset træk prøve
  - tøjnings-spændings kurve
  - Sand tøjnings-spændings kurve (også gældende efter UTS)
  - Anisotropi

Sand tøjnings-spændings kurve

Volume konstant=> $\varepsilon_{Tykkelse} = -\varepsilon_{bredde} - \varepsilon_{træk}$

Udregning af tykkelses tøjningen over bredden af indsnævringens zonen

Derved fås det aktuelle tværsnits areal af indsnævringens zonen

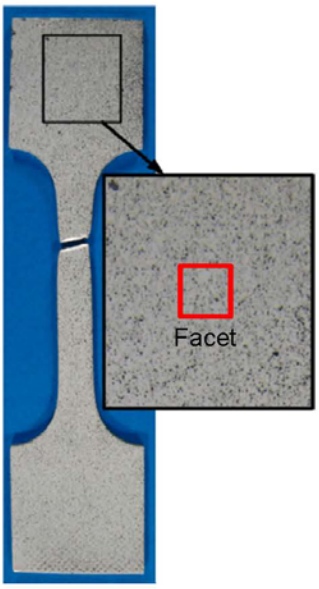

Sand tøjnings-spændings kurve

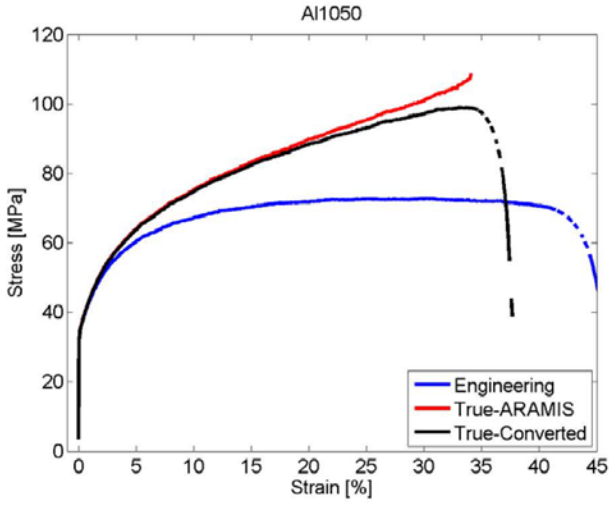

$$\sigma_t = \sigma_E(1+\varepsilon_E)$$

$$\varepsilon_t = \ln(1+\varepsilon_E)$$

Sand tøjnings-spændings kurve

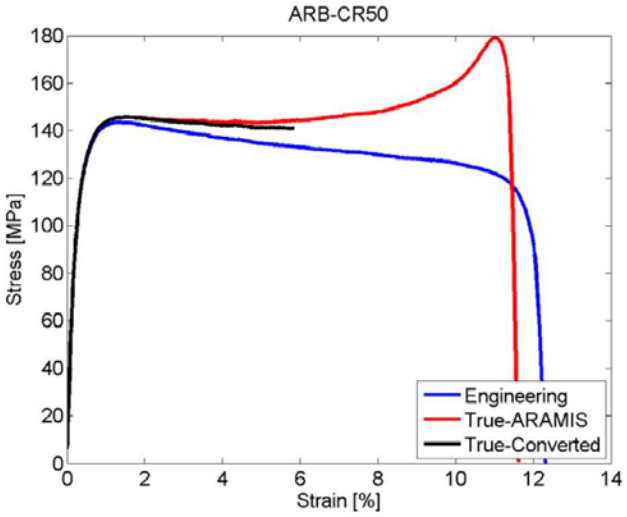

DTU Wind Energy, Technical University of Denmark

ARAMIS

- En-akset træk prøve
  - tøjnings-spændings kurve
  - Sand tøjnings-spændings kurve (også gældende efter UTS)
  - Anisotropi

DTU Wind Energy, Technical University of Denmark

Spørgsmål?

Tak for jeres opmærksomhed.

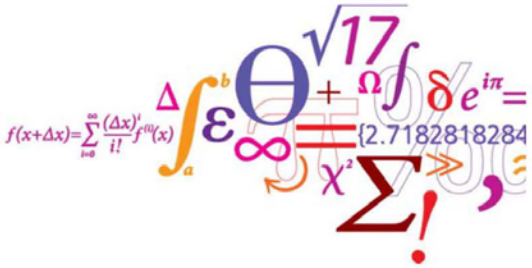

DTU Wind Energy
Department of Wind Energy

Baggrund for Innovationskonsortiet REEgain om magnetiske materialer

Jens Christiansen, Teknologisk Institut

TEKNOLOGISK
INSTITUT

Indhold

- Hvad er innovationskonsortier?
- Baggrunden for REEgain
- Virksomhedernes interesser
- Aktiviteterne REEgain

TEKNOLOGISK INSTITUT

Hvad er et innovationskonsortium?

- Konkrete samarbejdsprojekter mellem virksomheder, forskningsinstitutioner og teknologiske serviceinstitutter
- Formålet er, at parterne i fællesskab udvikler viden eller teknologi, som ikke blot gavner enkelte virksomheder, men hele brancher indenfor dansk erhvervsliv
- Mindst 2 virksomheder, en forskningsinstitution og et teknologisk serviceinstitut
- Varighed på mellem 2 og 4 år

TEKNOLOGISK INSTITUT

Hvad er et innovationskonsortium også?

- 'Kortslutning' mellem forskning, teknologiudvikling og produktudvikling
- Støtten til universiteterne og Teknologisk Institut balanceres med virksomhedernes indsats
- Ingen temaer, men vurderes ud fra virksomhedernes og samfundets behov
- Meget lidt bureaukrati, når projektet er i gang

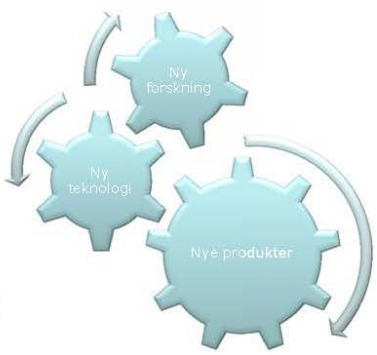

DANISH TECHNOLOGICAL INSTITUTE

Artikler om magneter og sjældne jordarter

TEKNOLOGISK INSTITUT

Skyhøje priser på vigtige råvarer

Priserne på **neodymium** er i denne måned røget helt op på en pris på **450 dollar eller knap 2.400 kr. pr. kilo**, der er den vigtigste af disse eftertragtede, strategisk vigtige råvarer. Det er en tidobling i forhold til prisen i slutningen af 2010. Samtidig svinger priserne meget, så de gør det svært og uforudsigeligt at indkøbe råvarer fra Kina. I dag betaler europæiske magnetproducenter over 30 procent mere for neodymium end de kinesiske konkurrenter.

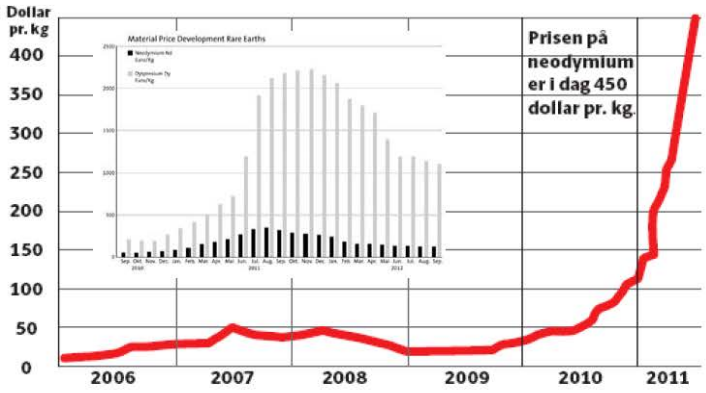

Berlingske Businenss, august 2011

DANISH TECHNOLOGICAL INSTITUTE

De Sjældne jordarter

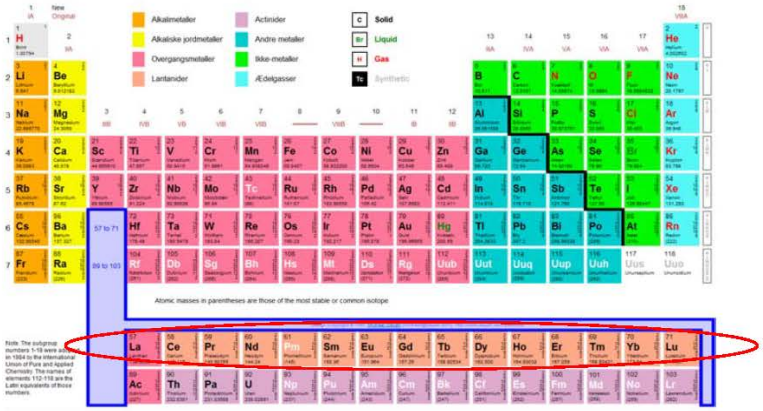

TEKNOLOGISK INSTITUT

Sjældne jordarters anvendelser

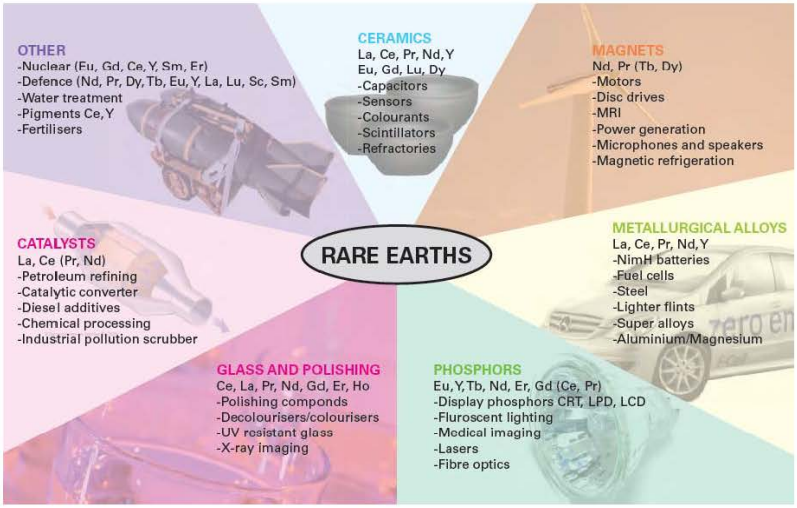

Kilde: mineralsUK

TEKNOLOGISK INSTITUT

Sjældne jordarter i Toyota Prius

Kilde: mineralsUK

DANISH TECHNOLOGICAL INSTITUTE

REEgain konsortiet

- DTU
- Syddansk universitet
- Teknologisk Institut

- Envision Energy APS
- FJ Industries A/S
- HJ Hansen A/S
- Holm Magnetics APS
- Sintex A/S
- Tanbreez Mining Greenland A/S
- Technoflex APS

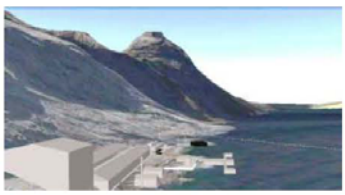

Konsortium med fødekæde

DANISH TECHNOLOGICAL INSTITUTE

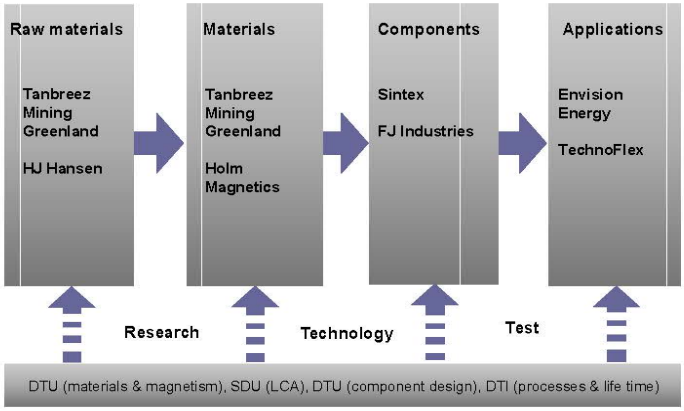

DANISH TECHNOLOGICAL INSTITUTE

TANBREEZ Mining Greenland A/S

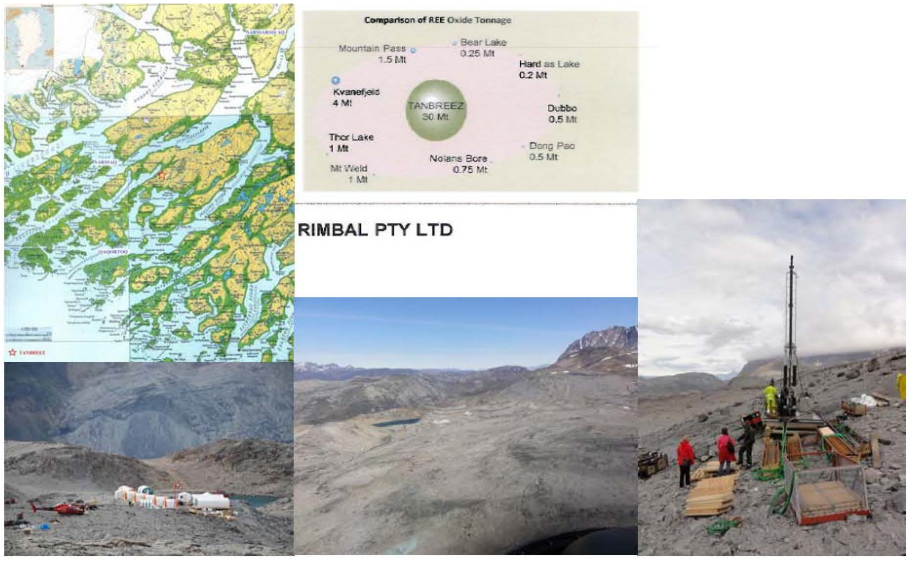

DANISH TECHNOLOGICAL INSTITUTE

Ta-Nb-REE-Z(r) - malm

Tre fraktioner:

1. Eudialyt (20%)
   - REE
   - Zirkonium
   - Niob
   - Tantal
2. Feldspat – nepheline (40%)
   - Kan sælges som byggemateriale
3. Arfvedsonit (40%)
   - Uudnyttet

Eudialyt	
Zirkonium oxide	1.8%
Niobium oxide	0.2%
Lette REE	0.5%
Tunge REE	0.15%

DANISH TECHNOLOGICAL INSTITUTE

Arfvedsonit - uudnyttet fraktion (40%)

Udnyttelse

- Indeholder stor forekomst af litium
- Magnetisk
- Udvikle metode til at udvinde litium fra arfvedsonit

Mulige anvendelser af arfvedsonit

- "Sort sand"
- Sorte mursten?
- Salget skal kun dække omkostninger ved transporten - deponeringsomkostninger udgås

Lithium-anvendelser:

- Li-ion-batterier
- Produktion af glas (Li_2CO_3)
- Smøremidler (LiOH)
- Medicin
- Organisk kemi ($LiAlH_4$)

DANISH TECHNOLOGICAL INSTITUTE

Genvinding af permanente magneter fra affald – *urban mining*

Magnetseparation fra kompressorer hos HJ Hansen

DANISH

DANISH TECHNOLOGICAL INSTITUTE

H.J.HANSEN
Udvikling gennem generationer

DANISH TECHNOLOGICAL INSTITUTE

Shredder: 100 biler i timen

Formgivning af NdFeB magneter med *Metal Injection Moulding*

TEKNOLOGISK INSTITUT

Styrker
- Kan automatiseres
- Mulighed for kompleks form
- Lavt spild
- snævre tolerancer i forhold til støbeprocesser

Svagheder
- Begrænsning på dimensioner
- Kræver stort styktal – eller høj stykpris

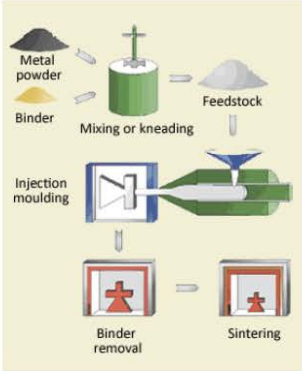

Udfordringer for MIM fremstillet NdFeB magneter

TEKNOLOGISK INSTITUT

- Forhindring af oxidation
- Kontrol af karbon - legering reagerer med bindemidler ved forhøjet temperatur
- Kontrol med kornstruktur
- Anisotropisk krympning af aligned NdFeB
- Ingen komprimeringstryk

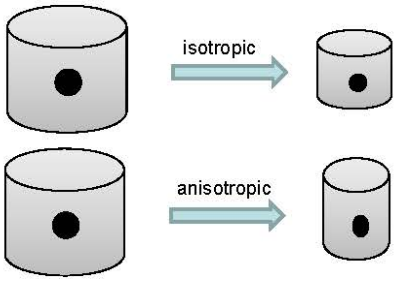

Magnetens evne til at modstå afmagnetisering

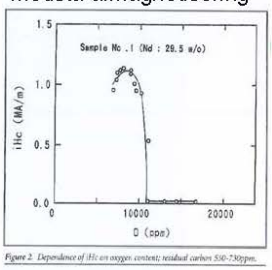

Figure 2. Dependence of iHc on oxygen content; residual carbon 530-730ppm.

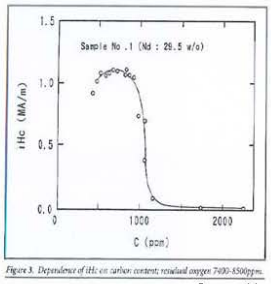

Figure 3. Dependence of iHc on carbon content; residual oxygen 7400-8500ppm.

Osamu Yamashita,1998

DANISH TECHNOLOGICAL INSTITUTE

Magneter til vindmøller

- Kan magneterne designes, så de blot skal remagnetiseres?
- Kan mængden af magnetisk materiale reduceres?
- Hvor store magneter kan vi lave?
- Har vi sjældne jordarter nok?
- Kan simple blandinger af sjældne jordarter benyttes?

Foto: ing.dk

DANISH TECHNOLOGICAL INSTITUTE

Pilotudstyr og analyselaboratorier Teknologisk Institut

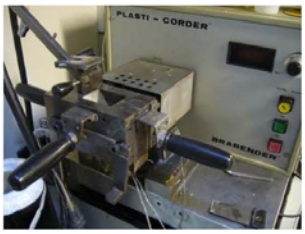

Delprojekter i REEgain

- Mixed Rare-Earth-Fe-B sintered magnets – DTU Energy Conversion (manager), Holm Magnetics (exploitation manager)
- Minimizing Magnetic Materials by design and recycling - DTU Elektro (manager), SDU, Envision Energy (Exploitation manager), HJ Hansen, Sintex
- Minerals chemistry, separation and recycling - Tanbreez (manager), DTI, HJ Hansen
- Materials investigation and processing - Sintex (manager), DTI, FJ Industries
- Operational magnetic systems - reliability and surface protection - Technoflex (manager), DTI, Envision Energy, Sintex

Følg med i projektet på www.reegain.dk

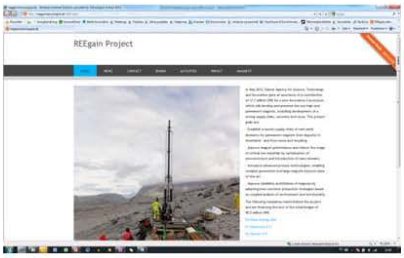


DANISH
TECHNOLOGICAL
INSTITUTE
Tak for opmærksomheden
Jens Christiansen, sektionsleder –
Materialedivisionen, jec@teknologisk.dk

Superleder tapes karakteriseret fra nanometer pinning til meter store spoler

Asger Bech Abrahamsen, DTU Vindenergi

Superconductors characterized from nanometer pinning sites to meter size coils for direct drive wind generators

Asger B. Abrahamsen[1] and Bogi Bech Jensen[2]

[1]Department of Wind Energy
[2]Department of Electrical Engineering

Technical University of Denmark

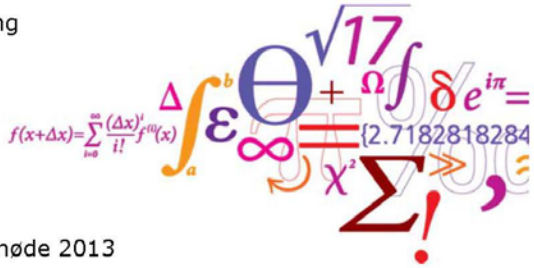

Dansk Metallurgisk Selskab, Vintermøde 2013
January 16-18, Kolding, Denmark

DTU Wind Energy
Department of Wind Energy

Outline

- **Motivation**
- **Scaling laws of turbines**
- **Superconductors**
- **Generators**
- **Conclusion**

Cost Of Energy (COE)

$$COE = \frac{CAPEX + OPEX}{Energy\ production}$$

CAPEX: Capital Expenditure

1.5 MEuro/MW* →

7.5 MEuro for 5 MW

OPEX: Operational Expenditure

*EU 2030 target for offshore wind

Motivation for superconducting generator

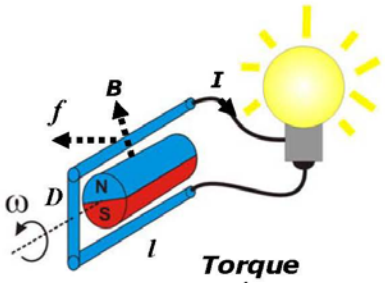

Torque

$$Power \propto \overbrace{BI}\ D^2 l\,\omega$$

- 1G : Copper + Iron
- 2G : $R_2Fe_{14}B$ magnets+Fe
  10 MW ~ 6 tons PM
- 3G : $RBa_2Cu_3O_{6+x}$ HTS + Fe
  10 MW ~ 10 kg RBCO

DTU Wind Energy, Technical University of Denmark

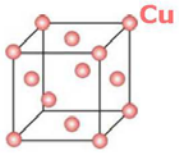

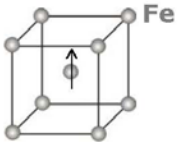

T_C = 1043 K
B_r ~ 0 Tesla

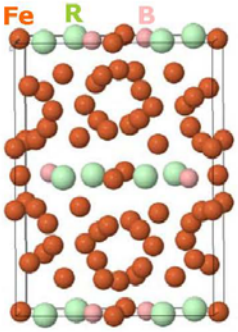

T_C = 583 K
B_r ~ 1.4 Tesla

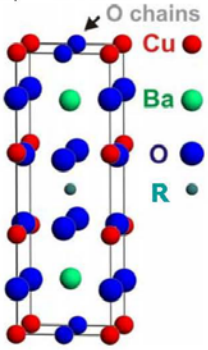

T_C = 93 K
B_{c2} ~ 100 Tesla

Motivation: Up-scaling the turbine power

Constant tip speed →	Rotor diameter	D_{rotor}	$\sim P^{1/2}$
	Torque	T	$\sim P^{3/2}$
	Generator diameter	D_{gen}	$\sim (BI)^{-1/2} P^{3/4}$

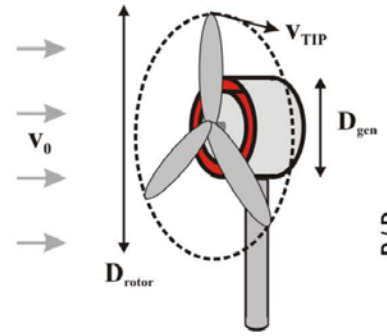

$$P = T\omega = \tfrac{1}{2}\rho D_{rotor}^2 v_0^3 C_p$$
$$= B_g I D_{gen}^2 L_{gen} \omega$$

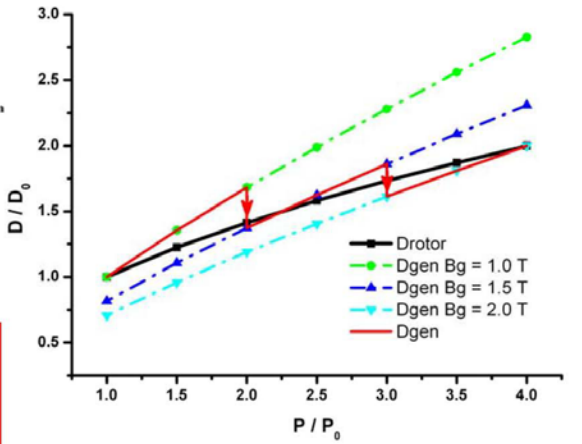

Abrahamsen et. al., ASC 4LF-04 (2012)

Superconductivity

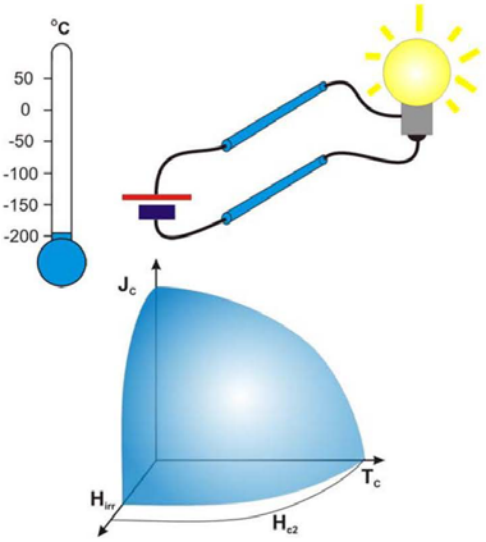

DTU Wind Energy, Technical University of Denmark

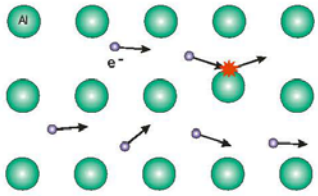

$P = R I^2$

$R = 0\ \Omega \rightarrow P = R I^2 = 0$ Watt

Critical fields

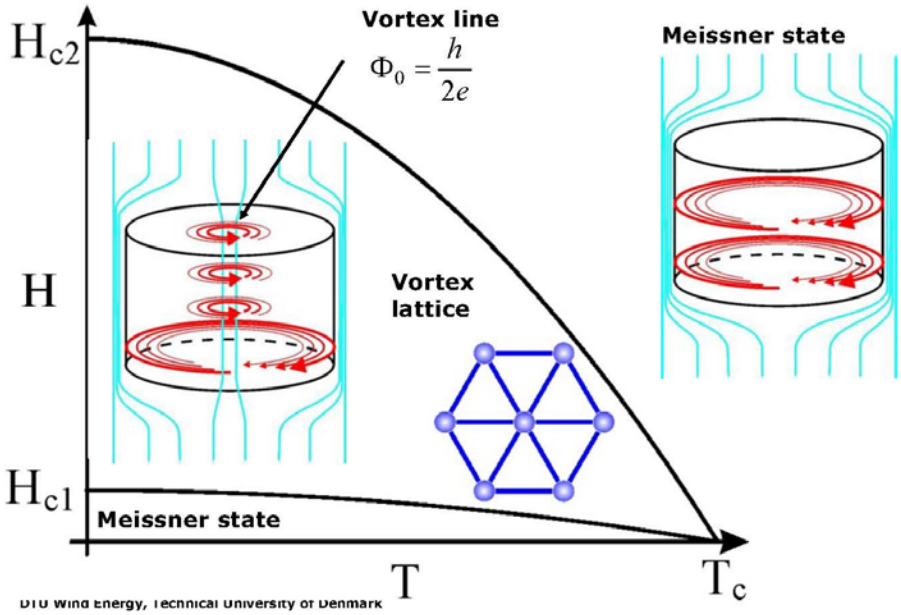

DTU Wind Energy, Technical University of Denmark

Critical current density

- Lorentz force on vortex line
- Pinning force
- Vortex movement when:

$$\vec{f} = \vec{J} \times \Phi_0 \vec{z}$$

$$f_{pin} = \frac{dU}{dx} \sim \frac{U_{pin}}{\xi}$$

$$f > f_{pin} \Rightarrow J_C \sim \frac{U_{pin}}{\xi \Phi_0}$$

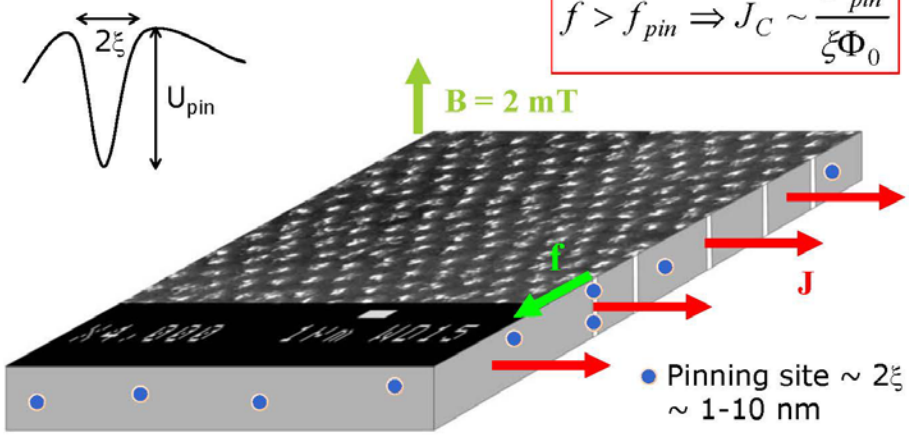

Choice of superconductor

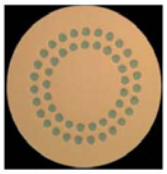

NbTi Bruker EST

0.4 €/m

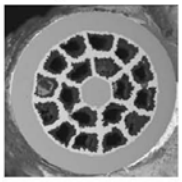

1-4 €/m

MgB_2 HyperTech

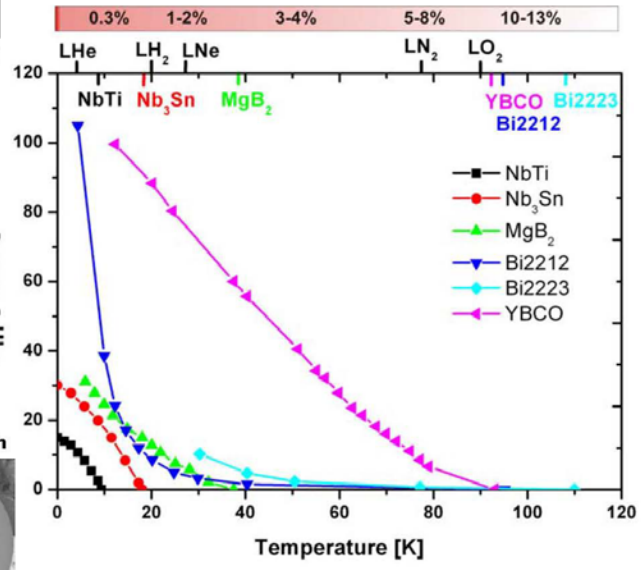

30 €/m 20 €/m

YBCO Bi-2223

Jensen, Mijatovic & Abrahamsen, EWEA 2012

HTC tapes and coils

Superwind.dk DTU

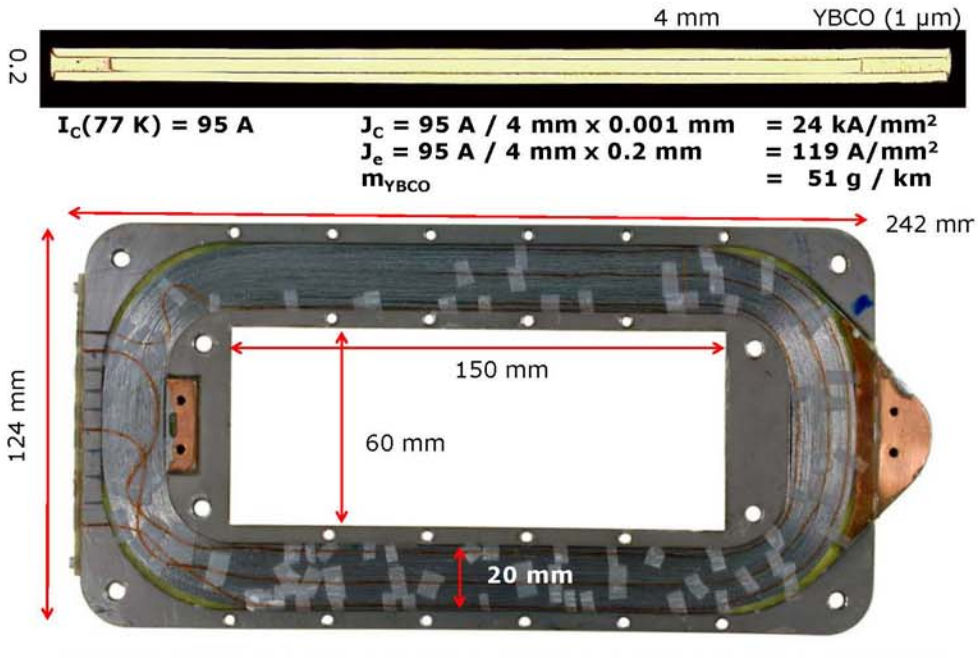

I_C(77 K) = 95 A

J_C = 95 A / 4 mm x 0.001 mm = 24 kA/mm²
J_e = 95 A / 4 mm x 0.2 mm = 119 A/mm²
m_{YBCO} = 51 g / km

DTU

IV curves of coils @ 77 K in liquid nitrogen

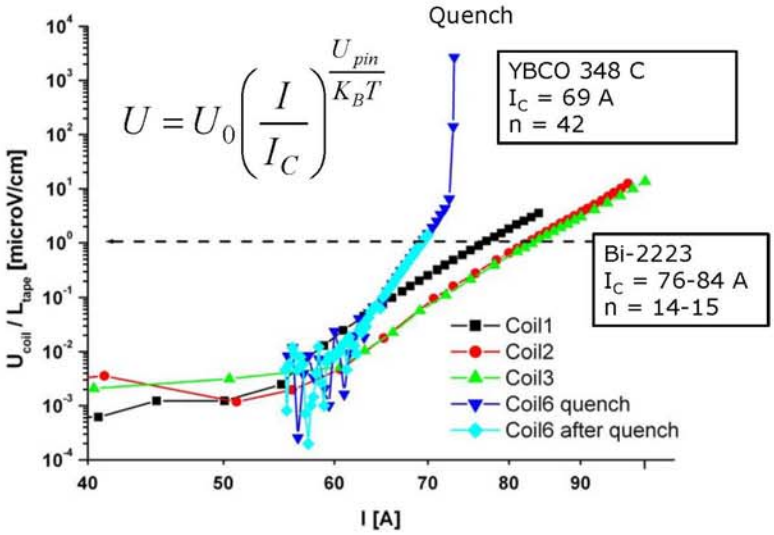

DTU Wind Energy, Technical University of Denmark

Abrahamsen *et. al.*,"Feasibility of 5 MW superconducting wind turbine generator", Physica C471, 1464 (2011)

Radial flux machine

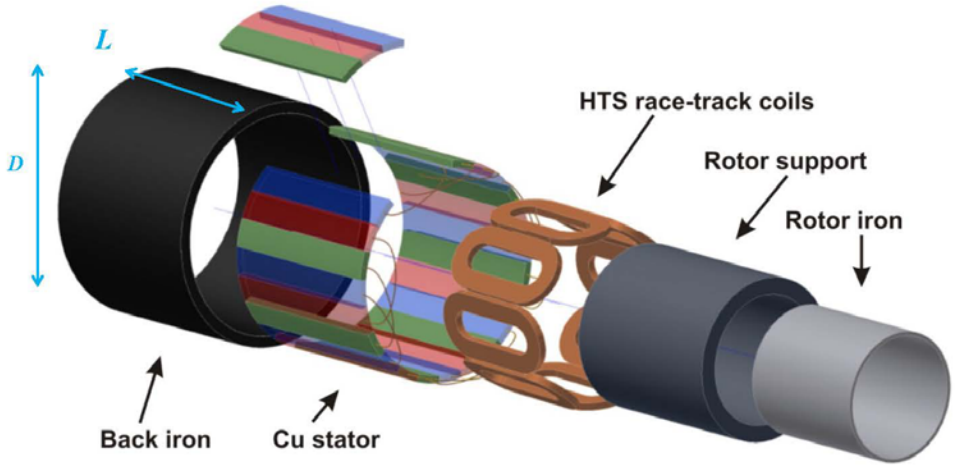

DTU Wind Energy, Technical University of Denmark

Abrahamsen et. al., SUST23,034019 (2010)

Superconducting generator and Je

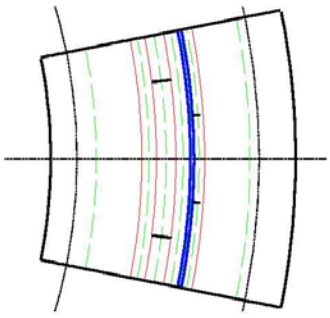

D = 4.2 m
L = 1.4 m

t_r = 0.25 m
t_{ic} = 0.04
t_s = 0.053
t_{oc} = 0.04
t_g = 0.01
t_{cu} = 0.029
t_{os} = 0.25

T = 4.2 MNm

B_{Fe} = 2.5 T
B_{airgap} = 2.4 T

Cu loss = 5 %

B_{sup} ~ 3.3 T (FE)

J_e = 70 A/mm²

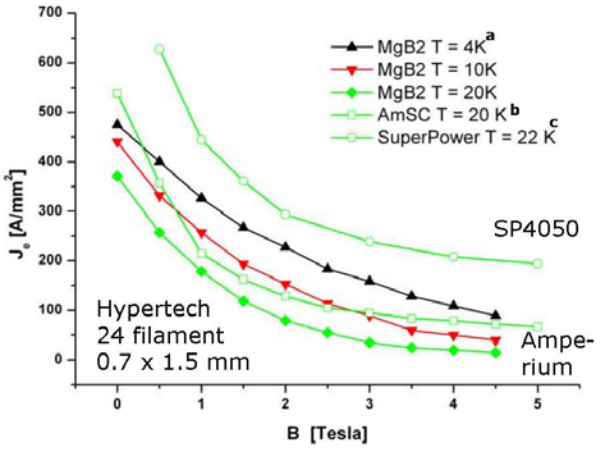

[a]S. Mine el al., *IEEE Trans. Appl. Supercond.* 22, 2012, p. 4400604.
[b]AmSC Amperium application note
[c]D.W. Hazelton and V. Selvamanickam, Proceedings of the IEEE, Vol. 97, 2009, p. 1831.

Coated conductor vs. MgB_2

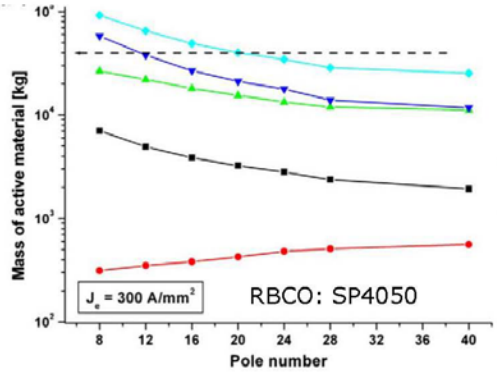

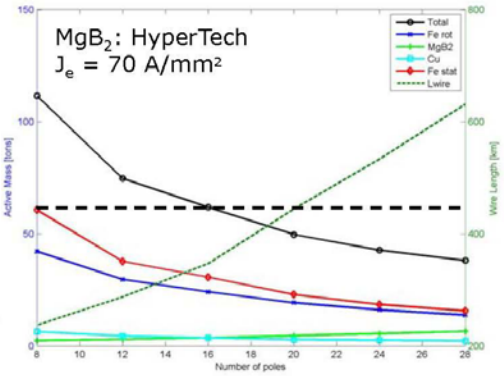

24 poles	**m ~40 tons**	**16 poles**	**m ~ 60 tons**
L = 134 km	**30 Euro/m**	**L = 347 km**	**1-3 Euro/m**
Tape cost ~	**4.0 Meuro**	**Wire cost ~**	**0.4-1.0 MEuro**

CAPEX fraction 53 % > 1/3

Abrahamsen *et. al.*, Physica C471, 1464 (2011)

CAPEX fraction 5-13 % < 1/3

Abrahamsen et. al., ASC 4LF-04 (2012)

Top head mass (nacelle + rotor)

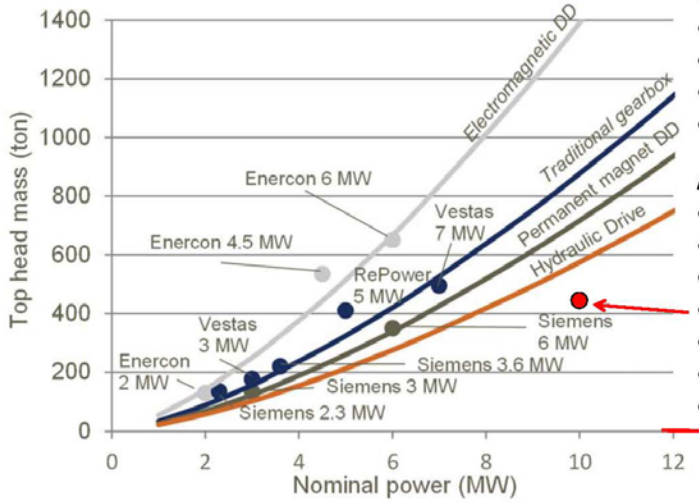

GE Global Research
- 10 MW DE-EE0005143
- m_{gen} ~142 tons
- D ~ 5 m
- Effic. ~ 90 %
- LTS NbTi wires
- Use of MRI technology
- Cost ~ 280 $/kW
- COE ~ 0.075 $/kWh

American Superconductors
- 10 MW SeaTitan
- m_{gen} ~ 160 tons
- D ~ 5 m
- $m_{nacelle}$ ~ 420 tons
- Effic. ~ 94 %
- HTS $YBa_2Cu_3O_{6+x}$
- COE ~ ?

Source: www.btm.dk
World market update 2011

DTU Wind Energy, Technical University of Denmark

Conclusion

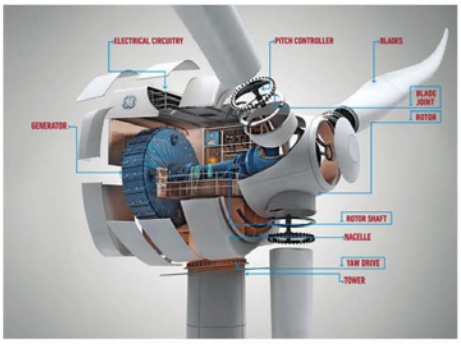

Magneto Resonant Imaging + Wind =

Superconducting direct drive generator

NbTi & MgB_2 almost cost competitive now. HTC in the long run.

Source: GE

Thank you for your attention

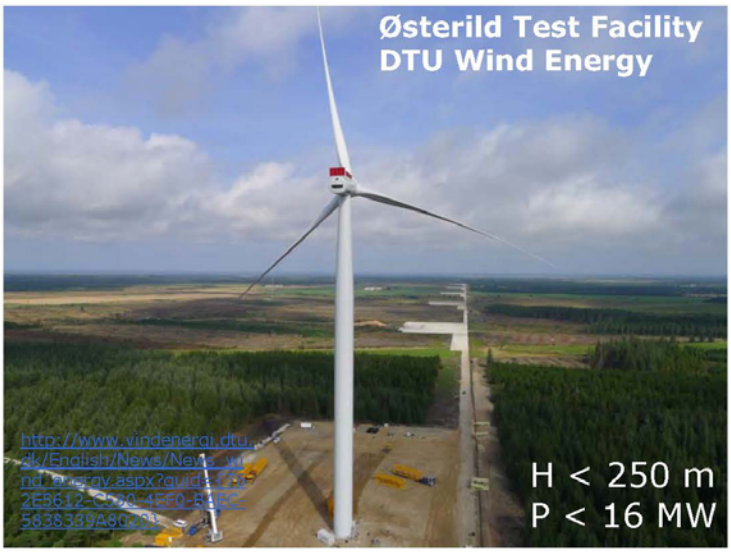

Copyright Siemens Denmark

Acknowledgement

Superwind.dk
DTU Globalization

INNWIND.EU
FP7 Energy
2012-2017

Superconducting generators
P = 10-20 MW

Mikrostruktur karakterisering af SG-støbejern

Karl-Martin Pedersen, Siemens Wind Power A/S

SIEMENS

Karakterisering af mikrostruktur i SG-jern

DMS Vintermøde 2013

Karl Martin Pedersen
Siemens Wind Power A/S

SIEMENS

Outline

- Mikrostrukturevaluering i SG jern
  - Visuel evaluering
  - Billedanalyse
- Grafit størrelsesfordeling i 2D og 3D
- Grafit på brudflader

SIEMENS

Hvorfor SG jern

Ved størkning
- Metaller svinder (=porøsiteter i centrum af emnet)
- Kulstof udvider sig ved dannelse af grafit (modvirker porøsiteter)
- Kulstof sænker størkne-temperaturen ca. 350°C i forhold til stål

Grafit-kugler i stedet for grafit-flager
- Højere styrke og sejhed

Processen
- Stor geometrisk frihed

Pris

Gråt støbejern

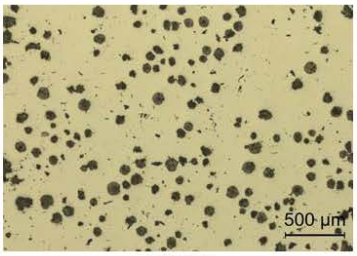

SG jern

SIEMENS

Karakterisering af mikrostruktur (Visuelt)

Grafitten
- Form og størrelse
- ISO 945-1

Matrixen
- Perlit/Ferrit indhold
- Evt. Karbider eller andet

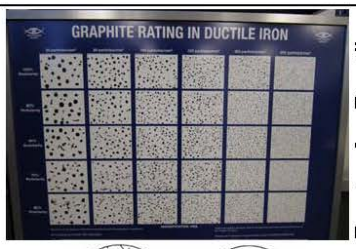

Poster fra Ductile Iron Society

Poster fra Ductile Iron Society

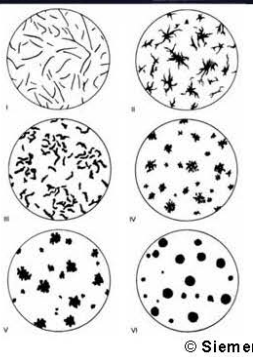

ISO 945-1

SIEMENS

Karakterisering af grafitform (Billedanalyse)

$$Aspect\ ratio = \frac{Minor\ axis}{Major\ axis}$$

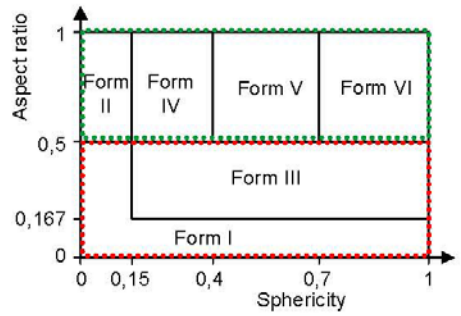

$$Sphericity = \frac{4 \times \pi \times Area}{(Perimeter)^2}$$

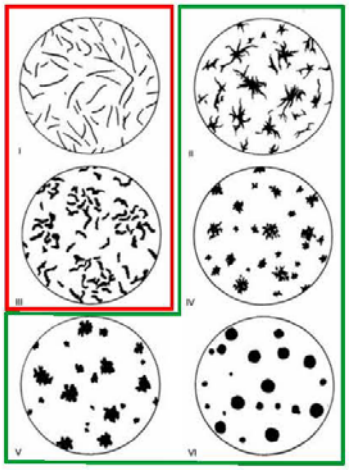

Har anvendt Image Pro®

Billedanalyse kan også give information om nodulantal pr areal, samt størrelsesfordeling.

SIEMENS

Validering af billedanalyse (ISO 945-1)

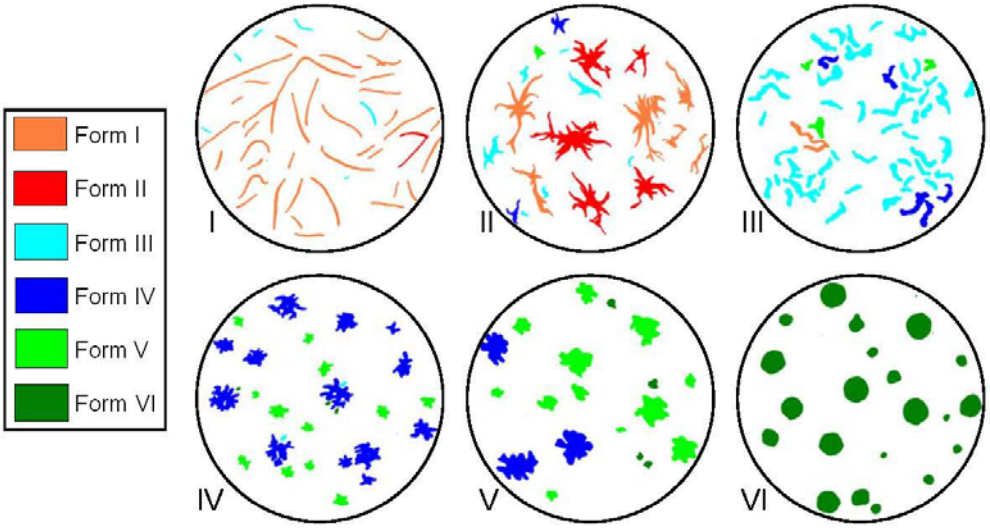

Validering af billedanalyse (ISO 945-1)

SIEMENS

Målt	Charts i Figur 1 i ISO 945-1					
	Form I	Form II	Form III	Form IV	Form V	Form VI
Form I	**90.6**	38.5	3.8	0	0	0
Form II	3.9	**46.7**	0	0	0	0
Form III	5.5	9.4	**80.1**	0.9	0	0
Form IV	0	4.1	11.5	**74.7**	36.1	0
Form V	0	1.3	4.7	23.4	**60.0**	0
Form VI	0	0	0	1.0	4.0	**100.0**

Validering af billedanalyse (Poster fra Ductile Iron Society)

SIEMENS

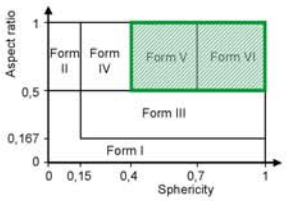

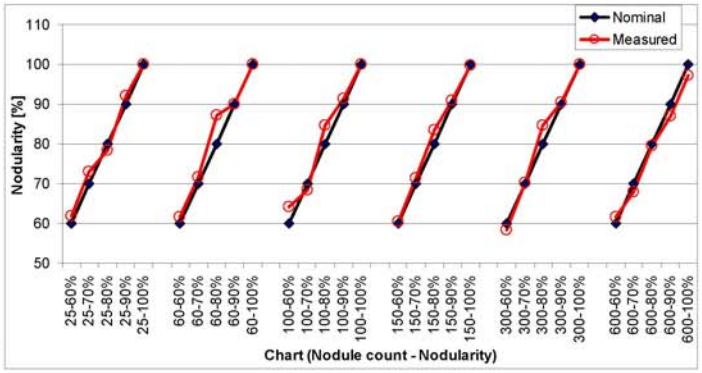

Både Form V og VI er acceptable

$$Nodularity = \frac{Area\ of\ acceptable\ graphite}{Total\ graphite\ area} \times 100\%$$

Nogle praktiske erfaringer om billedanalyse

SIEMENS

Præparering meget vigtig

Krav om flere billeder (bruger typisk 10 billeder)

Opgør fordeling af grafitform udfra areal, ikke udfra antal

Taget med få millimeters afstand

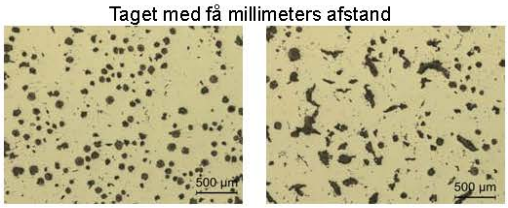

Ofte lige så hurtig at gøre det visuelt, men billedanalyse kan virke mere overbevisende.

Visuel evaluering kan udføres på ætsede emner eller på replica (sammen med vurdering af ferrit/perlit indhold). Billedanalyse skal udføres på polerede emner.

Billedanalyse har svært at tage højde for dårlig grafitform, f.eks. Chunky grafit (tilbagemelding til produktion)

Chunky grafit

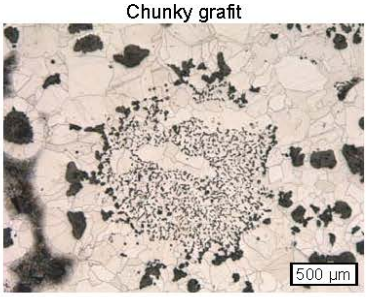

ISO/TR 945-2 Mikrostruktur i støbejern. Del 2: Grafitklassifikation ved billedanalyse

SIEMENS

Har ikke anvendt den endnu, men nogle få kommentarer:

Omhandler IKKE matematiske beskrivelser af grafitformer
Ikke anvendelig for fordeling af grafit i gråt støbejern.

Beskriver nogle krav eller ting til overvejelse (listen er ikke komplet):

- Præperering
- Billedtagning
  - Lysstyrke, skarphed, gråskala
  - Pixelstørrelse (1µm/pixel)
- Minimum 20 grafitpartikler pr billede
- Analysere mindst 400 til 1000 partikler
- Ikke grafit partikler/porer skal ekskluderes
- Opdel sammenhængende grafitpartikler
- Validering ved sammenligne med visuelle målinger

SIEMENS

Konvertering fra 2D til 3D

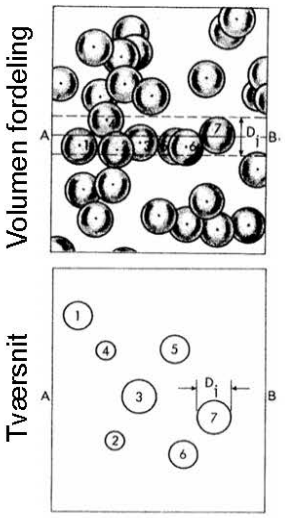

Forudsætning: Ensartet nodul størrelse

$$N_A = d \cdot N_V \qquad d = \left(\frac{6 f^g}{\pi N_V}\right)^{1/3} \qquad \Rightarrow \quad N_V = \left(\frac{\pi}{6 f^g}\right)^{1/2} (N_A)^{3/2}$$

$N_A = Area\ count\ \left[mm^{-2}\right]$

$N_V = Volume\ count\ \left[mm^{-3}\right]$

$d = Diameter\ [mm]$

$f^g = Fraction\ of\ graphite$

Varierende nodul størrelser:

$$N_V = \left(\frac{\pi}{6 f^g}\right)^{1/2} (\alpha N_A)^{3/2}$$

$\alpha = size\ distribution\ parameter\ (\approx 1.2)$

SIEMENS

3D størrelsesfordeling

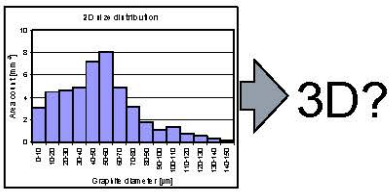

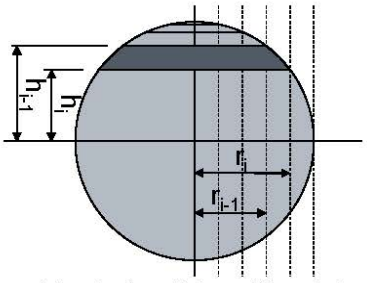

Vandret snit i grafitnodul

5 størrelsesintervaller

Visuelt på tværsnit

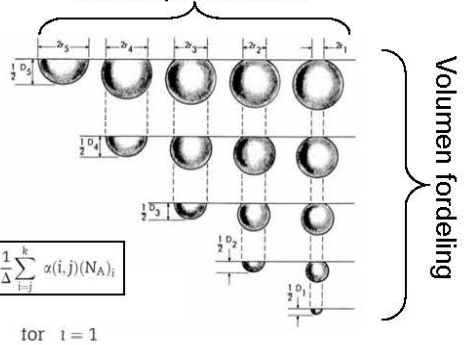

$$(N_V)_j = \frac{1}{\Delta} \sum_{i=j}^{k} \alpha(i,j)(N_A)_i$$

$$\alpha(i,i) = 1 \quad \text{for} \quad i = 1$$

$$\alpha(i,i) = \frac{2}{\pi} \ln\left(\frac{i + \sqrt{i^2 - (i-1)^2}}{i-1}\right) \qquad \forall\, i > 1$$

$$\alpha(i,j) = \frac{2}{\pi} \ln\left(\frac{i + \sqrt{i^2 - (j-1)^2}}{i + \sqrt{i^2 - j^2}} \times \frac{i - 1 + \sqrt{(i-1)^2 - j^2}}{i - 1 + \sqrt{(i-1)^2 - (j-1)^2}}\right) \qquad \forall\, i > j$$

SIEMENS

3D størrelsesfordeling

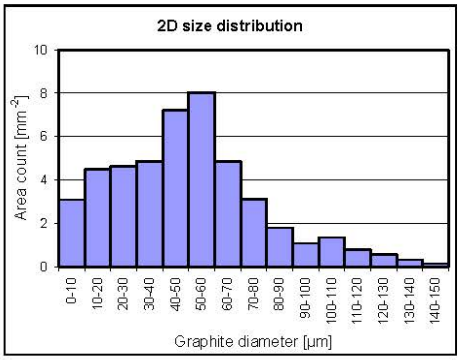

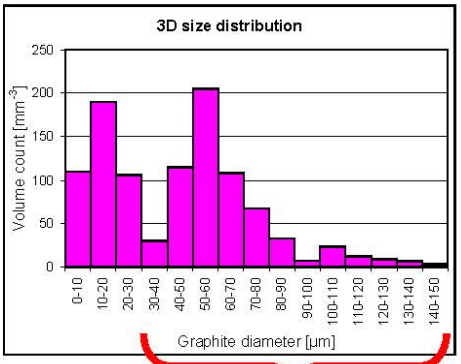

Grafit noduler

	2D	3D
Count (<30µm)	12,3 mm^{-2}	405 mm^{-3}
Count (>30µm)	34,2 mm^{-2}	621 mm^{-3}

SIEMENS

Grafitindhold på brudflade (Udmattelsestest, R = –1)

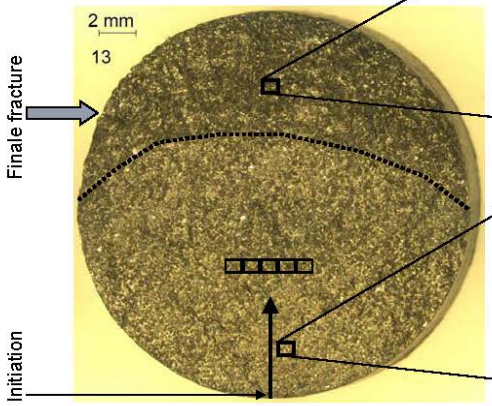

17 mm fra kant

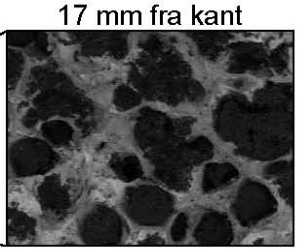

3 mm fra kant

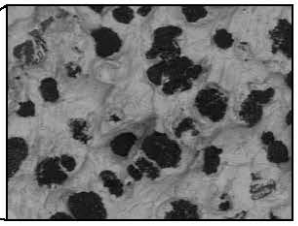

Grafitindhold på brudflade

SIEMENS

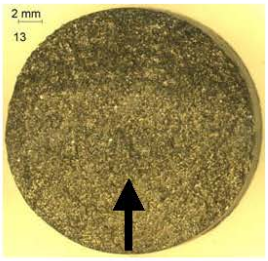

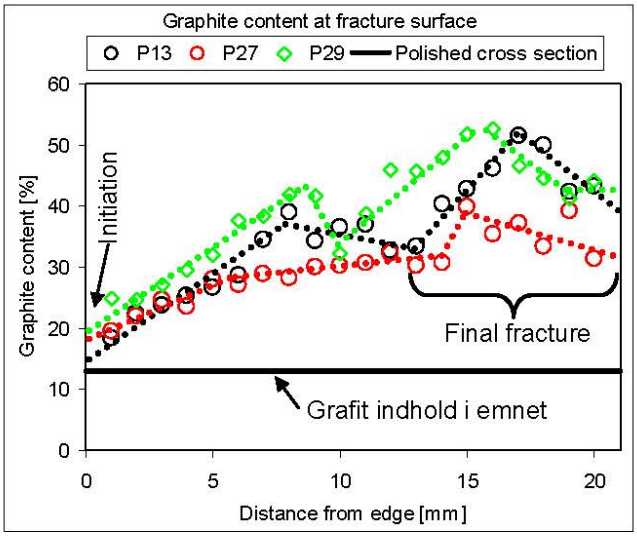

Plastic zone at crack tip

SIEMENS

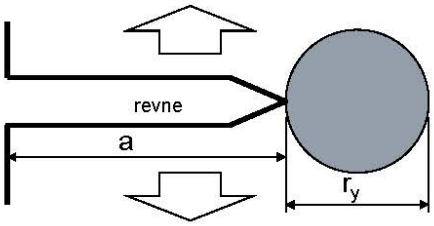

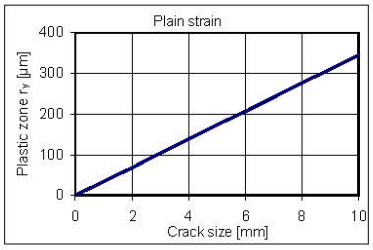

$$r_y = \frac{1}{2\pi}\left(\frac{K_{max}}{\sigma_{YS}}\right)^2 \quad (Plain\ stress)$$

$$r_y = \frac{1}{6\pi}\left(\frac{K_{max}}{\sigma_{YS}}\right)^2 \quad (Plain\ strain)$$

$$K_{max} = Y\sigma_{max}\sqrt{\pi a}$$

$$r_y = \frac{a}{6}\left(\frac{Y\sigma_{max}}{\sigma_{YS}}\right)^2 \quad (Plain\ strain)$$

K = spændings intensity factor

σ_{max} = max spænding

σ_{YS} = flydespænding

a = revnelængde

r_y = plastisk zone

Y = Form faktor

Plastisk zone og grafit noduler (lille zone)

SIEMENS

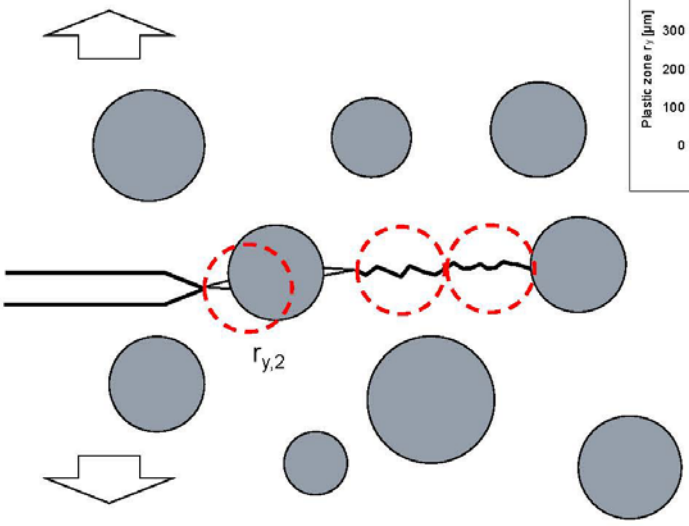

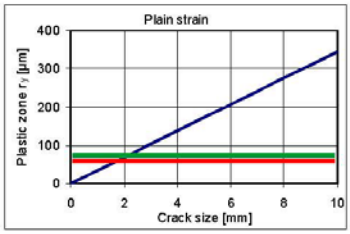

Middel afstand til nærmeste nabo

Middel grafitstørrelse

Plastisk zone og grafit noduler (stor zone)

SIEMENS

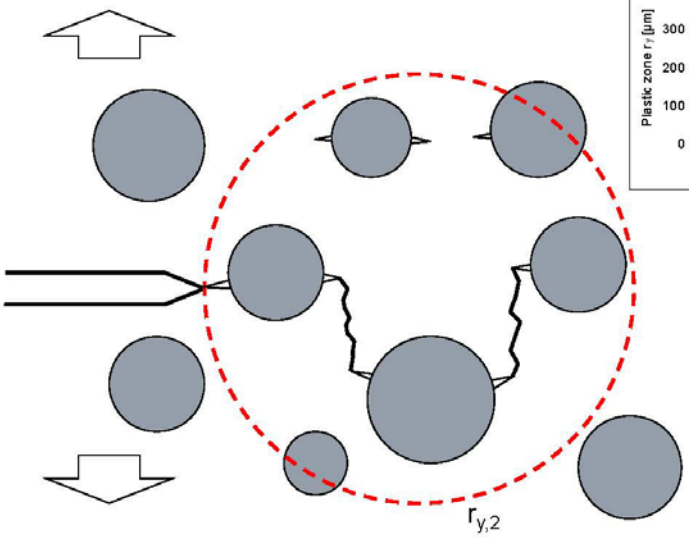

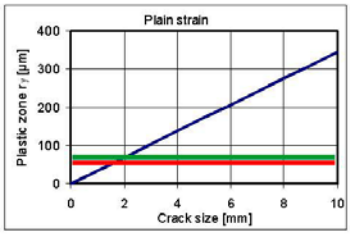

Middel afstand til nærmeste nabo

Middel grafitstørrelse

Plastisk zone og grafit noduler

SIEMENS

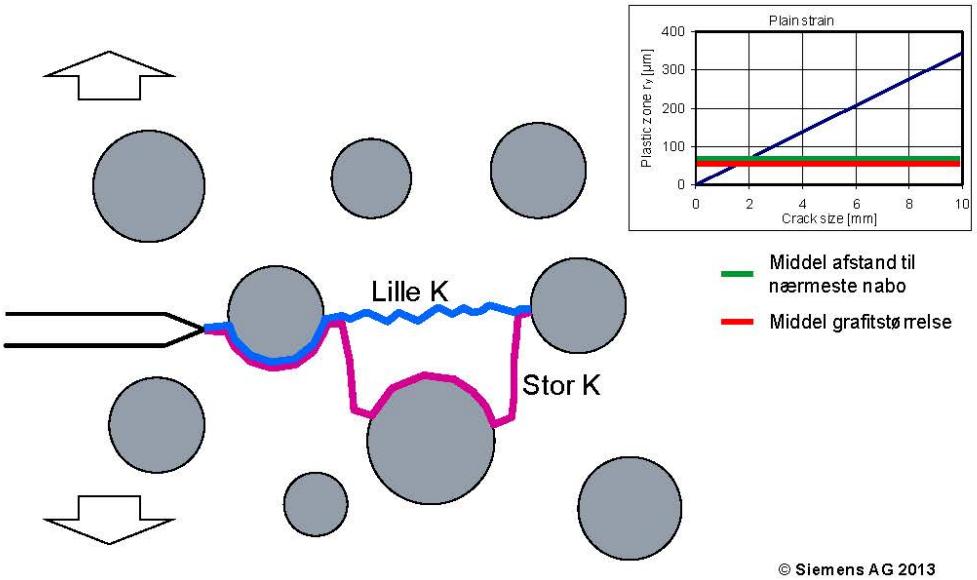

Cross section of fracture surface

SIEMENS

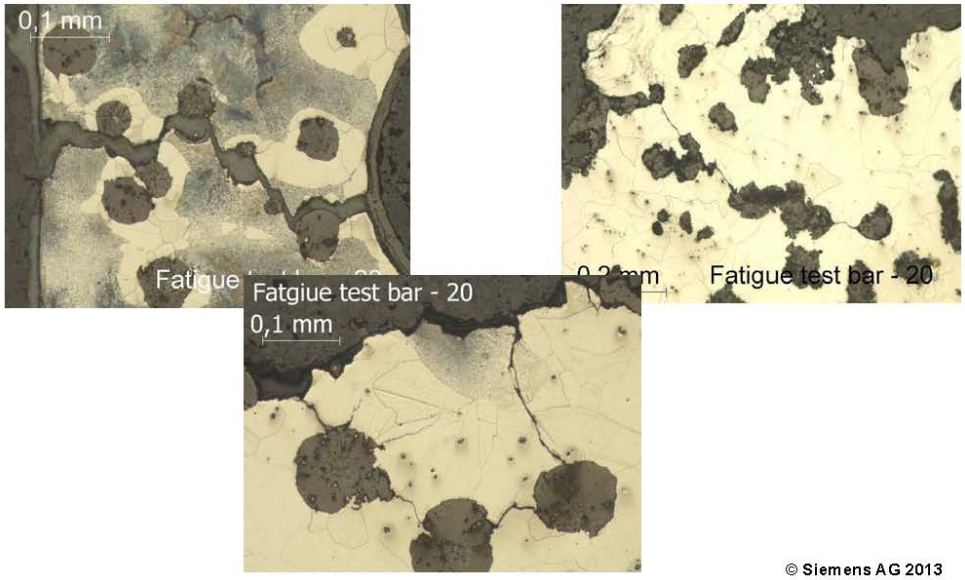

SIEMENS

Striation (8mm from edge)

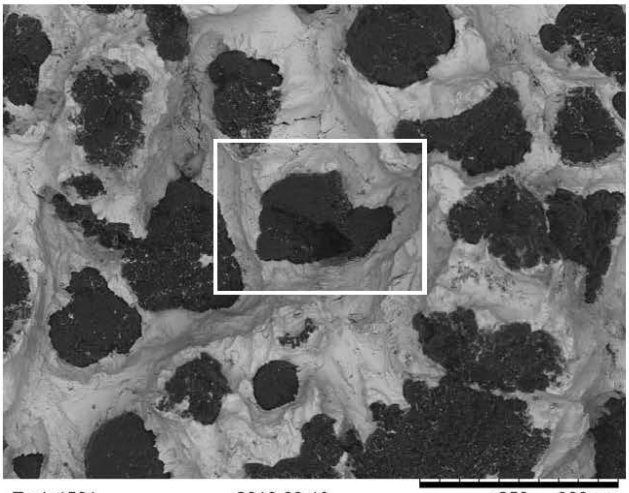

SIEMENS

Striation (8mm from edge)

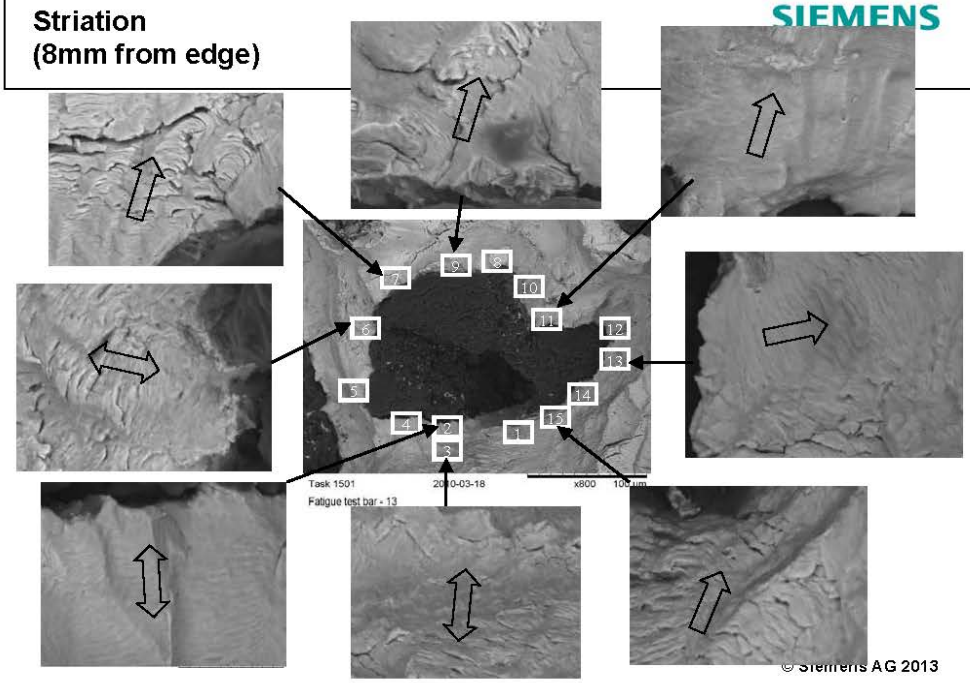

SIEMENS

Eksempel på fejlet komponent

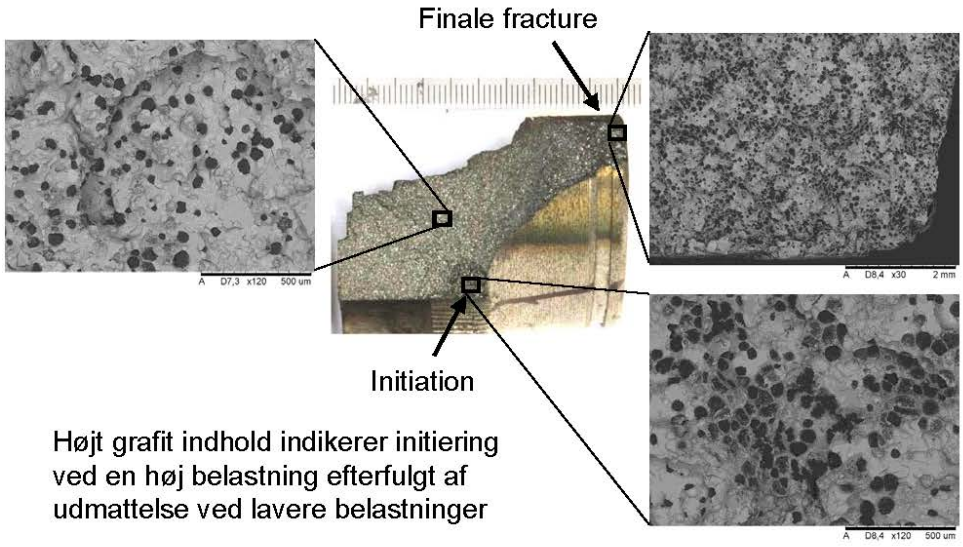

Højt grafit indhold indikerer initiering ved en høj belastning efterfulgt af udmattelse ved lavere belastninger

SIEMENS

Tak for jeres opmærksomhed

SIEMENS

Kilder

Grafit noduler i 2D og 3D:

- K.M. Pedersen and N.S. Tiedje: Graphite nodule count and size distribution in thin-walled ductile cast iron, Materials Characterization, Vol 8, p 1111-1121, 2008
- E.E. Underwood: Quantitative Stereology. Addison-Wesley Publishing Company; 1970. p. 109–145
- C.B. Basak and A.K. Sengupta: Development of a FDM based code to determine the 3-D size distribution of homogeneously dispersed spherical second phase from microstructure: a case study on nodular cast iron. Scripta Materialia, Vol 51, p. 255–260, 2004

Kvalitetssikring af støbegods i MAN B&W motorer

Knud Strande, MAN

Kvalitetssikring af Støbegods i
MAN B&W Motorer

Knud Strande
Production Support
Engineering
Marine Low Speed

Kvalitetssikring - MAN B&W Motorer

- MAN Diesel & Turbo – København
- Typiske støbte komponenter i MAN B&W motorer; Gråjern, Stål, SG jern og Kompakt grafit jern.
- Kvalitetssikring – Controlled Component Concept.
- "Dagligt arbejde" i Production Supports støbegruppe.
- Tekniske udfordringer foranlediget af design og af produktion – eksempler.
- Indløb og efterfødning – "god latin".
- Sammenfatning, kvalitetssikring - "Værktøjskassens" indhold.

MAN DIESEL & Turbo

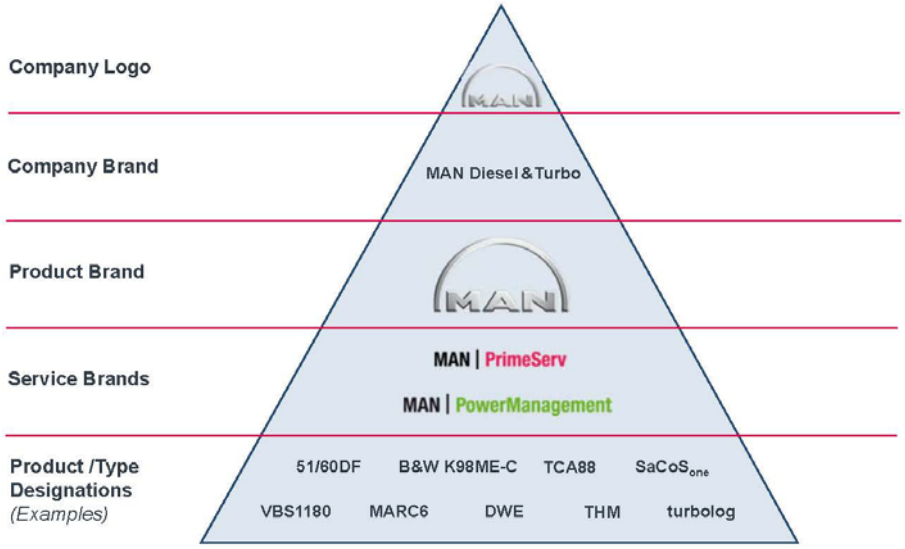

MAN B&W Motoren

- Størrelser: 26-98 cm cylinder diameter
- Effekt: 450 kW – 87.000 kW
- Typiske støbte komponenter: Gråjern, Stål, SG jern og CGI jern
- Ca. 30% af motorens vægt består af støbegods
- På en 6S60MC-C motor (~15 MW) svarer det til ~ 100t
- På 15 GW svarer det til ~ 100.000t

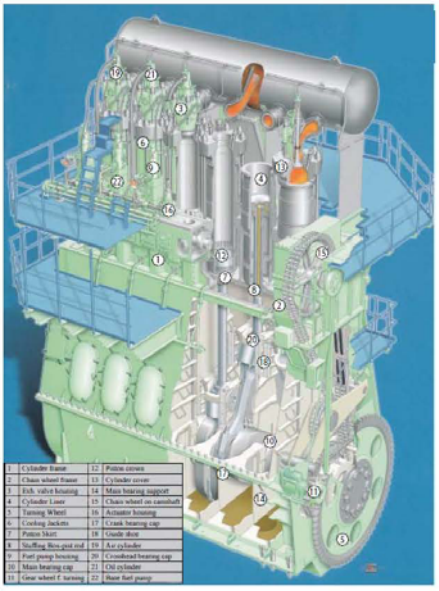

Støbegods i MAN B&W motorer

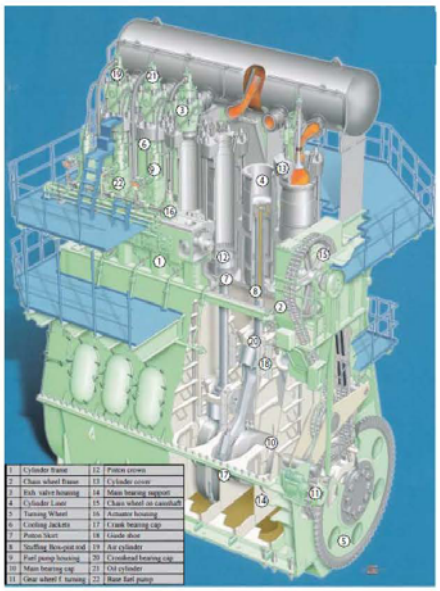

MAN B&W Motoren

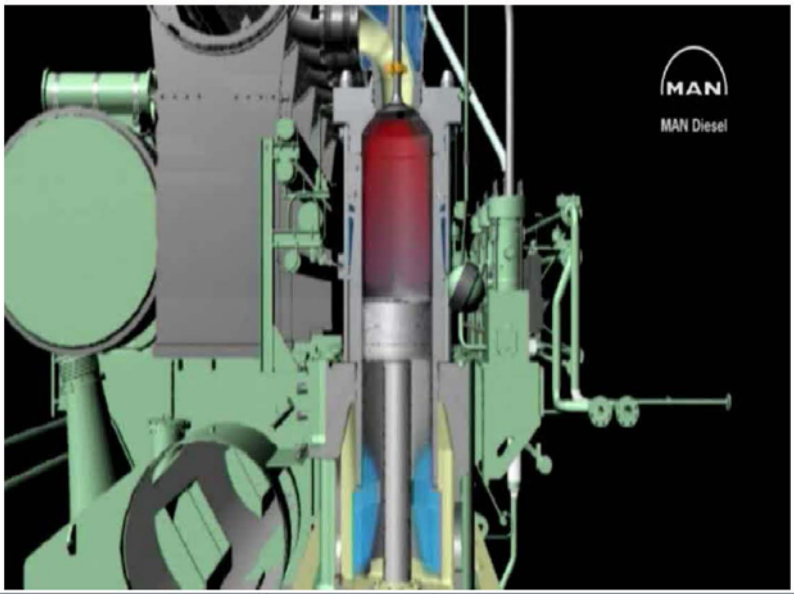

Kvalitetssikring – Controlled Components

- **Simple Components**
  Requirements to material properties (alloy), geometrical tolerances and surface tolerances stated on drawings and in general accepted standards.

- **Controlled Components**
  Components with certain functional requirements and/or components considered difficult to manufacture.

- **Quality Specification**
  States quality requirements, which always are based on expected component performance set by the designer (and experience).

- **First Time Approval Test (FTA)**
  Supplier has to show his technical ability before being approved.

- **Production Recommendation**
  Special process knowledge required.

Støbegruppens samarbejdspartnere

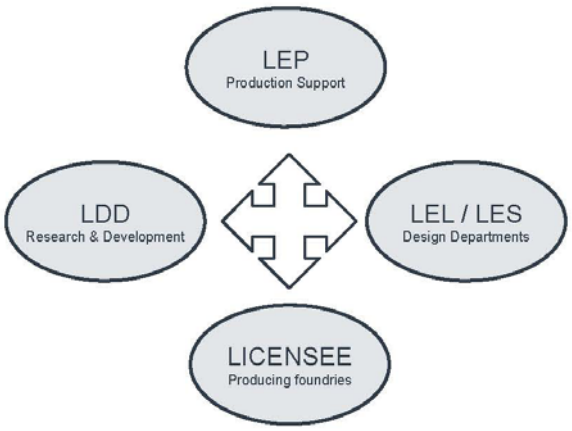

Eksempel på kvalitets specifikation

Cylinder Frames

Cylinder Frames, Grey Cast Iron

This document is valid for existing engine types on order as of the date of this document:

Engine types:

All two-stroke engine types
(Specified with C3Cu Cylinder Frames).

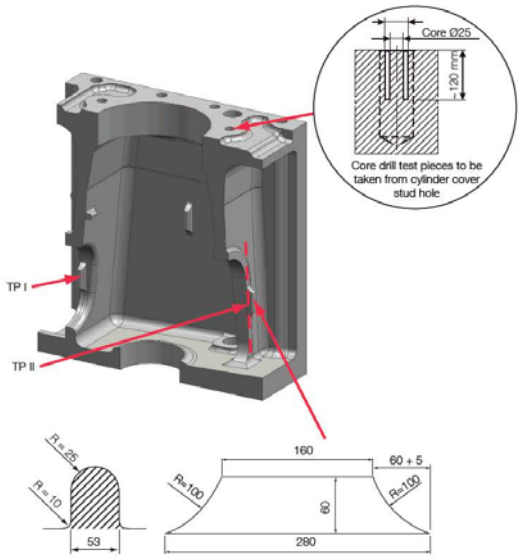

B&W Støberi 1885 – P. S. Krøyer

Casting Simulation
Filling, Absolute Velocity

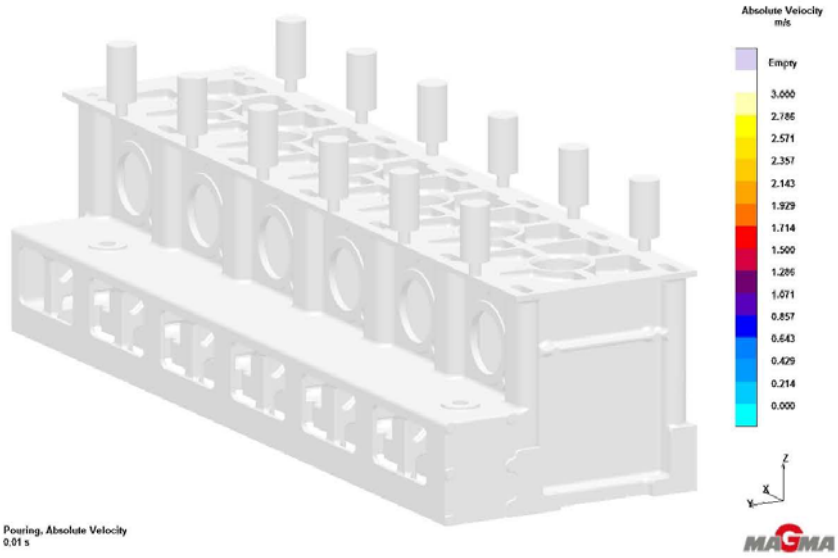

Feed back from "real life"
Cylinder frame castings – material strength

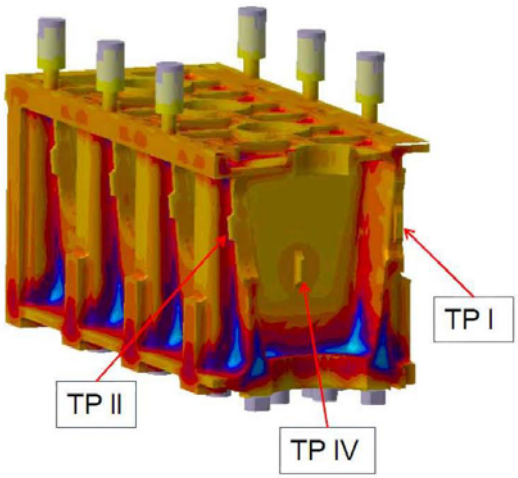

Cast-on test pieces according to QC 0743089-5.6

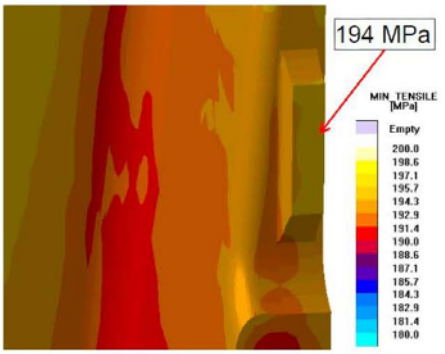

CHARGE No.	Test Piece No.	Tension Test		
		Tensile Strength	Yield Strength	Elongation
		N/mm²	N/mm²	%
Specification		min.150	—	—
S9X211 (Fore)	①	186	—	—
	②	181	—	—
	③	196	—	—

Feed back from "real life"

Cylinder frame castings – material strength

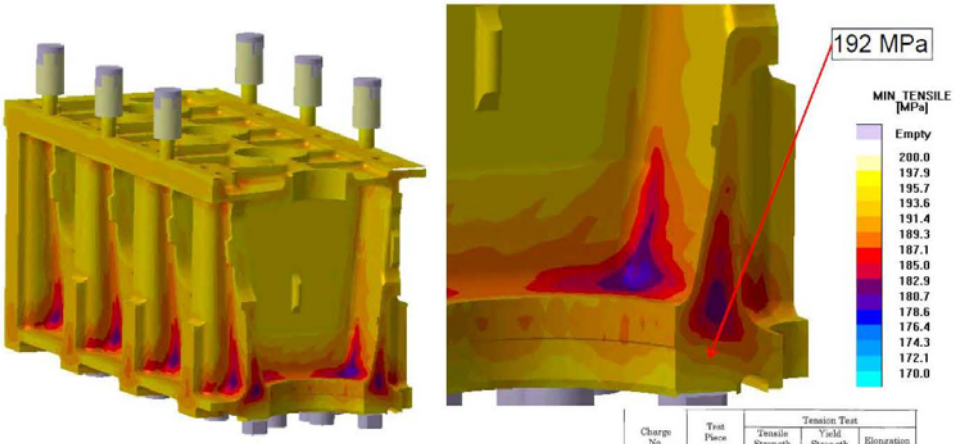

Charge No.	Test Piece No.	Tension Test		
		Tensile Strength N/mm²	Yield Strength N/mm²	Elongation %
Specification		≥140	—	—
S9X211 (Fore)	1	161	—	—
	5	158	—	—
	9	161	—	—
	10	160	—	—

Core drilled test pieces in according to QC 0743089-5.6

Feed back from "real life"

Cylinder frame castings – too low material strength

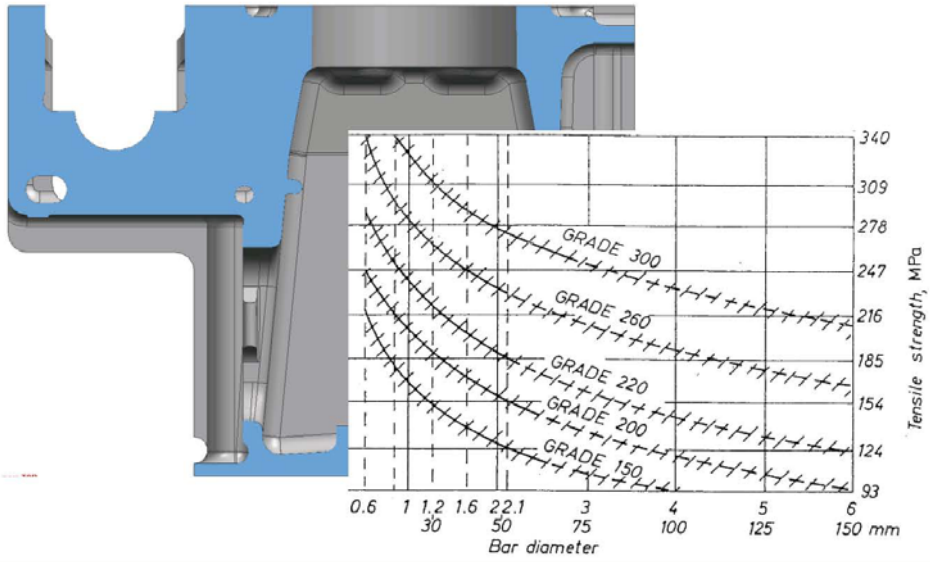

Feed back from "real life"

Cylinder frame castings – too low material strength

Feed back from "real life"

Cylinder frame castings – too low material strength

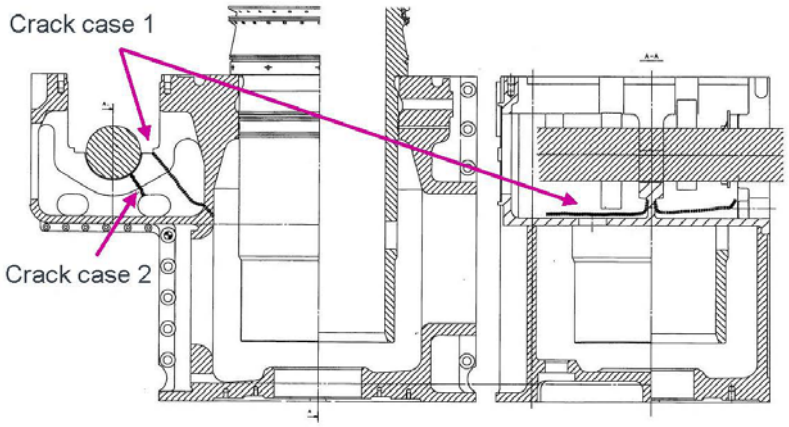

Feed back from ”real life”

Cylinder frame castings – shrinkage defects

Feed back from ”real life”

Cylinder frame castings – residual stresses

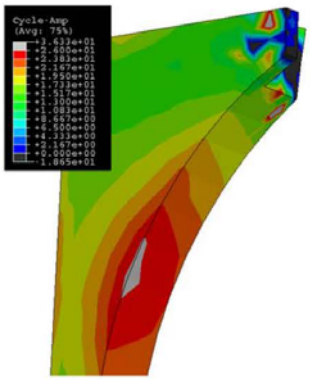

Stresses caused by engine operation

Feed back from "real life"
Cylinder frame castings – residual stresses

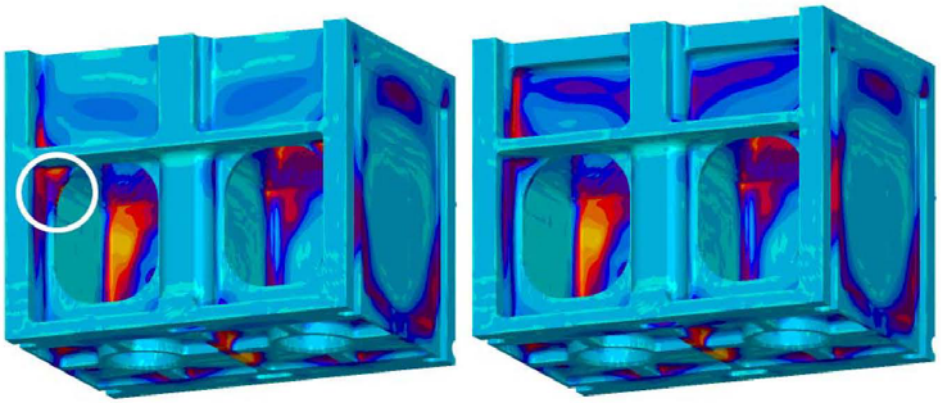

Reducing residual stresses by design modifications

Feed back from "real life"
Indeslutninger/overfladefejl

6S50ME-B9 cylinder frame

KPF, nodular cast iron

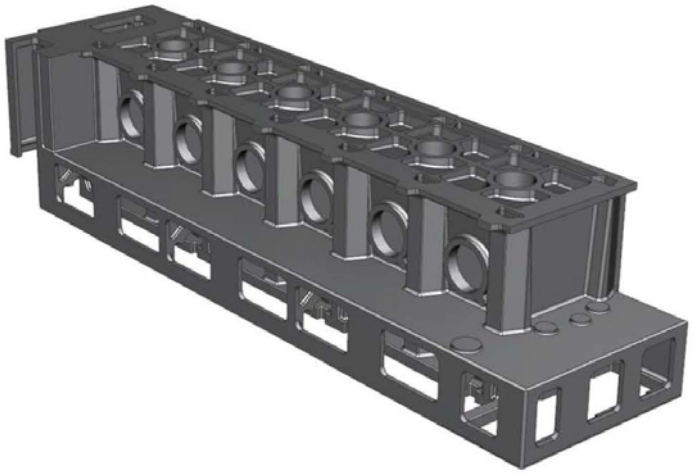

Dummy filling, layout 1

Vertical sprue, Ø90

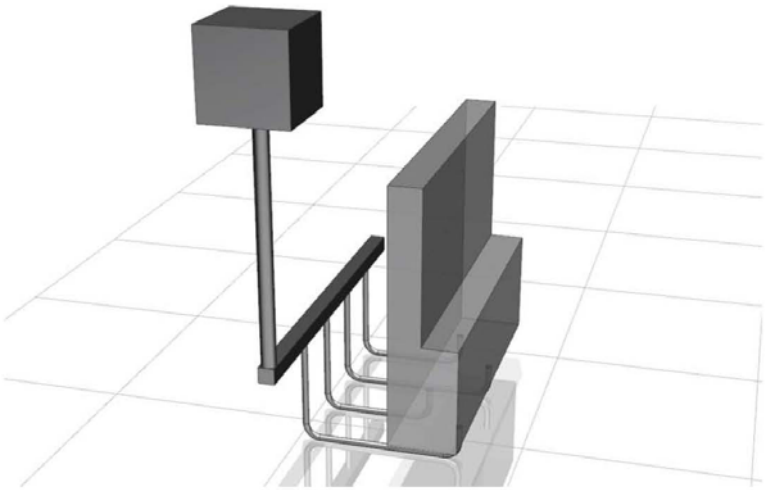

Dummy filling, layout 2
Split sprue, Ø100 & Ø90

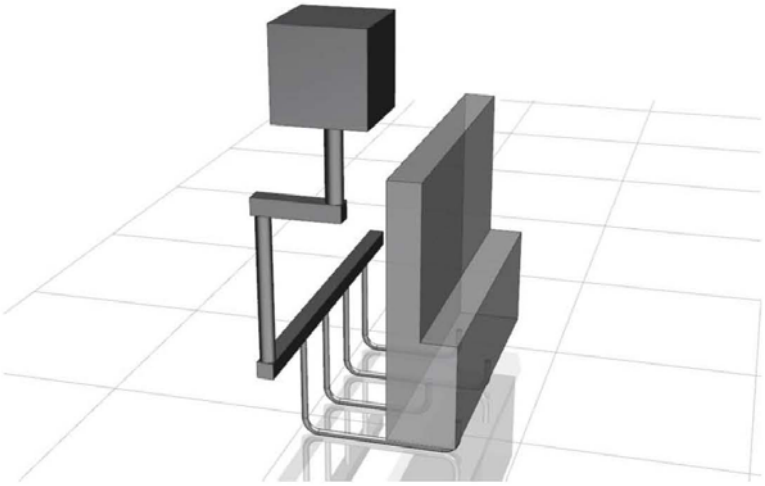

Dummy filling, layout 3
Split sprue, Ø100 & Ø90 - Ø50

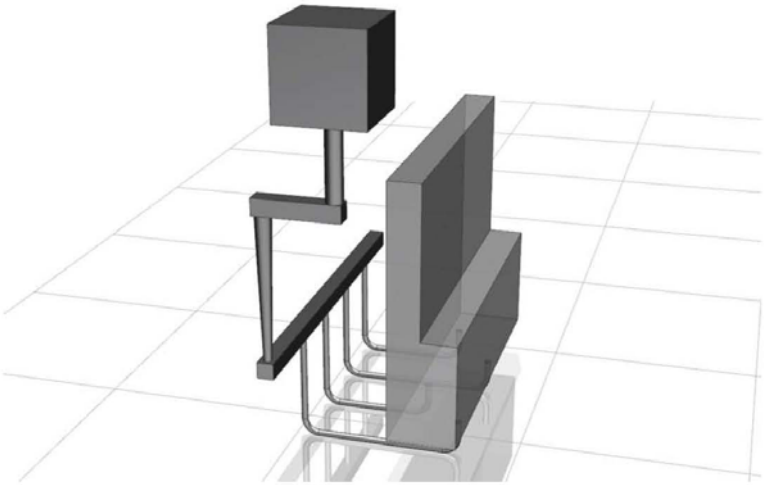

Dummy filling
Same pouring rate for all three layouts

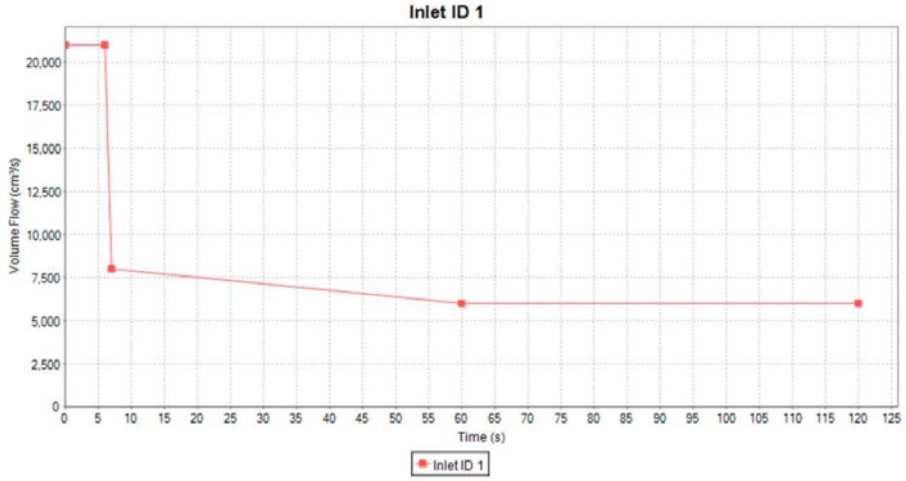

Layout 1
Absolute Velocity, fill time ~128s

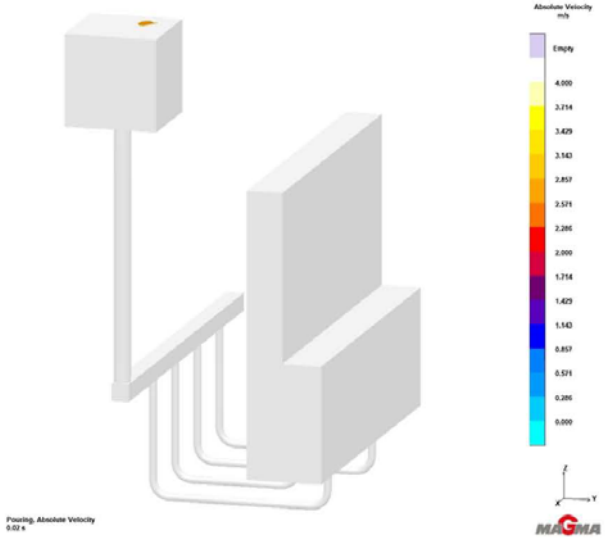

Layout 1
Absolute Velocity

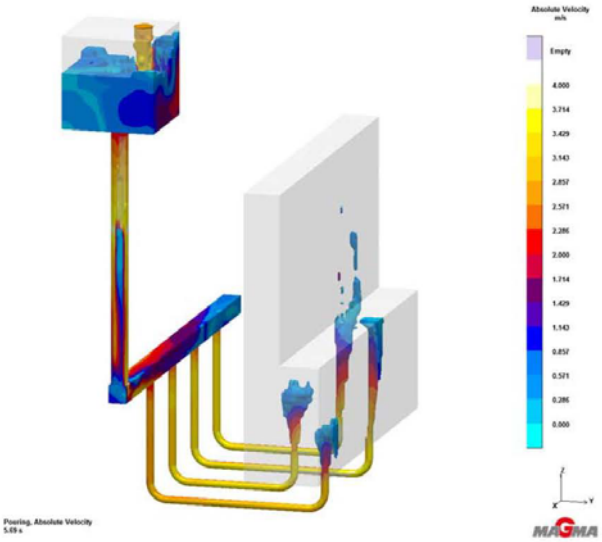

Layout 2
Absolute Velocity, fill time ~130s

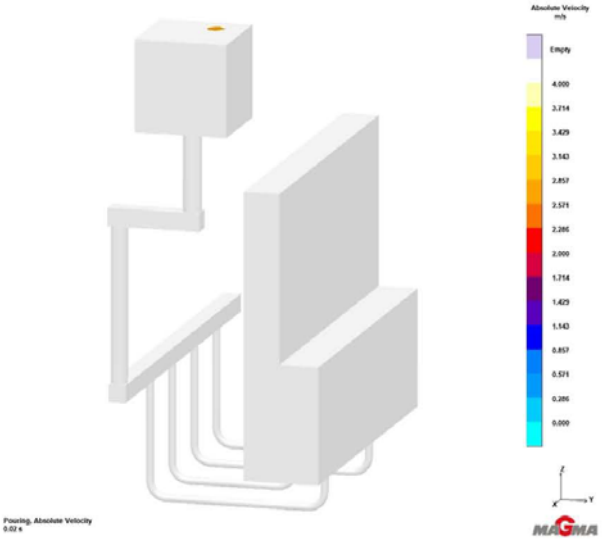

Layout 2
Absolute Velocity

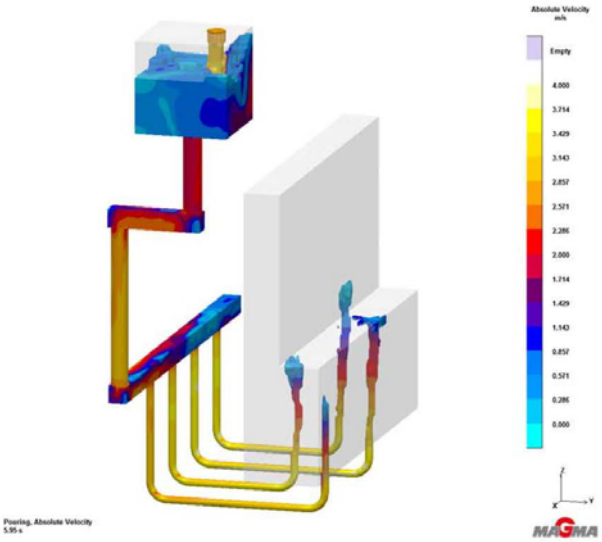

Layout 3
Absolute Velocity, fill time ~140s

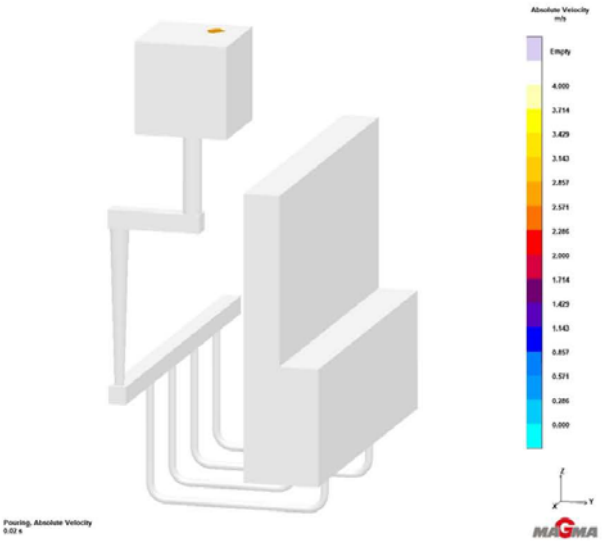

Layout 3
Absolute Velocity

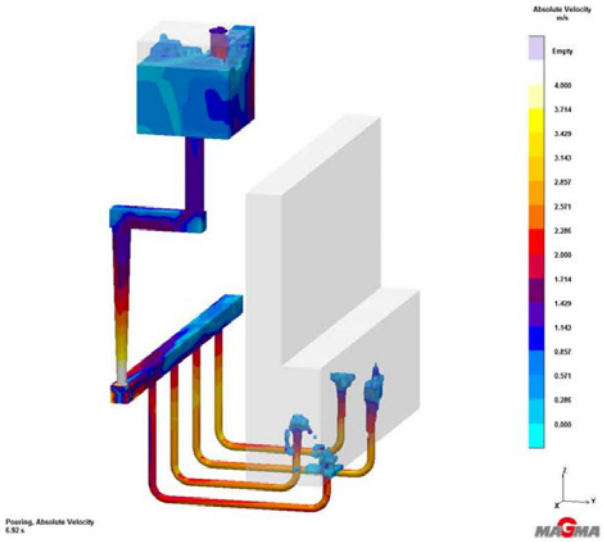

Comparison, ~6 sec.
Layout 2 Layout 3

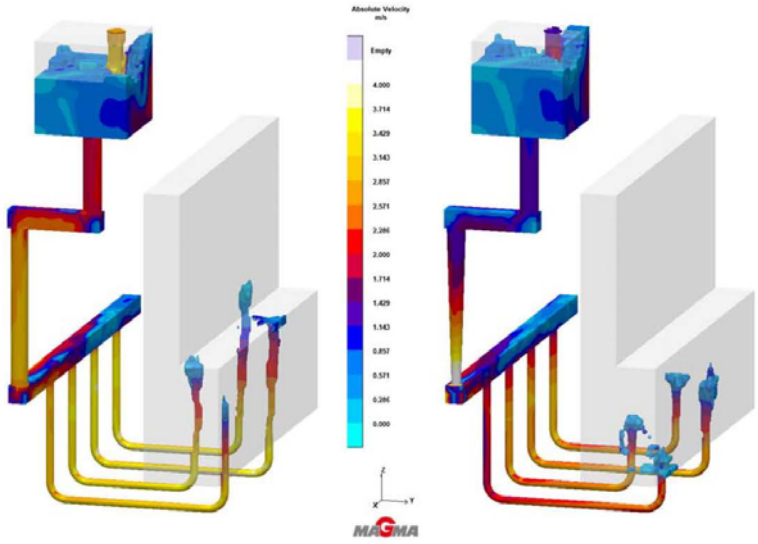

Comparison, ~45 sec.

Layout 2 Layout 3

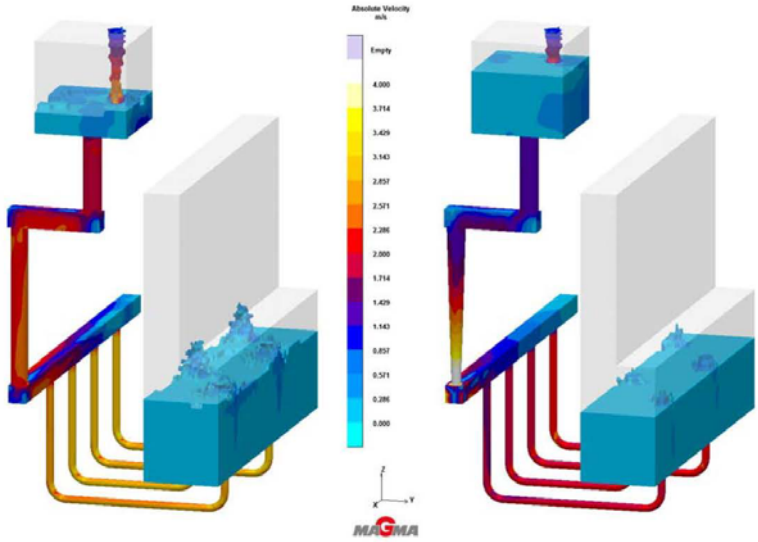

Cylinder liner G50ME-C

Grey cast iron – Tarkalloy A

Kvalitets sikring – internt & eksternt

Værktøjskassens indhold

- Optimere designet, så det er støbevenligt
  - **støbesimulering.**
- Udarbejde specifikationer og rekommandationer
  - **designkrav + erfaring + tilbagemeldinger fra producenter.**
- Hjælpe specifikke producenter med at optimere støbe layoutet
  - **støbesimulering.**
- Hjælpe specifikke producenter med at optimere smeltebehandlingen
  - **smeltemetallurgisk viden.**
- Hjælpe specifikke producenter med at optimere formmaterialerne
  - **viden om formsand og bindemidler.**

Ny metode til kvantificering af grafitstørrelse og –morfologi i støbejern

Steen Krogh Jensen, MAN

Ny metode til kvantificering af grafitstørrelse og –morfologi i støbejern

Disclaimer

All data provided on the following slides is for information purposes only, explicitly non-binding and subject to changes without further notice.

Agenda

1	Cylinderforing – gammel materialspecifikation
2	ISO 945 – graphite classification
3	Cylinderforing – eksempler på grafit struktur, matrix and hårdfase
4	Grafitstørrelse – en ny definition
5	Hårdfase – mængde og fordeling
6	Ferrit – mængde?
7	Cylinderforing – ny materialespecifikation
8	Eksempler fra støberier
9	Stempelring – materialespecifikation – nodularitet
10	ISO 16 112 – Compacted (vermicular) graphite cast irons - Classification

Cylinderforing
Gammel materialespecifikation

MAN B&W Diesel A/S

Cast Iron

Cast Iron for Cylinder Liners **Tarkall-C**

Mechanical Properties

Tensile Strength	R_m	N/mm²	min. 245[1]
Elongation	A_{50}	%	min. 0.3[2]
Brinell Hardness (ISO 6506-1981)	HBS	10/3000/15	180-230[3]

[1] In the upper part of the cylinder liner.
[2] Total elongation at fracture i. e. elastic + plastic elongation. See Q.C. 74 18 96-0.
[3] Measured on the inside of the cylinder liner, 100 mm from the top.

Microstructure

- Graphite (ISO 945-1975): I A 2/3/4.
- Matrix: Lamellar pearlite. Max. 3% ferrite. 3-7% cementite + steadite.

Microstructure

- **Graphite (ISO 945-1975): I A 2/3/4.**
- **Matrix: Lamellar pearlite. Max. 3% ferrite. 3-7% cementite + steadite.**

- **Figures and text in bold type denote imperative demands.** All other information - including Similar Standards - is given for guidance only. (See General Note).
- According to Quality Control No. 74 14 12-0 the foundry must carry out a first-time casting and obtain the approval of MAN B&W Diesel A/S as supplier of cylinder liners made of Tarkall-C.

Similar Standards

ISO
EN
JIS
These standards do not include any Cast Iron similar to the above quality.

Supply Form

Finished cylinder liners. Tarkall-C is an abbreviation of the trade name Tarkalloy C.

 Material Sheet P 676-2

Tribologi/Styrke/ Varmeledningsevne

Slidstyrke

Scuffing resistens

Styrke/Tribologi

Grafitform ifølge ISO 945

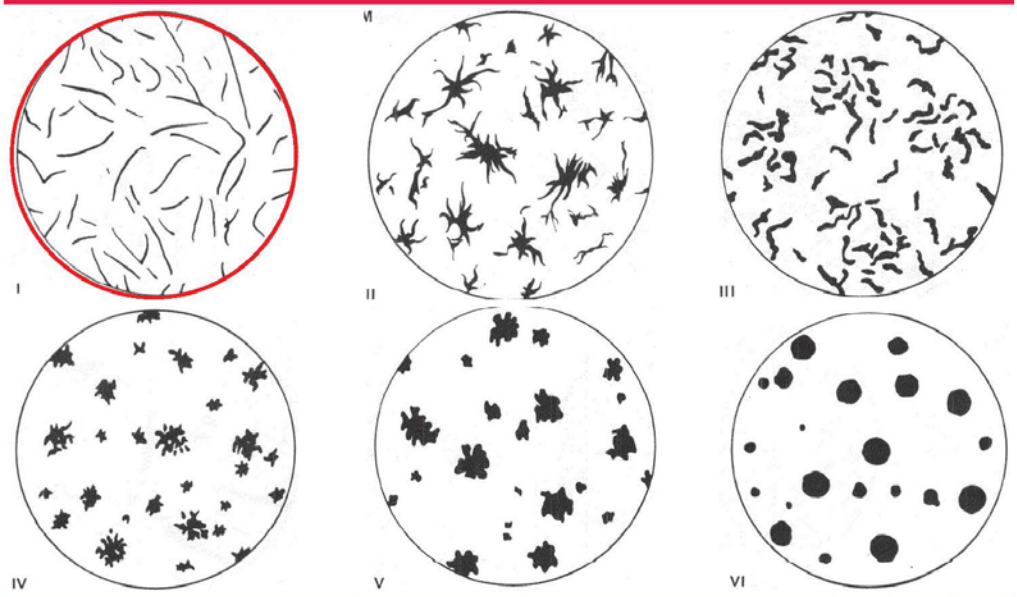

Grafitstørrelse ifølge ISO 945

Table 1 — Dimensions of graphite particle forms I to VI

Dimensions in millimetres

Size range reference number	Indication of the particle size observed at ×100 magnification	Actual dimension
1	⩾ 100	⩾ 1
2	50 to < 100	0,5 to < 1
3	25 to < 50	0,25 to < 0,5
4	12 to < 25	0,12 to < 0,25
5	6 to < 12	0,06 to < 0,12
6	3 to < 6	0,03 to < 0,06
7	1,5 to < 3	0,015 to < 0,03
8	< 1,5	< 0,015
NOTE 1	When determining size ranges 1 and 2, a lower magnification (×25 or ×50) may be used.	
NOTE 2	When determining size ranges 6 to 8, a higher magnification (×200 or ×500) may be used.	
NOTE 3	For determining size ranges, the largest visible graphite particle size is used.	

Grafiteform - 7 støberier

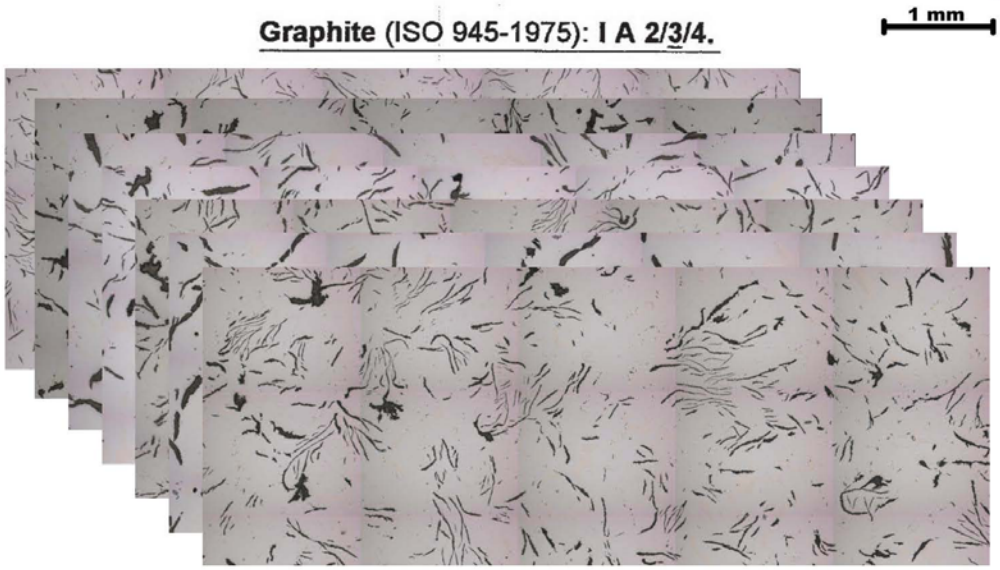

Matrix (perlit/ferrit)- 7 støberier

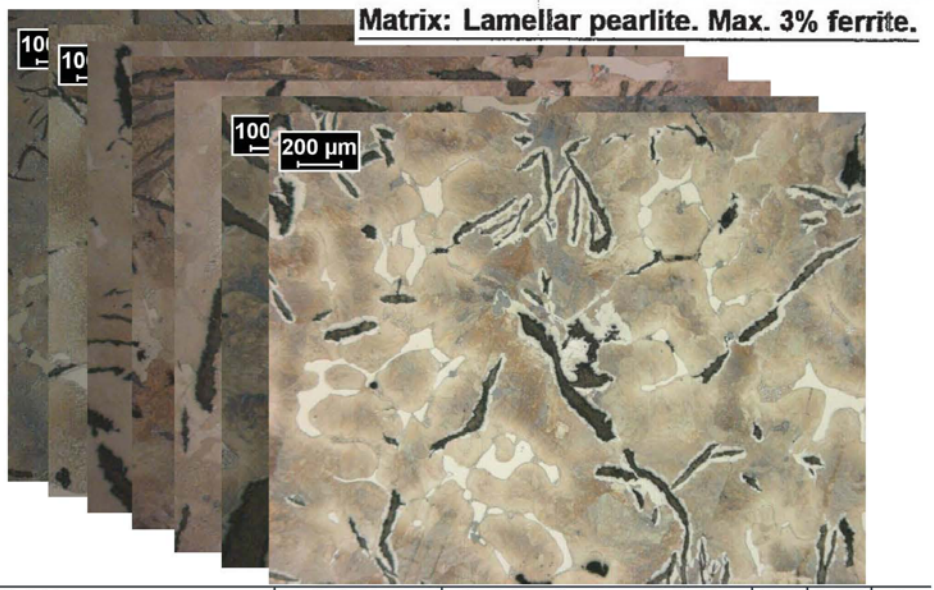

Hårdfase - 7 støberier

3-7% cementite + steadite.

1 mm

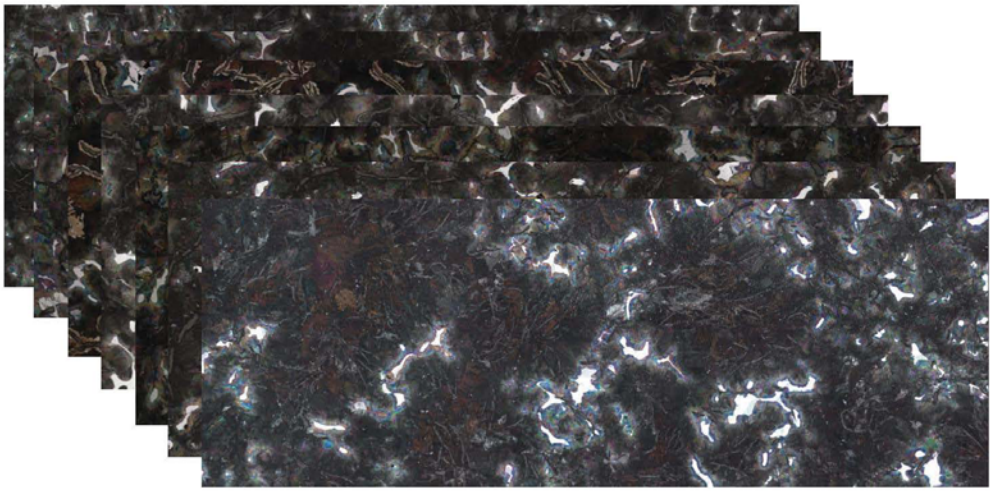

Samlet vurdering af Mikrostruktur 7 støberier

		Graphite type			% Cementite + Steadite			% Ferrite		
Position	Matrix	inside	centre	outside	inside	centre	outside	inside	centre	outside
MAN Diesel A/S	Pearlite	IA3/4/5	IA3/4/5	IA3/4/5	2.13	1.52	1.88	< 1	< 1	< 1
Leverandør nr. 1	Pearlite	A4			< 2			-		
MAN Diesel A/S	Pearlite	IA3/4/5	IA3/4/5	IA3/4/5	3.82	2.97	3.36	< 1	< 1	< 1
Leverandør nr. 3	Pearlite	A2-4			3 - 4			< 3		
MAN Diesel A/S	Pearlite	IA3/4/5	IA3/4/5	IA3/4/5	2.76	2.49	3.60	< 1	< 1	< 1
Leverandør nr. 4	Pearlite	A2-4			3 - 4			< 3		
MAN Diesel A/S	Pearlite	IA2/3/4	IA2/3/4/5	IA2/3/4/5	5.91	6.95	7.08	< 1	< 1	< 1
Leverandør nr. 2	Pearlite	IA3/4			4.2 - 6.4			Max. 1		
MAN Diesel A/S	Pearlite	IA2/3/4	IA2/3/4	IA2/3/4	4.48	5.50	5.88	~1	~1	~1
Leverandør nr. 6	Pearlite	-			-			-		
MAN Diesel A/S	Pearlite	IA2/3/4	IA2/3/4	IA3/4/5	4.46	4.27	3.29	< 1	< 1	< 1
Leverandør nr. 5	Pearlite	IA3	IA3	IA3	5.0	5.3	4.6	0	0	0
MAN Diesel A/S	Pearlite	IA2/3/4	IA2/3/4	IA2/3/4	5.7	5.3	6.1	< 1	< 1	< 1
Leverandør nr. 7	Pearlite	IA3/4	IA3/4	IA3/4	5.2	4.8	4.5	< 2	< 2	< 2
Spec. Takalloy-C	**Pearlite**	**IA2/3/4**			**3-7**			**Max. 3**		

- Ud fra ovenstående tabel er det svært at differentiere mellem forskellige leverandører
- Vurderingen af specielt grafitstørrelsen er delvis subjektiv
- Ikke særlig god overensstemmelse mellem vurderinger fra leverandører og MDT

Serviceerfaringer

Serviceerfaringer:

- Højere slid på nogle foringer end andre
- Større tilbøjelighed til scuffing på nogle foringer
- Revnede foringer

Observationer i mikrostrukturen:

- Stor forskel på grafitstørrelse (Længde/Bredde/Areal)
- Kæmpe forskel på mængden af hårdfase og fordelingen af denne
- Store variationer på mængden af ferrit
- Derudover fandtes store variationer på trækstyrken/udmattelsesstyrken

Brug for et generelt løft i kvaliteten:

- Målemetode til ensartet bestemmelse af grafitstørrelsen
- Bedre fordeling af hårdfasen – primære cellestørrelse
- Bestemmelse af ferritmængden

Grafitstørrelse – ISO 945
Forstørrelse: 100x

Repræsentativt?
Statistik?
Primær cellestørrelse?

Løsningen er

Mosaik!

Grafitstørrelse - Så er det jeres tur!

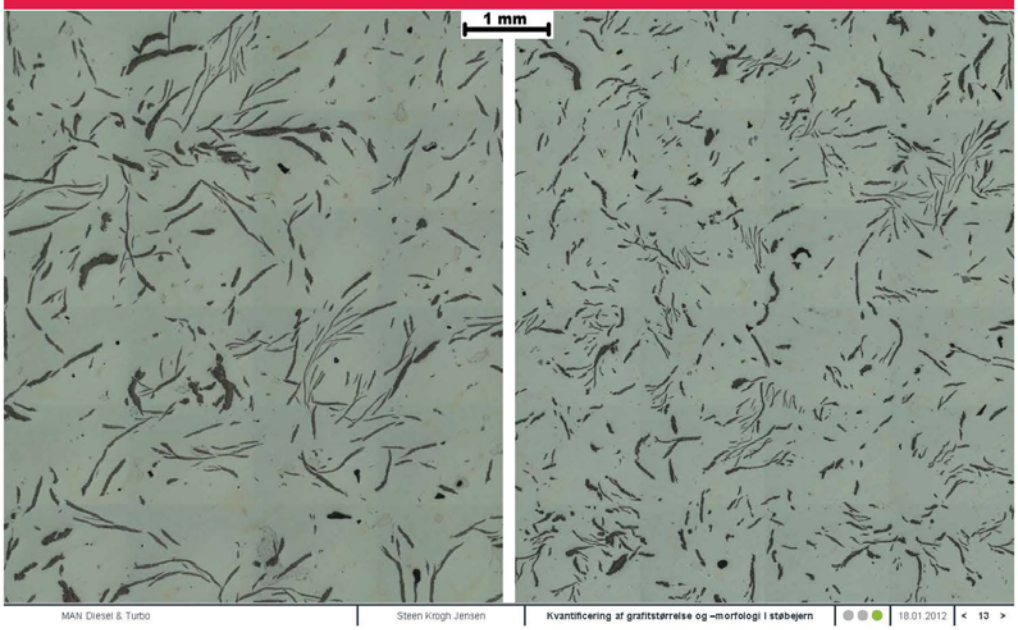

Grafitstørrelse - Lidt Hjælp

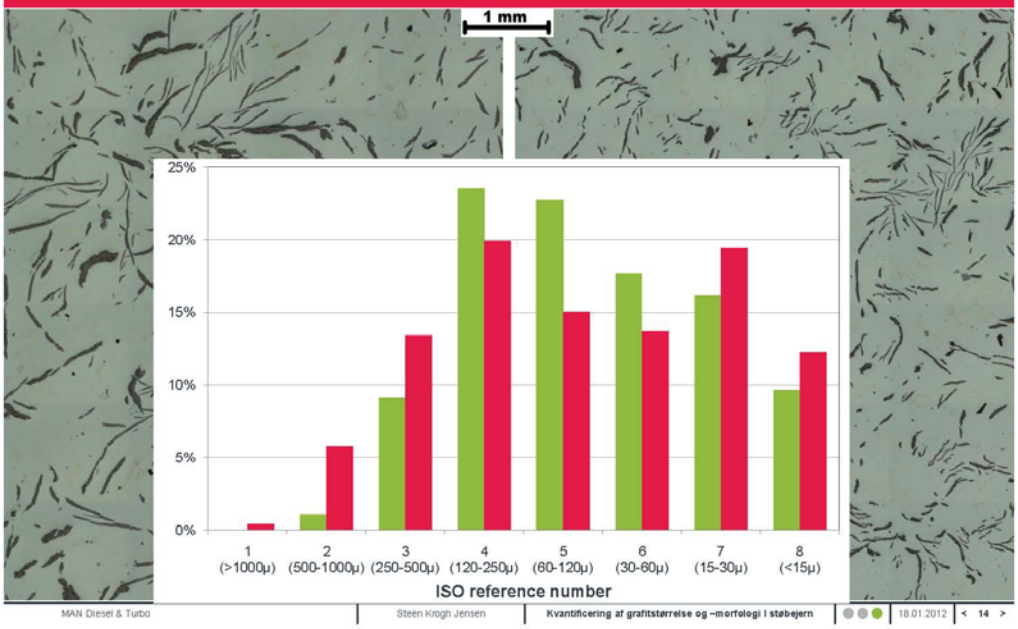

Grafitstørrelse
Lidt mere hjælp

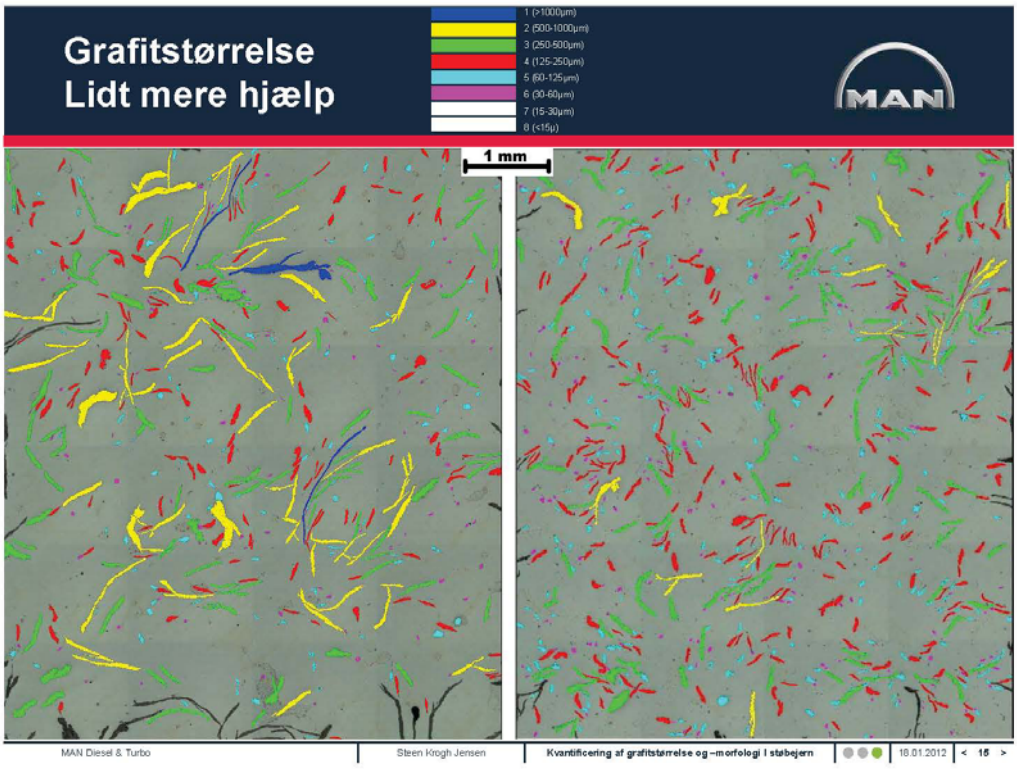

MAN Diesel & Turbo | Steen Krogh Jensen | Kvantificering af grafitstørrelse og –morfologi I støbejern | 18.01.2012 | < 15 >

Grafitstørrelse
Nu kommer det "nye" – Eksempel 1

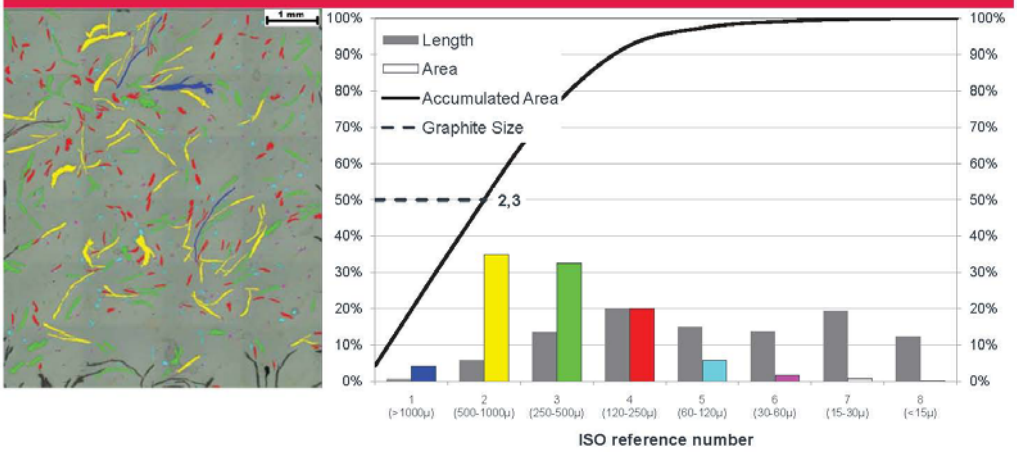

MAN Diesel & Turbo | Steen Krogh Jensen | Kvantificering af grafitstørrelse og –morfologi I støbejern | 18.01.2012 | < 16 >

Grafitstørrelse
Nu kommer det "nye" – Eksempel 2

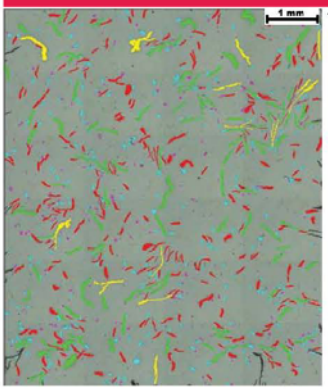

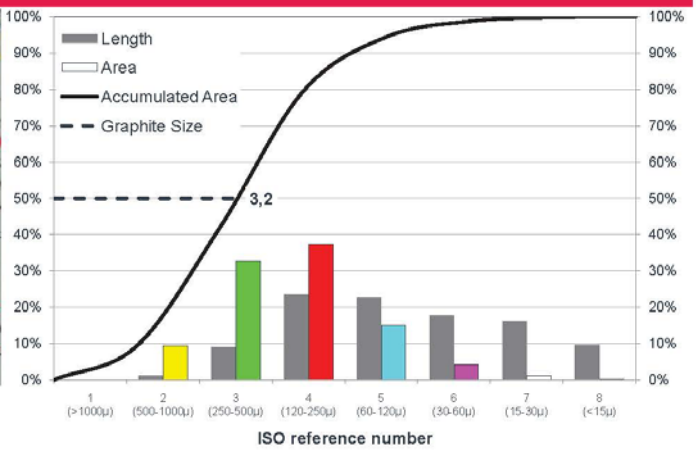

Grafitstørrelse
Nu kommer det "nye" – Eksempel 3

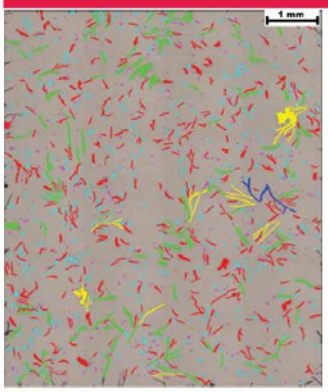

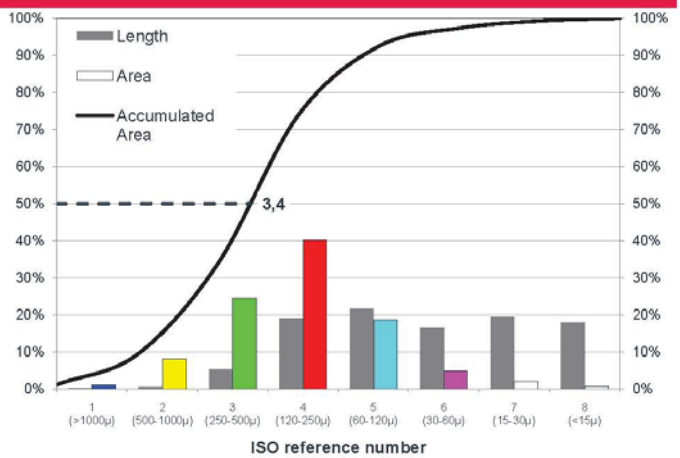

Grafitstørrelse - sammenfatning

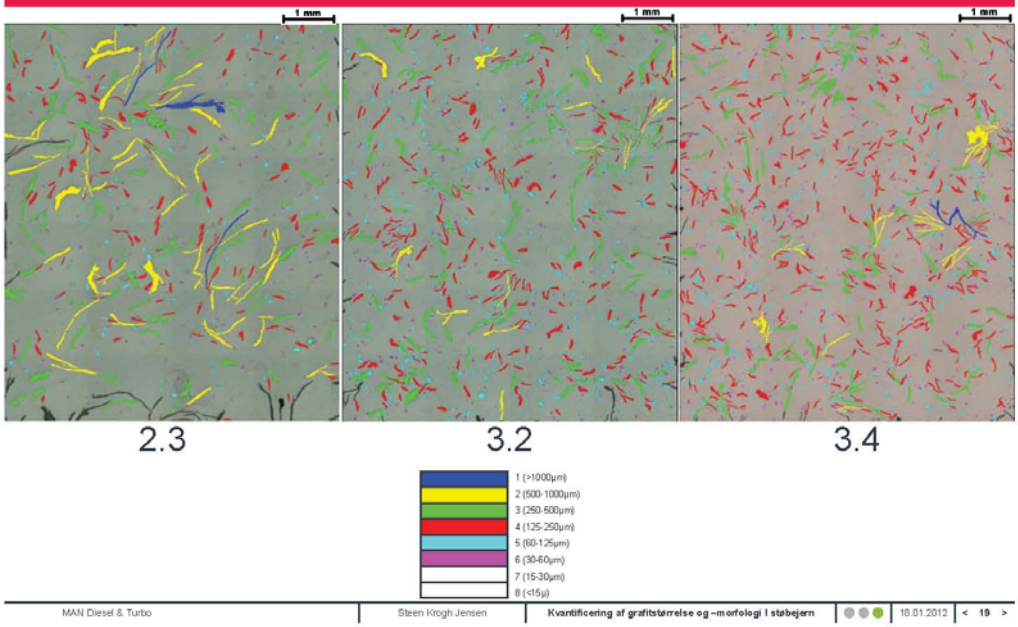

Hårdfase – Mængde og fordeling?

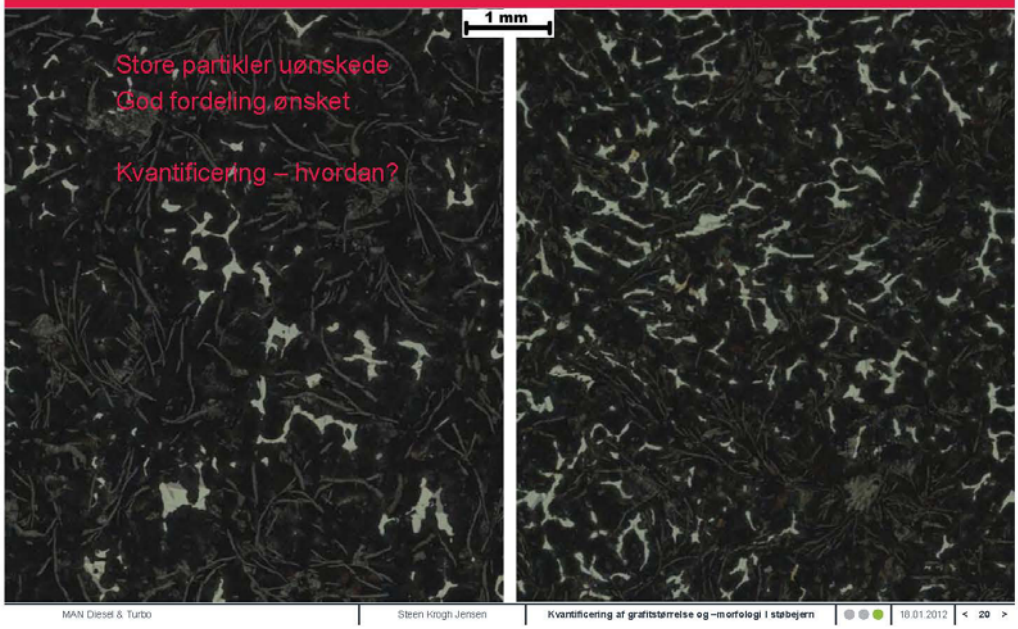

Hårdfase - Eksempler

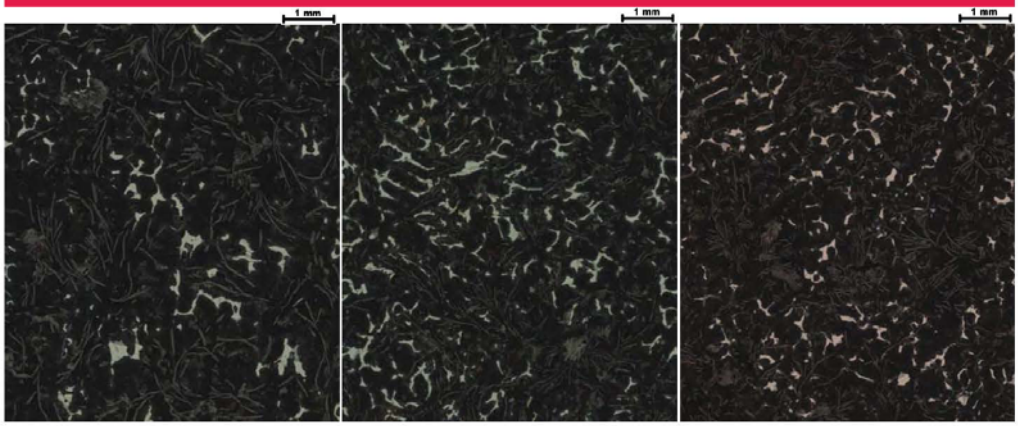

3.6% 6.4% 4.4%

Hårdfase - Sammenfatning

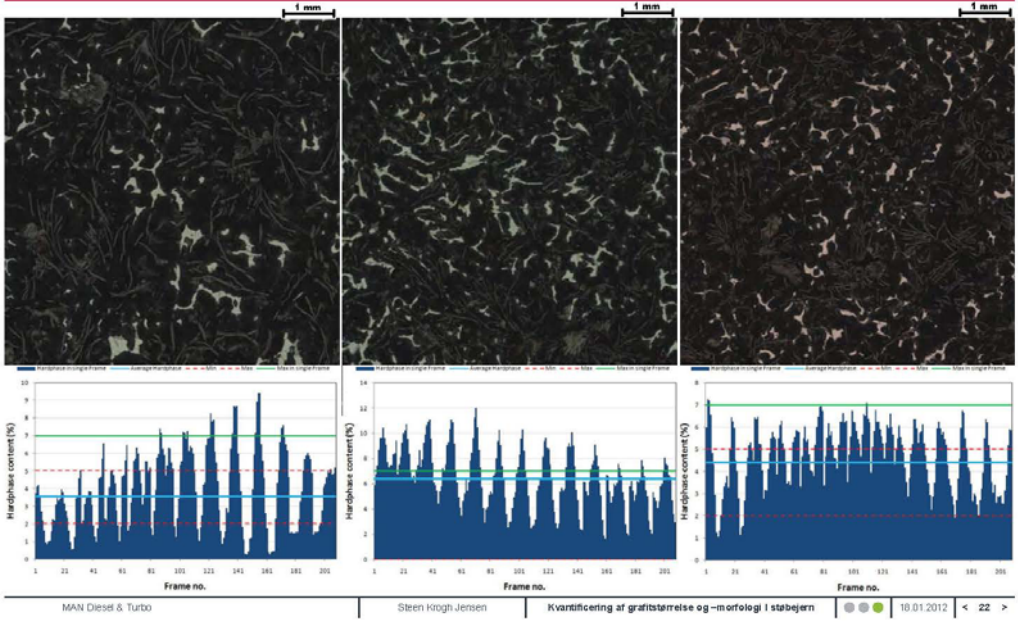

Ferrit?

Cylinderforing
"Komplet" beskrivelse af mikrostrukturen

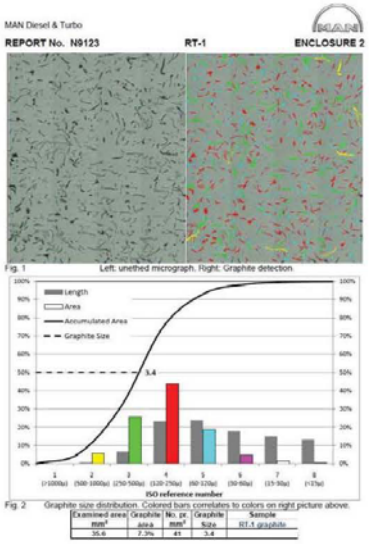

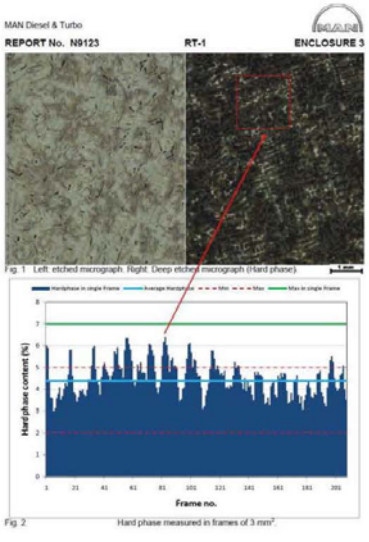

Cylinder foring
Samlet mikrostruktur evaluering

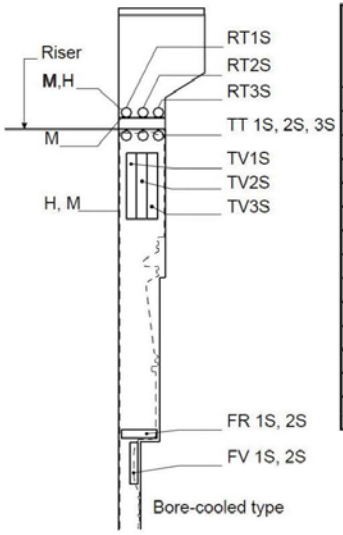

MDT Position	Matrix	Graphite				Cementite + Steadite		Ferrite		Enclosure
		Form	Distribution	Size	Area	Average	Max	Average	Max	
RT 1	Pearlite	I	A	3.0	8.3	6.1	12.6	<1	-	2 and 3
RT 2	Pearlite	I	A	3.2	7.8	6.7	12.6	<1	-	4 and 5
RT 3	Pearlite	I	A	3.1	7.2	5.4	9.6	<1	-	6 and 7
TT 1	Pearlite	I	A	2.9	8.0	5.1	9.2	<1	-	8 and 9
TT 2	Pearlite	I	A	3.0	8.6	4.9	9.7	<1	-	10 and 11
TT 3	Pearlite	I	A	2.9	7.6	4.9	8.0	<1	-	12 and 13
TV 1	Pearlite	I	A	3.0	8.6	4.4	9.0	<1	-	14 and 15
TV 2	Pearlite	I	A	2.9	7.9	5.1	8.8	<1	-	16 and 17
TV 3	Pearlite	I	A	3.0	8.2	4.6	9.1	<1	-	18 and 19
FR 1	Pearlite	I	A	3.2	7.5	6.8	12.5	<1		20 and 21
FR 2	Pearlite	I	A	3.1	7.4	4.1	6.8	<1		22 and 23
FV 1	Pearlite	I	A	3.2	7.9	5.6	9.0	<1		24 and 25
FV 3	Pearlite	I	A	3.4	6.2	5.6	10.0	<1		26 and 27
Spec. for Tarkalloy C	Pearlite	IA2/3/4			-	<7	-	<3	-	

Cylinderforing
Ny materialespecifikation

Gammel

MAN B&W Diesel A/S

Cast Iron

Cast Iron for Cylinder Liners **Tarkall-C**

Mechanical Properties

Tensile Strength	R_m	N/mm²	min. 245[a]
Elongation	A_{50}	%	min. 0.3[a][b]
Brinell Hardness (ISO 6506-1981)	HBS	10/3000/15	180-230[a]

[a] In the upper part of the cylinder liner.
[b] Total elongation at fracture i. e. elastic + plastic elongation. See Q.C. 74 18 96-0.
[a] Measured on the inside of the cylinder liner, 100 mm from the top.

Microstructure

- Graphite (ISO 945-1975): I A 2/3/4.
- Matrix: Lamellar pearlite. Max. 3% ferrite. 3-7% cementite + steadite.

Chemical Composition

	C%	Si%	Mn%	P%	S%	B%	Cu%	V%
Min.	3.0			0.2		0.02	1.0	
Nominal	3.2	1.1	0.8					
Max.				0.4	0.10	0.04	1.5	0.22

Heat Treatment

In case of demand for stress relieving: Heat max. 90°C/hour to 550°C, hold for 4 hours. Cool in furnace max. 50°C/hour to max. 150°C.

- Figures and text in bold type denote imperative demands. All other information - including Similar Standards - is given for guidance only. (See General Note).
- According to Quality Control No. 74 14 12-0 the foundry must carry out a first-time casting and obtain the approval of MAN B&W Diesel A/S as supplier of cylinder liners made of Tarkall-C.

Similar Standards

ISO
EN
JIS

These standards do not include any Cast Iron similar to the above quality.

Supply Form

Finished cylinder liners. Tarkall-C is an abbreviation of the trade name Tarkalloy C.

 Material Sheet P 676-2

Ny

MAN Diesel & Turbo

Iron, Cast

Cast Iron for Cylinder Liners Tarkalloy C

Data marked with "■" are imperative demands.

All other information, including "Guidance - Standards - References", are given for guidance only.

MDT SPECIFICATIONS

Q.C. 74141-0 Cylinder Liners - Tarkalloy C/A - First-Time Production Approval
Q.C. 745688-3 Evaluation of microstructures based on Image analysing equipment/software for Tarkalloy C/A Cylinder Liners
Q.S. 74317-3 Quality Specification for Two-Stroke Cylinder Liners

APPLICATION

Cylinder Liners

NOTES

New suppliers of TARKALL-C CYLINDER LINERS must be approved by MDT, see the Q.C. mentioned in the MDT Specifications.

MECHANICAL PROPERTIES

Standard Test Method	Condition	Position	Dimension [mm]	Temperature [°C]	Rp min [MPa]	Rm min [MPa]	Rmmax [MPa]	A50 min [%]	Rb min [MPa]	Rb max [MPa]
ISO 6892-2(1998)	40Hz	Liner Material	-	20		245		0.3		

MECHANICAL PROPERTIES - NOTES

- In the upper part of the cylinder liner.
- Total elongation at fracture(i.e. elastic + plastic elongation): See the Q.C. mentioned in the MDT Specifications.

HARDNESS - ROOM TEMPERATURE

Standard Test Method	Condition	Position	Dimension mm	HB min	HB max	HB nom	HV min	HV max	HV nom
ISO 2039-1 (1988)	40Hz	Liner Material	-	180					

HARDNESS NOTES

Measured on the inside of the cylinder liner, 100 mm from the top.

CHEMICAL COMPOSITION

Limit	Dimension [mm]	C%	Si%	Mn%	P%	S%	Cr%	Mo%	Ni%	Cu%	V%	Nb%	Ti%	B%	Mg%	Sn%
■ Min.	-	3.0	-	-	0.20	-	-	-	-	1.00	-	-	-	0.020	-	-
Nominal	-	3.2	1.1	0.8	-	-	-	-	-	-	-	-	-	-	-	-
■ Max.	-	-	-	-	0.40	0.10	-	-	-	1.50	0.22	-	-	0.040	-	-

COMPOSITION - NOTES

Nominal for chemical composition means "average". Normally a deviation of ± 10 % is fully acceptable, but this is not an imperative demand as long as the mechanical properties are fulfilled.

STRUCTURE - IRON ACCORDING TO ISO 945 (1975)

Dimension [mm]	Graphite Form	Graphite Distribution	Reference Size	Cementite+ Steadite %	Ferrite %	Pearlite %
■ > 100 mm	I	A	2-3/4	<7%	<3%	Rest
■ ≥ 100 mm	I	A	2-3/4	3-6%	≤ 1%	Rest

STRUCTURE - NOTES

The notes are valid only for group 3 cylinder liners - 0-40 mm from finish machined inside surface.

- Max 3% Ferrite - measured within a test area of app. 2 mm², where highest concentration is observed
- Max 7% Cem+Ste - measured within a test area of max 3 mm², where highest concentration is observed

HEAT TREATMENT

Stress Relieving in case of demand.

HEAT TREATMENT - NOTES

Treatment	Heating Rate	Temperature [°C]	Holding Time min [h]	Cooling Media1	Cooling Rate	Cool To [°C]	Cooling Media2	Application
Stress Relieving	< 90 °C/h	550	4	Furnace	50 °C/h	< 150	-	

 Material Technology & Research | Revised By EKB | Accepted By EKB | Issue Date March 2011 | Revision Date March 2011 | NdeoRov | New demands for group 5 liners | Revision No P 676-4

Printed: 02-Apr-12 Page 1 of 2

Cylinderforing
Ny materialespecifikation

Gammel

Microstructure

- **Graphite** (ISO 945-1975): **I A 2/3/4.**
- **Matrix: Lamellar pearlite. Max. 3% ferrite. 3-7% cementite + steadite.**

Ny

STRUCTURE - IRON ACCORDING TO ISO 945 (1975)

Dimension (mm)	Graphite Form	Graphite Distribution	Reference Size	Cementite+ Steadite %	Ferrite %	Pearlite %
< 800 mm	I	A	2-3-4	< 7%	< 3%	Rest
≥ 800 mm	I	A	2-3-4	2-5%	≤ 1%	Rest

STRUCTURE - NOTES

The notes are valid only for group 3 cylinder liners - 0-40 mm from finish machined inside surface:

- Max 3% Ferrite - measured within a test area of app. 2 mm², where highest concentration is observed
- Max 7% Cem+Ste - measured within a test area of max 3 mm², where highest concentration is observed

- Øget ensartethed
- Generelt kvalitetsløft
- "Ny" omgang FTA
- Fundet "aktive" leverandører
- Ferritmåling er endnu ikke automatiseret!
- Indkøb af billedbehandlingsudstyr hos underleverandører

Cylinderforing
Eksempler fra underleverandører

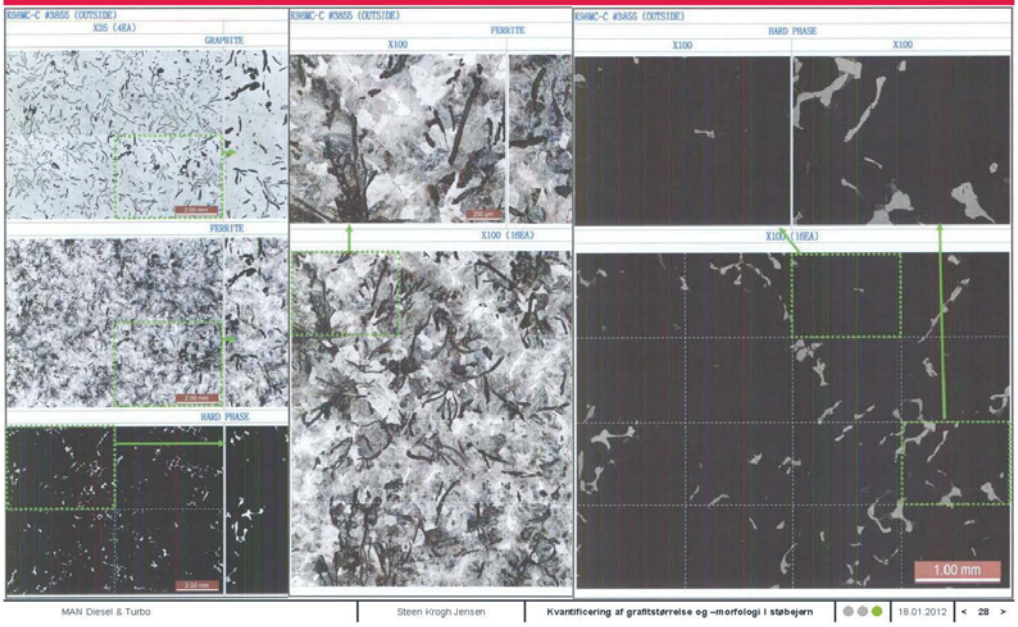

Cylinderforing
Eksempler fra underleverandører

MAN Diesel & Turbo | Steen Krogh Jensen | Kvantificering af grafitstørrelse og –morfologi I støbejern | 18.01.2012 | < 29 >

Cylinderforing
Eksempler fra underleverandører

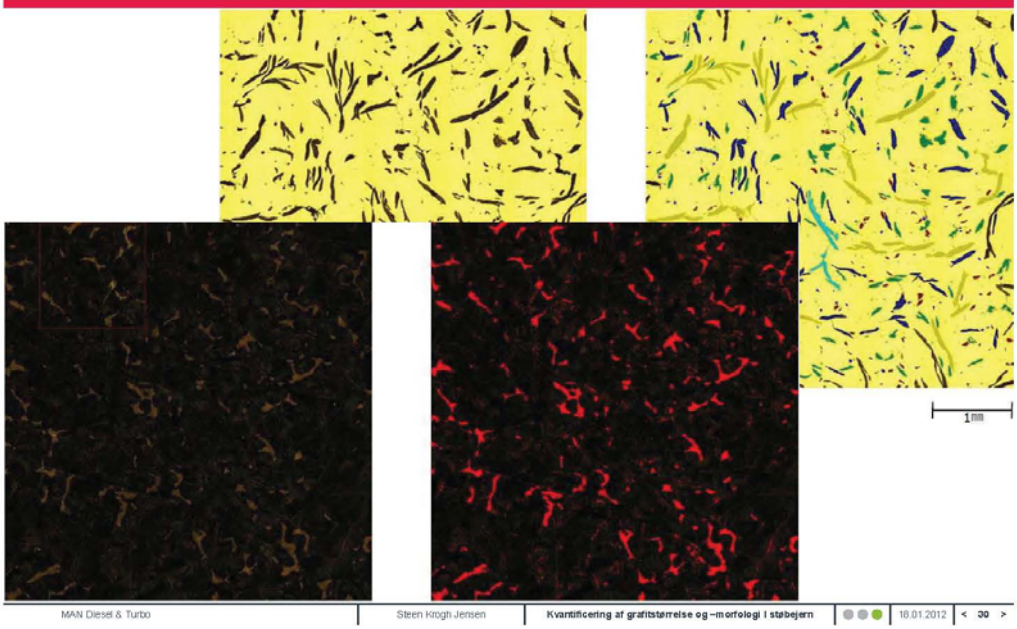

MAN Diesel & Turbo | Steen Krogh Jensen | Kvantificering af grafitstørrelse og –morfologi I støbejern | 18.01.2012 | < 30 >

Cylinderforing
Eksempler fra underleverandører

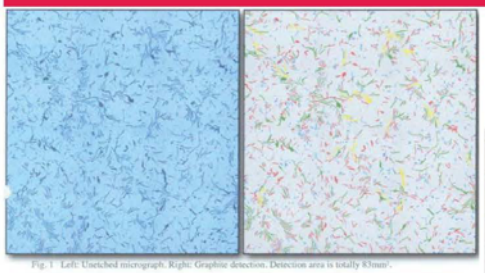

Fig. 1 Left: Unetched micrograph. Right: Graphite detection. Detection area is totally 83mm².

CLASS	1	2	3	4	5	6	7	8
Length	>1000µm	500-1000µm	250-500µm	120-250µm	60-120µm	30-60µm	15-30µm	<15µm
Area	0.29%	7.05%	27.20%	35.15%	16.49%	5.79%	4.10%	4.93%
Accumulated area	0.29%	7.34%	34.54%	69.69%	86.18%	91.97%	96.07%	100.00%

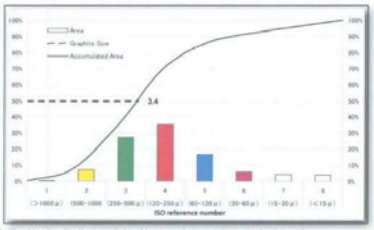

Fig. 2 Graphite size distribution. Colored bars correlates to colors on right picture above.

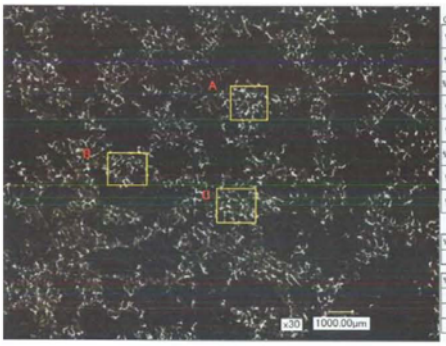

Chemical composition	
%C	3.34
%Si	1.05
%Mn	0.74
%P	0.222
%S	0.093
%Cu	1.15
%V	0.001
%B	0.023

%Cem+Ste Average
3.2

%Cem+Ste MAX	
A	9.5
B	7.7
C	9.0

Stempelring
Materialespecifikation

MAN Diesel & Turbo

Iron, Cast

Cast Iron for Piston Rings (Vermicular graphite) CV1

Data marked with "■" are imperative demands.

All other information, including "Guidance - Standards - References", are given for guidance only.

MDT SPECIFICATIONS

G.C. 742650-8 Piston Rings - First-Time Production Approval

APPLICATION

Finished piston rings.
The piston ring maker MUST be approved by MDT

NOTES

Previous part of datasheet: R/VK-C - RevisionNo P 649-2 Issued January 2003

MECHANICAL PROPERTIES

Standard Test Method	Condition	Position	Dimension [mm]	Temperature [°C]	Rp min [MPa]	Rm min [MPa]	Rm max [MPa]	A5d min [%]	Rb min [MPa]	Rb max [MPa]
ISO 6892 (2009)	+U+c	Ring	-	20		425		0.6	740	

MECHANICAL PROPERTIES - NOTES

■ Elongation (A): ≥ 0.6% (ring diameters ≥ 900 mm).

STRUCTURE - IRON ACCORDING TO ISO 945 (1975)

	Dimension (mm)	Graphite Form	Graphite Distribution	Reference Size	Cementite+ Steadite %	Ferrite %	Pearlite %
■	≥ ø 900	III; nodularity < 20 %	A	4/6	1-3	≤ 3	Rest
■	< ø 900	III; nodularity < 20 %	A	4/6	3-7	≤ 3	Rest

STRUCTURE - NOTES

■ The nodularity must be determined according to ISO16112 or JIS5502 respectively

■ The approved piston ring maker must produce piston rings in full agreement with own material specification, known and approved by MDT.

■ Any changes of the chemical composition already approved for the actual piston ring maker will result in a demand for a new approval test.

PHYSICAL PROPERTIES

Temperature [°C]	Density [kg/m3] Nom	MeanExpansion [10-6/°K] Nom	ThermalConductivity [W/m°K] Nom	MeanHeatCapacity [J/kg°K] Nom	Modulus Elasticity [GPa] Nom	Modulus Rigidity [GPa] Nom
20					165	

PHYSICAL - NOTES

For Modulus of Elasticity specified as "Nominal" a deviation of +/- 10% is acceptable. Must be verified during the "First Time Approval".

Nodularitet

- Evig diskussion!
- Subjektivt vurderet
- Indflydelse på varmeledningsevne
- Påvirker tribologiske egenskaber
- Ny standard – ISO 16112

Nodularity according to ISO 16112

$$\text{Roundness} = \frac{A}{A_m} = \frac{4 \times A}{\pi \times l_m^{\,2}}$$

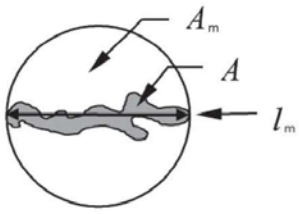

A_m area of circle of diameter l_m

A area of the graphite particle in question

l_m maximum axis length of the graphite particle in question = maximum distance between two points on the graphite particle perimeter

Roundness-shape factor	Graphite form
0,625 to 1	Nodular (ISO form VI)
0,525 to 0,625	Intermediate (ISO forms IV and V)
< 0,525	Compacted (ISO form III)
Flake graphite particles and graphite particles with maximum axis length less than 10 µm are not included in the analysis.	

Percent nodularity is calculated on an area basis as follows:

$$\text{Percent nodularity} = \frac{\sum A_{\text{nodules}} + 0{,}5 \times \sum A_{\text{intermediates}}}{\sum A_{\text{all particles}}} \times 100$$

A_{nodules} is the area of particles classified as speroidal (nodular) graphite;

$A_{\text{intermediates}}$ is the area of particles classified as intermediate forms of graphite;

$A_{\text{all particles}}$ is the area of all graphite particles greater than 10 µm.

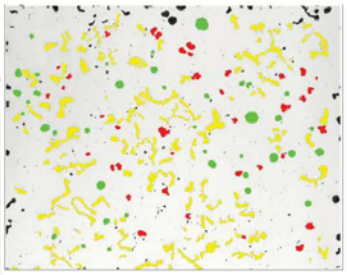

Nodularity according to JIS 5502

$$\text{Roundness} = \frac{A}{A_m} = \frac{4 \times A}{\pi \times l_m^{\,2}}$$

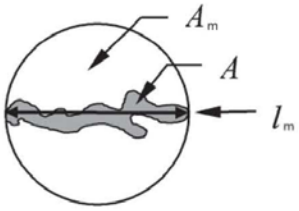

5. Image analysis (calculation of nodularity) procedure

(1) Import the image data of graphite structure ---------- 3. - a)

(2) Digitalization: split into black particles (graphite) and white part (matrix)

(3) Correction of digitalized images: eliminate graphite which size is not over 15 µm ------ 3. - b)

(4) Calculation of nodularity (automatic calculation)

i) Classification of graphite: divide graphite shape into **I -IV** and **V-VI**

*Classification method;

If a graphite area ratio against the minimum circumscribed circle of the graphite

(= (Area of graphite) x 100 / Area of minimum circumscribed circle) is:

- under 55% => **I -IV**
- over 55% => **V-VI**

ii) Calculation of nodularity of graphite ---------- 3. - c)

$$\frac{\text{Figure of shape V-VI graphite}}{\text{Figure of all graphite}} \times 100 = \text{Nodularity (\%)}$$

Nodularitet - Eksempler

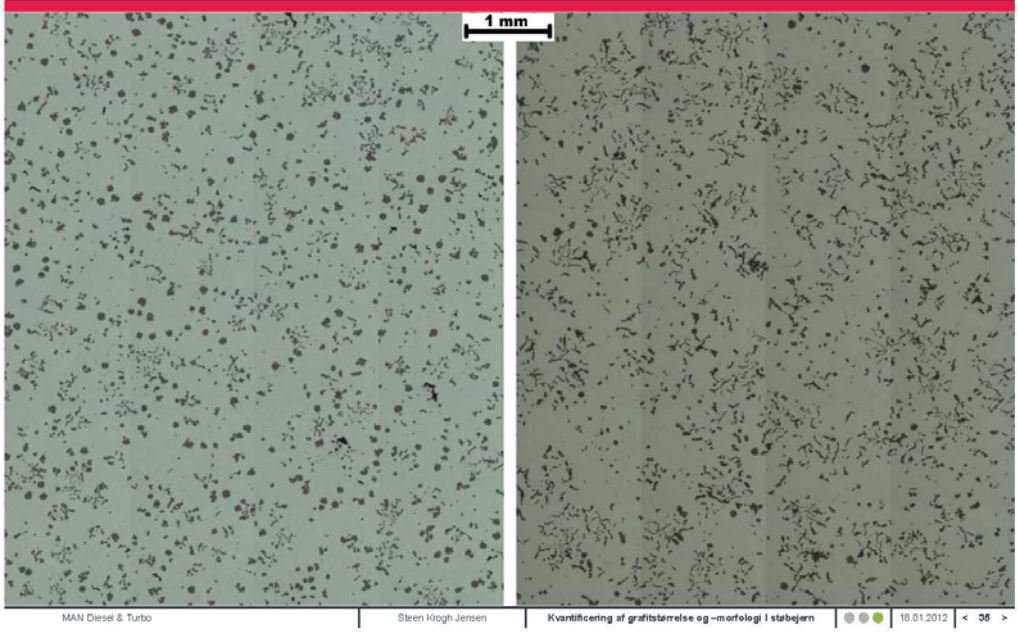

Nodularitet - Eksempler

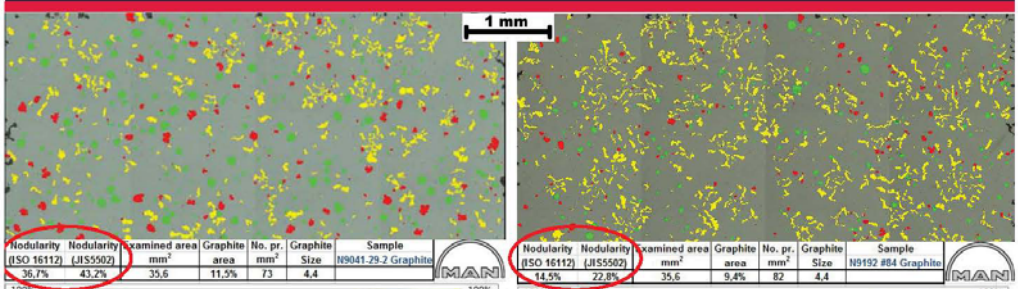

Nodularity (ISO 16112)	Nodularity (JIS5502)	Examined area mm²	Graphite area	No. pr. mm²	Graphite Size	Sample
36,7%	43,2%	35,6	11,5%	73	4,4	N9041-29-2 Graphite

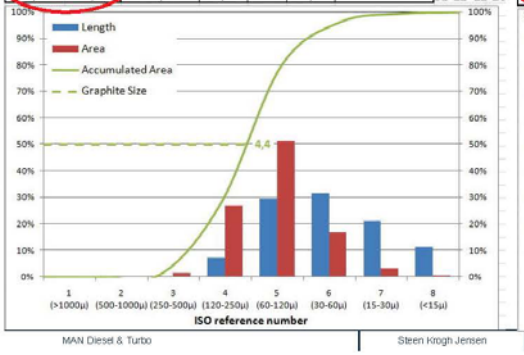

Nodularity (ISO 16112)	Nodularity (JIS5502)	Examined area mm²	Graphite area	No. pr. mm²	Graphite Size	Sample
14,5%	22,8%	35,6	9,4%	82	4,4	N9192 #84 Graphite

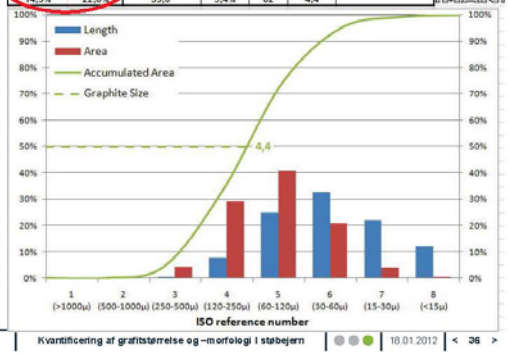

Stempelring
"Komplet" beskrivelse af mikrostrukturen

MAN Diesel & Turbo

REPORT No. NN9192 #84-4 ENCLOSURE 4

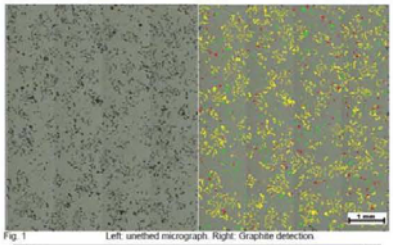

Fig. 1 Left: unethed micrograph. Right: Graphite detection

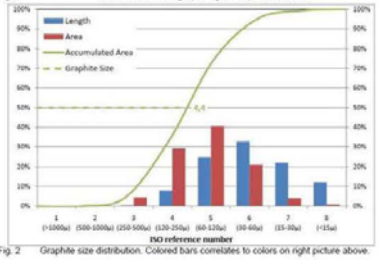

Fig. 2 Graphite size distribution. Colored bars correlates to colors on right picture above.

Nodularity (ISO 16112)	Nodularity (JIS5502)	Examined area mm²	Graphite area	No. pr. mm²	Graphite Size
14.5%	22.8%	35.6	9.4%	82	4.4

MAN Diesel & Turbo

REPORT No. N9192 #81-4 ENCLOSURE 3

Fig. 1 Left: etched micrograph. Right: Deep etched micrograph (Hard phase).

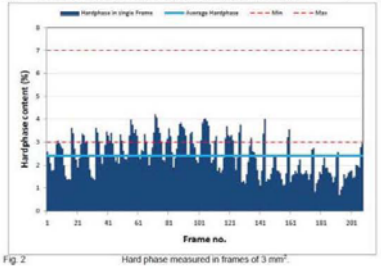

Fig. 2 Hard phase measured in frames of 3 mm².

Nodularitet - underleverandører

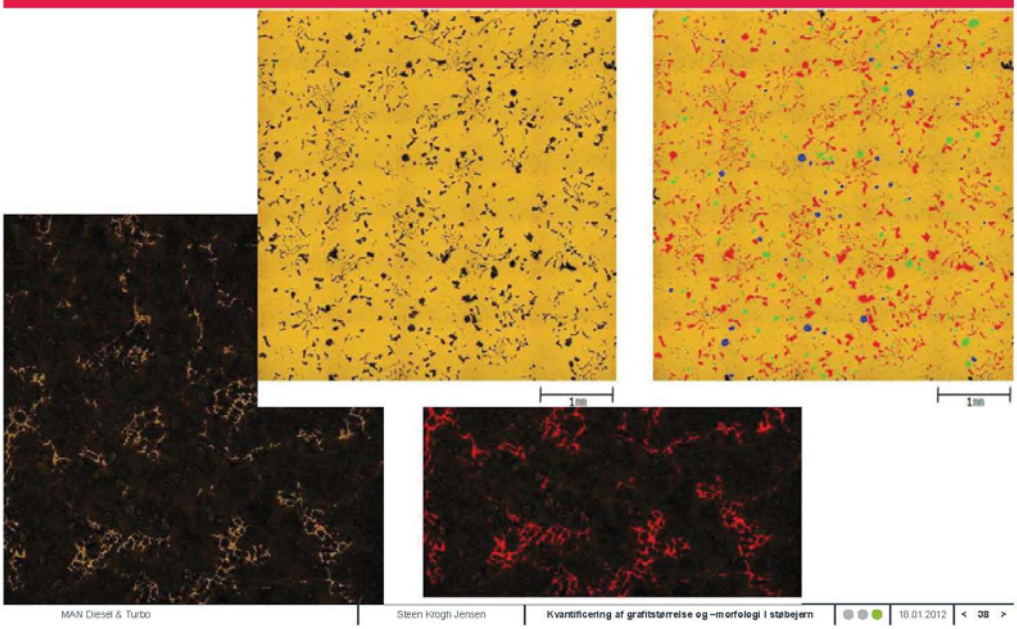

Disclaimer

All data provided in this document is non-binding.

This data serves informational purposes only and is especially not guaranteed in any way. Depending on the subsequent specific individual projects, the relevant data may be subject to changes and will be assessed and determined individually for each project. This will depend on the particular characteristics of each individual project, especially specific site and operational conditions.

Tak for opmærksomheden!

Materialevalg/Stålfremstilling

Stig Rubæk, Metal-Consult

DMS Vintermøde 2013

Materialevalg/Stålfremstilling

Særligt indlæg ved DMS´s Vintermøde 2013

på

Hotel Koldingfjord

16.-18 Januar 2013

Stig Rubæk /Metal-Consult

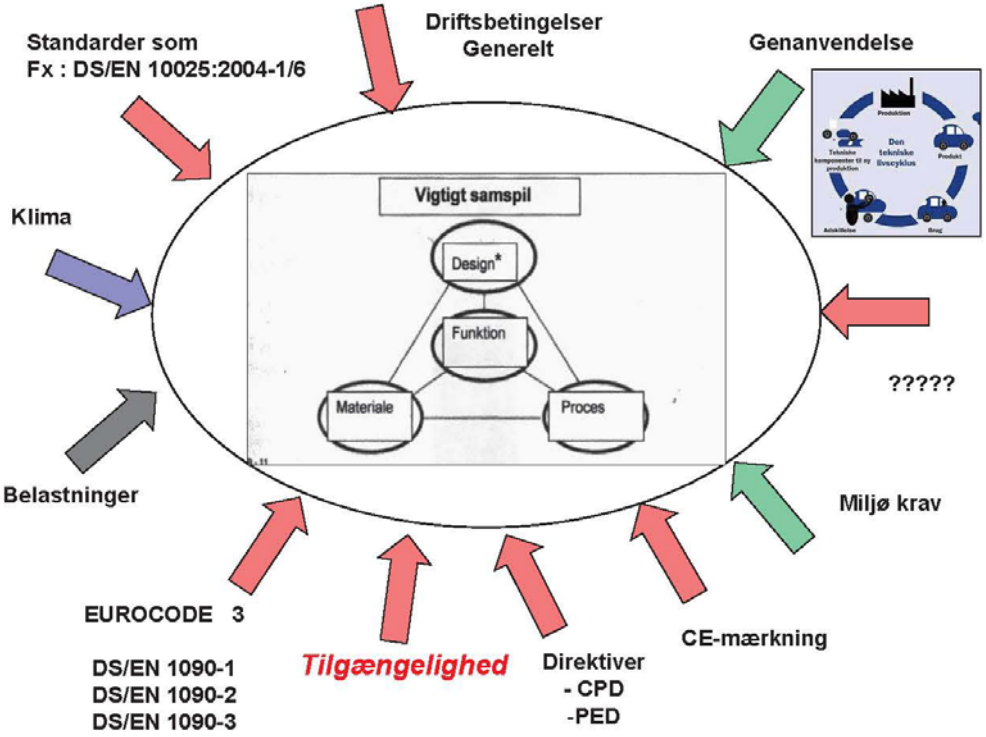

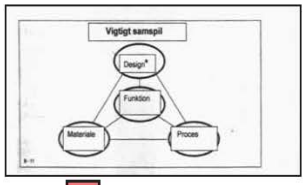

Materialernes egenskaber er altid det centrale element ved materialevalg. Eksempler på design-begrænsende egenskaber kan samles i nedenstående skema.

Klasse	Egenskab
Generel	Pris
	Densitet (massefylde)
Mekanisk	Elasticitetmodul (stivhed)
	Styrke (fx elasticetsgrænse)
	Sejhed
	Brudsejhed
	Dæmpningskapacitet
	Udmattelsesstyrke
Termisk	Termisk ledningsevne
	Specifik varmefylde
	Smeltepunkt
	Glastemperatur
	Termisk udvidelseskoefficient
	Krybemodstand
Slid	Slid-konstant
Korrosion/ Oxidation	Korrosionshastighed

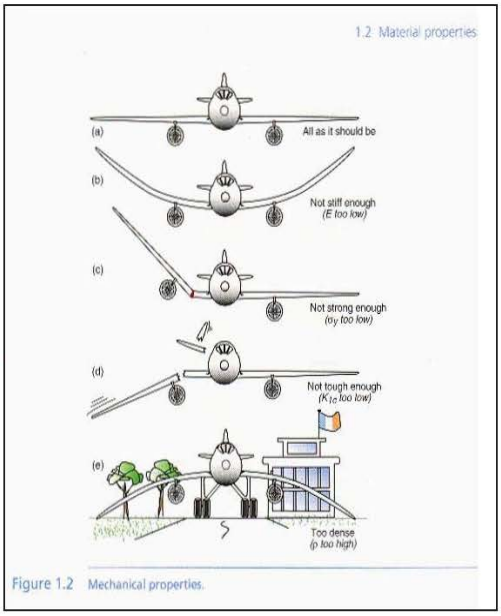

DMS

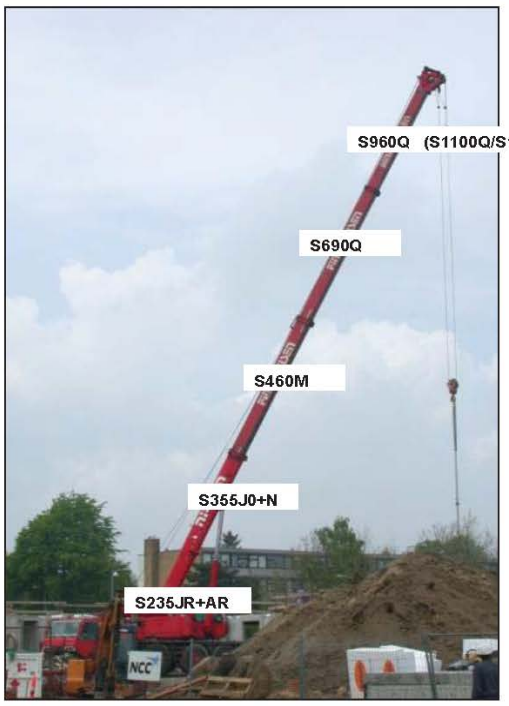

DS/EN 10025

DS/EN 10025 del 1 til 6

Del 1 Generelle tekniske leveringsbetingelser

Del 2 Tekniske leveringsbetingelser for ulegerede konstruktionsstål
(S235 -, S275 -, S355 - og S450- med undergrupperne *JR, J0 , J2 og K2,*
samt tillægsbetegnelserne +AR, +N og +M (kun lange produkter))

Del 3 *Tekniske leveringsbetingelser for (ovn)normaliserede/valsede normaliserede svejselige finkornskonstruktionsstål*
(S275 N/NL, S355N/NL , S420N/NL, S460N/NL)

Del 4 Tekniske leveringsbetingelser for *termomekanisk valsede* svejselige *finkornskonstruktionsstål*
(S275M/ML, S355M/ML, S420M/ML -, S460M/ML)

Del 6 Tekniske leveringsbetingelser for flade produkter af *højstyrke konstruktionsstål* i *sejhærdet tilstand*
(S460Q/QL/QL1, S500Q/QL/QL1, S550Q/QL/QL1, S620Q/QL/QL1, S690Q/QL/QL1, S890Q/QL/QL1, 960QQL)

Del 5 Tekniske leveringsbetingelser for konstruktionsstål med *fo[illegible] korrosionsbestandighed (korrosionstræge stål)*
(S235 –W, S355 -WP, S355 –W med undergrupperne *JR, J0 ,J2 og K2)*

DMS

Design Strategi: Hold dig over DBTT!

- Pre-WWII: Titanic
- WWII: Liberty skibe

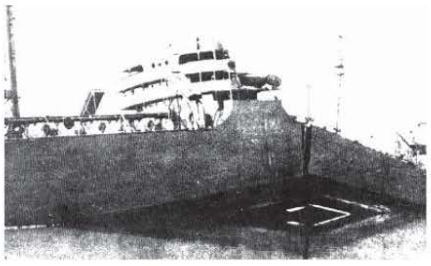

- Problem: Anvendelse af ståltyper med omslagstemperatur omkring rumtemperatur.

Slagprøvning

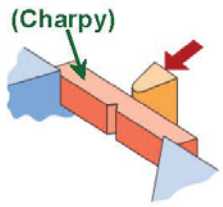

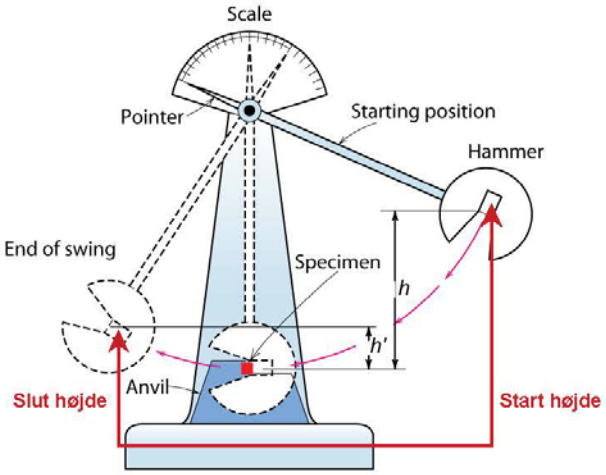

7

DMS

Omslags-Temperaturen

- Ductile-to-Brittle Transition Temperature (DBTT)...
  = Omslagstemperaturen

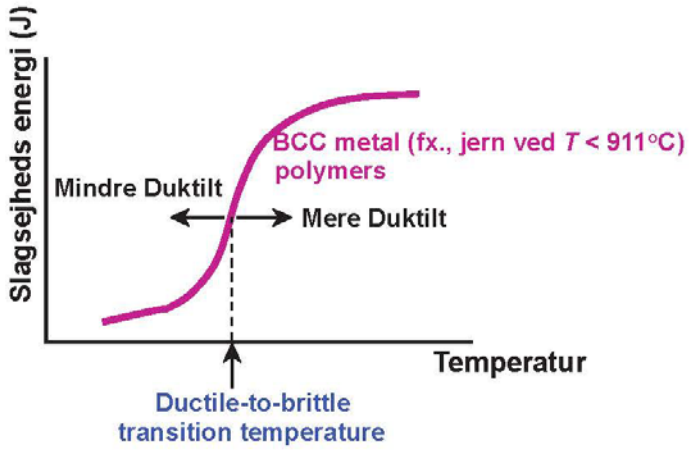

8

CEV (%) = C+ Mn/6+(Cr+Mo+V)/5 + (Ni+Cu)/15

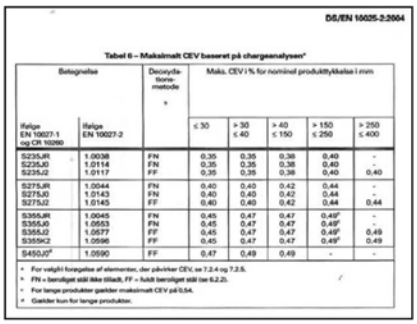

DS/EN 10025-2:2004

Tabel 6 – Maksimalt CEV baseret på chargeanalysen[a]

Betegnelse		Deoxyda-tions-metode	Maks. CEV i % for nominel produkttykkelse i mm				
Ifølge EN 10027-1 og CR 10260	Ifølge EN 10027-2		≤ 30	> 30 ≤ 40	> 40 ≤ 150	> 150 ≤ 250	> 250 ≤ 400
S235JR	1.0038	FN	0,35	0,35	0,38	0,40	-
S235J0	1.0114	FN	0,35	0,35	0,38	0,40	-
S235J2	1.0117	FF	0,35	0,35	0,38	0,40	0,40
S275JR	1.0044	FN	0,40	0,40	0,42	0,44	-
S275J0	1.0143	FN	0,40	0,40	0,42	0,44	-
S275J2	1.0145	FF	0,40	0,40	0,42	0,44	0,44
S355JR	1.0045	FN	0,45	0,47	0,47	0,49[c]	-
S355J0	1.0553	FN	0,45	0,47	0,47	0,49[c]	-
S355J2	1.0577	FF	0,45	0,47	0,47	0,49[c]	0,49
S355K2	1.0596	FF	0,45	0,47	0,47	0,49[c]	0,49
S450J0[d]	1.0590	FF	0,47	0,49	0,49	-	-

[a] For valgfri forøgelse af elementer, der påvirker CEV, se 7.2.4 og 7.2.5.
[b] FN = beroligat stål ikke tilladt, FF = fuldt beroligat stål (se 6.2.2).
[c] For lange produkter gælder maksimalt CEV på 0,54.
[d] Gælder kun for lange produkter.

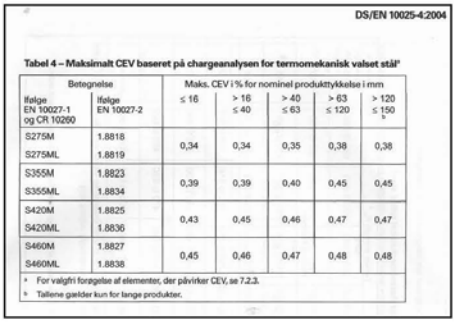

DS/EN 10025-4:2004

Tabel 4 – Maksimalt CEV baseret på chargeanalysen for termomekanisk valset stål[a]

Betegnelse		Maks. CEV i % for nominel produkttykkelse i mm				
Ifølge EN 10027-1 og CR 10260	Ifølge EN 10027-2	≤ 16	> 16 ≤ 40	> 40 ≤ 63	> 63 ≤ 120	> 120 ≤ 150 [b]
S275M	1.8818	0,34	0,34	0,35	0,38	0,38
S275ML	1.8819					
S355M	1.8823	0,39	0,39	0,40	0,45	0,45
S355ML	1.8834					
S420M	1.8825	0,43	0,45	0,46	0,47	0,47
S420ML	1.8836					
S460M	1.8827	0,45	0,46	0,47	0,48	0,48
S460ML	1.8838					

[a] For valgfri forøgelse af elementer, der påvirker CEV, se 7.2.3.
[b] Tallene gælder kun for lange produkter.

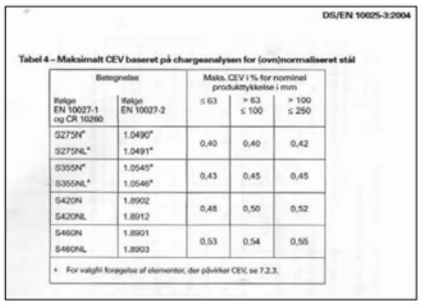

DS/EN 10025-3:2004

Tabel 4 – Maksimalt CEV baseret på chargeanalysen for (ovn)normaliseret stål

Betegnelse		Maks. CEV i % for nominel produkttykkelse i mm		
Ifølge EN 10027-1 og CR 10260	Ifølge EN 10027-2	≤ 63	> 63 ≤ 100	> 100 ≤ 250
S275N[a]	1.0490[a]	0,40	0,40	0,42
S275NL[a]	1.0491[a]			
S355N[a]	1.0545[a]	0,43	0,45	0,45
S355NL[a]	1.0546[a]			
S420N	1.8902	0,48	0,50	0,52
S420NL	1.8912			
S460N	1.8901	0,53	0,54	0,55
S460NL	1.8903			

[a] For valgfri forøgelse af elementer, der påvirker CEV, se 7.2.3.

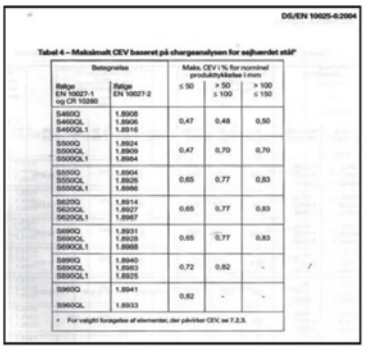

DS/EN 10025-6:2004

Tabel 4 – Maksimalt CEV baseret på chargeanalysen for sejhærdet stål[a]

Betegnelse		Maks. CEV i % for nominel produkttykkelse i mm		
Ifølge EN 10027-1 og CR 10260	Ifølge EN 10027-2	≤ 50	> 50 ≤ 100	> 100 ≤ 150
S460Q	1.8908	0,47	0,48	0,50
S460QL	1.8906			
S460QL1	1.8916			
S500Q	1.8924	0,47	0,70	0,70
S500QL	1.8909			
S500QL1	1.8984			
S550Q	1.8904	0,65	0,77	0,83
S550QL	1.8926			
S550QL1	1.8986			
S620Q	1.8914	0,65	0,77	0,83
S620QL	1.8927			
S620QL1	1.8987			
S690Q	1.8931	0,65	0,77	0,83
S690QL	1.8928			
S690QL1	1.8988			
S890Q	1.8940	0,72	0,82	-
S890QL	1.8983			
S890QL1	1.8925			
S960Q	1.8941	0,82	-	-
S960QL	1.8933			

[a] For valgfri forøgelse af elementer, der påvirker CEV, se 7.2.3.

DMS

Fremstilling af svejselige konstruktionsstål med udgangspunkt i :

EN 10025:2004 del 1-6

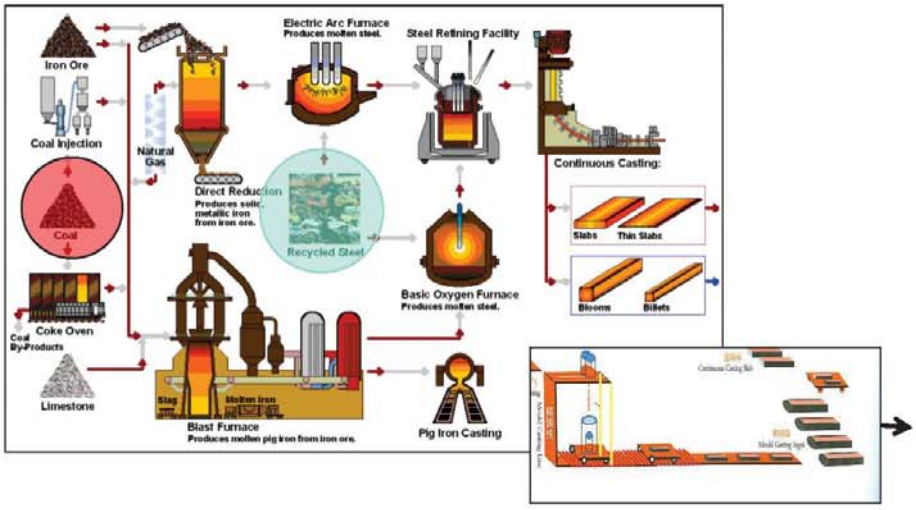

Blokstøbning
Ingot - /Mould Casting

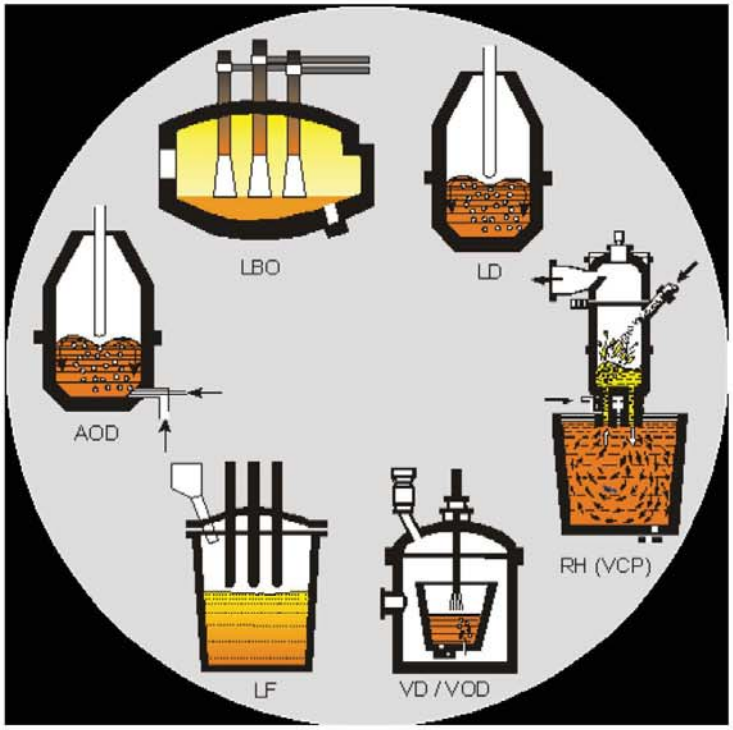

DMS

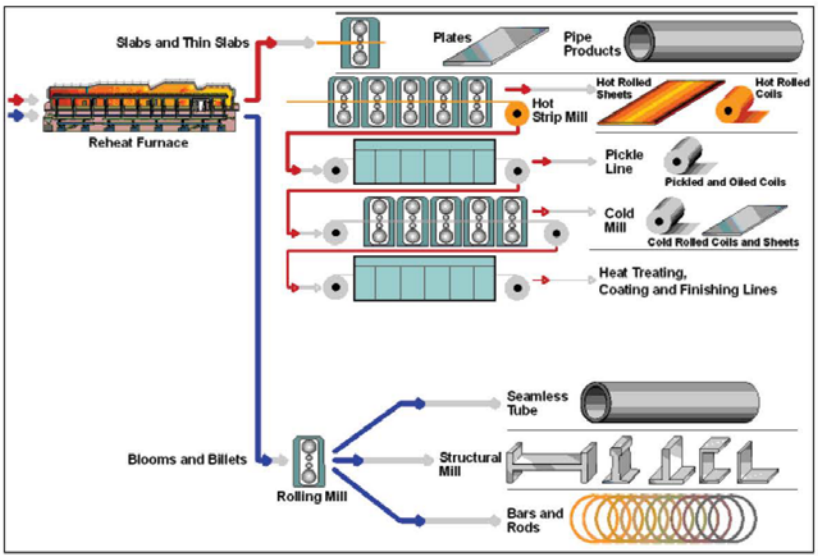

DMS

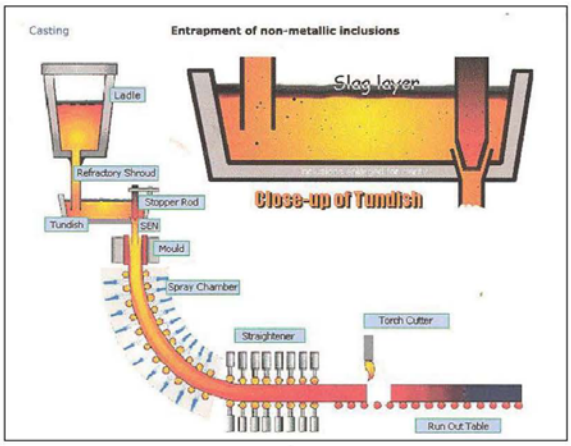

Z-prøvning (Z = 70%)

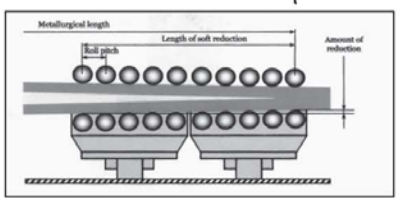

"Soft reduction"

Slabs tværsnit

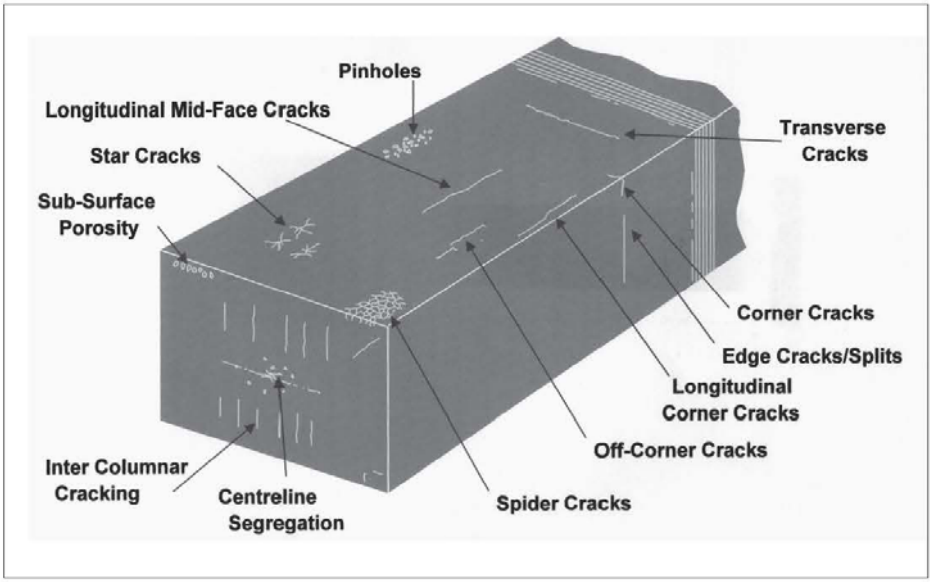

Varmvalsning

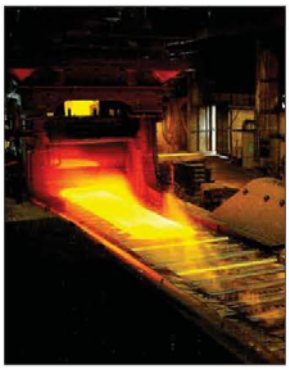

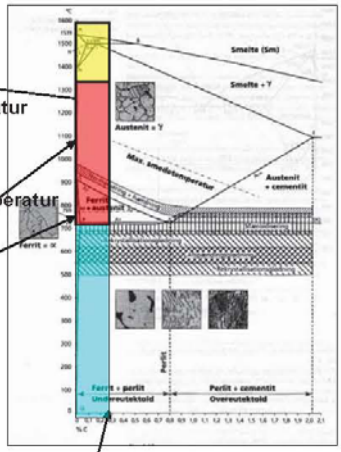

Slabs temperatur

Valse temperatur område

Max. kulstof(carbon) indhold for svejselige konstruktionsstål i overensstemmelse med DS/EN 10025: C_{max} = 0,24 %

Styrkeøgning

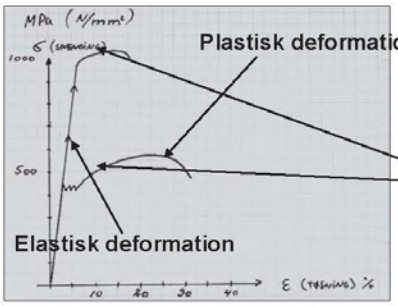

Dislokation

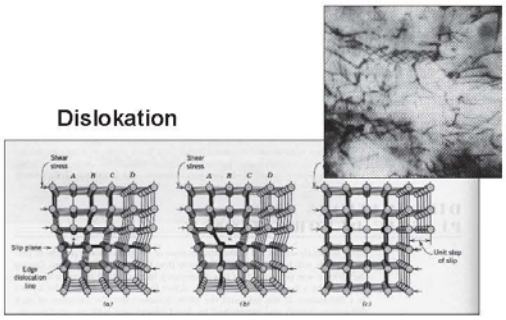

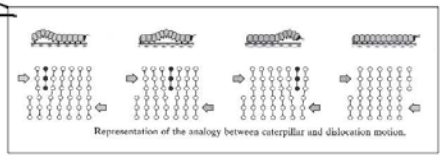

Dislokationbarierer/-bremser ➔ udvidelse af det elastiske område ➔ Styrkeøgning:

- Fremmedatomer (fx C og Mn)
- Korngrænser (ved kornforfining)
- Dislokationsforøgelse (deformationshærdning)
- Fremmede faser (ved modningshærdning)

DMS

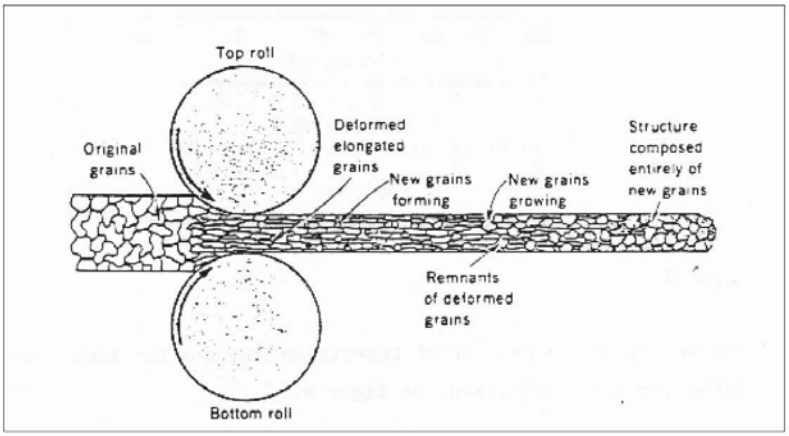

DMS

Valseprocesser

Kvarto- valseværk

ACC-udstyr

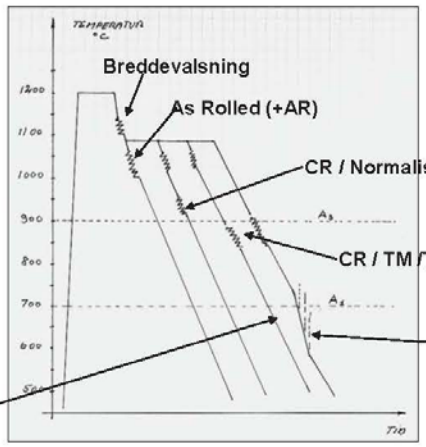

CR-valsning = Controlled Rolling

Valseprocesser

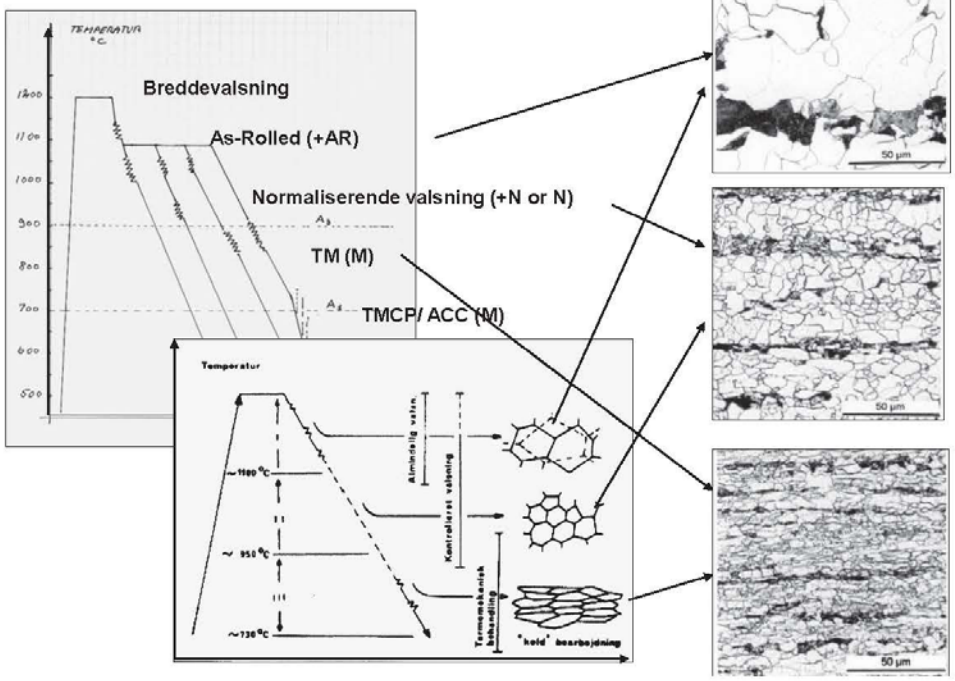

Egenskaber frembragt ved en valseproces.

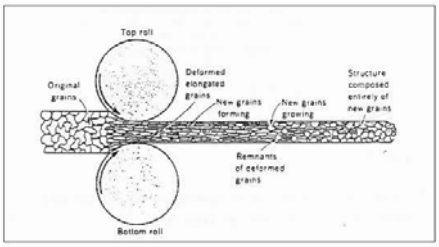

Varmvalsning

I) **Normal varmvalsning (Leveringstilstand as-rolled)**

En evt. breddevalsning udføres umiddelbart efter, at slabsen/blokken er udtaget af slabs/blokovnen.
Slabs/bloktemperaturen er typisk 1250 °C. Herefter vendes den breddevalsede slabs/blok, og længdevalsningen påbegyndes umiddelbart.

Længderetningen på pladen omtales som "hovedvalseretningen"

Det varmvalsede ståls struktur er relativt grovkornet (ASTM-kornstørrelse omkring 5-6, alt efter pladedimension).

II) **Kontrolleret (styret) valsning (CR-valsning = Controlled Rolling)**

Siden 30'erne er der udviklet kontrollerede (styrede) valseprocesser, som går under fællesbetegnelsen »Kontrolleret valsning, forkortet CR (Controlled Rolling).

CR-processerne omfatter en række processer, der som fælleskendetegn har det ene, at de sidste 20 %'s deformation foregår under nøje temperaturkontrol, dvs. i et bestemt temperaturinterval.

DMS

II.a) **Normaliserende valsning**

Valsningen udføres næsten som beskrevet under varmvalsning, men de sidste stik (tykkelsesreduktionen) udføres i det temperaturinterval, hvor stålet normalt (ovn)normaliseres, altså lige over A_3.

De resulterende mekaniske egenskaber skal modsvare det (ovn)normaliserede produkt. Det er væsentligt at påpege, at stålstandarderne ikke skelner imellem de to processer. Dette betyder derfor, at en forbruger ikke i certifikatet, uanset type, kan få oplyst, hvilken type normaliseret stål forbrugeren har modtaget.

II.b) **TMCP-stål (Thermo Mechanical controlled Process)**

TMCP-valsning dækker over et antal forskellige valseprocesser.

For de fleste af disse processer findes flere betegnelser, hvilket fra et forbrugersynspunkt kan være meget forvirrende. Det vil derfor altid i tvivlstilfælde være en god ide at gennemlæse specifikationen efter standarden for det aktuelle stål.

II.b.1) **TM-stål (Thermo Mechanical Rolling)**

Startvalsetemperaturen er normalt, men ikke nødvendigvis, en del lavere end for varmvalsning. Endvidere udføres slutvalsningen ved så lave temperaturer, at austenitten ikke rekrystalliserer, dvs, ved en temperatur lige over A_3 eller i tofaseområdet imellem A_3/A_1, og der dannes derfor en finkornet struktur.

I sidstnævnte tilfælde kan de højeste styrkeegenskaber opnås, idet der lidt populært sker en form for »kolddeformation» af de enkelte korn, som sammen med den finkornede struktur giver en mærkbar styrkeforøgelse, samt en god sejhed.

II.b.2) **ACC-stål (Accelerated Controlled Cooling)**

En japansk udviklet proces til fremstilling af højstyrkestål med særdeles gode egenskaber, hvad angår lav kulstofækvivalent (CEV), omslagstemperatur mm.

Udgangspunktet er et normaliseret valset/TM-stål. Den endnu varme plade føres igennem et langt køleanlæg (typisk 40-50 m), hvori pladen afkøles styret fra ca. 600 °C til ca. 600 °C, alt efter ønskede egenskaber. Derefter afkøling i luft.

Strukturen en ferritisk/finperlitisk/bainitisk

Varmebehandling

(Ovn) Normalisereng og sejhærdning

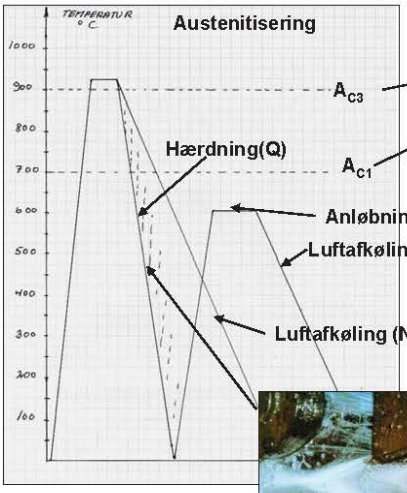

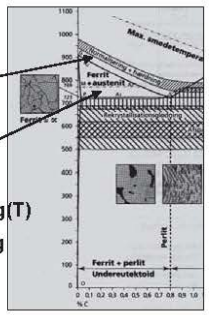

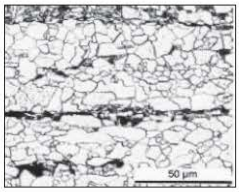

Normalisering (N)
Fin kornet perlit/ferrit

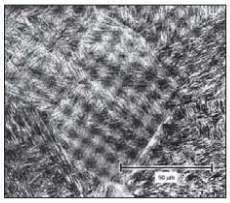

Hærdet (Q)
Martensit

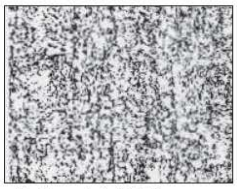

Sejhærdet (Q/T)
Anløbet martensit

Basis materiale: Varmvalset produkt (As-rolled)

"Roll quenching" udstyr

DMS

Egenskaber frembragt ved varmebehandling

I) (Ovn) Normalisering

Processen udføres ved at opvarme emnet til temperaturen over A_3-linien (til austenitområdet) i en ovn. Efter en kort holdetid, afkøling i luft.

Den opnåede struktur er finkornet ferritisk/perlitisk (ASTM-kornstørrelse 9-11, alt efter pladedimension).

Man opnår herved en forbedring af flydespændingen såvel som en sænkning af omslagstem-peraturen (en forbedring af slagsejhedsegenskaberne).

De opnåede egenskaber er ækvivalente med egenskaber opnået ved normaliserende valsning.

II) Q/T-stål (Quench/Tempering = (Martensit)hærdning/anløbning) På dansk er betegnelsen sejhærdning.

Som den engelske forkortelse antyder, er der her tale om to varmebehandlingsprocesser. En hærdning til martensit (quenching) efterfulgt af en anløbning (tempering),
Hærdningen udføres ved at opvarme et varmvalset produkt til en temperatur over A_3-linien (til austenitområdet). Efter en kort holdetid sendes pladen igennem et hærdeanlæg, hvor selve brat-kølin-gen og dermed martensitdannelsen finder sted.

Vær opmærksom på, at martensithårdheden udelukkende er et spørgsmål om kulstofindholdet, hvilket indebærer, at stærkere stål har et højere kulstof indhold

Anløbningen udføres fx i en normaliseringsovn, og temperaturintervallet imellem 600 °C og 660 °C. Forbrugeren bør være opmærksom på, at producenten normalt angiver anløbningstemperaturen i certifikatet, idet en overskridelse af denne temperatur fx i forbindelse med en varmbearbejdning kan føre til en reduktion af stålets styrkeegenskaber.

DMS

ACC-treatment ("alloying with water")

Accelereted Continuous/Controlled Cooling

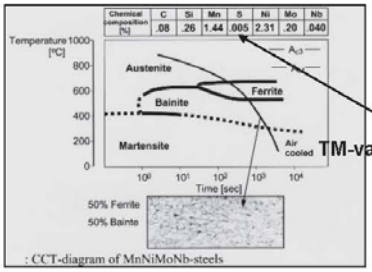

: CCT-diagram of MnNiMoNb-steels

TM-valset lavt legeret stål

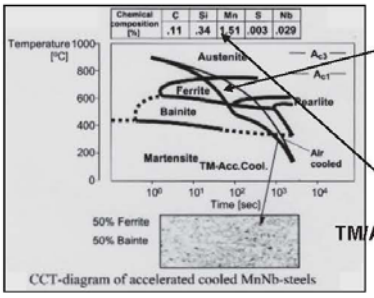

CCT-diagram of accelerated cooled MnNb-steels

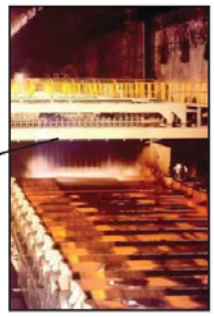

TM/ACC - behandlet u-legeret stål

DS/EN 10025-4-S420M

Ferritisk/bainitisk struktur

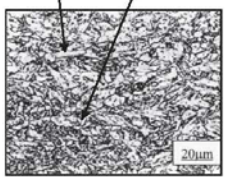

DS/EN 10025-4-S460ML

DMS

Hydrogen inducerede revner (ca. 1980)

Ståltype : St 52-3 Svovl : S 0 0,008 % Hydrogen : H < 0,0010 % ?

Slabs tværsnit

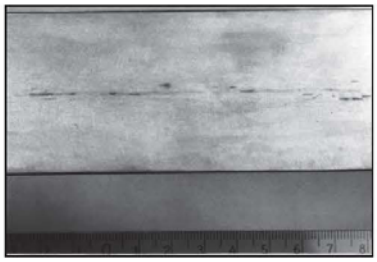

Plade tværsnit

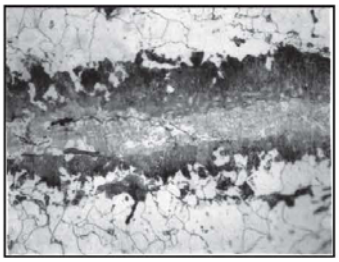

Microstruktur : 400 x

DMS

Hydrogen inducerede revner (ca. 2010)

Ståltype : S 355 J2 Svovl : S 0 0,002 % Hydrogen : H < 0,0002 % ?

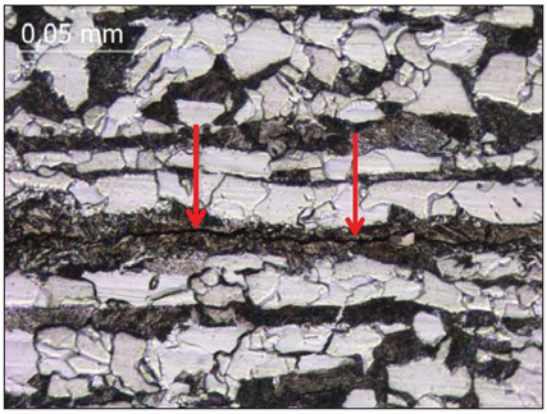

Revnen løber i det perlitiske bånd i den sejrede zone i pladens center

DMS

Blokstøbning

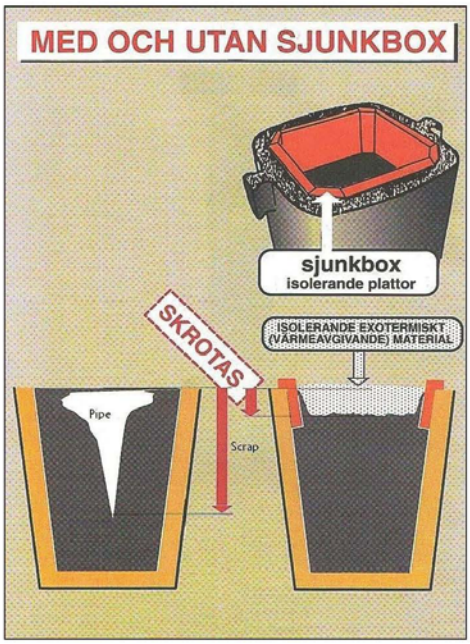

DMS

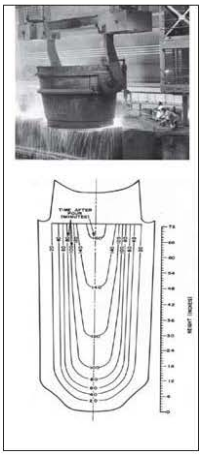

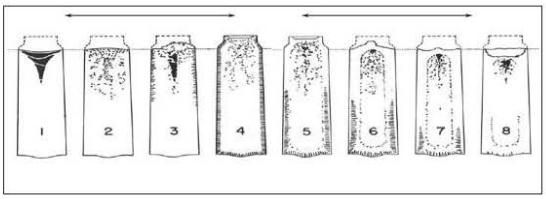

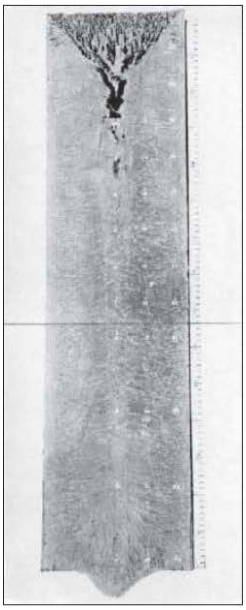

Makrostruktur

Moderne blokstøbning med vandkølet kobberkokille

Varmebehandling og karakterisering af nye udskilningshærdbare superlegeringer

Uffe Bihlet, MAN og DTU Mekanik

Varmebehandling og karakterisering af nye udskilningshærdbare superlegeringer

DMS Vintermøde 2013

Uffe D. Bihlet
ErhvervsPhD studerende
MAN Diesel & Turbo
DTU MEK

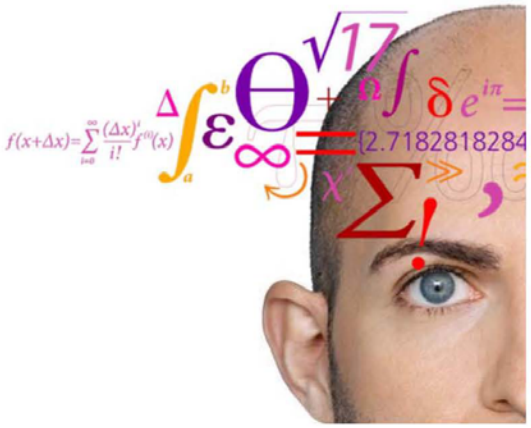

Agenda

- To-takts motoren og udstødningsventilen
- Udskilningshærdning i Inconel 718
- Ny legering
- Verificering af hærdningsmekanismen i ny legering
  - Røngtendiffraktion (XRD)
  - Focused Ion Beam Imaging (FIB)
  - TEM
- Wrap-up

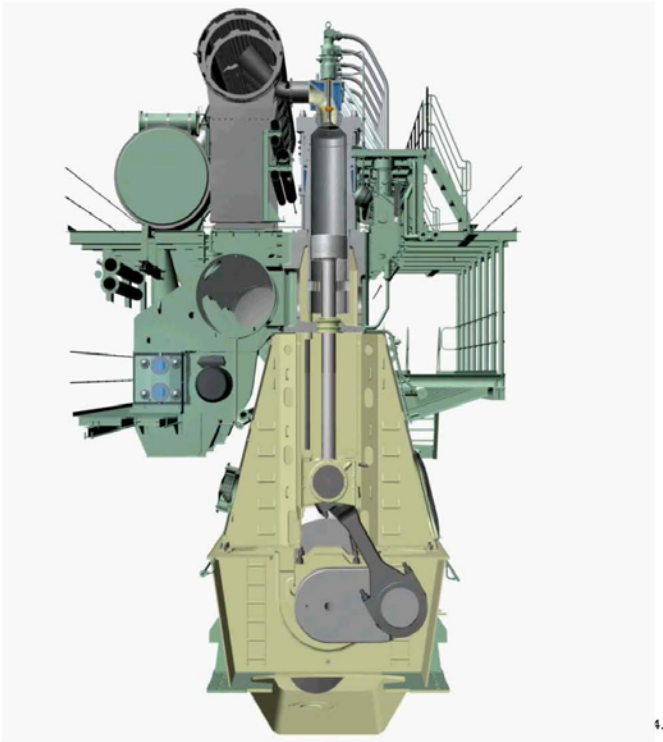

Ventilspindlen

Legering	Cr	Nb	Ti	Al	Fe	Mo	Ni
IN718	19	5	0.9	0.5	18	3	Bal

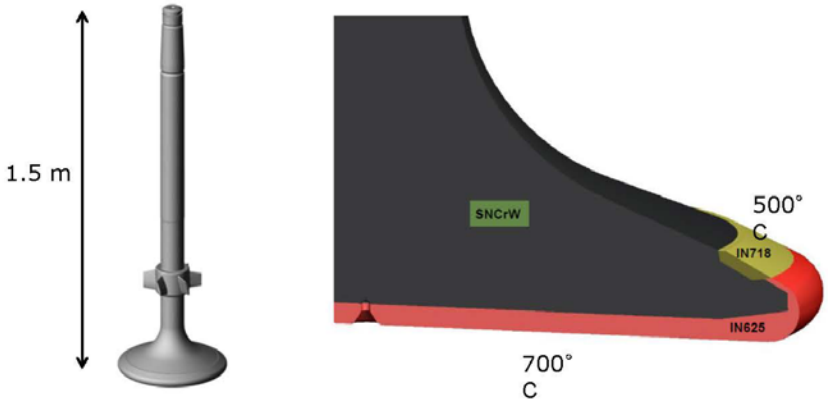

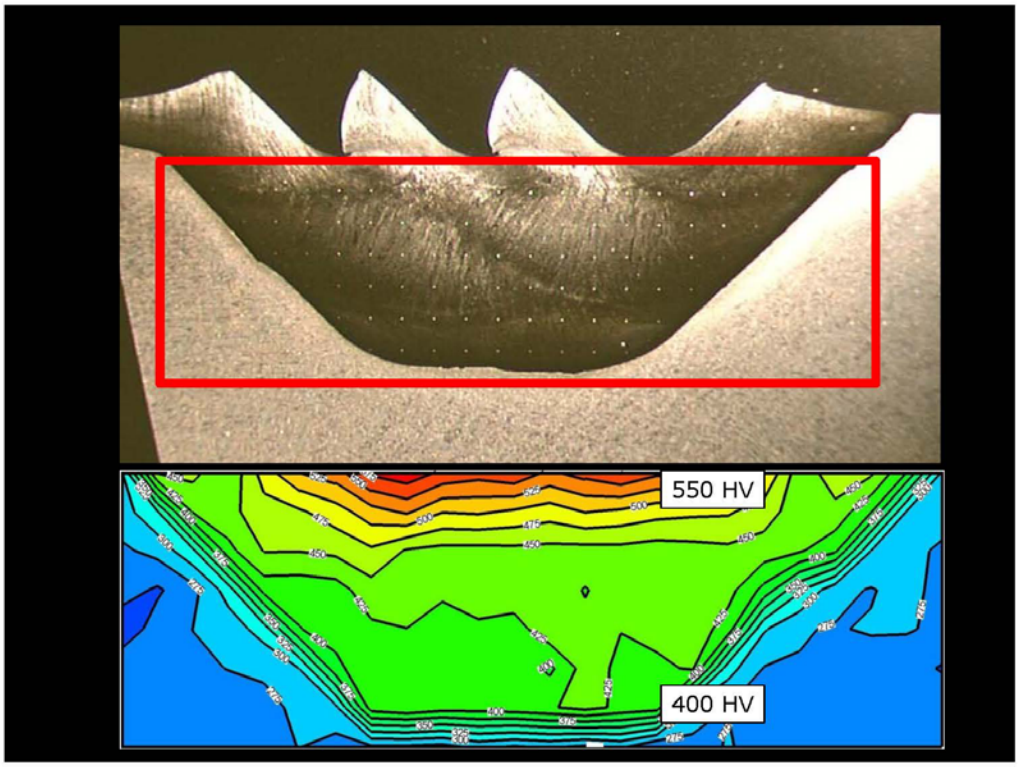
550 HV
400 HV

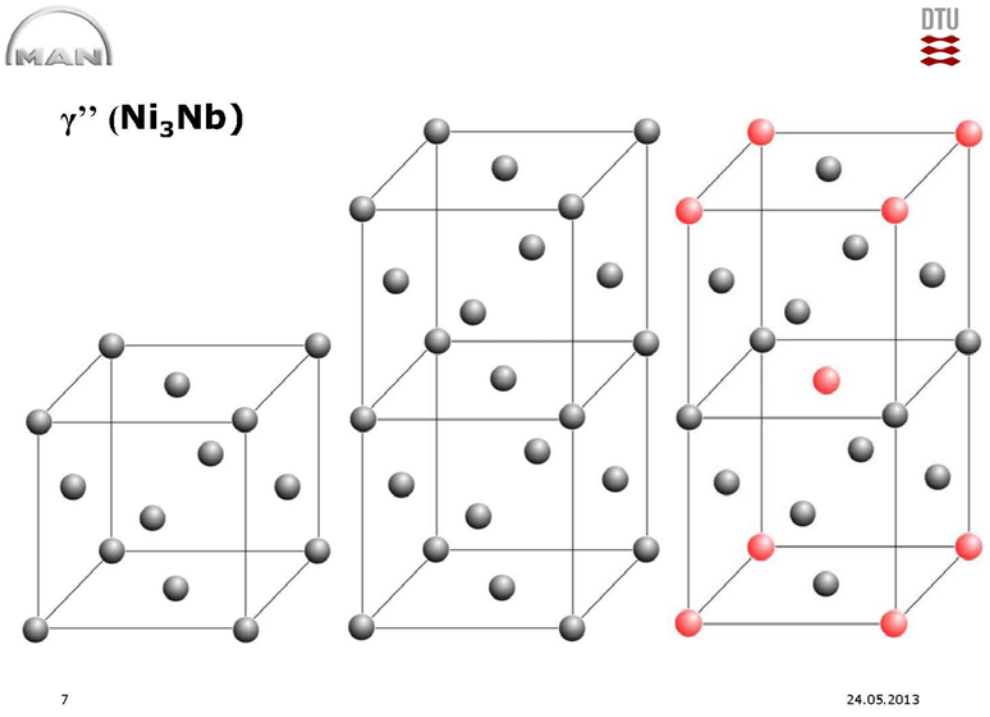
γ'' (Ni3Nb)
7
24.05.2013

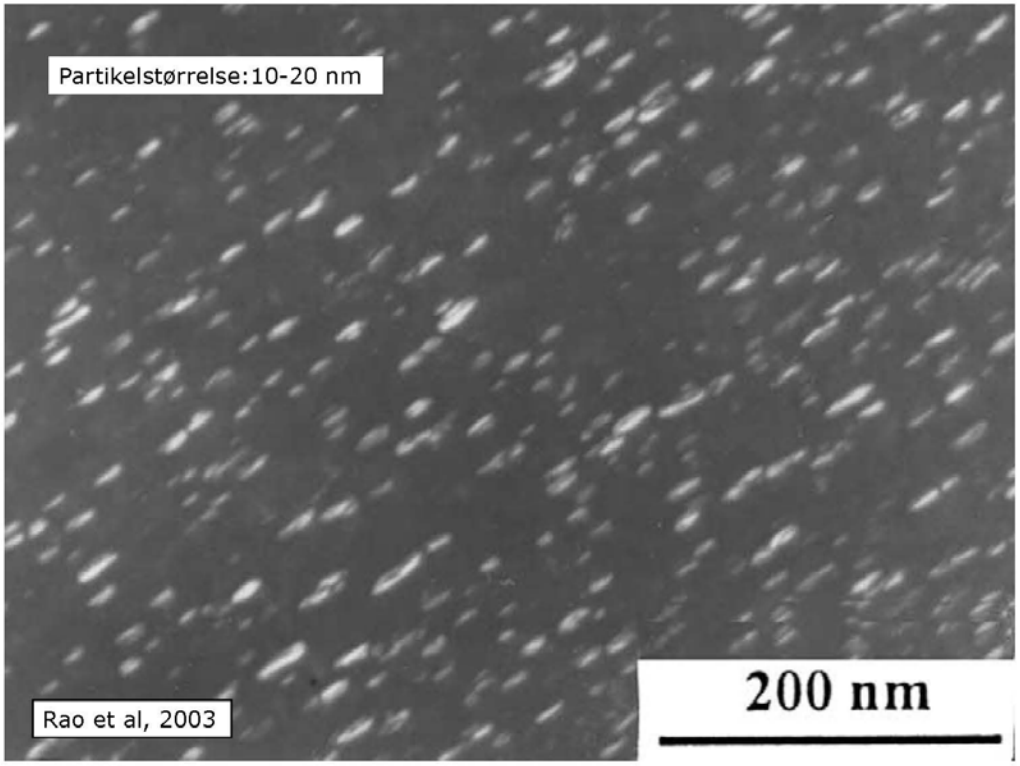
Partikelstørrelse:10-20 nm
Rao et al, 2003
200 nm

Agenda

- To-takts motoren og udstødningsventilen
- Udskilningshærdning i Inconel 718
- Ny legering
- Verificering af hærdningsmekanismen i ny legering
  - Røngtendiffraktion (XRD)
  - Focused Ion Beam Imaging (FIB)
  - TEM
- Wrap-up

Fra Inconel 718 -> ?

Legering	Cr	Nb	Ti	Al	Fe	Mo	Ni
IN718	19	5	0.9	0.5	18	3	Bal
No. 6	**40**	**3.5**	**0.5**	-	-	-	**Bal**

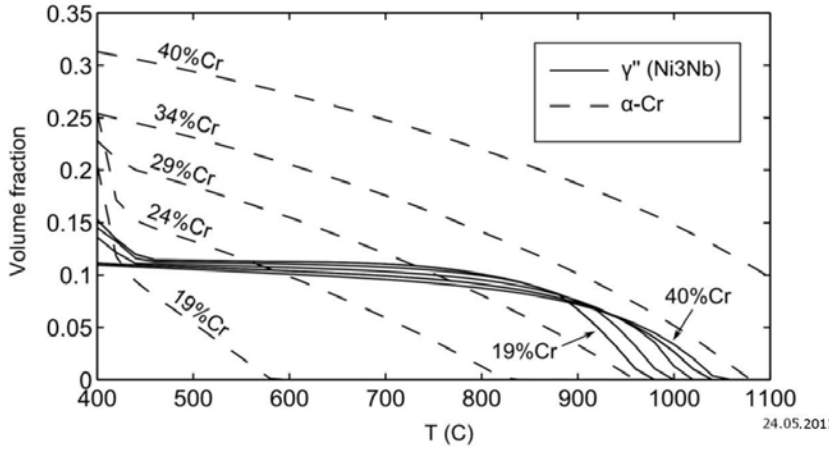

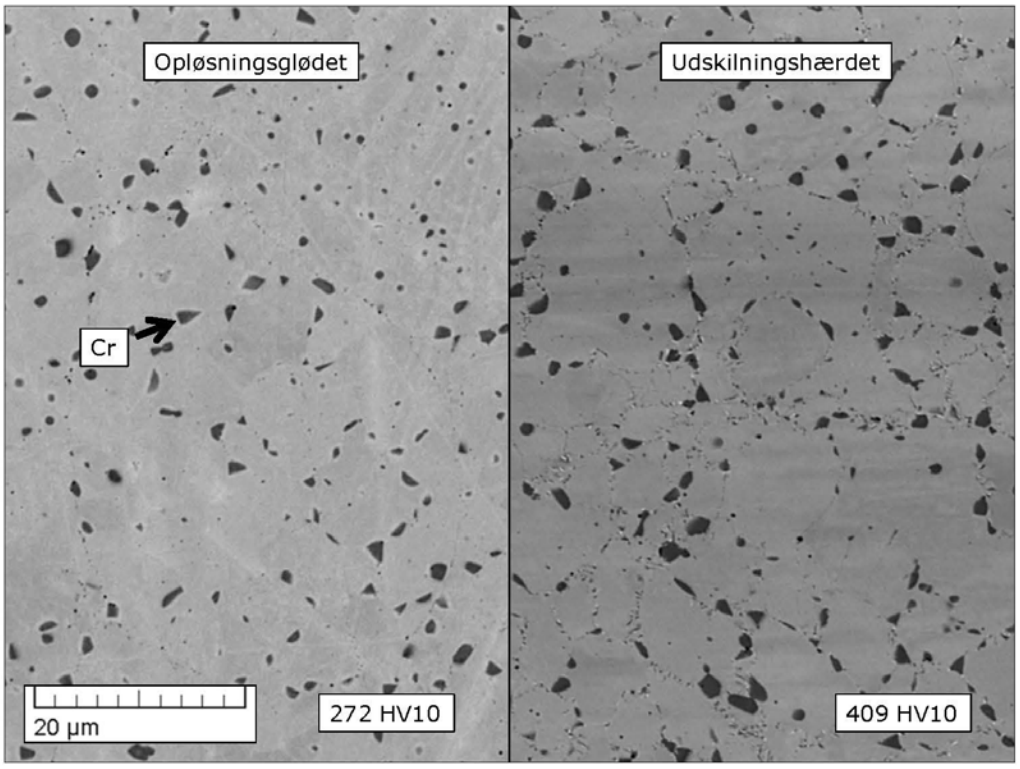

Agenda

- To-takts motoren og udstødningsventilen
- Udskilningshærdning i Inconel 718
- Ny legering
- Verificering af hærdningsmekanismen i ny legering
  - Røngtendiffraktion (XRD)
  - Focused Ion Beam Imaging (FIB)
  - TEM
- Wrap-up

Røngtendiffraktion (XRD)

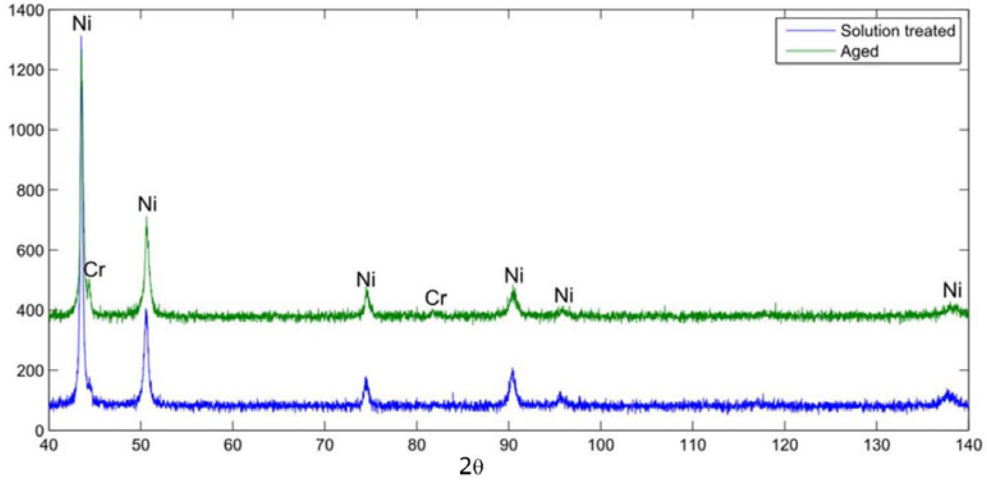

13 24.05.2013

Agenda

- To-takts motoren og udstødningsventilen
- Udskilningshærdning i Inconel 718
- Ny legering
- Verificering af hærdningsmekanismen i ny legering
  - Røngtendiffraktion (XRD)
  - Focused Ion Beam Imaging (FIB)
  - TEM
- Wrap-up

14 24.05.2013

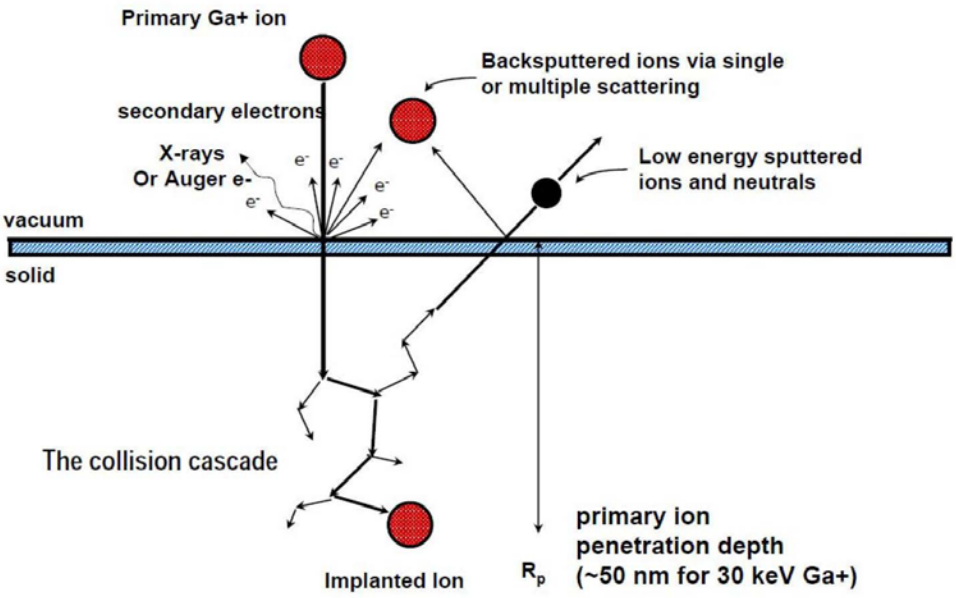
Primary Ga+ ion
Backsputtered ions via single
or multiple scattering
secondary electrons
X-rays
Or Auger e-
Low energy sputtered
ions and neutrals
vacuum
solid
The collision cascade
primary ion
penetration depth
(~50 nm for 30 keV Ga+)
Implanted Ion
R_p

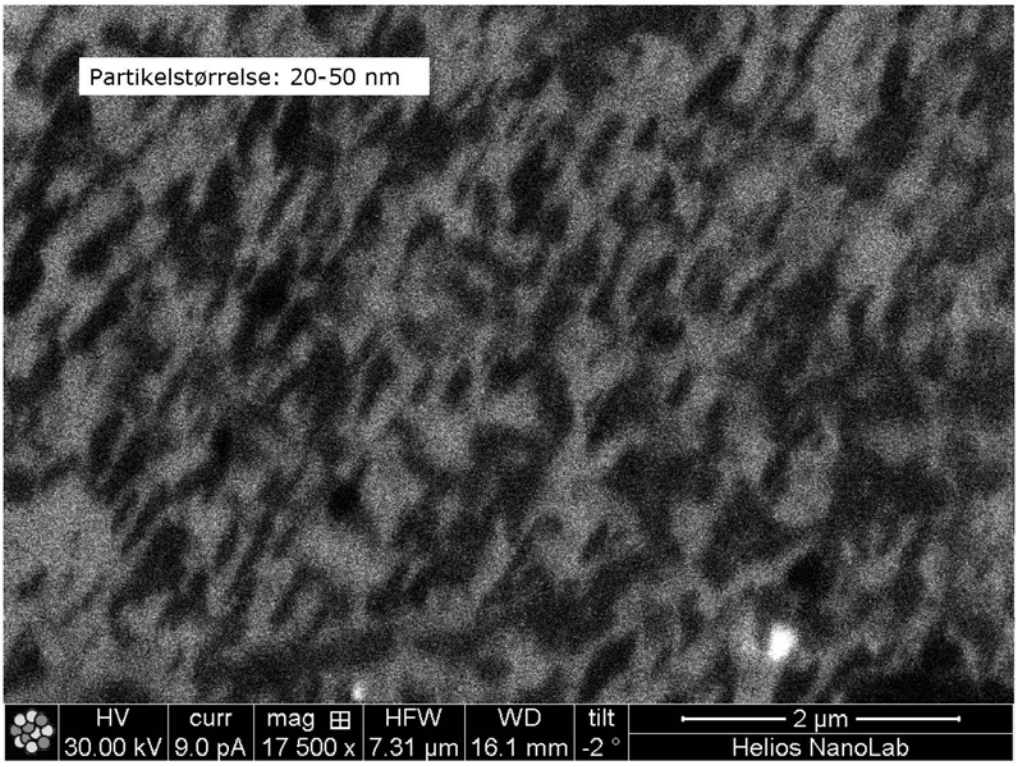
Partikelstørrelse: 20-50 nm
HV
30.00 kV
curr
9.0 pA
mag
17 500 x
HFW
7.31 µm
WD
16.1 mm
tilt
-2 °
2 µm
Helios NanoLab

Agenda

- To-takts motoren og udstødningsventilen
- Udskilningshærdning i Inconel 718
- Ny legering
- Verificering af hærdningsmekanismen i ny legering
  - Røngtendiffraktion (XRD)
  - Focused Ion Beam Imaging (FIB)
  - TEM
- Wrap-up

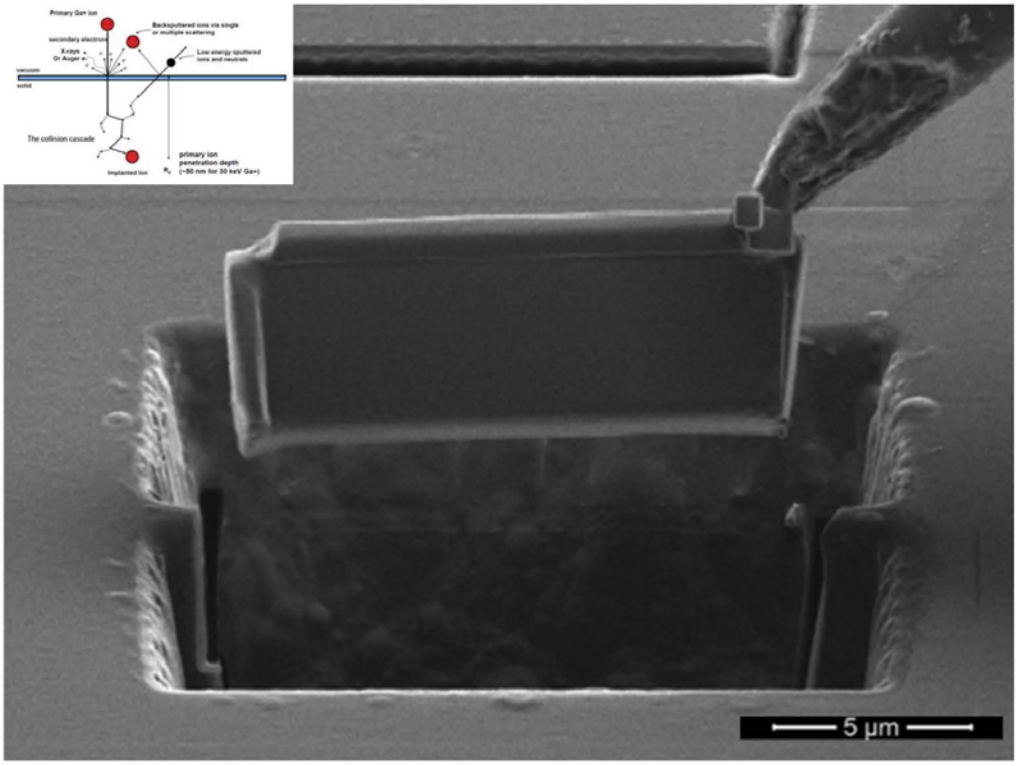

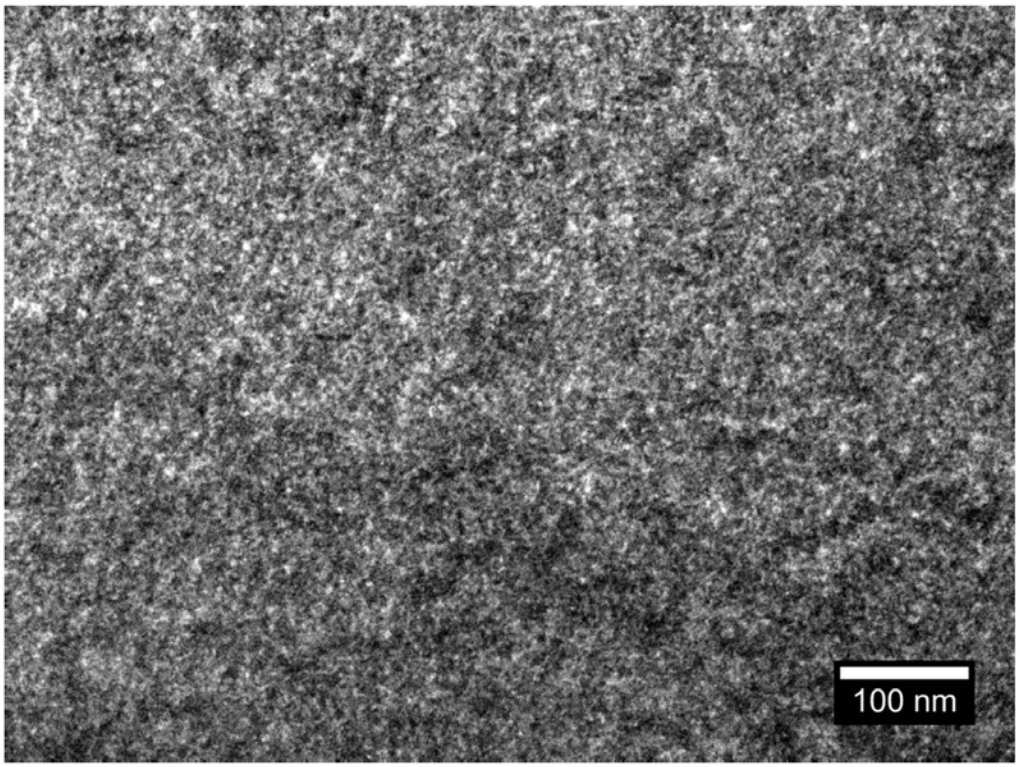
100 nm

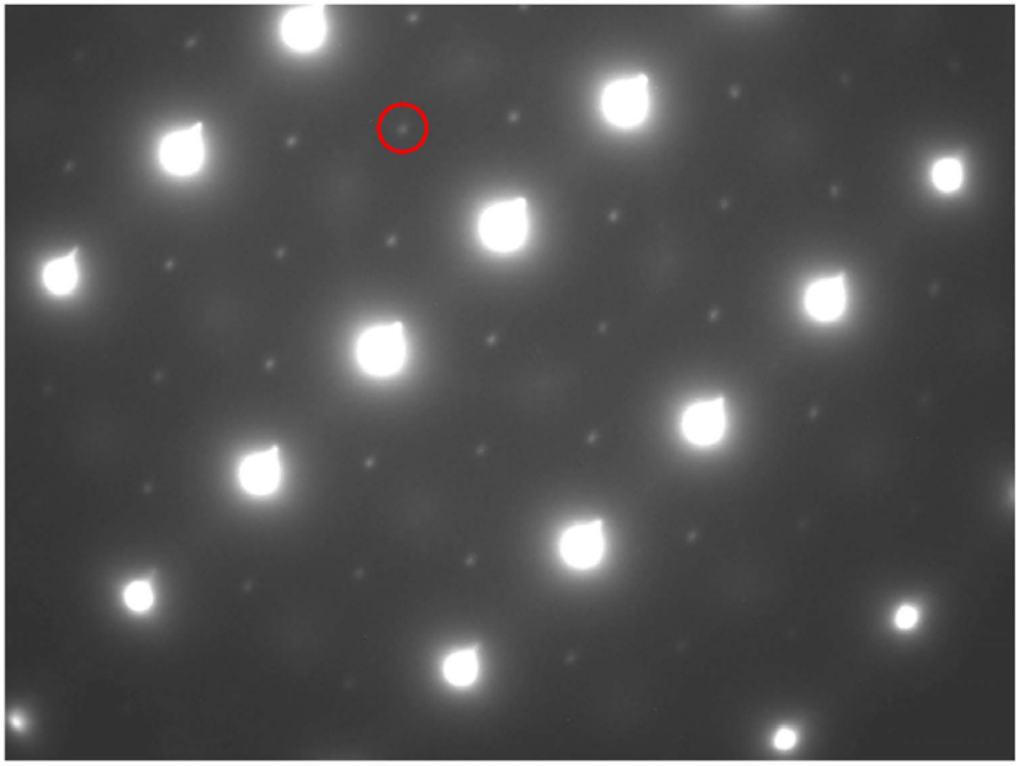

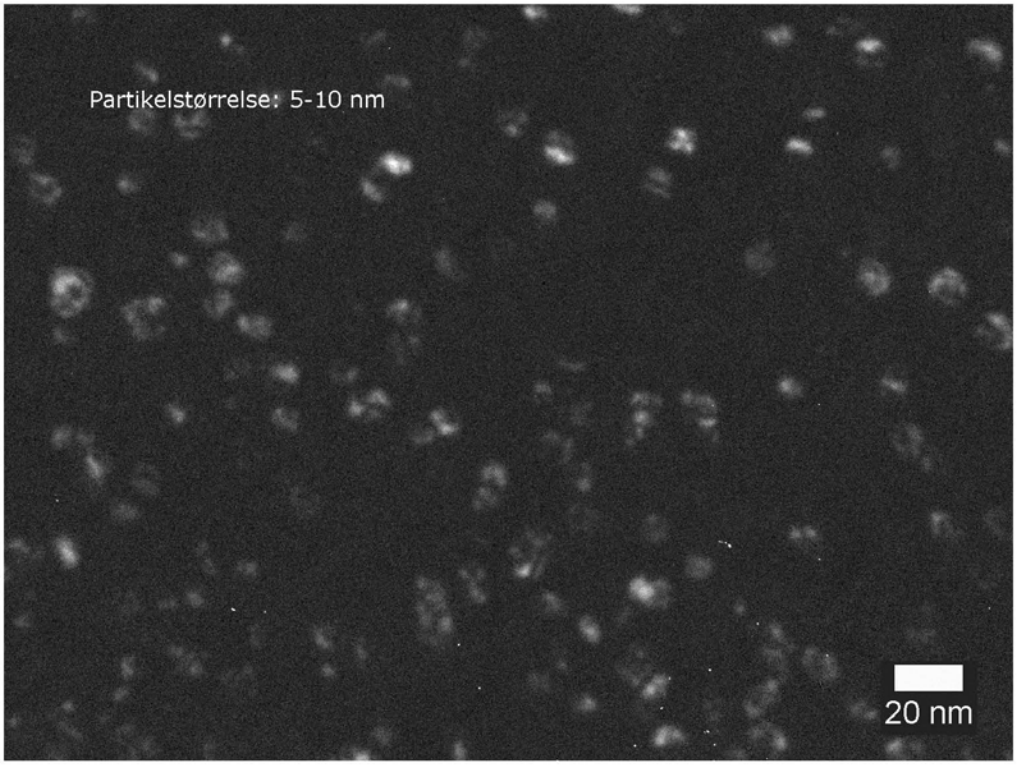

Agenda

- To-takts motoren og udstødningsventilen
- Udskilningshærdning i Inconel 718
- Ny legering
- Verificering af hærdningsmekanismen i ny legering
  - Røngtendiffraktion (XRD)
  - Focused Ion Beam Imaging (FIB)
  - TEM
- Wrap-up

GD-OES applications

Io Mizushima, IPU

Anvendelse af Glow Discharge Optical Emission Spectrometer (GD-OES)

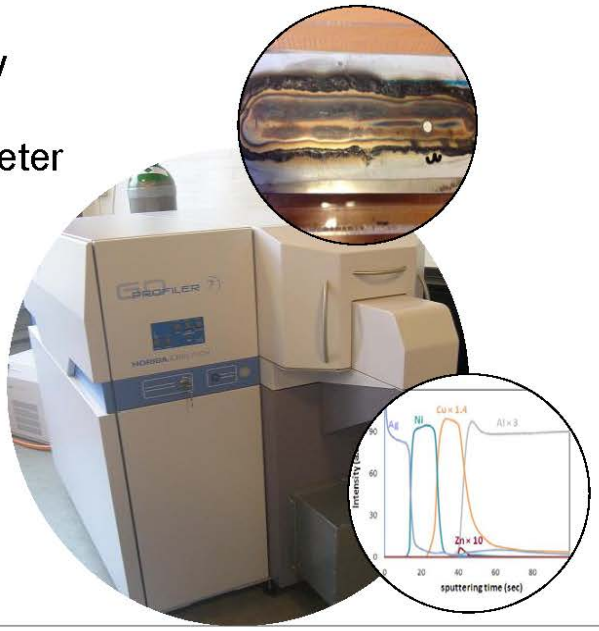

Io Mizushima

IPU

IPU

IPU: A dedicated on-campus innovation team

- A non-profit organisation at the TU of Denmark
- Research and development projects on contract
- Commercialisation of ideas, innovations, and patents

- 50 full-time staff
- 70+ associated DTU staff
- Co-location with DTU colleagues on campus
- Turnover: ~ 6 mill EUR/yr

... since 1956

IPU

Outline

1. GD-OES - princippet

2. Fordele og ulemper ved GD-OES

3. Eksempler
   Bulk-analyse
   Dybdeprofiler
   Praktiske anvendelser

4. Opsummering

IPU

GD-OES

GD-OES anvendes til analyse af den kemiske sammensætning.

Både bulk-materialer og overflader kan analyseres med dybdeprofiler (0,1-100µm).

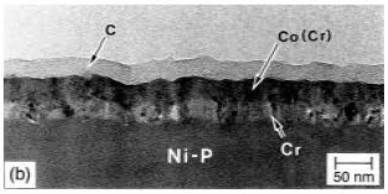

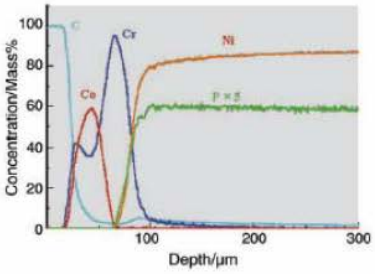

IPU

Machine components

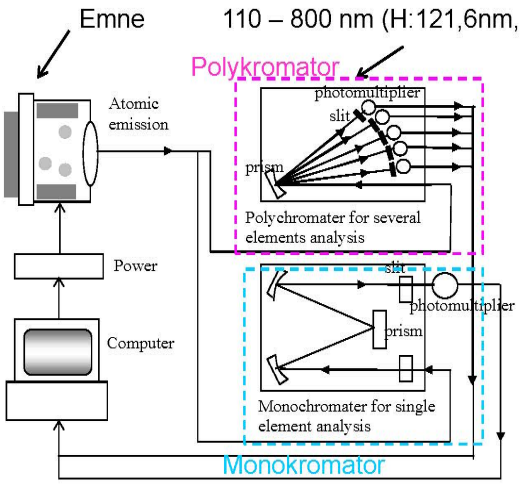

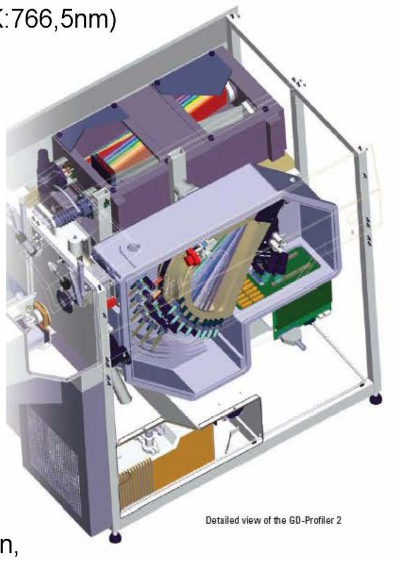

Bølgelængden kan vælges frit på monokromatoren, som i princippet kan måle alle elementer.

IPU

Optical emission lines

H	121,567	Sb	206,833
O	130,217	Ga	417,205
Cl	134,724	Cr	425,433
N	149,263	W	429,461
Be	313,042	Pb	220,353
Nb	316,34	In	451,132
Cu	324,754	Cd	228,802
Ag	328,068	Se	241,352
C	165,701	Au	242,795
Zn	334,502	B	249,678
Ni	341,477	Hg	253,652
Co	345,351	Mn	257,61
P	178,287	Pt	265,945
S	180,734	Ge	275,459
Ti	365,35	Mg	285,213
Fe	371,994	Hf	286,637
Sn	189,989	Si	288,158
Mo	386,411	Bi	306,772
Ca	393,367	Li	670,791
Al	396,152	K	766.49

GD-OES kan måle selv lette grundstoffer som f.eks. hydrogen.

IPU

GD-OES periodic table of available elements

Polykromator: udvalgte elementer (43)
Monokromator: ekstra element kan vælges frit

H																	He
Li	Be											B	C	N	O	F	Ne
Na	Mg											Al	Si	P	S	Cl	Ar
K	Ca	Sc	Ti	V	Cr	Mn	Fe	Co	Ni	Cu	Zn	Ga	Ge	As	Se	Br	Kr
Rb	Sr	Y	Zr	Nb	Mo	Tc	Ru	Rh	Pd	Ag	Cd	In	Sn	Sb	Te	I	Xe
Cs	Ba	La	Hf	Ta	W	Re	Os	Ir	Pt	Au	Hg	Tl	Pb	Bi	Po	At	Rn

IPU

Emission part

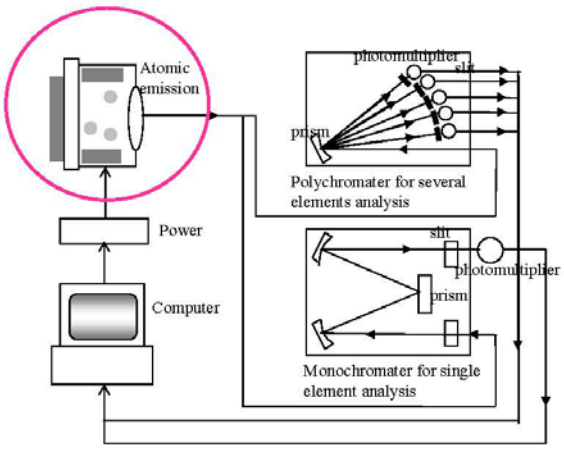

IPU

Emission part

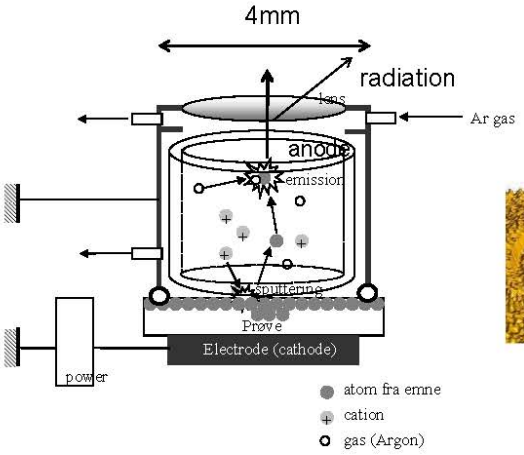

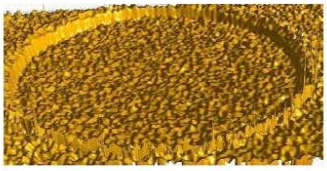

Sputtering af grundstoffer:
ioniseret argon → eksitering af grundstoffer → emission (udsender lys)

IPU

Intensitet ændring

Intensitet ændres ved-
- Tryk (pressure)
- Spænding (voltage)
- Afstand mellem anode og emne
- Urenheder på linsen
- Bulk materiale

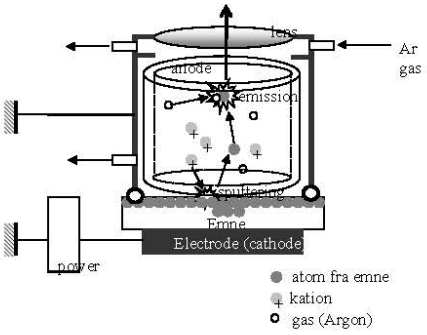

IPU

Sputtering hastighed

Side 11

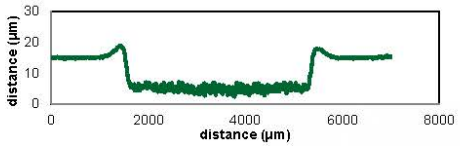

元素	濃度 (%)	スパッタリング速度 (µ/min)	密度 (g/cm3)
Ag	99.980	22.0	10.49
Al	99.500	3.6	2.69
Au	99.950	20.0	19.26
Co	99.900	3.6	8.90
Cr	99.900	5.2	7.19
Cu	99.994	9.6	8.93
Fe	99.570	4.6	7.87
Mg	99.900	12.0	1.74
Mo	99.950	6.4	10.20
Nb	99.900	3.6	8.57
Ni	99.700	5.2	8.90
Pb	99.990	40.0	11.34
Pd	99.950	13.0	12.16
Pt	99.980	8.0	21.45
Si	100.000	2.2	2.33
Sn	99.900	18.0	7.30
Ta	99.950	4.9	16.60
Ti	99.900	2.4	4.50
W	99.950	5.6	19.30
Zn	99.990	23.0	7.13

IPU

Intensitet ændring

Side 12

Intensitet ændres ved-
- Bulk materiale
- Tryk (pressure)
- Spænding (voltage)
- Afstand mellem anode og emne
- Urenheder på linsen

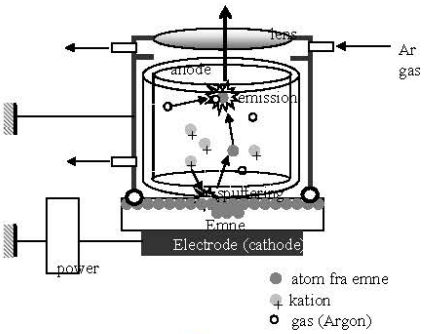

Udstyret skal rutinemæssigt kalibreres, og helst med standarder der er sammenlignelige med emnet der måles.

IPU

Fordele og ulemper ved GD-OES

Fordele
- 43 elementer kan analyseres på én gang
- lette stoffer, bl.a. hydrogen, ilt, kul, nitrogen og klorid kan måles
- meget små koncentrationer kan måles
- hurtig måling (1-10 µm/min.)

Ulemper
- emner skal være flade og skal have areal på mindst 5*5mm^2
- det tager lang tid at foretage kvantitative analyser grundigt
- emner skal være generelt elektrisk ledende

IPU

Eksempler

Bulk analyser

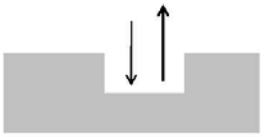

Dybdeprofiler

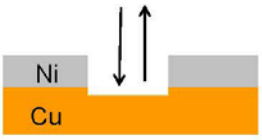

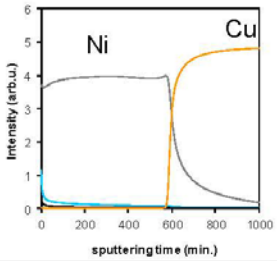

IPU

Eksempel 1 - bulk analyse

Emne – AlSi9Cu3Fe0.5 indeholdende Mn, Mg, Ti, Sr

Metode – B General Al
Referencer:
SQ-15KA Al-12%Si, 0,7%Fe, 0.5%Cu, 0,06%Mn, 1.2%Mg, 0.1%Ti, 0.03%Sr
SQ-12TL Al-1.1%Si, 0.6%Fe, 4.8%Cu, 1.1%Mn, 0.16%Mg
SQ-11PG Al-0.2%Si, 0,2%Fe, 0.5%Cu, 0,4%Mn, 3.1%Mg, 0.1%Ti

Resultat af måling på standarder:

	Si	Fe	Cu	Mn	Mg	Ti	Sr
15KA	12	0.78	0.41	0.08	1.1	0.09	0.04
12TL	0.95	0.73	3.9	1.3	0.14	-	-
11PG	0.18	0.22	0.44	0.49	2.7	0.09	

Genkalibration

Resultat af måling på testemne:

	Si	Fe	Cu	Mn	Mg	Ti	Sr
sample	8.7	0.65	2.4	0.46	0.34	0.06	0.04

IPU

Eksempler – Zinkat behandling

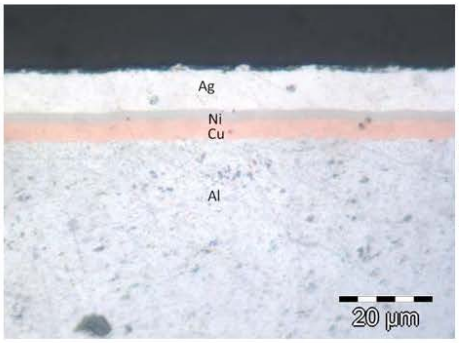

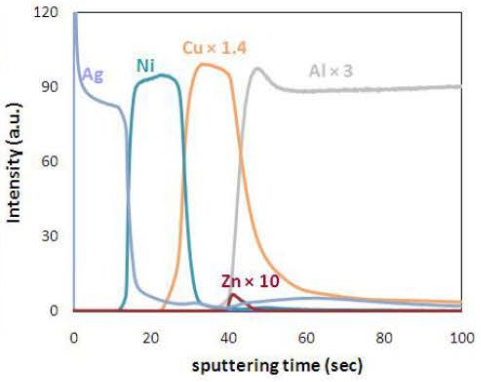

IPU

Eksempler – Elektropletteret silicium wafer

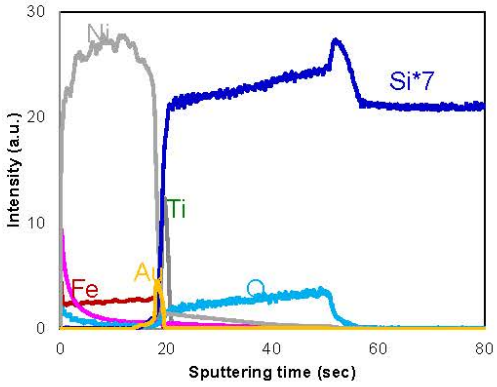

Analyseområde

IPU

Eksempler – Fejl i svejsning

Svejsning med plastiskfolie på bagside

Kan en slibning fjerne det brændte plastik fra overfladen?

IPU

GD-OES måling af emner med svejsninger

Side 19

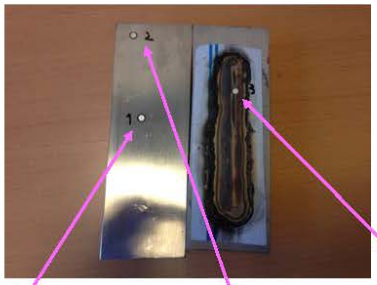

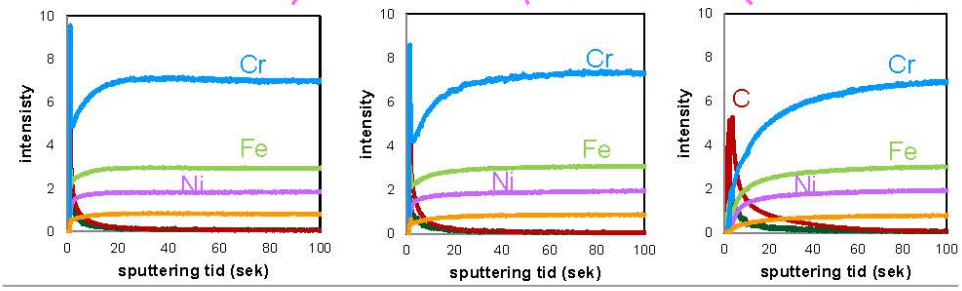

IPU

Korrosionstest og GD-OES-måling

Side 20

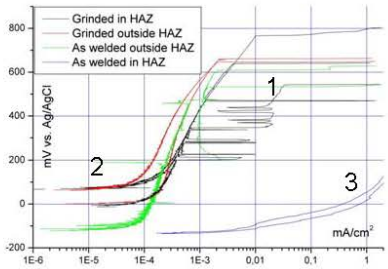

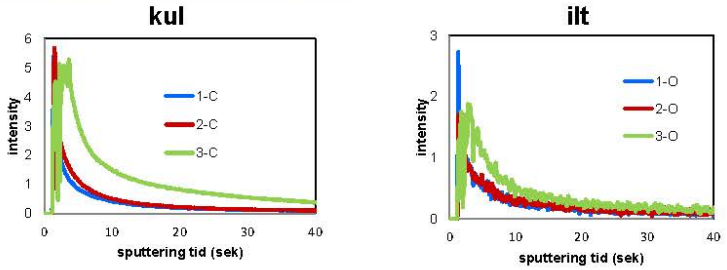

IPU

Forbehandling af aluminium

Aluminium plade forbehandlet med vådblæsning
(indeholder fint kalk pulver)

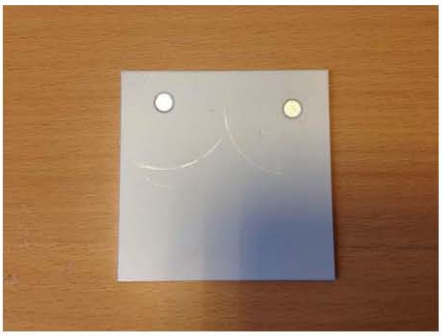

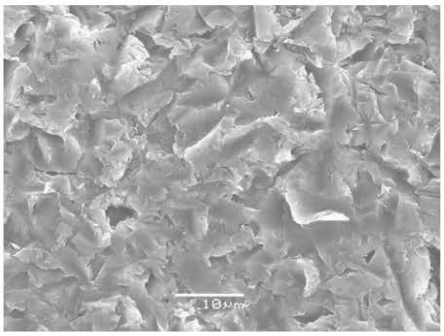

IPU

Forbehandling af aluminium

Original aluminium plade

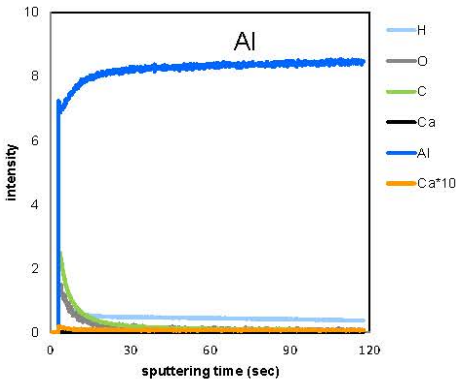

Efter vådblæsning

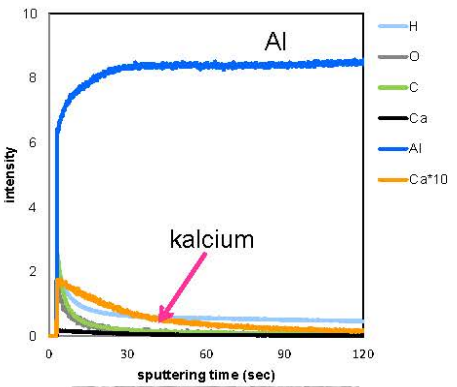

Meget calcium er stadig tilbage
→ høj pH
→ bakterier er døde

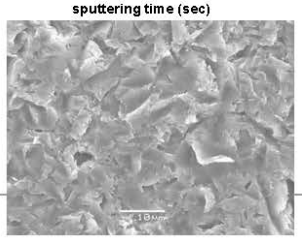

IPU

Kalcium målinger på Al forbehandlet på forskellige måder

Side 23

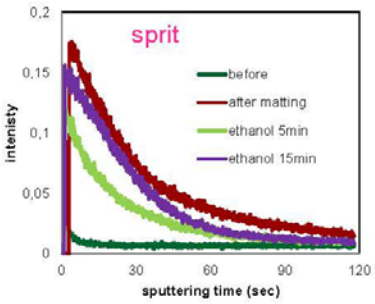

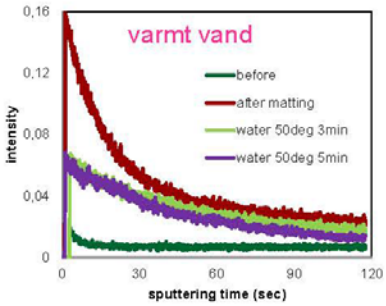

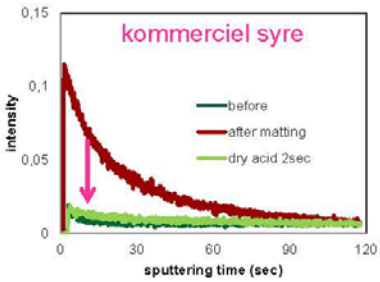

bedste måde

IPU

Deponering af guld med kobberforurening

Side 24

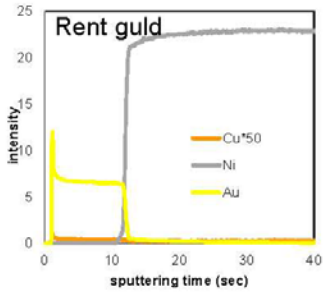

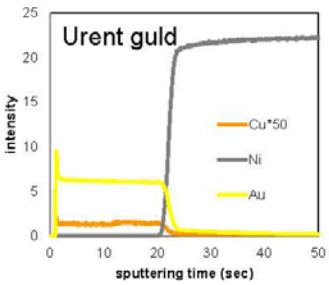

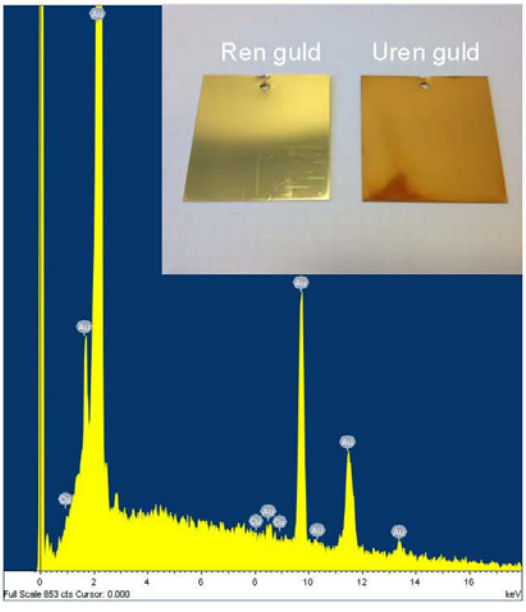

IPU

Fosfor aktiverede kobberanoder

Side 25

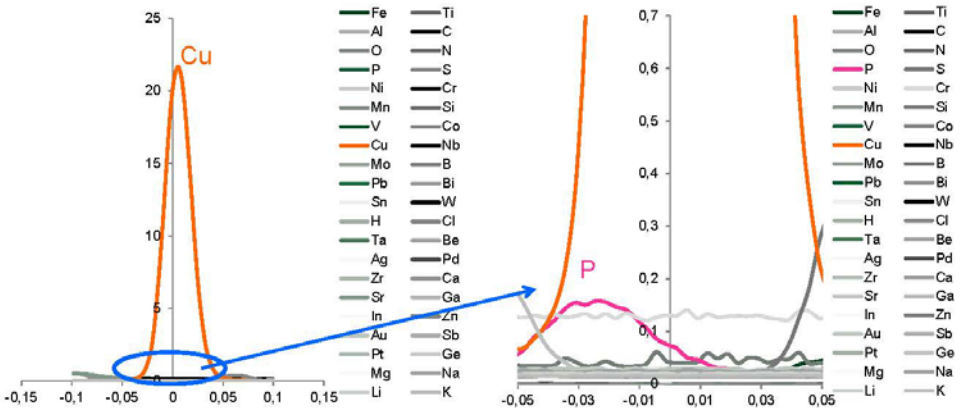

IPU

Ikke-ledende emner

Side 26

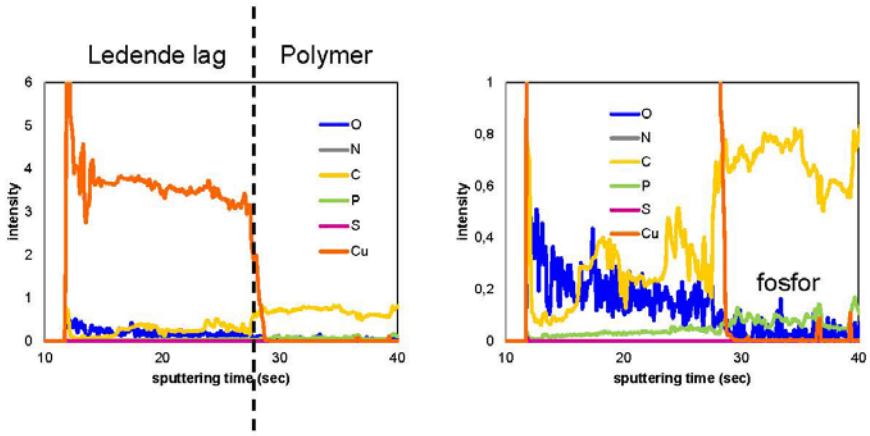

IPU

Summary

GD-OES kan anvendes til karakterisering af sammensætning, evt. kan en dybdeprofil opnås.

Det er vigtigt at kende fordele og ulemper ved metoden, når man foretager GD-OES måling.

Det kræver meget tid at gennemføre en ordentlig kvantitative analyse vha. GD-OES, dog er det muligt at måle selv lette grundstoffer præcist ved at bruge sammenlignelige standarder.

GD-OES kan benyttes til at måle urenheder der ikke kan detekteres med andre metoder.

IPU

Egenskaber for korrosion og rensbarhed af rustfri ståloverflader

Rasmus Lage

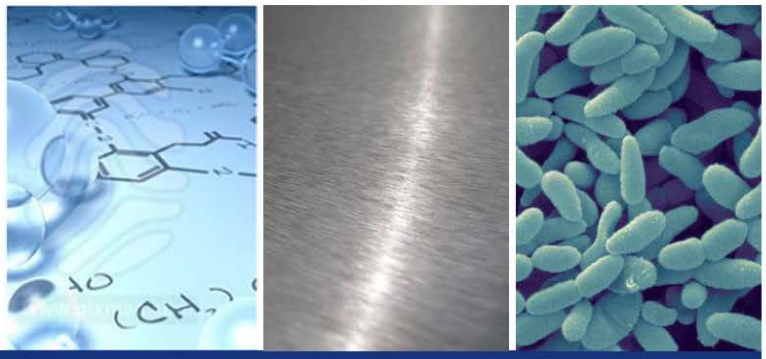

Præsentation – DMS Vintermøde

Korrosion og Cleanability Egenskaber for EN 1.4404 Rustfri Stål Overflader

Fredag d. 18/01 , 2013, Kolding.

Rasmus Lage – MSc Design & Innovation

DTU

Oplæg om korrosion og cleanability

Målsætning for dagens oplæg

- Gennemgå uddrag af udført studie i hvordan forskellige overfladebehandlinger kan have kraftig indvirkning på de efterfølgende egenskaber for korrosion og cleanability
- Sammenligne egenskaber for udsnit af nogle af de mest almindelige benyttede overflader i industrien
- Sammenholde ruhedsparametre for specificering af overflader med de resulterende egenskaber

Agenda

- Overordnede overvejelser for korrosion og cleanability
- Valgt legering og overfladebehandlinger
- Resultater for overflader, cleanabilty og korrosionsegenskaber
- Opsummering

Overordnede overvejelser for korrosion og cleanability

Overordnede overvejelser

- Overfladetopografi har stor indvirkning på cleanability og korrosionsbestandighed af overflader, selvom de er af samme type rustfri stållegering.
- Forskellige typer af overfladebehandlinger vil introducere vidt forskellige topografier afhængigt af den enkelte behandling.
- Valg af overfladebehandling og trade-offs?
  - Cleanabilty
  - Korrosionsbestandighed
  - Mekaniske egenskaber
  - Visuel karakteristika
  - Eksisterende praksis
  - Fastlagte krav
  - Pris

Valgt legering og overfladebehandlinger

Valgt legering og overfladebehandlinger

Valgt materialetype

- EN 1.4404 stål (316L)
- Analysearbejde foretages på 2 mm pladeemner.

Hvilke overflader er tilgængelige og benyttes i praksis?

- Slebne, matteret, børstet og rystepudset
- Poleret
- Blæste
- Vibrationsslebne og vibrationspolerede
- Slyngrenset
- Kemiske og elektrokemiske

Karakterisering af overflade topografi

Karakterisering af overflade topografi

Karakterisering af undersøgte overflader:

For tilstrækkeligt at kunne skelne mellem konsekvenserne af de enkelte overfladebehandlinger og deres indvirkning på korrosion og cleanabilty egenskaber, må den introducerede topografi undersøges i dybden.

Metoder til karakterisering:

- Scanning Electron Microscopy (SEM)
- Metallographic Cross Section
- Ruhedsmålinger (R_a i særdeleshed)

Karakterisering af overflade topografi

2B overflade

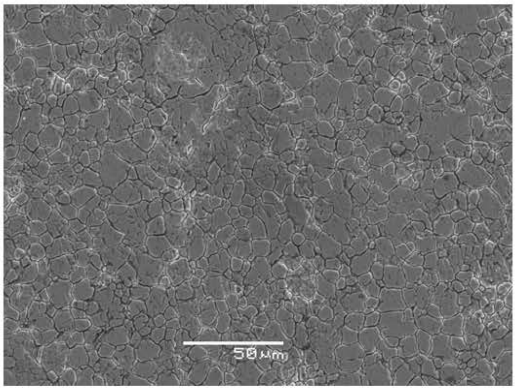

Fremstillingsproces

- Kold valset
- Annealed
- Bejdset
- Let valset

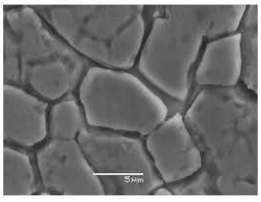

Korrosion og Cleanability Egenskaber for EN 1.4404 Rustfri Stål Overflader

Karakterisering af overflade topografi

Slebet korn 180 overflade

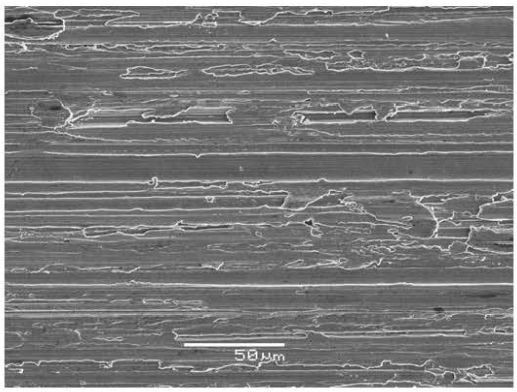

Fremstillingsproces

- Slebet korn 80
- Slebet korn 120
- Slebet korn 180

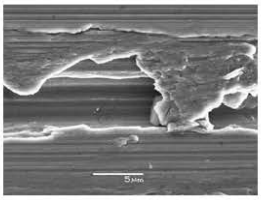

Korrosion og Cleanability Egenskaber for EN 1.4404 Rustfri Stål Overflader

Karakterisering af overflade topografi

Matteret overflade

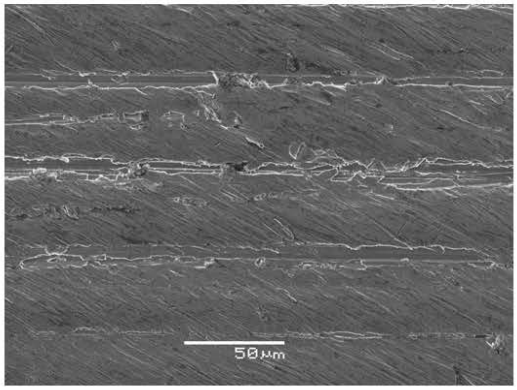

Fremstillingsproces

- Slebet korn 80
- Slebet korn 120
- Slebet korn 180
- Matteret m. 3M SC-BS A MED

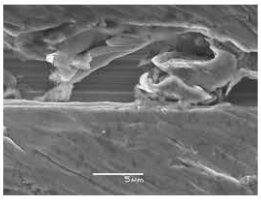

Korrosion og Cleanability Egenskaber for EN 1.4404 Rustfri Stål Overflader

Karakterisering af overflade topografi

Electropoleret overflade

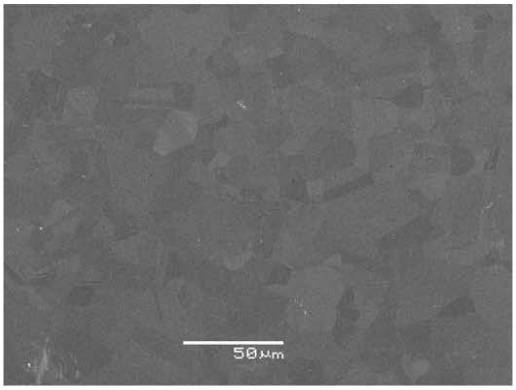

Fremstillingsproces

- Electropoleret
- 25 A/dm^2
- 15 min
- 50 C°

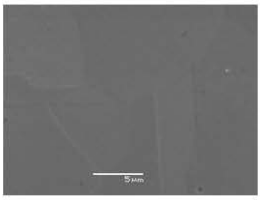

Korrosionsegenskaber og effekt af topografi

Korrosionsegenskaber og effekt af topografi

Cykliske Polarisationskurver (CYP)

CYP er en accelereret test for korrosionsbestandighed, hvor en nedsænket overflade påtvinges en gradvis stigende elektrisk spænding (potentiale).

Denne spænding er et udtryk for hvor aggressivt et miljø den pågældende overflade befinder sig i.

Der testes i en saltopløsning for at sikre at korrosion kan opstå.

Ved at måle den resulterende strøm mellem overflade og omkringliggende medie, kan begyndelsespunktet identificeres for korrosion (pitting potentialet)

Sammenligning af korrosionsegenskaber

Cykliske Polarisationskurver

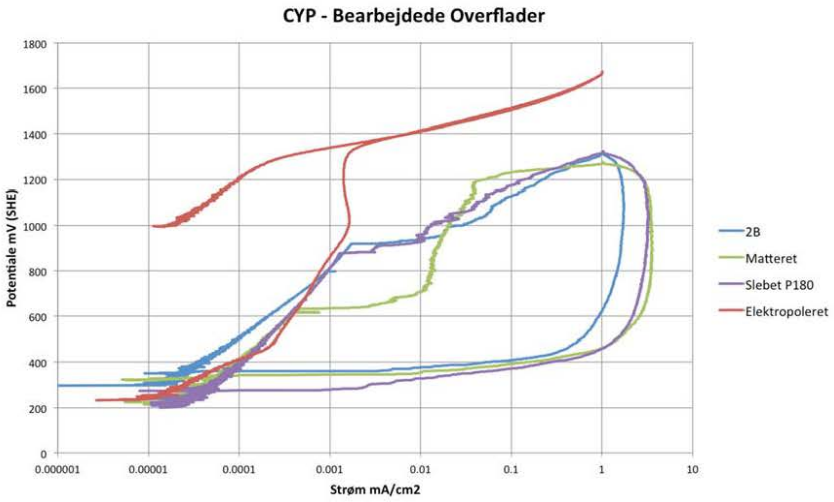

Sammenligning af korrosionsegenskaber

Cykliske Polarisationskurver

Slebet korn 180 overflade

Matteret overflade

Cleanability og effekt af topografi

Cleanability og effekt af topografi

Cleanabilty som resultat af topografi?

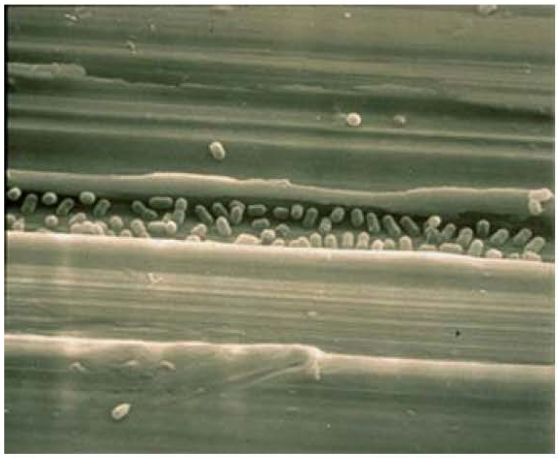

Ref: Professor Amy Wong – Microbewiki.

Cleanability og effekt af topografi

Kvantitativ metode - Impedans Analyse

Kvantitativ bedømmelse af resterende bakterier på undersøgte 10x15 mm samples efter rengøring. Antal af bakterier (Colony Forming Units - CFU) på overfladen bestemmes ved, at måle udviklingen af CO_2 der produceres af de resterende bakteries stofskifte.

Visuel methode – Agar Replica Plating

Visuel bedømmelse af resterende bakterier på undersøgte 10x15 mm samples efter rengøring. Bakteriel overførelse fra den rengjorte overflade opnås via aftryk på Agar substrat efterfulgt af observation af den mikrobiel vækst.

Korrosion og Cleanability Egenskaber for EN 1.4404 Rustfri Stål Overflader

Cleanability og effekt af topografi

Cleanability for udvalgte overflader:

Ground P180

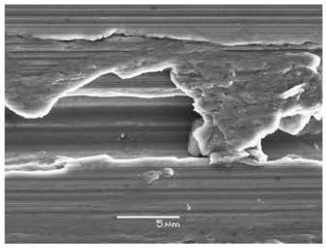

Replica Plating

CFU – 159580
(1,5 x 10^5)

Polished

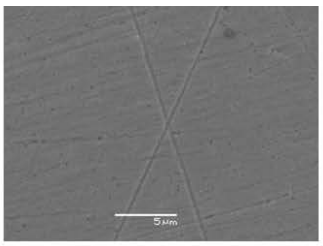

Replica Plating

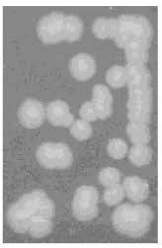

CFU – 3592
(3,5 x 10^3)

Pålidelighed af ruhedsmålinger som parameter

Pålidelighed af ruhedsmålinger som parameter

Nuværende brug af R_a værdier

- Mest almindelige ruhedsparameter til specificering af overflader.
- Velkendt og let at benytte.
- Bruges i langt de fleste nuværende standarder og guidelines for design af applikationer med henblik på korrosion og cleanabilty.
- Anklages for at være for upræcis til tilstrækkeligt at kunne afbillede overflade topografi og overfladeregenskaber.

Pålidelighed af ruhedsmålinger som parameter

Vurdering af nuværende standarder og guidelines i henhold til brugen af R_a

- R_a værdier kan ikke altid relateres til egenskaber for korrosion og cleanability.
- R_a værdier kan kun opfattes som tilnærmelser af den egentlige overflade topografi.
- R_a værdier vil for mange overflader have indlejret usikkerheder med hensyn til gengivelse af skjulte sprækker og revner.
- Nuværende standarder og guidelines tager ikke sådanne usikkerheder tilstrækkelig til efterretning.

Slebet P120

Korrosion og Cleanability Egenskaber for EN 1.4404 Rustfri Stål Overflader

Opsummering

Opsummering

- Valg af overfladebehandling har stor indvirkning på henholdsvis cleanabilty og korrosionsegenskaber. Anvendt behandling og de resulterende egenskaber bør derfor overvejes i henhold til den givne applikation.
- Nuværende specificering af overfladekriterier via eksisterende standarder og guidelines indeholder flere faldgrupper. Dette skyldes især brugen af R_a værdier som overfladekriterium.
- Via overvejelser omkring effekten af topografi kan der etableres et forbedret udgangspunkt for valg af overfladebehandling. Formidlingen af disse overvejelser kan assistere med udvælgelse og forbedret forståelse af overfladespecificering.

Korrosion og Cleanability Egenskaber for EN 1.4404 Rustfri Stål Overflader

Tak

Spørgsmål?